UNIVERSITY OF

SUSSEX

AT BRIGHTON

ROBUST ANALYSIS AND DESIGN OF CONTROL SYSTEMS WITH PARAMETRIC UNCERTAINTY

by

Nusret Tan

A thesis submitted in fulfilment of
the requirements for the degree of
Doctor of Philosophy
at the University of Sussex

School of Engineering, University of Sussex
Brighton, BN1 9QT, UK

November 1999

Declaration

The work described in this thesis, carried out in the School of Engineering, University of Sussex, is that of the author and has not been submitted in any form for any other degree at this or any other university.

Signed ....

Nusret Tan

School of Engineering, University of Sussex

Brighton, BN1 9QT, UK

November 1999

To My Parents

Ramazan Tan and Zakine Tan

Acknowledgements

I would like to take this opportunity to particularly thank my supervisor Professor Derek P. Atherton for drawing my attention to this field of research, and his skilful guidance and encouragement throughout this work.

I would also like to thank Ibrahim Kaya, Somanath Majhi, Muslum Arkan, Dr. Ilyas Cankaya, Dr. Ali Fuat Boz, the members of Control group and those of my friends whose names I did not mention here for their invaluable friendship, constructive discussion and all the good times we had together.

I am extremely grateful to my mother, my father, my brothers and sisters for their moral support, encouragement and belief in me.

Special thanks to the members of Department of Electrical and Electronics Engineering, Inonu University, Malatya, Turkey, for their friendship and support. The financial support for this study from Inonu University is greatly appreciated.

ABSTRACT

Classical control systems design uses fixed plant transfer functions yet engineers have known for many years that there is often considerable uncertainty regarding the parameters used in a transfer function representation. A major breakthrough on systems with uncertain parameters was achieved by the Russian mathematician Kharitonov who extended the Routh stability criterion to polynomials with an independent uncertainty structure known as interval polynomials, that is where the polynomial coefficients may be assumed to lie within a specific range rather than being fixed. Recently some important extensions, such as the edge theorem and the generalized Kharitonov theorem to the polynomials with more complex uncertainty structure, have been given. Motivated by these results, there has been a substantial amount of research in the field of robust control dealing with the analysis and design of systems containing parametric perturbations. This thesis presents additional results in this direction and the work can be divided in to three main parts.

The first part deals with interval systems, which is the simplest form of uncertain control systems. An extension of a new approach which is based on the Hermite-Biehler theorem to the $Lag/Lead$ controller structure for stabilizing a linear time-invariant plant is given. The approach is then used for computing the parameters of controllers for relative stabilization and interval plant stabilization. A user friendly software program, called "Analysis of Interval Systems Toolkit" (AISTK), has been developed in the MATLAB environment. The robust gain and phase margins and outer boundary of the Nyquist envelope of an interval plant family are discussed using the generalized Hermite-Biehler theorem. The gain crossover, phase crossover and the bandwidth frequencies of an interval plant are formulated.

The second part of the thesis considers control systems with affine linear uncertainty. An approach is given for plotting the Bode, Nyquist and Nichols envelopes of a transfer function with such parametric uncertainty. A novel feature of the approach is the use of the convex parpolygonal value set of a polynomial with affine linear uncertainty. Using these frequency envelopes, classical control design techniques are used to design robust control systems. Some results are developed on the determination of a robust small gain theorem, robust performance, strict positive realness and absolute stability problem of control systems with parametric as well as unstructured uncertainty.

The final part of the thesis studies the describing function analysis of nonlinear discrete interval systems. Using the results regarding the Schur stability of interval polynomials, a method is presented for investigating the stability of uncertain discrete systems with separable nonlinearities.

Contents

List of Figures

List of Tables

List of principal symbols

$\mathbf{q}, \mathbf{r}, \mathbf{a}$	Vectors of uncertain parameters
$a_i(\mathbf{q})$	Uncertain coefficient
Q, R	Uncertainty boxes
$\mathbf{R}$	Real number
$P(s, \mathbf{q})$	Uncertain polynomial family
$P(z, \mathbf{a})$	Discrete interval polynomial
$G(s)$	Transfer function of a plant
$C(s)$	Transfer function of a controller
$G(s, \mathbf{q}, \mathbf{r})$	Uncertain transfer function
$G(z, \mathbf{x}, \mathbf{y})$	Discrete interval transfer function
$G_K(s)$	Kharitonov plants family
$G_E(s)$	Extremal system of an uncertain plant
$Re[.]$	Real part
$Im[.]$	Imaginary part
$arg[.]$	Argument
$e(c_i, c_j)$	Edge with end points c_i and c_j
λ	A variable changing within $[0, 1]$
ω_{cg}	Gain crossover frequency
ω_{cp}	Phase crossover frequency
ω_b	Bandwidth frequency
$\partial(.)$	Denotes boundary
$N(A, \mathbf{p})$	Uncertain describing function
τ	Time delay
$\sigma(.)$	Signature of a polynomial
$\Vert . \Vert_\infty$	∞-norm

Chapter 1

INTRODUCTION

1.1 Introduction

Control theory within this century can be divided into four main periods: classical control, optimal control, control of multivariable systems and robust control. The period 1930-1960 can be classified as the "Classical Control" period. Here famous pioneers, like Bode [28], Nyquist [110] and Nichols [109], developed control design tools such as the Bode, Nyquist and Nichols plots. The root locus design methods became important, after the root locus technique was developed by Evans in 1948 [56]. Concepts such as gain and phase margins were introduced and have been widely used for controller design as a measure of stability margin. The results developed in this period have been successfully applied by practising control engineers.

The next period started from the early 1960's and can be called "Optimal Control". The state-space approach to optimal control and filtering theory was introduced in 1960 by Kalman [82]. Concepts such as controllability, observability, optimal state estimation and optimal state feedback were developed and introduced during this stage. These concepts were based on state space matrix equations rather than frequency domain transfer functions. Thus, these results shifted the emphasis in control engineering from the frequency domain to the time domain.

In the third stage of control theory development, control engineers dealt with the design of multivariable systems by frequency domain design methods. Extensions of the scalar classical frequency response techniques for multi-input multi-output (MIMO) systems were developed by Rosenbrock [114], MacFarlane [103] and Mayne [105].

The current fourth period from 1980 until today may be known as "Robust Control", which is one of the fastest growing and promising areas of research today. With robust control, researchers have begun to deal with systems which have uncertainties. Thus, more realistic and advantageous results have been developed.

1.2 What is Robust Control?

In modelling physical systems for control purposes, one normally needs to generate mathematical representations of the system. However, in general, it is difficult to obtain an exact mathematical description of a physical process. Therefore, it is necessary to make some simplifications in order to obtain a description of the system which is tractable. The difference between an exact model and its simplified form is called a perturbation. The requirement for a control design to be successful is that it must cope with any changes such as parametric variations which may occur in a system. This ability of a control system is known as robustness. Thus, robust control refers to the control of uncertain plants. The problem is to design a fixed controller which guarantees acceptable performance in the presence of uncertainty. Uncertainties in control systems can be broadly classified under two categories. They are:

i) structured (or parametric) uncertainty, representing lack of precise knowledge of the actual parameters. For example, the uncertain parameters can be the coefficients of a transfer function of a system.

ii) unstructured (or nonparametric) uncertainty which represents unmodelled dynamics, nonlinearities and error due to linearizations etc.. These types of uncertainties are usually given as norm bounded perturbations.

The purpose of robust control is to apply the well known techniques used in linear control system theory to, and develop new techniques for the analysis and design of systems with the uncertainties described above. In recent years there have been some important developments in the field of robust control [32] such as use of singular values as a measure of gain in transformations (Doyle and Stein [55]), the factorial approach in controller synthesis (Vidyasagar [132], Cailler and Desoer [31]), parametarization of stabilizing controllers (Youla *et al.* [137, 138], Desoer *et al.* [51]), H_∞ optimization (Zames [140], Zames and Francis [141], Helton [68]), robust stabilization and sensitivity minimization (Kimura [90], Vidyasagar and Kimura [133], Francis and Zames [60], Chang and Pearson [33]), computational aspect of H_∞ optimization (Delsarte *et al.* [50], Glover [66], Francis *et al.* [61]) and parametric theory-Kharitonov theorem and related approaches (Barmish [13], Ackermann [1], Bhattacharyya *et al.* [25], Djaferis [52]). One of the main reasons behind all these developments taking place in recent years is the striking advances in micro-processor design and computer technology. Among these topics, the takeoff point for this work is the parametric theory.

1.3 Parametric Theory

The analysis and design of systems which are subjected to parametric perturbations was largely ignored before the 1980's. The reason was mainly due to the fact that there were no theories which can be used for analysing or designing control systems with uncertain parameters. Of course, there are some notable exceptions. For example, the Evans root locus method [56], is an important tool for stability and robustness analysis for single parameter perturbations. In the book by Siljak [117], the issue of robust stability for systems with structured real parametric uncertainty is considered. For problems involving robustness analysis with uncertain parameters entering multilinearly into transfer function coefficients, a powerful tool is the mapping theorem given in the book by Zadeh and Desoer [139]. The book by Horowitz [78] made some contributions to robust synthesis.

However, after the mid-1980's, one can see a new explosion of research involving real parametric uncertainty. The reason for this explosion of results in the field of parametric theory is the seminal theorem of Kharitonov [88]. Kharitonov's theorem was originally published in 1978 in the Russian technical literature, however, it remained largely unknown for several years partly due to the fact that Kharitonov's original proof was complicated and difficult to understand. However, since the introduction of this remarkable theorem to the Western literature by Barmish [14], many papers have appeared providing new proofs of this theorem [29, 35, 106, 47] which are easy to understand.

The Kharitonov theorem is an extension of the Routh stability criterion to interval polynomials. An interval polynomial is a polynomial where each coefficient can vary in a prescribed interval. The Kharitonov theorem states that an interval polynomial family, which has an infinite number of members, is Hurwitz stable if and only if a finite small subset of the family which consists of four polynomials known as Kharitonov polynomials are Hurwitz stable. The most significant results following this theorem have been the edge theorem of Bartlett *et al.* [21] and the generalized Kharitonov theorem of Chapellat and Bhattacharyya [34]. The edge theorem considers a family of polynomials with affine linear uncertainty structure which means that the coefficients are not independent as in the case of interval polynomials. It proved that the whole family is stable if and only if all the exposed edges of the polytopic family are stable. Furthermore, the edge theorem is not restricted to Hurwitz stability and it can be applied to general stability regions. The generalized Kharitonov theorem is an improved version of the edge theorem. The advantage of the generalized Kharitonov theorem over the edge theorem is that the number of edges which are required for stability are not dependent on the number of uncertain parameters. Using these results, there have been many developments in the field of parametric robust control. Some of these developments are summarized shortly as follows:

1. Robust stability of uncertain polynomials (Argoun [3], Barmish [15], Soh [119], Rantzer [113], Datta and Bhattacharyya [49], Shaw and Jayasuriya [116], Levkovich *et al.* [101], Arhipov *et al.* [6], Hernandez *et al.* [69]);

2. Parametric stability margin computation (Chapellat *et al.* [40], Soh *et al.* [120], Blanchini *et al.* [27], Mahon *et al.* [104], Ke [86]);

3. Frequency response computation of uncertain systems (Bailey and Hui [10], Bartlett *et al.* [24], Hollot and Tempo [75], Keel and Bhattacharyya [87], Fu [62], Levkovich and Zehep [102], Tan and Atherton [121, 122, 123]);

4. Stabilization of systems with parametric uncertainty (Ghosh [65], Hollot and Yang

[76], Barmish *et al.* [16], Djaferis [54], Naimark and Zehep [108], Ho *et al.* [70], Tan and Atherton [124, 125]);

5. Robust root locus (Barmish and Tempo [17], Chen *et al.* [41], Hwang *et al.* [79], Hwang and Chen [80]);

6. Analysis of time delay sytems with parametric perturbations (Barmish and Shi [18], Fu *et al.* [63], Tsypkin and Fu [131], Kogan and Leizarowitz [94]);

7. Robust Schur stability of interval polynomials (Bose *et al.* [30], Cieslek [44], Hollot and Bartlett [77], Kraus *et al.* [93], Katbab and Jury [84]);

8. Describing function analysis of uncertain nonlinear systems (Fadali and Chachavalvoong [57], Ferreres and Fromion [58], Impram and Munro [81], Tan and Atherton [126]);

9. Probabilistic robustness (Chen and Zhou [42, 43], Lagoa *et al.* [97], Barmish *et al.* [19]);

10. Critical direction theory (Latchman *et al.* [98, 99, 100]);

11. Multi-input/Multi-output(MIMO) uncertain systems (Santis and Vicino [115], Yeung and Winnie [135], Kontogiannis and Munro [95, 96])

12. Absolute stability of parametrically uncertain systems (Dasgupta [48], Grujic and Petkovski [67], Chapellat *et al.* [37, 38, 39], Tesi and Vicino [129], Dahleh *et al.* [46], Foo and Soh [59], Mori *et al.* [107], Tan and Atherton [127, 128])

An extensive discussion about all the results introduced so far and some further results can be found in the books [1, 13, 25, 52]. Despite all of these developments, the field of parametric robust control is still an active research area. There are many open problems which need to be answered.

1.4 Outline of the Thesis

This work aims to do further investigation and research on control systems with parametric uncertainty. Computation of stabilizing controller parameters using the generalized

Hermite-Biehler theorem, development of user friendly programs for the analysis of interval systems, developments of methods for computing frequency responses of uncertain systems, extensions of these methods to the different control problems such as the determination of the robust small gain theorem, robust performance, strict positive realness and absolute stability problem of systems with parametric as well as unstructured perturbations, and describing function analysis of uncertain systems are the main objectives of this work. The research work is organized as follows:

Chapter 2: Kharitonov Theorem and Related Approaches

In this chapter a description of parametric uncertainty structure is first given. Then some technical tools such as the value set concept, the zero exclusion principle, the segment lemma, the Kharitonov theorem and the edge theorem which play an important role while analysing the robust stability of polynomials with parametric uncertainty are summarized. Finally, the sixteen Kharitonov plants family and thirty-two systems which are the two fundamental concepts behind many results developed in the field of parametric robust control are introduced.

Chapter 3: Feedback Stabilization Using the Hermite Biehler Theorem

This chapter deals with the stabilization of control systems using a recently developed new approach. The approach is based on a new result [71] generalizing the classical Hermite-Biehler theorem to the case of not necessarily Hurwitz polynomials and considers the stabilization of feedback systems using *P, PI* and *PID* controllers. In this chapter, an extension of the results given in [72, 73, 74] to the $Lag/Lead$ controller structure for stabilizing a given transfer function is first given. The approach is then developed for PI, $Lag/Lead$ and PID controllers to achieve relative stabilization. Finally, the stabilization of an interval plant family is discussed using the sixteen Kharitonov plants family and the generalized Hermite-Biehler theorem.

Chapter 4: A Software Package Program for Analysis of Interval Systems

The chapter describes a software program called "Analysis of Interval Systems ToolKit (AISTK)" which is a collection of algorithms developed in the MATLAB environment. AISTK is a user friendly toolkit like control kit and deals with the analysis of uncertain systems defined by an interval plant structure. In addition the procedures for constructing various envelopes that contain the entire frequency responses of an interval system are given. The outer boundary of the Nyquist envelope of an interval plant family is discussed using the generalized Hermite-Biehler theorem. The formulation of gain crossover, phase crossover and bandwidth frequencies of an interval plant are also given. The application of a simple autotuning method to an interval plant is given by an example.

Chapter 5: Frequency Response of Systems with Affine Linear Uncertainy

In this chapter, effective procedures are proposed for computing the Bode, Nyquist and Nichols envelopes of a transfer function with an affine linear uncertainty structure. The procedures are based on the convex parpolygonal value set of a polytopic polynomial family. Using this family of plots, classical control design techniques are used to design robust control systems.

Chapter 6: Analysis of Control Systems with Mixed Perturbations

Extensions of results developed in the previous chapter to problems such as the determination of a robust small gain theorem, robust performance, strict positive realness and the absolute stability problem of control system with parametric uncertainty is made. Thus, the chapter studies control systems with parametric as well as unstructured uncertainty. The unstructured uncertainty is modelled as norm bounded perturbations and sector bounded nonlinear gains and the parametric uncertainty is represented by a transfer function whose numerator and denominator polynomials are polynomials with affine linear uncertainty.

Chapter 7: The Describing Function Analysis of Nonlinear Discrete Interval Systems

The describing function analysis of discrete interval systems with separable nonlinearities is studied. Some of the results developed in the area of parametric robust control related to the stability of discrete interval polynomials are combined with the describing function method to analyze the stability problem of discrete nonlinear interval systems.

Chapter 8: Conclusion

This chapter outlines the new contributions of the work presented in this thesis and makes suggestions for future research.

Chapter 2

KHARITONOV'S THEOREM AND RELATED APPROACHES

2.1 Introduction

The stability analysis of control systems is a very important issue and therefore has always been a major concern of control engineers. Autonomous stability means that, in the absence of external excitation, all signals in the system decay to zero. A control system is stable if and only if all the roots of the characteristic equation of the system lie in the left-half s plane. In classical control there are some powerful tools, which were developed for a fixed nominal system, such as the Routh-Hurwitz criterion for continuous systems, Jury's test for discrete systems and the well known frequency domain plots (Nyquist, Bode and Nichols plots) for stability analysis and controller design. However, as mentioned in Chapter 1, in real physical systems, the parameter variations of the transfer functions is an unavoidable fact. Thus, the fundamental problem in the study of control systems with parametric uncertainty is to determine whether or not all the polynomials in a given family of characteristic polynomials are Hurwitz stable. This property is known as robust stability which is one of the main subjects of parametric robust control.

Parametric robust control has made tremendous strides related to the robust stability analysis of parametrically uncertain systems since the publication of Kharitonov's celebrated theorem [88]. The Kharitonov theorem simply stated that the robust stability of an interval polynomial can be determined by testing the stability of just four polynomials in the real coefficient case. With this surprising result the entire field of parametric robust control came alive and researchers have addressed the following questions: To what extent can the Kharitonov theorem on the uncertain structure be relaxed? How can it be used for the analysis and design of control systems? The edge theorem of Bartlett et al. [21] and the generalized Kharitonov theorem(GKT) of Chapellat and Bhattacharyya [34] are the most significant results in this direction.

The organization of this chapter is as follows: Section 2.2 introduces the issue of uncertainty structure. In Section 2.3 some fundamental concepts, namely the value set concept, zero exclusion principle and segment lemma which are repeatedly used while analysing robust stability of uncertain polynomials, are first given. Then, the famous Kharitonov theorem and a major theorem developed during the post-Kharitonov era known as the edge theorem are introduced. Application of the Kharitonov theorem to a control system is considered in Section 2.4. In this section, the sixteen Kharitonov plant family and thirty-two systems are given. The final section gives a summary of the chapter.

2.2 The Issue of Uncertainty Structure

No matter how accurately one tries to mathematically model an engineering system, the model never describes exactly the system's behaviour. Environmental changes as well as component production tolerances affect the values of the system's parameters. Therefore, it is more realistic to assume a model with uncertainties.

Consider the standard feedback system shown in Figure 2.1 with a fixed plant

$$G(s) = \frac{N(s)}{D(s)} \tag{2.1}$$

and a compensator

$$C(s) = \frac{N_c(s)}{D_c(s)} \tag{2.2}$$

The classical stability problem for this standard configuration leads to examination of the closed loop polynomial $N(s)N_c(s) + D(s)D_c(s)$. In practice, however, as stated above the physical parameters entering into the model of a control system may not be known exactly. Typically, these physical parameters are known to vary in prescribed intervals, this leads to a resulting closed-loop polynomial which includes perturbations associated with these parameters. One can denote [20] these unknown parameters by a vector $\mathbf{q} = [q_1, q_2, ..., q_q]^T$ which is restricted to a prescribed *bounding hyper rectangle* (uncertainty box) Q in $\mathbf{R}^q$ as

$$Q = \{\mathbf{q}\in\mathbf{R}^q : q_i\in[\underline{q_i}, \overline{q_i}], i = 1, 2, ..., q\} \tag{2.3}$$

where $\underline{q_i}$ and $\overline{q_i}$ are specified lower and upper bounds of the ith perturbation q_i, respectively. Such an uncertainty box is shown in Figure 2.2 for three unknown parameters. Now, assume that the fixed transfer function of the configuration given in Figure 2.1 is an uncertain transfer function of the form

$$G(s, \mathbf{q}) = \frac{N(s, \mathbf{q})}{D(s, \mathbf{q})} \tag{2.4}$$

where $N(s, \mathbf{q})$ and $D(s, \mathbf{q})$ are uncertain polynomials. This means that each of these polynomial coefficients are a function of $\mathbf{q}$. In this case, the closed-loop characteristic polynomial is

$$P(s, \mathbf{q}) = N(s, \mathbf{q})N_c(s) + D(s, \mathbf{q})D_c(s) \tag{2.5}$$

which can be written in a more general form as

$$P(s, \mathbf{q}) = a_0(\mathbf{q}) + a_1(\mathbf{q})s + a_2(\mathbf{q})s^2 + ... + a_n(\mathbf{q})s^n \tag{2.6}$$

whose coefficients depend on the uncertainty vector $\mathbf{q}$. For the stability analysis of a polynomial family of the form of Eq.(2.6), the type of coefficient function $a_i(\mathbf{q})$ plays an important role. There are four classes of uncertain polynomials [13] depending on the structure of the coefficient function $a_i(\mathbf{q})$ which are

1. *Independent Uncertainty Structure(Interval Polynomials)*: An uncertain polynomial is an interval polynomial if each $a_i(\mathbf{q})$ of Eq.(2.6) is dependent only on one parameter such as $a_0(\mathbf{q}) = q_0$, $a_1(\mathbf{q}) = q_1$,..., $a_n(\mathbf{q}) = q_n$.

2. *Affine Linear Uncertainty Structure*: The polynomial of Eq.(2.6) is said to have an affine linear uncertainty structure if $a_i(\mathbf{q})$ is an affine linear function for $i = 0, 1, 2, ..., n$; that is, a linear function plus a constant. For example, $a_i(\mathbf{q}) = 3q_1 + q_2 + 8q_3 + 2$ is an affine linear function. These types of polynomials are also known as polytopic polynomial families.

3. *Multilinear Uncertainty Structure*: An uncertain polynomial $P(s, \mathbf{q})$ is said to have a multilinear uncertainty structure if each of the coefficients $a_i(\mathbf{q})$ is a multilinear function such as $a_i(\mathbf{q}) = 3q_1q_2q_3 + 2q_2 - q_3 + 10q_2q_3 + 3$.

4. *Polynomial Uncertainty Structure*: If each of the coefficients function of $a_i(\mathbf{q})$ of the polynomial of Eq.(2.6) is a multivariable polynomial in the components of $\mathbf{q}$ then $P(s, \mathbf{q})$ is said to have a polynomial uncertainty structure. For example, $a_i(\mathbf{q}) = 2q_1q_3 - 6q_1q_2 + q_3^2$ is a polynomial function.

Four different types of uncertainty structures for polynomials have been given. Let $P_{indep.}$, P_{affine}, $P_{multilin.}$ and $P_{poly.}$ denote the uncertain polynomials with independent, affine linear, multilinear and polynomic uncertainty structures, respectively, then the hierarchy can be stated as

$$P_{indep.} \subset P_{affine} \subset P_{multilin.} \subset P_{poly.} \tag{2.7}$$

From this hierarchy it can be seen that the most simple uncertainty structure is the independent one. An effective result on the independent uncertainty structure is the well known Kharitonov theorem. The next level of difficulty is the affine linear uncertainty structure. For affine linear uncertainty, the edge theorem is a useful tool. The multilinear and polynomial uncertainty structures have higher levels of difficulty. There is no straightforward method to deal with these types of uncertainty structures. One possible way to deal with these types of polynomials is to apply the so-called *overbounding technique* [13] which enables one to convert a dependent uncertainty structure to an independent one. However, this technique is a conservative technique. On the other hand, in the literature, some results related to uncertain polynomials with multilinear and polynomial uncertainty have been developed [13] using the *mapping theorem* [139].

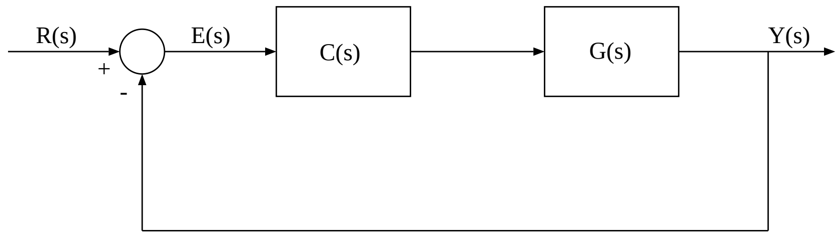

Figure 2.1: A standard feedback system

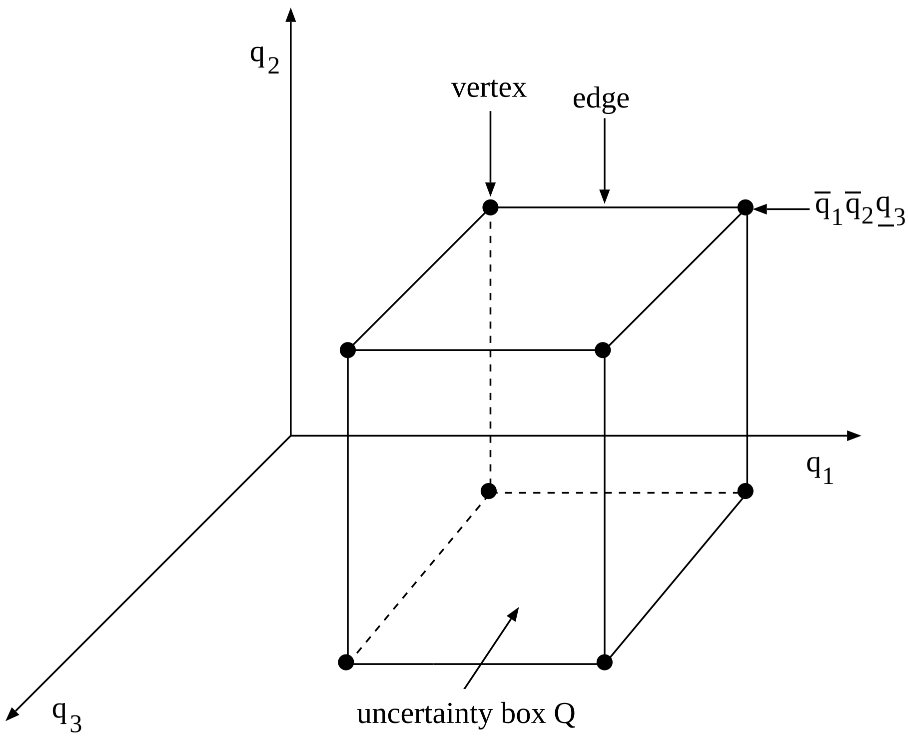

Figure 2.2: An uncertainty box in parameter space for $q = 3$ uncertain parameters

2.3 Some Essential Tools of Robust Control Under Parametric Uncertainty

In this section, some technical tools which play an important role in the field of parametric robust control are briefly mentioned. An understanding of these tools enables one to see the logic behind the many developments in robust control theory.

2.3.1 Value Set Concept

This is an important concept which is widely used in robust control under parametric uncertainty for checking the stability of uncertain systems, computing frequency responses of uncertain systems etc.. For a fixed polynomial the image of the polynomial at a fixed frequency is a point in the complex plane. However, for an uncertain polynomial the image is a set of points. These sets are referred to as value sets. Simply, the value set of an uncertain polynomial can be formulated as follows: Suppose that $P(s, \mathbf{q})$ is an uncertain polynomial defined by Eq.(2.6), at a fixed real frequency ω^* the value set is given by

$$P(j\omega^*, Q) = \{P(j\omega^*, \mathbf{q}) : \mathbf{q} \in Q\} \tag{2.8}$$

In the general case when the coefficients of $P(s, \mathbf{q})$ are multilinear or polynomic, there is no efficient analytical representation for the value set, and its construction may be quite difficult. However, in some important cases such as polynomials with independent and affine linear uncertainty, the shape of the value set can be described very simply [53, 130].

The power of the value set approach is derived from the fact that it is essentially a two dimentional set in the complex plane whereas the uncertain parameter box belongs to $\mathbf{R}^q$. Therefore, it is easier to deal with it computationally. The value set concept together with the zero exclusion principle which is given in the next subsection is a powerful tool for the stability analysis of uncertain polynomials.

Example 2.1

Consider

$$P(s, \mathbf{q}) = s^3 + 8s^2 + [5.5, 6.5]s + 3 \tag{2.9}$$

In order to obtain the value set of this uncertain polynomial family at each frequency, one needs to find the real and imaginary part of $P(s, \mathbf{q})$. Substituting $s = j\omega$

$$P(j\omega, \mathbf{q}) = -j\omega^3 - 8\omega^2 + j[5.5, 6.5]\omega + 3 = -8\omega^2 + 3 + j\omega(-\omega^2 + [5.5, 6.5]) \qquad (2.10)$$

Thus, the real and imaginary parts of $P(s, \mathbf{q})$ can be written as

$$Re[P] = -8\omega^2 + 3 \qquad (2.11)$$

and

$$-\omega^3 + 5.5\omega \leq Im[P] \leq -\omega^3 + 6.5\omega \qquad (2.12)$$

From these equations the value sets of $P(s, \mathbf{q})$ can be obtained. The value sets of $P(s, \mathbf{q})$ for 100 evenly spaced frequencies in the range $0 \leq \omega \leq 3$ are shown in Figure 2.3.

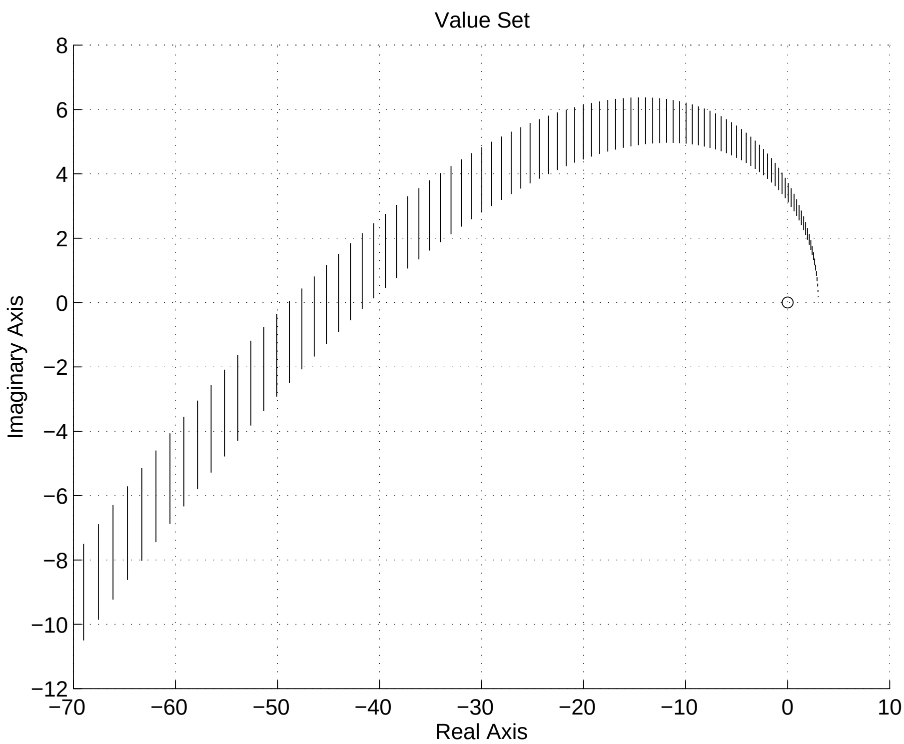

Figure 2.3: Value sets of the polynomial of Eq.(2.9)

2.3.2 Zero Exclusion Principle

Assume that the family of polynomials of Eq.(2.6) is of invariant degree (by invariant degree we mean that all polynomials under consideration should have the same degree. This means that the coefficient of the highest degree term should not vanish for any value of the parameter), and contains at least one stable polynomial. Then, it is easy to show using the *boundary crossing theorem* [36] that the entire family is stable if and only if the value sets of $P(s, \mathbf{q})$ do not include the origin for all real ω which can be written as [13]

$$0 \notin P(j\omega, Q) \tag{2.13}$$

As mentioned before, the value set concept combined with the zero exclusion principle constitutes a powerful tool to determine robust stability of uncertain polynomials. This comes from the fact that, the inclusion or exclusion of the origin in the value set of an uncertain polynomial can be checked using the boundary of the value set. Thus, when the value sets of an uncertain polynomial are readily constructable, the analysis of such a polynomial will also be easy. For example, one member of the uncertain polynomial family given in Example 2.1 such as $p(s) \in P(s, \mathbf{q}) = s^3 + 8s^2 + 5.5s + 3$ is stable and from Figure 2.3 since $0 \notin P(j\omega, Q)$ for all real ω, one can conclude that the family of polynomials $P(s, \mathbf{q})$ of Eq.(2.9) is robustly stable.

2.3.3 Segment Lemma

In this section, the problem of determining the stabilty of a line segment joining two fixed polynomials which are called end point polynomials is studied. Suppose $\delta_1(s)$ and $\delta_2(s)$ are polynomials of degree n then the segment of polynomials can be written as

$$\delta(s, \lambda) = (1 - \lambda)\delta_1(s) + \lambda\delta_2(s), \quad \lambda \in [0, 1] \tag{2.14}$$

In general, the stability of end points does not guarantee that of the entire segment of polynomials. For example, consider the segment joining the following two polynomials

$$\delta_1(s) = 3s^4 + 3s^3 + 5s^2 + 2s + 1$$

and

$$\delta_2(s) = s^4 + s^3 + 5s^2 + 2s + 5$$

it can be seen that although $\delta_1(s)$ and $\delta_2(s)$ are Hurwitz stable, the polynomial $\delta(s, \lambda) = (1 - \lambda)\delta_1(s) + \lambda\delta_2(s)$ for $\lambda = 0.5$ is not Hurwitz stable.

One possible way of determining the stability of a line segment is to conduct a sweep of λ, i.e. to test the stability of the polynomial starting from $\lambda = 0$ and increasing its value using a sufficiently small step until $\lambda = 1$ is reached. This approach is, however, time consuming and not exact. On the other hand, using the segment lemma, the stability of a segment can be checked by using the end point polynomials as follows: Let $\delta_1(s)$ and $\delta_2(s)$ be stable polynomials of degree n with leading coefficients of the same sign. Then the line segment $(1 - \lambda)\delta_1(s) + \lambda\delta_2(s)$ is Hurwitz stable for all $\lambda \in [0, 1]$ if and only if there exists no real $\omega > 0$ such that all of the following three conditions which can be obtained from Figure 2.4 are met [25]

$$\begin{aligned} &1)\ \ \delta_1^e(\omega)\delta_2^o(\omega) - \delta_2^e(\omega)\delta_1^o(\omega) = 0 \\ &2)\ \ \delta_1^e(\omega)\delta_2^e(\omega) \leq 0 \\ &3)\ \ \delta_1^o(\omega)\delta_2^o(\omega) \leq 0 \end{aligned} \tag{2.15}$$

where $(\delta_1^e(\omega), \delta_1^o(\omega))$ and $(\delta_2^e(\omega), \delta_2^o(\omega))$ are the even and odd parts of $\delta_1(s)$ and $\delta_2(s)$, respectively.

Example 2.2

Consider a line segment with the following end points

$$\delta_1(s) = s^3 + 3s^2 + 4.4s + 1.25$$

and

$$\delta_2(s) = 2s^3 + 4s^2 + 5.4s + 2.25$$

It can be seen that $\delta_1(s)$ and $\delta_2(s)$ are Hurwitz stable. The objective is to check the robust

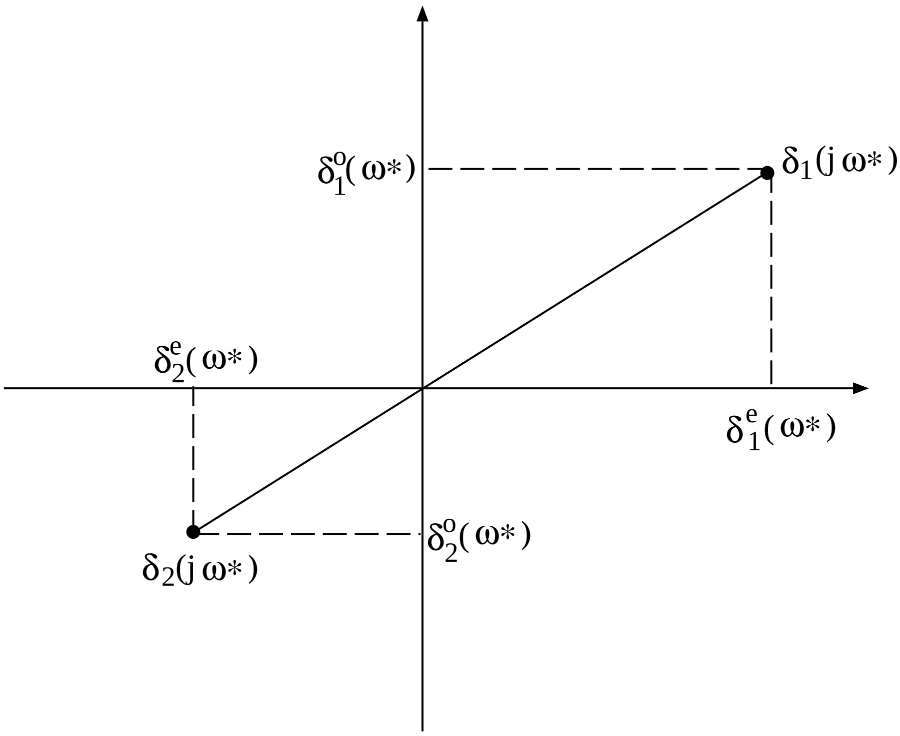

Figure 2.4: Geometric interpretation of segment lemma

stability of

$$\delta(s,\lambda) = (1-\lambda)\delta_1(s) + \lambda\delta_2(s) = (\lambda+1)s^3 + (\lambda+3)s^2 + (\lambda+4.4)s + (\lambda+1.25) \quad (2.16)$$

where $\lambda \in [0,1]$. To apply the segment lemma it is necessary to find the positive real roots of the polynomial

$$\delta_1^e(\omega)\delta_2^o(\omega) - \delta_2^e(\omega)\delta_1^o(\omega) = 2\omega^4 + 1.15\omega^2 - 3.15 = 0 \quad (2.17)$$

There is one positive real root which is $\omega = 1$. However, for $\omega = 1$ it can be seen that $\delta_1^e(\omega)\delta_2^e(\omega) = 3.06 > 0$ and $\delta_1^o(\omega)\delta_2^o(\omega) = 11.56 > 0$. Therefore, from the segment lemma, one can say that the line segment of Eq.(2.16) is stable. Although frequency sweeping is not necessary, the value sets of the segment are shown in Figure 2.5 which exclude the origin as expected.

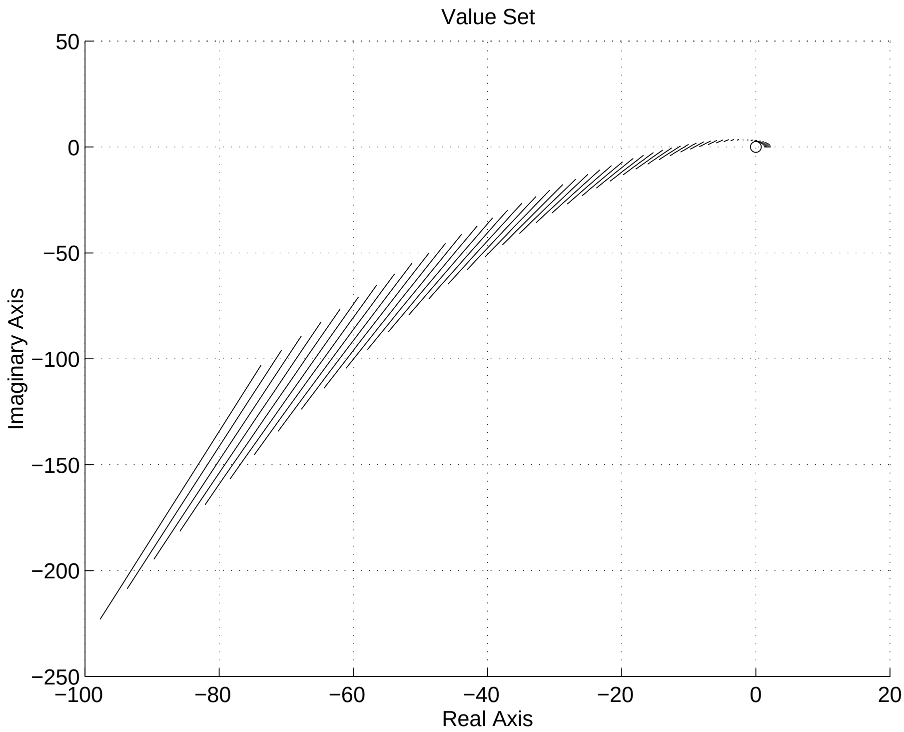

Figure 2.5: Value sets of the segment of Eq.(2.16)

2.3.4 The Kharitonov Theorem

This section deals with a result proved in 1978 by V. L. Kharitonov regarding the Hurwitz stability of a family of interval polynomials (each element of $\mathbf{q}$ enters into only one coefficient of (2.6)) known as the Kharitonov theorem. The Kharitonov theorem proves that the robust stability of an interval polynomial can be determined by testing the stability of just four polynomials which can be easily obtained by using upper and lower values of unknown parameters. The implication of this theorem goes far beyond the result embodied in it and has provided the spark for the activities of a large body of researchers all over the world. The Kharitonov theorem can be summarized as follows:

Consider a real interval polynomial of invariant degree n as

$$P(s,\mathbf{q}) = q_0 + q_1 s + q_2 s^2 + q_3 s^3 + ... + q_n s^n \tag{2.18}$$

where

$$Q = \{\mathbf{q} : q_i \in [\underline{q_i}, \overline{q_i}], i = 0, 1, \cdots, n\} \tag{2.19}$$

The given interval polynomial $P(s, \mathbf{q})$ is Hurwitz stable if and only if the following four extreme polynomials (four Kharitonov polynomials) are Hurwitz stable:

$$\begin{aligned}
p_1(s) \in P(s, \mathbf{q}) &= \underline{q_0} + \underline{q_1}s + \overline{q_2}s^2 + \overline{q_3}s^3 + \underline{q_4}s^4 + \ldots\ldots\ldots\ldots \\
p_2(s) \in P(s, \mathbf{q}) &= \underline{q_0} + \overline{q_1}s + \overline{q_2}s^2 + \underline{q_3}s^3 + \underline{q_4}s^4 + \ldots\ldots\ldots\ldots \\
p_3(s) \in P(s, \mathbf{q}) &= \overline{q_0} + \underline{q_1}s + \underline{q_2}s^2 + \overline{q_3}s^3 + \overline{q_4}s^4 + \ldots\ldots\ldots\ldots \\
p_4(s) \in P(s, \mathbf{q}) &= \overline{q_0} + \overline{q_1}s + \underline{q_2}s^2 + \underline{q_3}s^3 + \overline{q_4}s^4 + \ldots\ldots\ldots\ldots \qquad (2.20)
\end{aligned}$$

The original proof of this theorem by Kharitonov is complicated. Meanwhile, much simpler proofs can be found in [29, 35, 106, 47]. Generally using the value set concept together with the zero exclusion principle, the logic behind the Kharitonov theorem can be understood. It can be easily shown that the value set of the interval polynomial at a fixed frequency is a rectangle (*Kharitonov rectangle*) whose sides are parallel to the real and imaginary axes. Figure 2.6 shows the value set of the interval polynomial of Eq.(2.18) at $s = j\omega^*$. The four Kharitonov polynomials ($p_1(s)$, $p_2(s)$, $p_3(s)$ and $p_4(s)$) at $s = j\omega^*$ as shown in Figure 2.6 constitute the corners of the rectangle. From this rectangular value set, the Kharitonov polynomials of Eq.(2.20) can be easily obtained using the maximum and minimum values of the even and odd parts of $P(s, \mathbf{q})$ as follows

$$\begin{aligned}
p_1(s) &= P_{min}^{even}(s) + P_{min}^{odd}(s) \\
p_2(s) &= P_{min}^{even}(s) + P_{max}^{odd}(s) \\
p_3(s) &= P_{max}^{even}(s) + P_{min}^{odd}(s) \\
p_4(s) &= P_{max}^{even}(s) + P_{max}^{odd}(s) \qquad (2.21)
\end{aligned}$$

Since the sides of the rectangular value set are parallel to the real and imaginary axes, it can be easily shown that the inclusion or the exclusion of the origin from this rectangular value set can be checked by using corner points which correspond to the Kharitonov polynomials.

For a general nth order interval polynomial, the Kharitonov theorem suggests testing a set of four fixed polynomials. However, for polynomials of degree 5, 4 and 3, the Kharitonov test can be simplified [2]. The corresponding Kharitonov polynomials are 3,

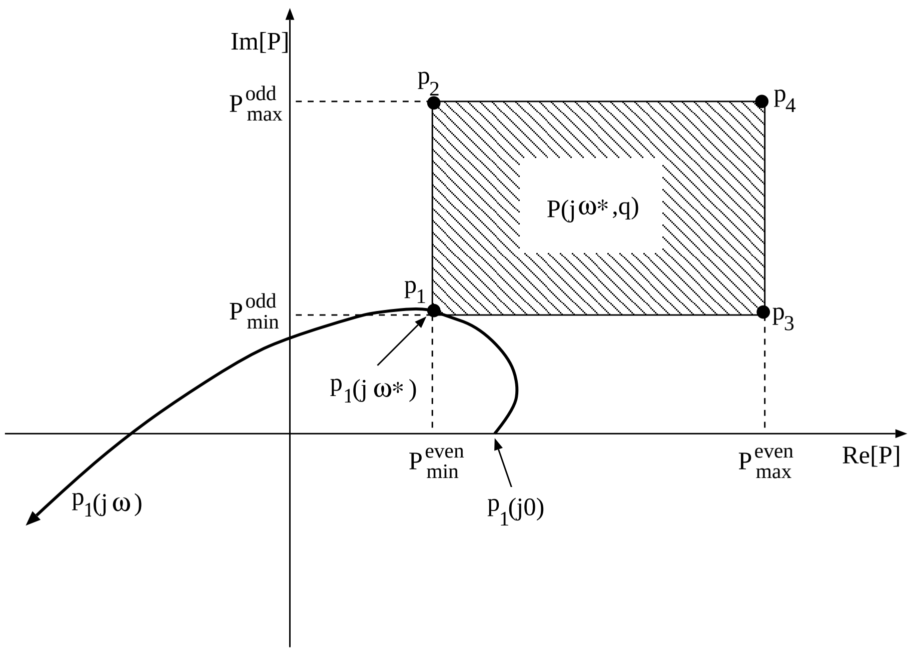

Figure 2.6: Kharitonov rectangle

2 and 1 in number as against 4 in the general case.

Example 2.3

Consider the following interval polynomial

$$P(s, \mathbf{q}) = s^4 + [4.95, 5.02]s^3 + [4.9, 7.1]s^2 + [2.5, 9.5]s + [0.32, 0.67] \tag{2.22}$$

The four Kharitonov polynomials are

$$\begin{aligned}
p_1(s) &= s^4 + 5.02s^3 + 7.1s^2 + 2.5s + 0.32 \\
p_2(s) &= s^4 + 4.95s^3 + 7.1s^2 + 9.5s + 0.32 \\
p_3(s) &= s^4 + 5.02s^3 + 4.9s^2 + 2.5s + 0.67 \\
p_4(s) &= s^4 + 4.95s^3 + 4.9s^2 + 9.5s + 0.67
\end{aligned} \tag{2.23}$$

Since these four Kharitonov polynomials are stable it can be concluded that the family of polynomials given in Eq.(2.22) is Hurwitz stable. The movement of the Kharitonov rectangles is shown in Figure 2.7.

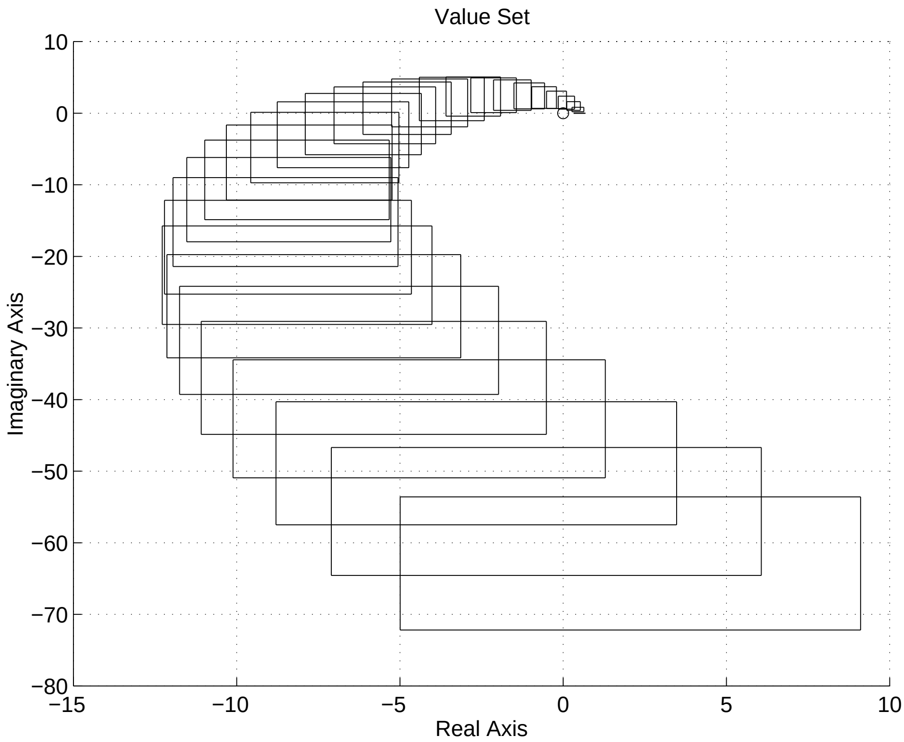

Figure 2.7: Movement of the Kharitonov rectangles

2.3.5 The Edge Theorem

Although the Kharitonov theorem gives an elegant solution to the stability problem of interval polynomials, it suffers from two basic limitations. These are: 1) The coefficients of the polynomials are assumed to vary independently. In other words no q_i enters into more than one coefficient. This is too restrictive for physical problems. In the general case, an uncertain polynomial can be represented by Eq.(2.6) where the coefficients can be affine linear, multilinear or polynomial functions. 2) Another important limitation is that the Kharitonov theorem can only be applied to problems where the stability region corresponds to the open left half plane. For example, the robust $\mathcal{D}$ stability (let $\mathcal{D}$ be a region in the complex plane then a polynomial is said to be $\mathcal{D}$ stable if all its roots lie in the region $\mathcal{D}$) cannot be checked by using the Kharitonov theorem.

Considerable research effort has been devoted to remove these limitations [13]. The most significant result in this direction is the one obtained by Bartlett *et al.* [21]. Their result, known as the edge theorem, deals with the stability of uncertain polynomials of the form of Eq.(2.6) with an affine linear uncertainty structure. As mentioned before, this type of polynomial is also known as a polytopic polynomial family. The edge theorem states that the corresponding polytope of polynomials of Eq.(2.6) with an affine linear uncertainty structure in the coefficient space has 2^q vertices and $(2^{q-1}(2^q - 1))$ edges joining 2^q vertices. Among these edges only the $(q2^{q-1})$ exposed edges of the polytope need to be checked to verify stability of the family of polynomials.

Since another version of the edge theorem shows that the root space of a polytopic polynomial family can be obtained from the root set of the exposed edges, it is also useful when one considers the general problem of robust $\mathcal{D}$ stability.

Example 2.4

Consider a polynomial family with affine linear uncertainty structure as

$$P(s, \mathbf{q}) = q_3 s^2 + (q_1 + q_2 + q_3)s + 2q_1 + q_2 \tag{2.24}$$

where

$$Q = \{\mathbf{q} = [q_1\ q_2\ q_3]^T : q_1 \in [1, 3],\ q_2 \in [4, 6],\ q_3 \in [0.2, 2.8]\} \tag{2.25}$$

It is quite clear that it is not possible to use the Kharitonov theorem for this uncertain family. On the other hand, since the uncertainty structure is affine linear, the edge theorem can be used successfully. Since there are three unknown parameters ($q = 3$), the corresponding polytope of the family of Eq.(2.24) in the coefficient space has $2^3 = 8$ vertices and $(3)2^2 = 12$ exposed edges (see Figure 2.2).

The vertex polynomials can be easily obtained as follows

$$\begin{aligned}
v_1(s) &= \underline{q_3}s^2 + (\underline{q_1} + \underline{q_2} + \underline{q_3})s + 2\underline{q_1} + \underline{q_2} \\
v_2(s) &= \underline{q_3}s^2 + (\overline{q_1} + \underline{q_2} + \underline{q_3})s + 2\overline{q_1} + \underline{q_2} \\
v_3(s) &= \underline{q_3}s^2 + (\underline{q_1} + \overline{q_2} + \underline{q_3})s + 2\underline{q_1} + \overline{q_2} \\
v_4(s) &= \underline{q_3}s^2 + (\overline{q_1} + \overline{q_2} + \underline{q_3})s + 2\overline{q_1} + \overline{q_2} \\
v_5(s) &= \overline{q_3}s^2 + (\underline{q_1} + \underline{q_2} + \overline{q_3})s + 2\underline{q_1} + \underline{q_2} \\
v_6(s) &= \overline{q_3}s^2 + (\overline{q_1} + \underline{q_2} + \overline{q_3})s + 2\overline{q_1} + \underline{q_2} \\
v_7(s) &= \overline{q_3}s^2 + (\underline{q_1} + \overline{q_2} + \overline{q_3})s + 2\underline{q_1} + \overline{q_2}
\end{aligned}$$

$$v_8(s) \quad = \quad \overline{q_3}s^2 + (\overline{q_1} + \overline{q_2} + \overline{q_3})s + 2\overline{q_1} + \overline{q_2} \tag{2.26}$$

Using these vertex polynomials, the exposed edges can be obtained. For example, the vertex polynomials $v_1(s)$ and $v_2(s)$ have the same structure except the parameter q_1 is its lower value ($\underline{q_1}$) in $v_1(s)$ and its upper value ($\overline{q_1}$) in $v_2(s)$. Thus, one of the exposed edges is $(1-\lambda)v_1(s) + \lambda v_2(s)$. Similarly, the remaining 11 exposed edges can be constructed. Once all the exposed edges are constructed then the stability can be determined using the segment lemma (since each exposed edge is a line segment) or the value set concept together with the zero exclusion principle (because the value sets at each frequency are bounded by the images of the exposed edges). The value sets of the family are shown in Figure 2.8 which exclude the origin. Therefore, the family is stable.

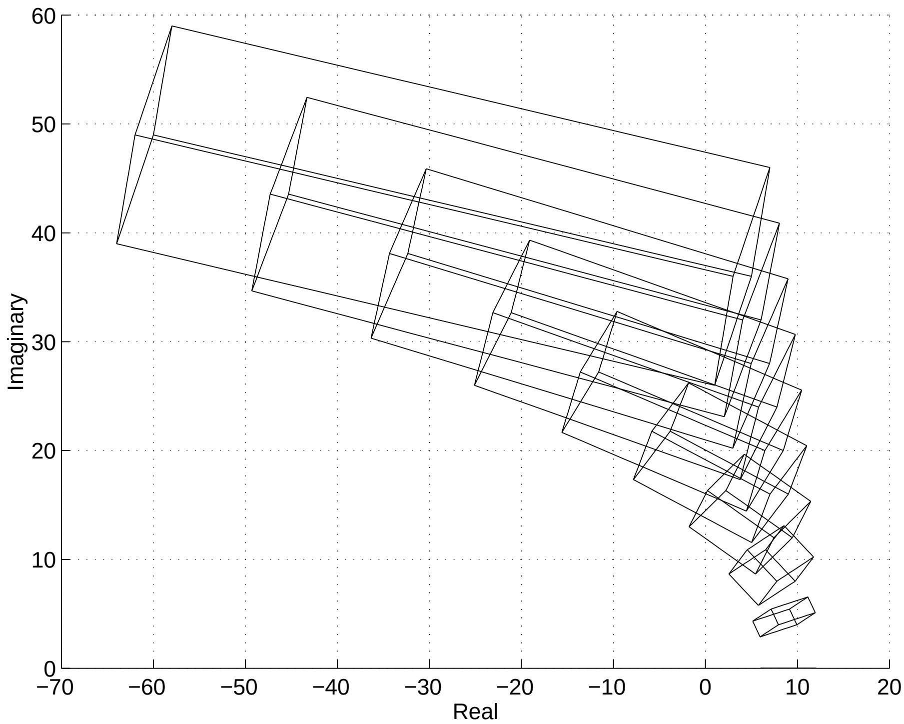

Figure 2.8: Value sets of the polynomials of Eq.(2.24)

2.4 The Interval Plant Concept

In this section, the sixteen Kharitonov plant family and thirty-two systems obtained from an interval plant are introduced. The sixteen Kharitonov plant family and the thirty-two systems are two fundamental theories behind many *extreme point results* developed in the field of parametric robust control. A definition of this terminolgy (*extreme point result*) is given in Barmish [20] as follows: An *extreme point result* is a result which enables one to infer that some desired property of a control system is robustly satisfied by checking the satisfication of this property on a finite subset of extreme systems which may arise. For example, is it possible to find the robust(minimum) gain and phase margin of a transfer function with independent uncertainty structure from a subset of fixed transfer functions? If so then one can say that an extreme point result holds. Of course, our intention in this section is not to report all the extreme point results of a control system with parametric uncertainty. An extensive research and discussion in this direction can be found in the books [1, 13, 25, 52], survey papers [20, 45, 112, 118] and the references there in. However, a brief introduction to these two important tools and a short discussion of some dominating extreme point results related to these tools are given.

2.4.1 Sixteen Kharitonov Plant Family

An interval plant is one in which the parameters are not known exactly, but are assumed to lie within specified intervals. More precisely, an interval plant can be formulated as

$$G(s,\mathbf{q},\mathbf{r}) = \frac{N(s,\mathbf{r})}{D(s,\mathbf{q})} = \frac{r_m s^m + r_{m-1}s^{m-1} + ... + r_0}{q_n s^n + q_{n-1}s^{n-1} + ... + q_0} \tag{2.27}$$

As usual, $Q = \{\mathbf{q} : q_i \in [\underline{q_i}, \overline{q_i}], i = 0, 1, ..., n\}$ and $R = \{\mathbf{r} : r_i \in [\underline{r_i}, \overline{r_i}], i = 0, 1, ..., m\}$ denote the boxes bounding the uncertain parameters vectors $\mathbf{q}$ and $\mathbf{r}$, respectively. Since the numerator and the denominator polynomials $N(s,\mathbf{r})$ and $D(s,\mathbf{q})$ are interval polynomials, from the Kharitonov theorem, one can obtain four Kharitonov polynomials for the numerator as

$$\begin{aligned}
N_1(s) &= \underline{r_0} + \underline{r_1}s + \overline{r_2}s^2 + \overline{r_3}s^3 + \underline{r_4}s^4 + ...\\
N_2(s) &= \underline{r_0} + \overline{r_1}s + \overline{r_2}s^2 + \underline{r_3}s^3 + \underline{r_4}s^4 + ...\\
N_3(s) &= \overline{r_0} + \underline{r_1}s + \underline{r_2}s^2 + \overline{r_3}s^3 + \overline{r_4}s^4 + ...\\
N_4(s) &= \overline{r_0} + \overline{r_1}s + \underline{r_2}s^2 + \underline{r_3}s^3 + \overline{r_4}s^4 + ...
\end{aligned} \tag{2.28}$$

and four Kharitonov polynomials for the denominator as

$$\begin{aligned}
D_1(s) &= \underline{q_0} + \underline{q_1}s + \overline{q_2}s^2 + \overline{q_3}s^3 + \underline{q_4}s^4 + \ldots\ldots\ldots\ldots \\
D_2(s) &= \underline{q_0} + \overline{q_1}s + \overline{q_2}s^2 + \underline{q_3}s^3 + \underline{q_4}s^4 + \ldots\ldots\ldots\ldots \\
D_3(s) &= \overline{q_0} + \underline{q_1}s + \underline{q_2}s^2 + \overline{q_3}s^3 + \overline{q_4}s^4 + \ldots\ldots\ldots\ldots \\
D_4(s) &= \overline{q_0} + \overline{q_1}s + \underline{q_2}s^2 + \underline{q_3}s^3 + \overline{q_4}s^4 + \ldots\ldots\ldots\ldots
\end{aligned} \tag{2.29}$$

By taking all combinations of the $N_i(s)$ and $D_i(s)$ for $i, j = 1, 2, 3, 4$, the following sixteen Kharitonov plant family can be obtained

$$G_K(s) = G_{ij}(s) = \frac{N_i(s)}{D_j(s)} \tag{2.30}$$

where $i, j = 1, 2, 3, 4$. This family is important both from the analysis and synthesis points of view. For example, the results given in [16, 26] known as the sixteen plants theorem states that a unity feedback system with a first order controller $C(s)$ and an interval plant of Eq.(2.27) is stable if $C(s)G_K(s)$ is stable. In Hollot and Tempo [75], it has been shown that the outer boundary of the Nyquist envelope of a stable interval plant is covered by the Nyquist plots of the sixteen Kharitonov plants. Thus, the worst case gain and phase margins can be computed from this family as well.

2.4.2 Thirty-Two Systems

As we have seen in the previous sections, the Kharitonov theorem deals with the robust stability problem of the polynomials which have an independent uncertainty structure. In attempting to apply this theorem directly to a control system with a fixed controller and an interval plant one meets a difficulty. This difficulty is mainly due to the fact that the characteristic polynomial coefficients do not perturb independently. The edge theorem can be used in this type of situation. However, the solution given by the edge theorem, in general, requires one to carry out the checking of all exposed edges which are exponentially dependent on the number of uncertain parameters. On the other hand a generalization of the Kharitonov theorem was given in [34]. Generally, the generalized Kharitonov theorem deals with the robust stability problem of polynomials of the form

$$K(s) = F_1(s)P_1(s, \mathbf{q}_1) + F_2(s)P_2(s, \mathbf{q}_2) + ... + F_m(s)P_m(s, \mathbf{q}_m) \tag{2.31}$$

where $F_1(s)$, $F_2(s)$,..., $F_m(s)$ are fixed polynomials in s and $P_1(s, \mathbf{q}_1)$, $P_2(s, \mathbf{q}_2)$,..., $P_m(s, \mathbf{q}_m)$ are interval polynomials. The details of this theorem can be found in the book by Bhattacharya *et al.* [25] where Chapter 7 has been totally devoted to the generalized Kharitonov theorem. Here, the thirty-two systems or Kharitonov's thirty-two segments which are a direct result of the generalized Kharitonov theorem are introduced.

Consider the interval plant family which is represented by Eq.(2.27) with the Kharitonov polynomials $N_1(s)$, $N_2(s)$, $N_3(s)$ and $N_4(s)$ for the numerator and $D_1(s)$, $D_2(s)$, $D_3(s)$ and $D_4(s)$ for the denominator. Then, the four Kharitonov segments for the numerator are

$$(1 - \lambda)N_i(s) + \lambda N_j(s) \tag{2.32}$$

and the four Kharitonov segments for the denominator are

$$(1 - \lambda)D_i(s) + \lambda D_j(s) \tag{2.33}$$

where $\lambda \in [0, 1]$ and $(i, j) \in \{(1, 2), (1, 3), (2, 4), (3, 4)\}$. Using the Kharitonov segments and Kharitonov polynomials for the numerator and the denominator polynomials, the following 32 subsets of the family can be obtained [25]

$$G_E(s) = \frac{N_i(s)}{(1 - \lambda)D_j(s) + \lambda D_k(s)} \cup \frac{(1 - \lambda)N_j(s) + \lambda N_k(s)}{D_i(s)} \tag{2.34}$$

where $\lambda \in [0, 1]$, $i = 1, 2, 3, 4$ and $(j, k) \in \{(1, 2), (1, 3), (2, 4), (3, 4)\}$. From these thirty-two systems, the Bode, Nyquist and Nichols envelopes of a control system with a fixed controller and an interval plant can be constructed [87]. For stability of a control system with a higher order controller and an interval plant, the stability of $C(s)G_E(s)$ is necessary and sufficient [34].

2.5 Conclusion

In this chapter, attention has been focused on the problem of robust stability of polynomials with parametric uncertainty. The points discussed in the chapter can be summarized as follows:

1. Using the Kharitonov theorem, the stability of interval polynomials can be determined by checking the stability of four Kharitonov polynomials. However, the Kharitonov theorem is not applicable when the coefficient perturbations are not independent.

2. The edge theorem covers problems of greater generality but it is computationally expensive. It can be applied in cases where the polynomial coefficients are affine linear in the parameters. Also, it is applicable to the different stability regions in the complex plane.

3. The value set concept, zero exclusion principle and the segment lemma are three important tools widely used in the field of parametric robust control while discussing the robust stability of uncertain polynomials.

4. The sixteen Kharitonov plants family and the thirty-two systems are two important developments for the analysis and design of control systems with parametric uncertainty.

Chapter 3

FEEDBACK STABILIZATION USING THE HERMITE BIEHLER THEOREM

3.1 Introduction

Recently, a new approach to the feedback stabilization using *P, PI* and *PID* controllers has been introduced in [72, 73, 74]. The approach is based on an appropriately generalized version of the Hermite-Biehler theorem [71]. The power of this method over the classical approaches such as the root locus technique, the Nyquist stability criterion and the Routh-Hurwitz criterion is that the first two classical methods are graphical and do not provide an analytical procedure to find all stabilizing values of the controller parameters. Although the Routh-Hurwitz criterion gives an analytical procedure, one needs to solve a set of polynomial inequalities which may be nonlinear to obtain stabilizing controller parameters. On the other hand, the stabilizing procedures based on the generalized Hermite-Biehler theorem provide an analytical solution to the problem of calculating the set of all stabilizing feedback gains for a given plant as well as providing a computational characterization of all stabilizing parameters of PI and PID controllers.

In this chapter, the application of the new method proposed in [72, 73, 74] is given for the $Lag/Lead$ controller structure. Indeed, most of the controllers used in industry today are PI, PID and $Lag/Lead$ controllers. Therefore, it is significant to extend the new approach to the $Lag/Lead$ controller structure. Thereafter, the approach is further developed for PI, $Lag/Lead$ and PID controllers for relative stabilization. In addition, the stabilization of uncertain systems defined by an interval plant is also discussed using the sixteen Kharitonov plant family and the Hermite-Biehler theorem.

The chapter is organized as follows: In Section 3.2, the Hermite-Biehler theorem and its generalized versions are given without proof which can be found in [74]. Stabilization of a given transfer function using a $Lag/Lead$ controller structure and the generalized Hermite-Biehler theorem is given in Section 3.3. In Section 3.4, the approach is further developed for relative stabilization. The stabilization of interval plants using the Kharitonov theorem and the Hermite-Biehler theorem is considered in Section 3.5.

3.2 The Hermite-Biehler Theorem

In this section, the Hermite-Biehler theorem and some further results are summarized. The details of all the results given here can be found in [74].

Let $\delta(s) = \delta_0 + \delta_1 s + ... + \delta_n s^n = \delta_e(s^2) + s\delta_o(s^2)$ be a given real polynomial of degree n where $\delta_e(s^2)$ and $\delta_o(s^2)$ are the even and odd parts of $\delta(s)$. Then the classical Hermite-Biehler theorem [36] can be stated as follows:

Theorem 3.1: Let $\omega_{e1}, \omega_{e2}, ...$ and $\omega_{o1}, \omega_{o2}, ...$ denote the positive real zeros of $\delta_e(-\omega^2)$ and $\delta_o(-\omega^2)$. Then $\delta(s)$ is Hurwitz stable if and only if all the zeros of $\delta_e(-\omega^2)$ and $\delta_o(-\omega^2)$ are real and distinct, δ_n and δ_{n-1} are of the same sign, and the positive real zeros satisfy the following interlacing property

$$0 < \omega_{e1} < \omega_{o1} < \omega_{e2} < \omega_{o2} < ...... \tag{3.1}$$

An equivalent analytical charcterisation of the Hermite-Biehler theorem is given by the following lemma using the signum function

$$sgn[x] = \begin{cases} -1 & \text{if } x < 0 \\ 0 & \text{if } x = 0 \\ 1 & \text{if } x > 0 \end{cases} \tag{3.2}$$

Lemma 3.1 [74]: Denote $\delta(j\omega) = p(\omega) + jq(\omega)$ where $p(\omega) = \delta_e(-\omega^2)$ and $q(\omega) = \omega\delta_o(-\omega^2)$. Let $\omega_{e1}, \omega_{e2}, ...$ denote the non-negative real zeros of $\delta_e(-\omega^2)$ and let $\omega_{o1}, \omega_{o2}, ...$ denote the non-negative real zeros of $\delta_o(-\omega^2)$, both arranged in ascending order of magnitude. Then the following conditions are equivalent:

1) $\delta(s)$ is Hurwitz stable.

2) δ_n and δ_{n-1} have the same sign and

$$n = \begin{cases} sgn[\delta_o].\{sgn[p(0)] - 2sgn[p(\omega_{o1})] + 2sgn[p(\omega_{o2})] + ... + (-1)^{m-1}.2sgn[p(\omega_{om-1})] \\ +(-1)^m.sgn[p(\infty)]\}, for \;\; n = 2m \\ \\ sgn[\delta_o].\{sgn[p(0)] - 2sgn[p(\omega_{o1})] + 2sgn[p(\omega_{o2})] + ... + (-1)^{m-1}.2sgn[p(\omega_{om-1})] \\ +(-1)^m.2sgn[p(\omega_{om})]\}, for \;\; n = 2m+1 \end{cases} \tag{3.3}$$

3) δ_n and δ_{n-1} have the same sign and

$$n = \begin{cases} sgn[\delta_o].\{2sgn[q(\omega_{e1})] - 2sgn[q(\omega_{e2})] + 2sgn[q(\omega_{e3})] + ... + (-1)^{m-2}.2sgn[q(\omega_{em-1})] \\ +(-1)^{m-1}.2sgn[q(\omega_m)]\}, for \;\; n = 2m \\ \\ sgn[\delta_o].\{2sgn[q(\omega_{e1})] - 2sgn[q(\omega_{e2})] + 2sgn[q(\omega_{e3})] + ... + (-1)^{m-1}.2sgn[q(\omega_{em})] \\ +(-1)^m.sgn[q(\infty)]\}, for \;\; n = 2m+1 \end{cases} \tag{3.4}$$

This lemma is not applicable to non-Hurwitz polynomials. In order to use the Hermite Biehler theorem as a tool for solving the stabilization problem, it needs to be generalized to the case of not necessarily Hurwitz polynomials. Define the normalized polynomial of

$\delta(j\omega)$ as [72].

$$\delta_f(j\omega) = \frac{p(\omega)}{f(\omega)} + j\frac{q(\omega)}{f(\omega)} = p_f(\omega) + jq_f(\omega) \ where \ f(\omega) = (1+\omega^2)^{n/2} \tag{3.5}$$

Such a normalization will make sure that $\delta_f(j\omega)$ intersects the real axis or the imaginary axis as $\omega \rightarrow \pm\infty$ and also preserve the finite frequencies at which $\delta(s)$ intersects the real and imaginary axes. Define also the signature of the polynomial $\delta(s)$ by $\sigma(\delta(s))$ and write

$$\sigma(\delta(s)) = l - r \tag{3.6}$$

where l and r are the number of open left and right half plane zeros of $\delta(s)$, respectively.
Theorem 3.2 [74]: Let $\delta(s)$ be a given real polynomial of degree n with no $j\omega$ axis roots except for possibly one at the origin. Let $0 = \omega_0 < \omega_1 < \omega_2 < .... < \omega_{m-1}$ be the real, non-negative , distinct finite zeros of $q_f(\omega)$ with odd multiplicities. Define also $\omega_m = \infty$. Then

$$\sigma(\delta) = \begin{cases} \{sgn[p_f(\omega_0)] - 2sgn[p_f(\omega_1)] + 2sgn[p_f(\omega_2)] + ... + (-1)^{m-1}.2sgn[p_f(\omega_{m-1})] \\ +(-1)^m.sgn[p_f(\omega_m)]\}.(-1)^{m-1}sgn[q(\infty)], \ if \ n \ is \ even \\ \\ \{sgn[p_f(\omega_0)] - 2sgn[p_f(\omega_1)] + 2sgn[p_f(\omega_2)] + ... \\ +(-1)^{m-1}.2sgn[p_f(\omega_{m-1})]\}.(-1)^{m-1}sgn[q(\infty)], \ if \ n \ is \ odd \end{cases} \tag{3.7}$$

Theorem 3.3 [74]: Let $\delta(s)$ be a given real polynomial of degree n with no roots on the $j\omega$ axis (the normalized plot $\delta_f(j\omega)$ does not pass through the origin). Let $0 < \omega_1 < \omega_2 < .... < \omega_{m-1}$ be the real, non-negative , distinct finite zeros of $p_f(\omega)$ with odd multiplicities. Also define $\omega_m = \infty$. Then

$$\sigma(\delta) = \begin{cases} -\{2sgn[q_f(\omega_1)] - 2sgn[q_f(\omega_2)] + ... \\ +(-1)^{m-2}.2sgn[q_f(\omega_{m-1})]\}.(-1)^m sgn[p(\infty)], \ if \ n \ is \ even \\ \\ -\{2sgn[q_f(\omega_1)] - 2sgn[q_f(\omega_2)] + ... + (-1)^{m-2}.2sgn[q_f(\omega_{m-1})] \\ +(-1)^{m-1}sgn[q_f(\omega_m)]\}.(-1)^m sgn[p(\infty)], \ if \ n \ is \ odd \end{cases} \tag{3.8}$$

3.3 Stabilization Using Lag/Lead Controller

In this section, the generalization of the Hermite-Biehler theorem is used in order to find the set of stabilizing values of the parameters of a *Lag/Lead* controller. Consider a unity feedback control system with a plant $G(s) = N(s)/D(s)$ and a controller $C(s)$.

a) Let $C(s)$ be a *Lag/Lead* controller of the form

$$C(s) = K\frac{s+\alpha}{s+\beta} \tag{3.9}$$

By using the even and odd parts of $N(s)$ and $D(s)$, $G(s)$ can be written as

$$G(s) = \frac{N_e(s^2) + sN_o(s^2)}{D_e(s^2) + sD_o(s^2)} \tag{3.10}$$

the characteristic equation of the system is

$$\begin{aligned}\delta(s,K,\alpha,\beta) = 1 + C(s)G(s) = 0 = {} & [K\alpha N_e(s^2) + \beta D_e(s^2) + s^2(KN_o(s^2) + D_o(s^2))] \\ & + s[KN_e(s^2) + K\alpha N_o(s^2) + D_e(s^2) + \beta D_o(s^2)]\end{aligned} \tag{3.11}$$

Substituting $s = j\omega$,

$$\begin{aligned}\delta(j\omega,K,\alpha,\beta) &= p(\omega,K,\alpha,\beta) + jq(\omega,K,\alpha,\beta) = \\ & [K\alpha N_e(-\omega^2) + \beta D_e(-\omega^2) - \omega^2(KN_o(-\omega^2) + D_o(-\omega^2))] \\ & + j\omega[KN_e(-\omega^2) + K\alpha N_o(-\omega^2) + D_e(-\omega^2) + \beta D_o(-\omega^2)]\end{aligned} \tag{3.12}$$

From Eq.(3.12) since both $p(\omega,K,\alpha,\beta)$ and $q(\omega,K,\alpha,\beta)$ depend on (K,α,β) this makes the application of lemma 3.1, theorem 3.2 or theorem 3.3 difficult. For example, in order to use theorem 3.2, one needs to find the positive real roots of $q(\omega,K,\alpha,\beta) = 0$ which depend on three unknown parameters (since the normalization given in Eq.(3.5) does not change the real roots of the even and odd parts and for clarity of presentation we will not invoke it). To partially overcome this difficulty , the following procedure can be used [74].

Assume the greatest common divisor of $N_e(s^2)$ and $N_o(s^2)$ is $e(s^2)$, and define

$$N'_e(s^2) = \frac{N_e(s^2)}{e(s^2)},\ N'_o(s^2) = \frac{N_o(s^2)}{e(s^2)} \tag{3.13}$$

from Eq.(3.13)

$$N'(s) = N'_e(s^2) + sN'_o(s^2) \tag{3.14}$$

and define

$$N^*(s) = N'(-s) = N'_e(s^2) - sN'_o(s^2) \tag{3.15}$$

$N'(s)$ has no $j\omega$ axis roots except possibly a single root at the origin. If one multiplies $\delta(s, K, \alpha, \beta)$ by $N^*(s)$ then the signature function of the multiplication can be written as

$$\sigma(\delta(s, K, \alpha, \beta)N^*(s)) = \sigma(\delta(s, K, \alpha, \beta)) + \sigma(N^*(s)) = \sigma(\delta(s, K, \alpha, \beta)) - \sigma(N'(s)) \tag{3.16}$$

By multiplying the characteristic equation with $N^*(s)$, one gets

$$\begin{aligned}
&\delta(s, K, \alpha, \beta)N^*(s) = \\
&\quad [s^2(D_o(s^2)N'_e(s^2) - D_e(s^2)N'_o(s^2)) + K\alpha(N_e(s^2)N'_e(s^2) - s^2N_o(s^2)N'_o(s^2)) \\
&\quad \beta(D_e(s^2)N'_e(s^2) - s^2D_o(s^2)N'_o(s^2))] + s[D_e(s^2)N'_e(s^2) - s^2D_o(s^2)N'_o(s^2) \\
&\quad +K(N_e(s^2)N'_e(s^2) - s^2N_o(s^2)N'_o(s^2)) + \beta(D_o(s^2)N'_e(s^2) - D_e(s^2)N'_o(s^2))]
\end{aligned} \tag{3.17}$$

and for $s = j\omega$, it can be seen that

$$\delta(j\omega, K, \alpha, \beta)N^*(j\omega) = \overline{p}(\omega, K, \alpha, \beta) + j\overline{q}(\omega, K, \beta) \tag{3.18}$$

Here, it is clear that one parameter of $q(\omega, K, \alpha, \beta)$ was eliminated and $\overline{q}(\omega, K, \beta)$, which is not dependent on α, is obtained. Now, let the degree of $\delta(s, K, \alpha, \beta)$ be n then $\delta(s, K, \alpha, \beta)$ is Hurwitz stable if and only if $\sigma(\delta(j\omega, K, \alpha, \beta)) = n$. Thus, the given plant is Hurwitz stable if and only if

$$\sigma(\delta(s, K, \alpha, \beta)N^*(s)) = n + \sigma(N^*(s)) = n - \sigma(N'(s)) \tag{3.19}$$

It is seen that for every fixed K value sweeping over β values and using theorem 3.2 or lemma 3.1 (if $N^*(s)$ is Hurwitz stable) and Eq.(3.19) (or conversely for each fixed β value sweeping over K values) the set of values of (K, α, β) for the system to be Hurwitz stable can be calculated. The range of β values for fixed K (or the range of K values for fixed

β) over which the sweeping needs to be done can be reduced by using the root locus idea given in [74] (see Appendix A). For example, for a known K value if one writes $\overline{q}(\omega, K, \beta)$ as

$$\overline{q}(\omega, K, \beta) = \omega(U(\omega, K) + \beta V(\omega)) \tag{3.20}$$

where β varies from $-\infty$ to $+\infty$ then the real breakaway points on the root locus of $U(\omega, K) + \beta V(\omega) = 0$ correspond to a real multiple root and must satisfy

$$\frac{U(\omega, K)\frac{dV(\omega)}{d\omega} - V(\omega)\frac{dU(\omega,K)}{d\omega}}{U^2(\omega, K)} = 0 \tag{3.21}$$

The real breakaway points are the real zeros of Eq.(3.21). And the corresponding β values can be found by using these zeros. Thus, the real root distribution of $U(\omega, K) + \beta V(\omega) = 0$ with respect to the origin can be calculated.

b) The lead controller is often used with unit gain at d.c. This means $K = \beta/\alpha$ and the transfer function can be written as

$$C(s) = \frac{1 + sT1}{1 + sT2} \tag{3.22}$$

with $T1 = 1/\alpha$ and $T2 = 1/\beta$. Now, assume $N'(s)$ which is defined in Eq.(3.14) has not got any root on the $j\omega$ axis and write the characteristic equation of the system

$$\begin{aligned} \delta(s, T1, T2) \quad &= \quad [N_e(s^2) + D_e(s^2) + s^2(T1N_o(s^2) + T2D_o(s^2))] \\ &\quad + s[N_o(s^2) + D_o(s^2) + T1N_e(s^2) + T2D_e(s^2)] \end{aligned} \tag{3.23}$$

multiplying $\delta(s, T1, T2)$ with $N^*(s)$ and substituting $s = j\omega$

$$\begin{aligned} &\delta(j\omega, T1, T2)N^*(j\omega) = p(\omega, T2) + jq(\omega, T1, T2) = [N_e(-\omega^2)N'_e(-\omega^2) + D_e(-\omega^2) \\ &N'_e(-\omega^2) - \omega^2 T2(D_o(-\omega^2)N'_e(-\omega^2) - D_e(-\omega^2)N'_o(-\omega^2)) + \omega^2 N'_o(-\omega^2)(N_o(-\omega^2) \\ &+D_o(-\omega^2))] + j\omega[D_o(-\omega^2)N'_e(-\omega^2) - D_e(-\omega^2)N'_o(-\omega^2) + T1(N_e(-\omega^2)N'_e(-\omega^2) \\ &+\omega^2 N_o(-\omega^2)N'_o(-\omega^2)) + T2(D_e(-\omega^2)N'_e(-\omega^2) + \omega^2 D_o(-\omega^2)N'_o(-\omega^2))] \end{aligned} \tag{3.24}$$

For every fixed $T2$, the zeros of $p(\omega, T2)$ do not depend on $T1$. Therefore by sweeping over all $T2$ values and using theorem 3.3 or lemma 3.1 (if $N^*(s)$ is stable), all the stabilizing values of $(T1, T2)$ can be calculated. From Eq.(3.24), if $N^*(s)$ is not Hurwitz stable, one needs to use theorem 3.3. Since theorem 3.3 is not applicable to a polynomial which has $j\omega$ axis roots, in this case, it is necessary to assume that $N'(s)$ or $N^*(s)$ must not have any roots on the $j\omega$ axis.

Example 3.1

Consider

$$G(s) = \frac{N(s)}{D(s)} = \frac{s^3 - 4s^2 + s + 2}{s^5 + 8s^4 + 32s^3 + 46s^2 + 46s + 17} \tag{3.25}$$

This plant is to be stabilized, if possible, using a *Lag/Lead* controller of the form

$$C(s) = \frac{s + \alpha}{s + \beta} \tag{3.26}$$

where K is assumed to be equal to one. From Eq.(3.11), the following closed loop characteristic equation is obtained

$$\begin{aligned}\delta(s, \alpha, \beta) = {} & s^6 + (8 + \beta)s^5 + (33 + 8\beta)s^4 + (42 + 32\beta + \alpha)s^3 \\ & + (47 + 46\beta - 4\alpha)s^2 + (19 + 46\beta + \alpha)s + 17\beta + 2\alpha \end{aligned} \tag{3.27}$$

Using the Routh-Hurwitz criterion to determine the stabilizing values for α and β, one can see that the following inequalities must hold.

$$
\begin{cases}
8+\beta>0 \\
\\
8\beta^2+68\beta-\alpha+222>0 \\
\\
210\beta^3+175\beta^2+12\beta^2\alpha+6651\beta+101\beta\alpha-\alpha^2+444\alpha-6468>0 \\
\\
(6852\beta^5+(111208-336\alpha)\beta^4+(670097-4933\alpha-48\alpha^2)\beta^3+(1380558-21446\alpha- \\
832\alpha^2)\beta^2+(-2611461+13818\alpha-5420\alpha^2+4\alpha^3)\beta+32\alpha^3-14712\alpha^2+359520\alpha- \\
3245472)>0 \\
\\
(1655352\beta^8+(40973724-250704\alpha)\beta^7+(4386511378-31392\alpha^2-6470823\alpha)\beta^6+ \\
(2523875448-773838\alpha^2-576\alpha^3-69801312\alpha)\beta^5+(7481585892-382258482\alpha- \\
8457189\alpha^2-8676\alpha^3)\beta^4+(6781242090-886670883\alpha-51534270\alpha^2-59583\alpha^3+ \\
120\alpha^4)\beta^3+(-20150281620+548874960\alpha-172578204\alpha^2-324222\alpha^3+1755\alpha^4)\beta^2+ \\
(-50509542114+5713694541\alpha-266724597\alpha^2-1444566\alpha^3+10272\alpha^4-6\alpha^5)\beta- \\
48\alpha^5+31320\alpha^4-4689096\alpha^3+60051600\alpha^2+603684576\alpha-3689400896)>0 \\
\\
17\beta+2\alpha>0
\end{cases}
$$

It is clear that, these inequalities are nonlinear and there is not a straightforward method for their solution.

Now, to see how the generalized Hermite-Biehler theorem can be used to determine the values of α and β for them $\delta(s,\alpha,\beta)$ of Eq.(3.27) is Hurwitz stable. From Eq.(3.15)

$$N^*(s)=-s^3-4s^2-s+2 \tag{3.28}$$

and multiplying $\delta(s,\alpha,\beta)$ by $N^*(s)$, one gets

$$
\begin{aligned}
&\delta(j\omega,\alpha,\beta)N^*(j\omega)=p(\omega,\alpha,\beta)+jq(\omega,\beta)= \\
&\quad[-(12+\beta)\omega^8+(183+65\beta+\alpha)\omega^6+(-183-246\beta+14\alpha)\omega^4-(75-22\beta-17\alpha)\omega^2
\end{aligned}
$$

$$+4\alpha + 34\beta] + j\omega[-\omega^8 + (65 + 12\beta)\omega^6 - (232 + 180\beta)\omega^4 + (39 + 91\beta)\omega^2 + 38 + 75\beta] \tag{3.29}$$

Since the signature of $N^*(s)$ is equal to 1 and the order of $\delta(s, \alpha, \beta)$ is equal to 6, $\delta(s, \alpha, \beta)$ is Hurwitz stable if and only if the signature of $\delta(s, \alpha, \beta)N^*(s)$ is equal to 7. From theorem 3.2 this implies that $q(\omega, \beta)$ must have at least 4 positive real roots. Since $q(\omega, \beta)$ has one root at the origin,

$$q_s(\omega, \beta) = \frac{q(\omega, \beta)}{\omega} = -\omega^8 + (65 + 12\beta)\omega^6 - (232 + 180\beta)\omega^4 + (39 + 91\beta)\omega^2 + 75\beta + 38 \tag{3.30}$$

must have at least three positive real roots. From Eq.(3.21), the distribution of the positive real roots of $q_s(\omega, \beta)$ was calculated as

$$\beta \in (-\infty, -0.5067) : 2 \; positive \; real \; root$$

$$\beta \in (-0.5067, \infty) : 3 \; positive \; real \; root$$

Thus the only possible region for stabilization is $\beta \in (-0.5067, \infty)$. For a fixed value of β such as $\beta^* \in (-0.5067, \infty)$, from theorem 3.2, since $(-1)^{m-1} sqn[q(\infty)] = 1$, for stability the following inequalities must hold

$$p(0, \alpha, \beta^*) > 0, \;\; p(\omega_1, \alpha, \beta^*) < 0, \;\; p(\omega_2, \alpha, \beta^*) > 0, \;\; p(\omega_3, \alpha, \beta^*) < 0 \tag{3.31}$$

where ω_1, ω_2 and ω_3 are the positive real roots of $q_s(\omega, \beta^*)$. For example, when $\beta^* = 0 \in (-0.5067, \infty)$, the positive real roots of $q_s(\omega, 0)$ are

$$\omega_1 = 0.7416, \;\; \omega_2 = 1.8834 \;\; and \;\; \omega_3 = 7.8244$$

Using inequalities of Eq.(3.31), it was computed for $\beta^* = 0$ and $\alpha \in (0, 3.7890)$, $\delta(s, \beta, \alpha)$ is Hurwitz stable. It was found that for all values of β within $(-0.5067, \infty)$ there are stabilizing values of α. For example, all the stabilizing values of α and β for $\beta \in [-0.5, 200]$ are shown in Figure 3.1.

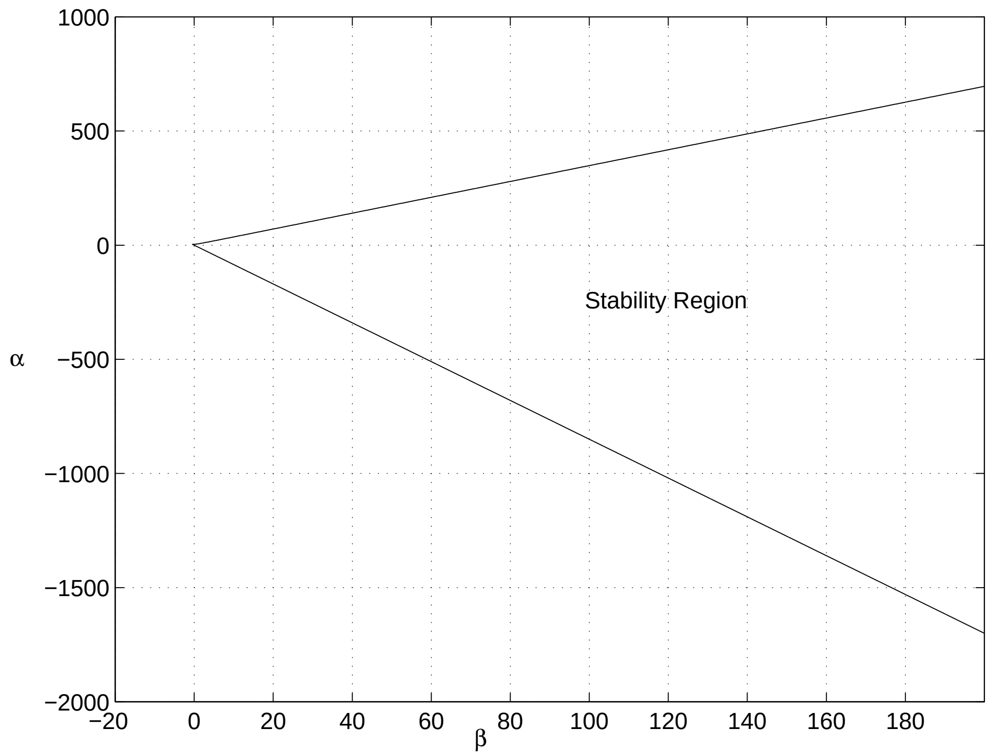

Figure 3.1: Stabilizing values of (α, β) for $K = 1$

Example 3.2

Consider the $C(s)$ and $G(s)$ of a unity feedback system as

$$C(s) = K\frac{s+\alpha}{s+\beta} \ \ and \ \ G(s) = \frac{3s+15}{s^3+3s^2+3s+5} \tag{3.32}$$

The characteristic equation is

$$\delta(s, K, \alpha, \beta) = s^4+(3+\beta)s^3+(3+3K+3\beta)s^2+(5+15K+3K\alpha+3\beta)s+5\beta+15K\alpha \tag{3.33}$$

From Eq.(3.15)

$$N^*(s) = 5 - s \tag{3.34}$$

and multiplying $\delta(j\omega, K, \alpha, \beta)$ by $N^*(j\omega)$, one gets

$$\delta(j\omega, K, \alpha, \beta)N^*(j\omega) = p(\omega, K, \alpha, \beta) + jq(\omega, K, \beta) = [(2-\beta)\omega^4 - (10+12\beta-3K\alpha)\omega^2 \\ +25\beta + 75K\alpha] + j\omega[-\omega^4 - (12-3K+2\beta)\omega^2 + 25 + 10\beta + 75K] \tag{3.35}$$

The signature of $N^*(s)$ is -1 and the order of $\delta(s, K, \alpha, \beta)$ is 4. Therefore, the $\delta(s, K, \alpha, \beta)$ is Hurwitz stable if and only if the signature of $\delta(s, K, \alpha, \beta)N^*(s)$ is equal to 3. Thus, from theorem 3.2,

$$q_s(\omega, K, \beta) = \frac{q(\omega, K, \beta)}{\omega} = -\omega^4 - (12 - 3K + 2\beta)\omega^2 + 25 + 10\beta + 75K \tag{3.36}$$

must have at least 1 positive real root. For example, for $K = 1$, $q_s(\omega, K, \beta)$ has 1 positive simple real root when $\beta \in (-10, \infty)$. Using theorem 3.2, for $K = 1$ and a value of $\beta \in (-10, \infty)$, since $(-1)^{m-1} sgn[q(\infty, K, \beta)] = 1$, for stability the following inequalities must be satisfied

$$25\beta + 75K\alpha > 0\ , \ \ (2 - \beta)\omega_1^4 - (10 + 12\beta - 3K\alpha)\omega_1^2 + 25\beta + 75K\alpha < 0$$

where ω_1 is the positive real root of $q_s(\omega, K, \beta)$. The stabilizing values of controller parameters for $K = 1$ and $\beta \in [1, 200]$ are shown in Figure 3.2. Figure 3.3 shows all the stabilizing values of the controller parameters when $K \in [1, 10]$ and $\beta \in [1, 200]$.

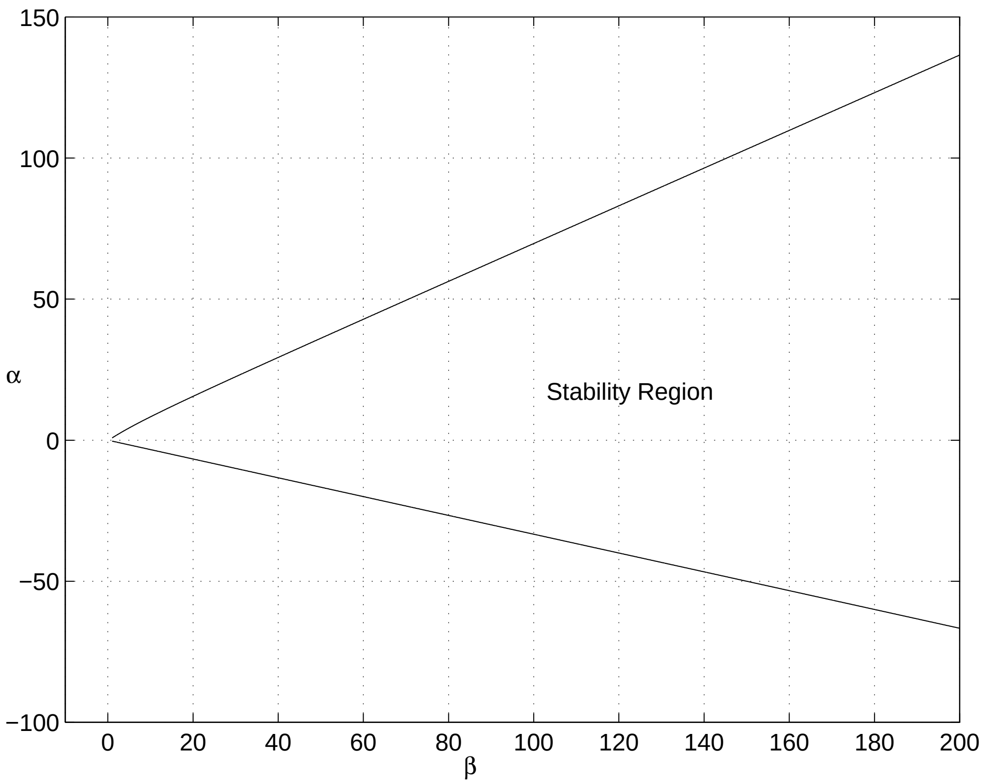

Figure 3.2: Stabilizing values of (α, β) for $K = 1$

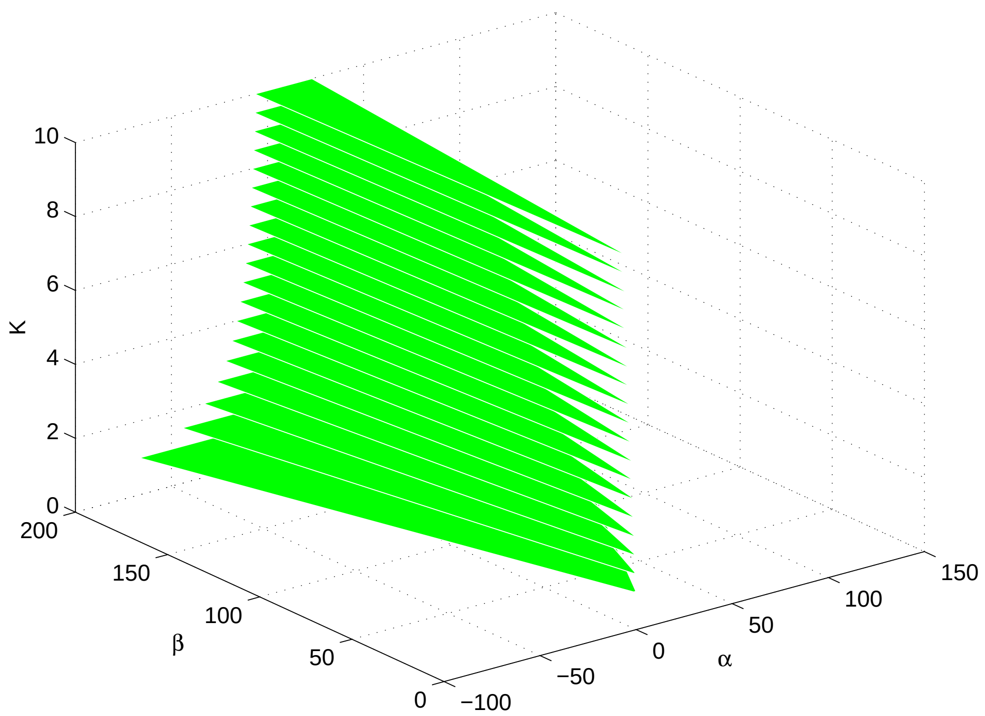

Figure 3.3: Stabilizing values of (α, β) for $K \in [1, 10]$

3.4 Relative stabilization

In this section, the stabilization of a given plant using the controllers defined as

$$C_1(s) = \frac{K_p s + K_p \rho + K_i}{s + \rho} \tag{3.37}$$

$$C_2(s) = \frac{K s + K \rho + K \alpha}{s + \rho + \beta} \tag{3.38}$$

$$C_3(s) = \frac{K_d s^2 + (2K_d \rho + K_p)s + \rho(K_d \rho + K_p) + K_i}{s + \rho} \tag{3.39}$$

where ρ is a known constant and K, α, β, K_p, K_i and K_d are unknown parameters is studied. In order to explain the aim of defining these controller structures, consider a PI controller and a plant as

$$C(s) = \frac{K_p s + K_i}{s}, \quad G(s) = \frac{N(s)}{D(s)} \tag{3.40}$$

To find all values of K_p and K_i which put all closed loop poles to the left of $s = \rho$ ($\rho = constant$), with $\widehat{C}(s)$ and $\widehat{G}(s)$ for $C(s)$ and $G(s)$ with $s = s + \rho$, then

$$\widehat{C}(s) = C(s+\rho) = \frac{K_p s + K_p \rho + K_i}{s+\rho}, \quad \widehat{G}(s) = G(s+\rho) = \frac{N(s+\rho)}{D(s+\rho)}$$

Now, if the characteristic equation, $\delta(s) = 1 + \widehat{C}(s)\widehat{G}(s) = 0$, is Hurwitz stable then one can be sure that all the closed loop poles of the system are to the left of $s = \rho$. Also, it is clear that $C_1(s)$ is exactly equal to the structure of $\widehat{C}(s)$. Similarly, it can be seen that for a *Lag/Lead* controller of the form $C(s) = K(s+\alpha)/(s+\beta)$ the structure of $C_2(s)$ and for a *PID* controller the structure of $C_3(s)$ can be obtained.

a) If the controller structure is in the form of $C_1(s)$ then the characteristic equation can be written as

$$\begin{aligned}&\delta(s, K_p, K_i) = 1 + C_1(s)G(s) = 0 = [\rho D_e(s^2) + (K_p\rho + K_i)N_e(s^2) + \\ &s^2(K_p N_o(s^2) + D_o(s^2))] + s[K_p N_e(s^2) + (K_p\rho + K_i)N_o(s^2) + D_e(s^2) + \rho D_o(s^2)]\end{aligned} \tag{3.41}$$

By multiplying the characteristic equation with $N^*(s)$ which is defined in Eq.(3.15) and putting $s = j\omega$, one gets

$$\begin{aligned}&\delta(j\omega, K_p, K_i)N^*(j\omega) = p(\omega, K_p, K_i) + jq(\omega, K_p) = [(K_p\rho + K_i)(N_e(-\omega^2)N_e'(-\omega^2) + \\ &\omega^2 N_o(-\omega^2)N_o'(-\omega^2) + \rho D_e(-\omega^2)N_e'(-\omega^2) + \omega^2(D_e(-\omega^2)N_o'(-\omega^2) + \rho D_o(-\omega^2)N_o'(-\omega^2) \\ &-D_o(-\omega^2)N_e'(-\omega^2)] + j\omega[K_p(N_e(-\omega^2)N_e'(-\omega^2) + \omega^2 N_o(-\omega^2)N_o'(-\omega^2)) + D_e(-\omega^2) \\ &N_e'(-\omega^2) + (D_o(-\omega^2)N_e'(-\omega^2) - D_e(-\omega^2)N_o'(-\omega^2)) + \omega^2 D_o(-\omega^2)N_o'(-\omega^2)]\end{aligned} \tag{3.42}$$

It is clear that for every fixed K_p value, the roots of $q(\omega, K_p)$ do not depend on K_i. Thus, sweeping over K_p values and using Eq.(3.19) and the results of Section 3.3, the set of all stabilizing (K_p, K_i) values for which the given plant is Hurwitz stable can be calculated. The range of K_p values over which the sweeping needs to be done can be reduced by using the root locus as explained in Section 3.3.

b) For $C_2(s)$, the characteristic equation of the system can be written as

$$\delta(s, K, \alpha, \beta) = 1 + C_2(s)G(s) = 0 = [(\rho+\beta)D_e(s^2) + K(\rho+\alpha)N_e(s^2) + s^2(D_o(s^2)$$

$$+KN_o(s^2)) + s[D_e(s^2) + (\rho+\beta)D_o(s^2) + KN_e(s^2) + K(\rho+\alpha)N_o(s^2)] \tag{3.43}$$

Multiplying $\delta(j\omega, K, \alpha, \beta)$ with $N^*(j\omega)$

$$\delta(j\omega, K, \alpha, \beta)N^*(j\omega) = p(\omega, K, \alpha, \beta) + jq(\omega, K, \beta) = [(\rho+\beta)(D_e(-\omega^2)N_e'(-\omega^2) + \omega^2$$
$$D_o(-\omega^2)N_o'(-\omega^2)) + K(\rho+\alpha)(N_e(-\omega^2)N_e'(-\omega^2) + \omega^2 N_o(-\omega^2)N_o'(-\omega^2)) - \omega^2(D_o(-\omega^2)$$
$$N_e'(-\omega^2) - D_e(-\omega^2)N_o'(-\omega^2))] + j\omega[K(N_e(-\omega^2)N_e'(-\omega^2) + \omega^2 N_o(-\omega^2)N_o'(-\omega^2)) + (\rho+\beta)$$
$$(D_o(-\omega^2)N_e'(-\omega^2) - D_e(-\omega^2)N_o'(-\omega^2)) + D_e(-\omega^2)N_e'(-\omega^2) + \omega^2 D_o(-\omega^2)N_o'(-\omega^2)] \tag{3.44}$$

Here, $q(\omega, K, \beta)$ depends on two parameters; namely, K and β. Therefore, it has to be assumed that one of the parameters K or β is known. Otherwise, it will be difficult to apply the generalized Hermite-Biehler theorem. For example, say that K is known then the range of β values over which sweeping needs to be done can be found by using the root locus. Thus, for every fixed K sweeping over the values of β or for every fixed β sweeping over the values of K and using the Hermite-Biehler theorem, all the stabilizing values of (K, α, β) can be calculated.

c) Let the controller be $C_3(s)$ then the characteristic equation of the system is

$$\delta(s, K_p, K_i, K_d) = 1 + C_3(s)G(s) = 0 = [\rho D_e(s^2) + s^2(D_o(s^2 + K_d N_e(s^2) + (2K_d\rho$$
$$+K_p)N_o(s^2)) + (\rho(K_d\rho + K_p) + K_i)N_e(s^2)] + s[D_e(s^2) + \rho D_o(s^2) + (2K_d\rho + K_p)$$
$$N_e(s^2) + (\rho(K_d\rho + K_p) + K_i)N_o(s^2) + s^2 K_d N_o(s^2)] \tag{3.45}$$

multiplying Eq.(3.45) with $N^*(s)$ and substituting $s = j\omega$

$$\delta(j\omega, K_p, K_i, K_d)N^*(j\omega) = p(\omega, K_p, K_i, K_d) + jq(\omega, K_p, K_d) = [\rho D_e(-\omega^2)N_e'(-\omega^2)$$
$$+\omega^2(D_e(-\omega^2)N_o'(-\omega^2) + \rho D_o(-\omega^2)N_o'(-\omega^2) - D_o(-\omega^2)N_o'(-\omega^2)) + K_d(-\omega^2 N_e(-\omega^2)$$
$$N_e'(-\omega^2) - \omega^4 N_o(-\omega^2)N_o'(-\omega^2)) + (\rho(K_d\rho + K_p) + K_i)(N_e(-\omega^2)N_e'(-\omega^2) + \omega^2 N_o(-\omega^2)$$
$$N_o'(-\omega^2))] + j\omega[D_e(-\omega^2)N_e'(-\omega^2) + \omega^2 D_o(-\omega^2)N_o'(-\omega^2) + \rho(D_o(-\omega^2)N_e'(-\omega^2)$$
$$-D_e(-\omega^2)N_o'(-\omega^2)) + (2K_d\rho + K_p)(N_e(-\omega^2)N_e'(-\omega^2) + \omega^2 N_o(-\omega^2)N_o'(-\omega^2))]$$
$$\tag{3.46}$$

It is seen that similar to $C_2(s)$ the $q(\omega, K_p, K_d)$ depends on the parameters K_p and K_d. For a fixed value of K_p or K_d, sweeping over values of the nonfixed parameter all the stabilizing values of (K_p, K_i, K_d), if there are any, can be determined.

Example 3.3

Consider a PID controller and a plant as

$$C(s) = \frac{K_d s^2 + K_p s + K_i}{s} \quad and \quad G(s) = \frac{N(s)}{D(s)} = \frac{s+1}{s^3 + s^2 + s + 1} \tag{3.47}$$

The objective is to find the parameters of the given controller for relative stabilization. At first, assume that $\rho = 0$. Then, the characteristic equation is

$$\delta(s, K_p, K_i, K_p) = s^4 + (1 + K_d)s^3 + (1 + K_p + K_d)s^2 + (1 + K_p + K_i)s + K_i \tag{3.48}$$

From eq.(3.15)

$$N^*(s) = 1 - s \tag{3.49}$$

multiplying the characteristic equation with $N^*(j\omega)$, one gets

$$\begin{aligned} \delta(j\omega, K_p, K_i, K_d)N^*(j\omega) = p(\omega, K_p, K_i, K_d) + jq(\omega, K_p) = \\ [-K_d\omega^4 - (K_d - K_i)\omega^2 + K_i] + j\omega[-\omega^4 + K_p\omega^2 + K_p + 1] \end{aligned} \tag{3.50}$$

It can be seen that for every fixed K_p, the zeros of $q(\omega, K_p)$ do not depend on K_i and K_d. Thus, by sweeping over all real K_p values, one can determine the set of all stabilizing (K_p, K_i, K_d) values. The range of K_p values over which the sweeping needs to be done can be reduced using the root locus. Since the signature of $N^*(s)$ is equal to -1 and the order of $\delta(s, K_p, K_i, K_d)$ is equal to 4, from Eq.(3.19) $\delta(s, K_p, K_i, K_d)$ is Hurwitz stable if and only if the signature of $\delta(s, K_p, K_i, K_d)N^*(s)$ is equal to 3. Since $q(\omega, K_p)$ has one root at the origin, in order to make the signature of $\delta(s, K_p, K_i, K_d)N^*(s)$ equal to 3, from theorem 3.2

$$q_s(\omega, K_p) = \frac{q(\omega, K_p)}{\omega} = -\omega^4 + K_p\omega^2 + K_p + 1 \tag{3.51}$$

must have at least one positive real root. Using the root locus, the distribution of the positive real roots of $q_s(\omega, K_p)$ was calculated as

$$K_p \in (-1, \infty) : \; 1 \, positive \; real \; root$$

$$K_p \in (-\infty, -1) : \; no \; positive \; real \; root$$

Thus, the only possible interval of K_p for stabilization is $K_p \in (-1, \infty)$. For example, for $K_p = 18 \in (-1, \infty)$, from theorem 3.2, for stability the following inequality must hold

$$0 < K_i < 19K_d \tag{3.52}$$

From this inequality it can be seen that for all $K_d \in (0, \infty)$ there are stabilizing values for K_i. Taking an upper value for K_d such as $K_d \in (0, 100]$, the set of all stabilizing values of (K_i, K_d) was computed and is shown in Figure 3.4.

Now, for the same $K_p = 18$, let us find all the stabilizing values of K_d and K_i for $\rho = -0.3$. Substituting $s - 0.3$ instead of s, one gets

$$\widehat{C}(s) = C(s - 0.3) = \frac{K_d s^2 + (18 - 0.6K_d)s + 0.09K_d + K_i - 5.4}{s - 0.3} \tag{3.53}$$

and

$$\widehat{G}(s) = G(s - 0.3) = \frac{s + 0.7}{s^3 + 0.1s^2 + 0.67s + 0.763} \tag{3.54}$$

The characteristic equation is

$$\begin{aligned} \delta(j\omega, K_d, K_i) &= 1 + \widehat{C}(j\omega)\widehat{G}(j\omega) = 0 = p(\omega, K_d, K_i) + jq(\omega, K_d, K_i) = \\ &\omega^4 - (18.64 + 0.1K_d)\omega^2 + 0.063K_d + 0.7K_i - 4.0089 \\ &+ j\omega(-(K_d - 0.2)\omega^2 + (7.762 - 0.33K_d + K_i)\omega) \end{aligned} \tag{3.55}$$

Multiplying $\delta(j\omega, K_d, Ki)$ of Eq.(3.55) with $N^*(j\omega) = 0.7 - j\omega$, it becomes

$$\begin{aligned} &\delta(j\omega, K_d, K_i)N^*(j\omega) = p(\omega, K_d, K_i) + jq(\omega, K_d) = \\ &((0.9 - K_d)\omega^4 - (5.328 + 0.4K_d - K_i)\omega^2 + 0.0441K_d + 0.49K_i - 2.80613) \\ &+ j\omega(-\omega^4 - (-18.78 + 0.6K_d)\omega^2 + 9.4129 - 0.294K_d) \end{aligned} \tag{3.56}$$

It can be seen that for Hurwitz stability of Eq.(3.56), the signature of Eq.(3.56) must be equal to 3. This implies that

$$q_s(\omega, K_d) = \frac{q(\omega, K_d)}{\omega} = -\omega^4 - (-18.78 + 0.6K_d)\omega^2 + 9.4129 - 0.294K_d \tag{3.57}$$

must have at least one positive real root. It was found that

$$K_d \in (-\infty, 32) : \ 1 \, positive \ real \ root$$

$$K_p \in (32, \infty) : \ no \ positive \ real \ root$$

So, the only possible interval for stability is $K_d \in (-\infty, 32)$. Sweeping over K_d values within this interval all stabilizing values of K_d and K_i which put the poles of the characteristic equation to the left of $\rho = -0.3$ were computed and sketched in Figure 3.5. Figure 3.6 shows the stabilizing values for different ρ values.

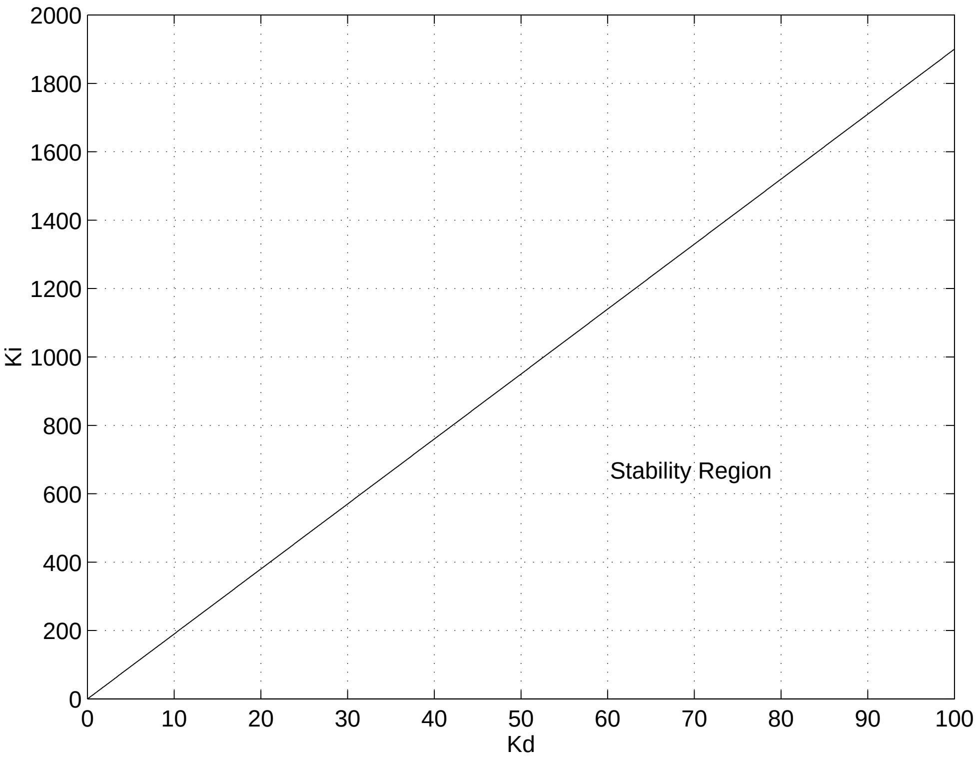

Figure 3.4: All the stabilizing values of (K_d, K_i) for $K_p = 18$ and $\rho = 0$

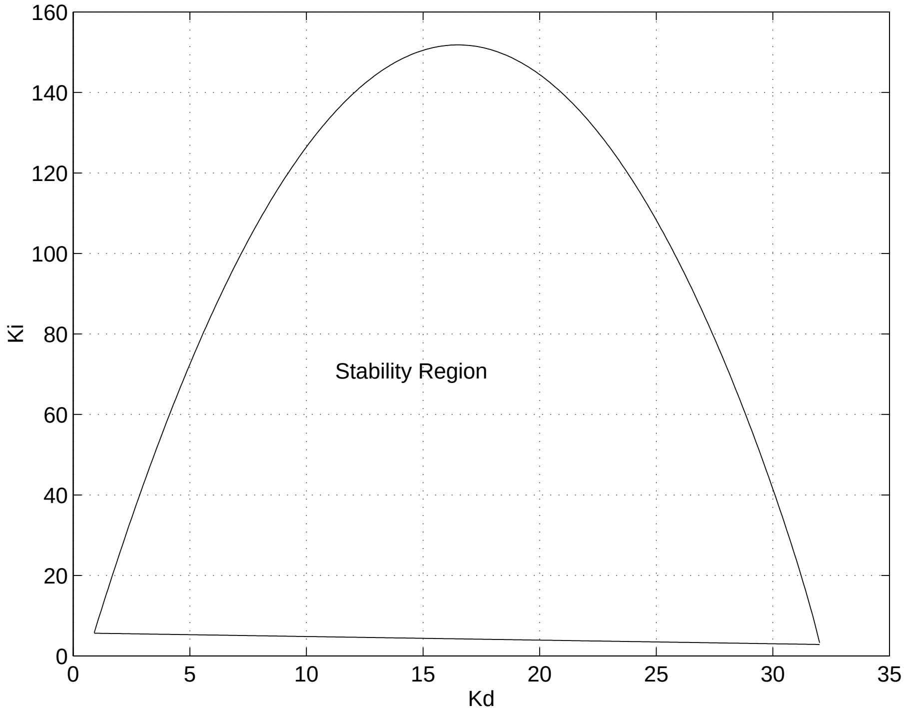

Figure 3.5: All the stabilizing values of (K_d, K_i) for $\rho = -0.3$ and $K_p = 18$

Example 3.4

Consider a PID controller and a plant as

$$C(s) = K_p + \frac{K_i}{s} - 0.3s \quad and \quad G(s) = \frac{1}{s+5}(\frac{1-0.5s}{1+0.5s}) \tag{3.58}$$

where $G(s)$ is a simple Pade approximation for a plant with transfer function $e^{-s}/(s+5)$. It is required to find all the values of (K_p, K_i) which put the poles of the characteristic equation of the system to the left of the line $s = -1 + j\omega$. Substituting $s - 1$ instead of s, one gets

$$\widehat{C}(s)=C(s-1)=\frac{-0.3s^2 + (K_p + 0.6)s - 0.3 - K_p + K_i}{s-1} \quad and \quad \widehat{G}(s)=\frac{-0.5s + 1.5}{0.5s^2 + 2.5s + 2} \tag{3.59}$$

The characteristic equation is

$$\delta(j\omega, K_p, K_i) = 1 + \widehat{C}(j\omega)\widehat{G}(j\omega) = p(\omega, K_p, K_i) + jq(\omega, K_p, K_i) =$$
$$(1.25 - 2.5K_p)\omega^2 - 2.45 - 1.5K_p + 1.5K_i + j\omega(-0.65\omega^2 + 0.55 + 2K_p - 0.5K_i) \tag{3.60}$$

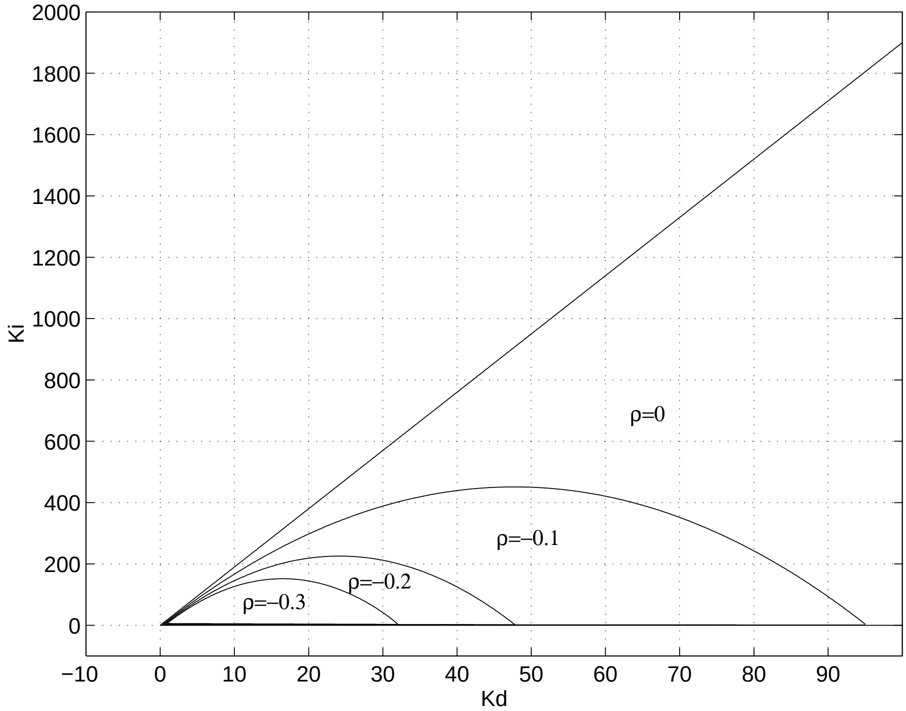

Figure 3.6: All the stabilizing values of (K_d, K_i) for $\rho = 0, -0.1, -0.2, -0.3$ and $K_p = 18$

Multiplying $\delta(j\omega, K_p, Ki)$ with $N^*(j\omega) = 3 + j\omega$, it becomes

$$\delta(j\omega, K_p, K_i)N^*(j\omega) = p(\omega, K_p, K_i) + jq(\omega, K_p) =$$
$$0.65\omega^4 - (4.3 + 0.5K_p - 0.5K_i)\omega^2 - 7.35 - 4.5K_p + 4.5K_i + j\omega(-(3.2 - 0.5K_p)\omega^2 - 0.8 + 4.5K_p) \tag{3.61}$$

From

$$q_s(\omega, K_p) = \frac{q(\omega, K_p)}{\omega} = -(3.2 - 0.5K_p)\omega^2 - 0.8 + 4.5K_p \tag{3.62}$$

It can be easily seen that for $K_p \in (0.1778, 6.4)$ there is one positive real root of $q_s(\omega, K_p)$. Thus, sweeping over the values of K_p and using results given in previous sections, all the values of K_p and K_i for which Eq.(3.60) is Hurwitz stable were computed and sketched in Figure 3.7.

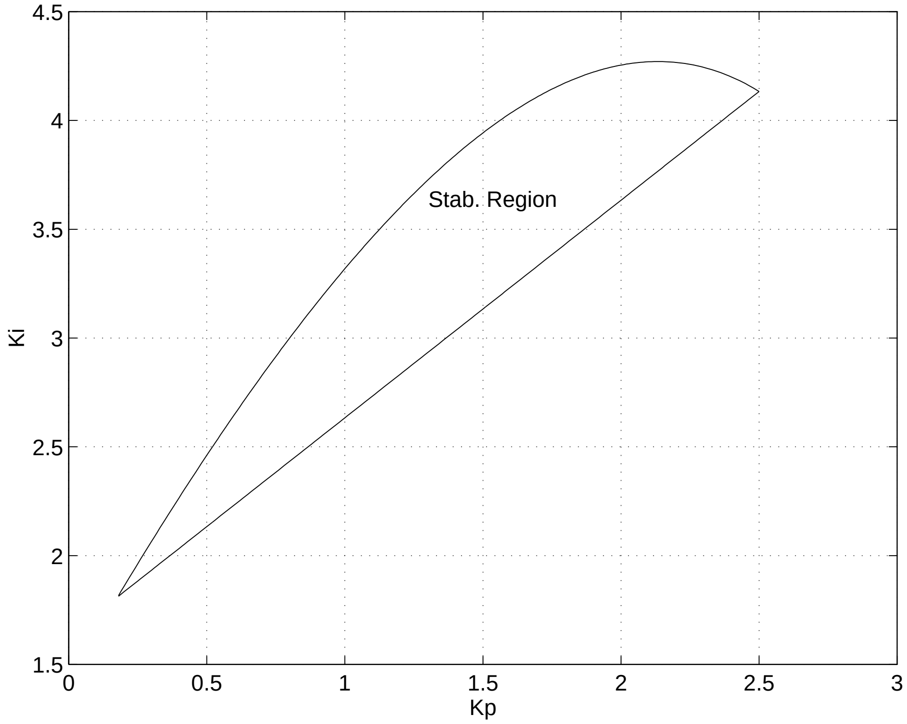

Figure 3.7: All the stabilizing values of (K_p, K_i) for $K_d = -0.3$

3.5 Interval plant stabilization

There are some important results in the literature about stabilization of interval systems. For example, in [65], it was shown that a constant gain controller stabilizes an interval plant family if and only if it stabilizes a set of eight of the extreme plants. In [76], it was shown that a first order controller stabilizes an interval plant if it stabilizes the set of extreme plants. The best results regarding this subject were given in [16, 26] where it was proved that a first order controller stabilizes an interval plant if and only if it simultaneously stabilizes the sixteen Kharitonov plant family which was introduced in Chapter 2. In this section, instead of using Routh tables, which were used in [16] in order to characterize all the parameters of a first order controller which stabilize an interval plant, the Hermite-Biehler theorem is used to find all the values of the parameters of a first order controller for which the given interval plant is Hurwitz stable.

Define the set $S(C(s)G(s))$ which contains all the values of the parameters of the controller $C(s)$ which stabilize $G(s)$, then the set of all the stabilizing values of parameters of a first order controller which stabilize the interval plant of Eq.(2.27) can be written as

$$S(C(s)G(s,\mathbf{q},\mathbf{r})) = S(C(s)G_K(s)) = S(C(s)G_{11}(s)) \cap S(C(s)G_{12}(s)) \cap ...... \cap S(C(s)G_{44}(s)) \tag{3.63}$$

where $G_K(s)$ represents the sixteen Kharitonov plant family which is given in Chapter 2 via Eq.(2.30). Now, let the controller be

$$C(s) = K \tag{3.64}$$

By using the even and odd parts of the numerator and the denominator polynomials, the sixteen Kharitonov plant family can be written as

$$G_K(s) = G_{ij}(s) = \frac{N_{ie}(s^2) + sN_{io}(s^2)}{D_{je}(s^2) + sD_{jo}(s^2)} \quad where \ i,j = 1,2,3,4 \tag{3.65}$$

For the constant gain controller of Eq.(3.64), the characteristic equation of the system is

$$\delta_{ij}(s,K) = [KN_{ie}(s^2) + D_{je}(s^2)] + s[KN_{io}(s^2) + D_{jo}(s^2)] \tag{3.66}$$

For $s = j\omega$, multiplying the characteristic equation with $N_i^*(s)$ gives

$$\begin{gathered}\delta_{ij}(j\omega,K)N_i^*(j\omega) = p_{ij}(\omega,K) + jq_{ij}(\omega) = [N_{ie}'(-\omega^2)(KN_{ie}(-\omega^2) + D_{je}(-\omega^2)) + \\ \omega^2 N_{io}'(-\omega^2)(KN_{io}(-\omega^2) + D_{jo}(-\omega^2))] + j\omega[N_{ie}'(-\omega^2)D_{jo}(-\omega^2) - N_{io}'(-\omega^2)D_{je}(-\omega^2)]\end{gathered} \tag{3.67}$$

Now, let the degree of $\delta_{ij}(s,K)$ be n then $\delta_{ij}(s,K)$ is Hurwitz stable if and only if $\sigma(\delta_{ij}(j\omega,K)) = n$. Thus, the given interval system is Hurwitz stable if and only if

$$\sigma(\delta_{ij}(s,K)N_i^*(s)) = n + \sigma(N_i^*(s)) = n - \sigma(N_i'(s)) \tag{3.68}$$

is satisfied for all $i,j = 1,2,3,4$.

From Eq.(3.67), for each Kharitonov plant, it is seen that using the positive real roots of $q_{ij}(\omega)$ and applying theorem 3.2 or lemma 3.1, all the stabilizing values of K can be calculated. Similarly, the related equations for PI and $Lag/Lead$ controllers can be obtained.

Example 3.5

Consider the interval plant given in [16]

$$G(s, \mathbf{q}, \mathbf{r}) = \frac{[54, 74]s + [90, 166]}{s^4 + [2.8, 4.6]s^3 + [50.4, 80.8]s^2 + [30.1, 33.9]s + [-0.1, 0.1]} \tag{3.69}$$

The objective is to calculate all the parameters of a PI controller

$$C(s) = K_p + \frac{K_i}{s} \tag{3.70}$$

which stabilize $G(s, \mathbf{q}, \mathbf{r})$. To find if stabilizing gains K_p and K_i exist, one possible approach would be as follows: First, construct sixteen Routh tables (one for each Kharitonov plant with controller $C(s)$ of Eq.(3.70)). Then, from the positivity requirement of the first column of these tables for stability, obtain sets of inequalities. Finally, compute the intersection of these sets of inequalities. For example, consider the first Kharitonov plant ($i = 1$ *and* $j = 1$). From Eq.(2.30), one of the Kharitonov plants is

$$G(s) = G_{11}(s) = \frac{54s + 90}{s^4 + 4.6s^3 + 80.8s^2 + 30.1s - 0.1} \tag{3.71}$$

The characteristic equation is

$$\delta_{11}(s, K_p, K_i) = 1 + C(s)G_{11}(s) = s^5 + 4.6s^4 + 80.8s^3 + a_1 s^2 + a_2 s + a_3 \tag{3.72}$$

where $a_1 = 30.1 + 54K_p, a_2 = -0.1 + 90K_p + 54K_i$ and $a_3 = 90K_i$. In order to find all the stabilizing values of (K_p, K_i) by using the Routh table, one needs to solve the following inequalities:

$$\begin{gathered} 371.8 - a_1 > 0\ ,\ a_3 > 0\ ,\ a_1(371.68 - a_1) - 4.6(4.6a_2 - a_3) > 0 \\ a_1(371.68 - a_1)(4.6a_2 - a_3) - 4.6(4.6a_2 - a_3)^2 - a_3(371.68 - a_1)^2 > 0 \end{gathered} \tag{3.73}$$

It is clear that solving these inequalities will not be very easy. Now, applying the Hermite

Biehler theorem, from Eq.(3.15),

$$N_1^*(s) = \frac{90 - 54s}{18} = 5 - 3s \tag{3.74}$$

Multiplying $\delta_{11}(j\omega, K_p, K_i)$ with $N_1^*(j\omega)$, one gets

$$\delta_{11}(j\omega, K_p, K_i)N_1^*(j\omega) = p_{11}(\omega, K_i) + jq_{11}(\omega, K_p) =$$
$$3\omega^6 - 219.4\omega^4 - (150.8 - 162K_i)\omega^2 + 450K_i + j\omega(-8.8\omega^4 - (313.9 - 162K_p)\omega^2 - 0.5 + 450K_p)$$

Now, it is seen that $q_{11}(\omega, K_p)$ is dependent only on K_p. Since the signature of $N_1^*(j\omega)$ is equal to -1 and the order of $\delta_{11}(j\omega, K_p, K_i)$ is equal to 5, $\delta_{11}(j\omega, K_p, K_i)$ is Hurwitz stable if and only if the signature of $\delta_{11}(j\omega, K_p, K_i)N_1^*(j\omega)$ is equal to 4. This implies that $q_{11}(\omega, K_p)$ must have at least two positive real roots. Since $q_{11}(\omega, K_p)$ has one root at the origin,

$$q_s(\omega, K_p) = \frac{q_{11}(\omega, K_p)}{\omega} = -8.8\omega^4 - (313.9 - 162K_p)\omega^2 - 0.5 + 450K_p \tag{3.75}$$

must have at least one positive real root. Using the root locus, the distribution of the positive real roots of $q_s(\omega, K_p)$ was calculated as follows

$$K_p \in (0.0011, \infty): \quad 1 \; positive \; real \; root$$

$$K_p \in (-\infty, 0.0011): \quad no \; real \; root$$

Thus, the only possible region for stabilization is $K_p \in (0.0011, \infty)$. Using theorem 3.2, for stability the following inequalities must be satisfied

$$p_{11}(0, K_i) = 450K_i > 0, \;\; p_{11}(\omega_1, K_i) = 3\omega_1^6 - 219.4\omega_1^4 - (150.8 - 162K_i)\omega_1^2 + 450K_i < 0$$

where ω_1 is the positive real root of $q_s(\omega, K_p)$. Sweeping over the values of K_p and using theorem 3.2, the stabilizing values obtained of (K_p, K_i) for $G_{11}(s)$ are shown in Figure 3.8. Figure 3.9 shows the stability regions of the sixteen Kharitonov plants where the intersection of these regions is shown by 'x'. From Eq.(3.63), the region 'x' was computed and sketched in Figure 3.10.

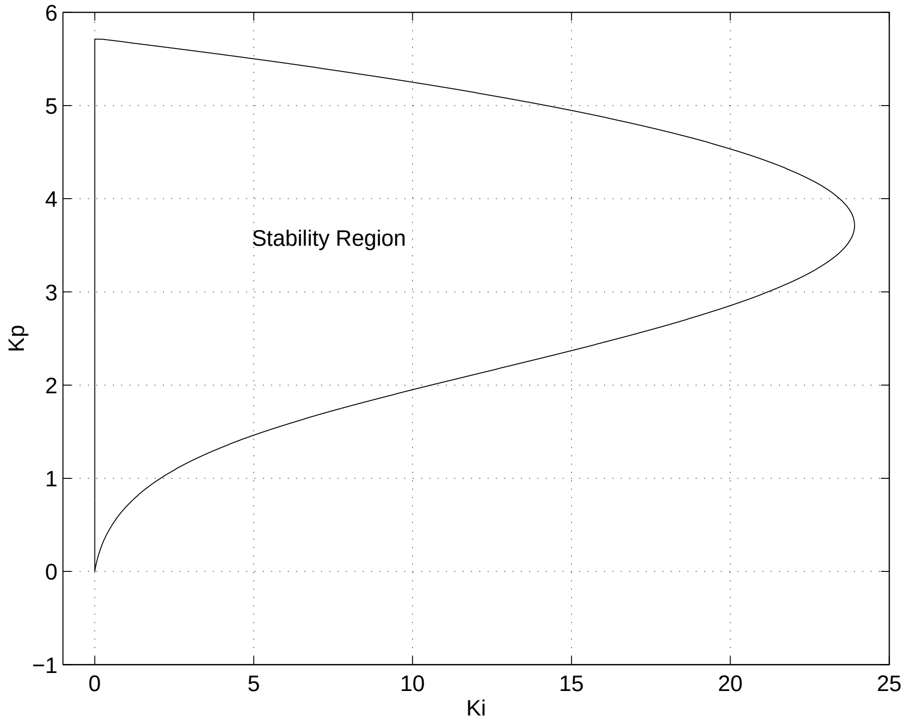

Figure 3.8: All the stabilizing values of (K_p, K_i) for $G_{11}(s)$

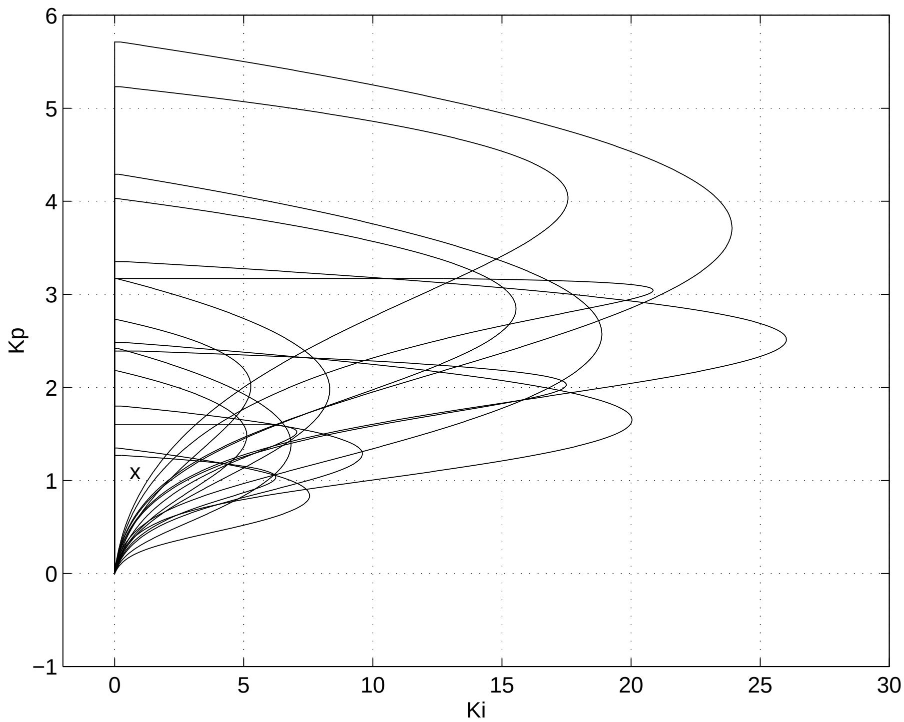

Figure 3.9: Stabilizing values of (K_p, K_i) for 16 Kharitonov plants

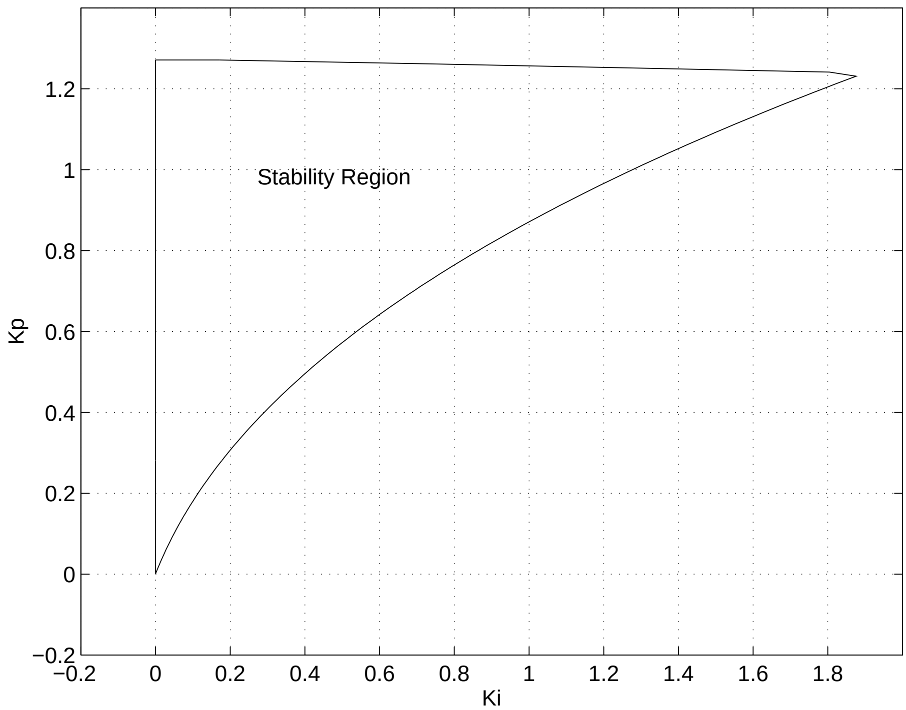

Figure 3.10: All the stabilizing values of (K_p, K_i) for the interval plant

3.6 Conclusion

In this chapter, an extension of a new approach which is based on the Hermite-Biehler theorem to the $Lag/Lead$ controller structure for stabilizing a given plant has been given. The approach was then further developed for PI, $Lag/Lead$ and PID controllers for relative stabilization. In addition, the stabilization of uncertain systems defined by an interval plant structure was also discussed using the sixteen Kharitonov plant family. Since the method is analytical and does not involve solving inequalities which may be nonlinear, it is superior to the existing results.

Chapter 4

A SOFTWARE PACKAGE PROGRAM FOR ANALYSIS OF INTERVAL SYSTEMS

4.1 Introduction

The striking advances in microprocessor design and computer technology have changed the approach to control system design in such a way that computationally demanding techniques no longer present a problem to the control engineer. This fact is obviously one of the main reasons why there have been many developments in the field of robust control since the 1980s. The power of computers enables the control engineer to try ideas easily and rapidly with the aid of specialized computer software. One of the effective software programs, which is widely used in control theory, is known as MATLAB.

MATLAB, standing for MATrix LABoratory, is a high performance interactive software package program. It provides numerical analysis, matrix calculations and graphical facilities. MATLAB allows the user to solve numerical problems using some simple commands rather than writing a program in a language such as Fortran, Basic or C. MATLAB also has various toolboxes such as the control toolbox, H_∞ toolbox, μ-toolbox, optimization toolbox and so on. Toolboxes are comprehensive collections of MATLAB functions (M-files) that extend the MATLAB environment in order to solve particular classes of problems such as control problems. Probably the most important feature of MATLAB is its easy extensibility which allows one to create different toolboxes.

In this chapter, a software package program, called Analysis of Interval Systems ToolKit (AISTK), which has been developed in the MATLAB environment is described. MATLAB has two toolboxes within the context of robust control systems which are the H_∞ toolbox and the μ-toolbox. These toolboxes use the well known H_∞ technique and the structured singular value to address the robustness problem, therefore, they are not helpful for control systems with parametric uncertainty. On the other hand, AISTK is a user friendly toolbox like the control kit and can be successfully used for analysis of interval systems. Although our intention in this chapter is to introduce AISTK, some theoretical results such as a discussion of robust gain and phase margins and the Nyquist envelope of an interval plant using the generalized Hermite-Biehler theorem for interval polynomials, formulation of gain crossover, phase crossover and bandwidth frequencies of interval plants etc. are also given.

The chapter is organized as follows: In section 4.2, the generalized Hermite-Biehler theorem for real and complex interval polynomials is given. Section 4.3 discusses the frequency response of interval systems. In this section, using the generalized version of the Hermite-Biehler theorem for interval polynomials, the robust gain and phase margins and the outer boundary of the Nyquist envelope of an interval plant are discussed. The section also gives procedures for computing the gain crossover, phase crossover and bandwidth frequencies of an interval transfer function. The problem of finding the maximum allowable perturbation bounds of parameters of a linear system while preserving stability is discussed in Section 4.4. The description of the software package program, AISTK, is given in Section 4.5. Some concluding remarks are given in the final section.

4.2 The Generalized Hermite-Biehler Theorem for Real and Complex Interval Polynomials

In Chapter 3, the classical Hermite-Biehler theorem and its generalized form for controller design were introduced. In this section, the generalized form of the Hermite-Biehler theorem for real and complex interval polynomials is given.

a) The Hermite-Biehler theorem for real interval polynomials [4]: Let the polynomial

$$P(s,\mathbf{q}) = q_0 + q_1 s + q_2 s^2 + q_3 s^3 + \dots\dots\dots + q_n s^n \tag{4.1}$$

be an nth order, real interval polynomial where the coefficients vary as $q_i \in [\underline{q_i}, \overline{q_i}], i = 0, 1, 2, ..., n$. Substituting $s = j\omega$ and $\mu = \omega^2$, one gets

$$P(\mu,\mathbf{q}) = R(\mu) + j\omega Q(\mu) \tag{4.2}$$

where

$$\begin{aligned} maxR(\mu) &= \overline{q_0} - \underline{q_2}\mu + \overline{q_4}\mu^2 - \underline{q_6}\mu^3 + \dots\dots\dots \\ minR(\mu) &= \underline{q_0} - \overline{q_2}\mu + \underline{q_4}\mu^2 - \overline{q_6}\mu^3 + \dots\dots\dots \\ maxQ(\mu) &= \overline{q_1} - \underline{q_3}\mu + \overline{q_5}\mu^2 - \underline{q_7}\mu^3 + \dots\dots\dots \\ minQ(\mu) &= \underline{q_1} - \overline{q_3}\mu + \underline{q_5}\mu^2 - \overline{q_7}\mu^3 + \dots\dots\dots \end{aligned} \tag{4.3}$$

Let the roots of $maxR(\mu) = 0$ and $minR(\mu) = 0$ be ω_{maxr1}, ω_{maxr2},...... and ω_{minr1}, ω_{minr2},......, respectively. Similarly, let the roots of $maxQ(\mu) = 0$ and $minQ(\mu) = 0$ be ω_{maxq1}, ω_{maxq2},...... and ω_{minq1}, ω_{minq2},......, respectively. Then the stability of the interval polynomials $P(s,\mathbf{q})$ can be stated as follows: The real interval polynomial $P(s,\mathbf{q})$ of Eq.(4.1) is strictly robust Hurwitz if and only if the frequency bands $[\omega_{minr1}, \omega_{maxr1}]$,

$[\omega_{minq1}, \omega_{maxq1}]$, $[\omega_{minr2}, \omega_{maxr2}]$, $[\omega_{minq2}, \omega_{maxq2}]$...... are simple, real, positive, interlacing and do not overlap. A graphical illustration of this interlacing property is shown in Figure 4.1.

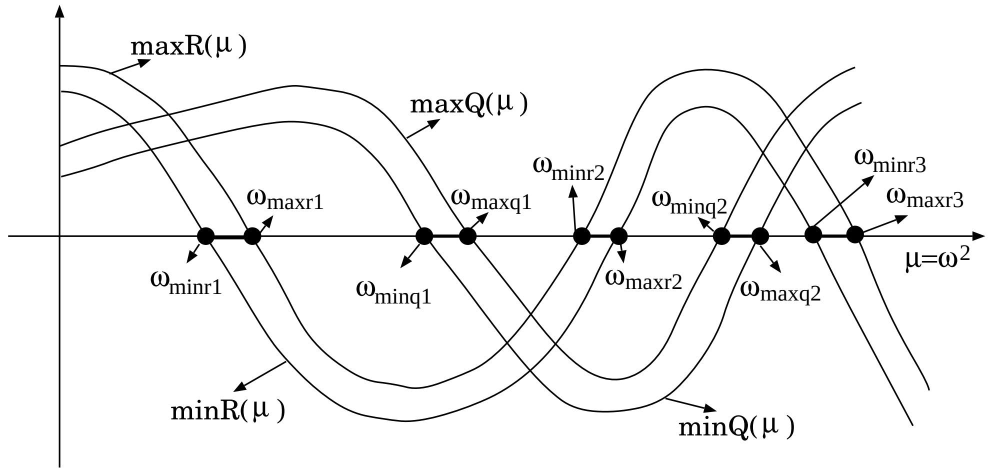

Figure 4.1: Interlacing property of an interval polynomial

b) The Hermite-Biehler theorem for complex interval polynomials [85]: Let the polynomial of Eq.(4.1) be a complex interval polynomial with

$$q_i = a_i + jb_i, \; i = 0, 1, 2, ..., n \tag{4.4}$$

where

$$a_i \in [\underline{a_i}, \overline{a_i}], \; b_i \in [\underline{b_i}, \overline{b_i}], \; i = 0, 1, 2, ..., n \tag{4.5}$$

In this case, one can write $P(s, \mathbf{q})$ as

$$P(j\omega, \mathbf{q}) = U(\omega) + jV(\omega) \tag{4.6}$$

By using the intervals of the parameters, the four extreme polynomials for $\omega \geq 0$ can be defined as

$$\begin{aligned}
maxU^{+}(\omega) &= \overline{a_0} - \underline{b_1}\omega - \underline{a_2}\omega^2 + \overline{b_3}\omega^3 + ... \\
minU^{+}(\omega) &= \underline{a_0} - \overline{b_1}\omega - \overline{a_2}\omega^2 + \underline{b_3}\omega^3 + ... \\
maxV^{+}(\omega) &= \overline{b_0} + \overline{a_1}\omega - \underline{b_2}\omega^2 - \underline{a_3}\omega^3 + ...
\end{aligned}$$

$$minV^{+}(\omega) = \underline{b_0} + \underline{a_1}\omega - \overline{b_2}\omega^2 - \overline{a_3}\omega^3 + ... \quad (4.7)$$

For the negative range of ω, the four extreme polynomials are:

$$\begin{aligned}
maxU^{-}(\omega) &= \overline{a_0} - \overline{b_1}\omega - \underline{a_2}\omega^2 + \underline{b_3}\omega^3 + ... \\
minU^{-}(\omega) &= \underline{a_0} - \underline{b_1}\omega - \overline{a_2}\omega^2 + \overline{b_3}\omega^3 + ... \\
maxV^{-}(\omega) &= \overline{b_0} + \underline{a_1}\omega - \underline{b_2}\omega^2 - \overline{a_3}\omega^3 + ... \\
minV^{-}(\omega) &= \underline{b_0} + \overline{a_1}\omega - \overline{b_2}\omega^2 - \underline{a_3}\omega^3 + ... \quad (4.8)
\end{aligned}$$

Similar to the case of polynomials with real coefficients, let the roots of $maxU^{+}(\omega) = 0$ and $minU^{+}(\omega) = 0$ be $\omega_{maxu^{+}1}$, $\omega_{maxu^{+}2}$,...... and $\omega_{minu^{+}1}$, $\omega_{minu^{+}2}$,...... and the roots of $maxV^{+}(\omega) = 0$ and $minV^{+}(\omega) = 0$ be $\omega_{maxv^{+}1}$, $\omega_{maxv^{+}2}$,...... and $\omega_{minv^{+}1}$, $\omega_{minv^{+}2}$,......, respectively. The Hermite-Biehler theorem for this case is: The interval polynomial $P(s, \mathbf{q})$ with complex coefficients of Eqs.(4.4-4.5) is strictly robust Hurwitz if and only if the frequency bands $[\omega_{minu^{+}1}, \omega_{maxu^{+}1}]$, $[\omega_{minv^{+}1}, \omega_{maxv^{+}1}]$, $[\omega_{minu^{+}2}, \omega_{maxu^{+}2}]$, $[\omega_{minv^{+}2}, \omega_{maxv^{+}2}]$..... are simple, real, interlacing and do not overlap and repeat the same process for the negative range of frequency.

Example 4.1

Consider the interval polynomial

$$P(s, \mathbf{q}) = [2,3]s^5 + [13,15]s^4 + [22,30]s^3 + [28,32]s^2 + [15,20]s + [5,8] \quad (4.9)$$

From Eq.(4.3)

$$maxR(\mu) = 8 - 28\mu + 15\mu^2; \;\; minR(\mu) = 5 - 32\mu + 13\mu^2 \quad (4.10)$$

and

$$maxQ(\mu) = 20 - 22\mu + 3\mu^2; \;\; minQ(\mu) = 15 - 30\mu + 2\mu^2 \quad (4.11)$$

The roots of $maxR(\mu)$ are: 0.352, 1.515; the roots of $minR(\mu)$ are: 0.168, 2.294; the roots of $maxQ(\mu)$ are: 1.063, 6.270 and the roots of $minR(\mu)$ are: 0.518, 14.482. Thus, it can be seen that the following interlacing condition is satisfied

$$[0.168, 0.352] < [0.518, 1.063] < [1.515, 2.294] < [6.270, 14.482] \tag{4.12}$$

Therefore, one can conclude that the given real interval polynomial is Hurwitz stable.

4.3 Frequency Response of Interval Systems

A frequency response of a physical system is an important fundamental subject in the field of control engineering. In classical control, there are graphical methods such as the Nyquist plot, Bode plot and Nichols chart for designing and analysing control systems. However, these methods were developed for a fixed nominal plant. So, in general, these methods are not applicable to interval systems. In this case, it is necessary to calculate the frequency response of the entire family of the system in order to carry out analysis and design. Some recent work in this direction can be found in [10, 11, 12, 22, 23, 24, 62, 83, 75, 87].

In this section, the procedures for constructing various envelopes that contain the entire frequency responses of an interval system are discussed.

4.3.1 Minimum(Robust) Gain and Phase Margins and Nyquist Envelope

As mentioned in Chapter 2, the subject of robust stability of control systems with parameter variations has been a focus of attention of researchers in recent years. However, beyond stability, it is important to guarantee some measure of robust performance for systems with parameter variations. In classical control theory, phase and gain margins are two important frequency domain performance measures widely used for controller design. For systems with a nominal transfer function these margins are computed from the Nyquist or Bode plots of the open loop transfer function. However, in the case of systems with parametric uncertainties, the computation of the gain and phase margins becomes much more complex. To overcome this complexity or difficulty, one needs to compute the frequency response of uncertain systems, such as the Nyquist or Bode envelopes, or to convert the problem to one of robust stability of uncertain polynomials.

The robust gain and phase margins of interval systems have been treated in Argoun and Bayoumi [5] and Hollot and Tempo [75]. In [5], the generalized Hermite-Biehler theorem for real and complex interval polynomials is used for computing robust gain and phase margins. In [75], it was shown that the outer boundary of the Nyquist envelope of a stable interval plant is covered by the Nyquist plots of the sixteen Kharitonov plants family. Here, the same problem is dealt with by using the generalized Hermite-Biehler theorem.

Consider the configuration shown in Figure 4.2 where

$$G_c = K_c e^{-j\phi} \tag{4.13}$$

is the frequency-independent gain-phase compensator. Thus, the closed loop characteristic equation of the system can be written as

$$1 + K_c e^{-j\phi} G(s) = 0 \tag{4.14}$$

For $\phi = 0$, the value of K_c for which the Eq.(4.14) just becomes unstable gives the gain margin. And for $K_c = 1$, the value of ϕ for which the Eq.(4.14) just becomes unstable gives the phase margin of the system.

Let the plant in Figure 4.2 be a stable nth order all pole interval system (for simplicity an all pole interval system is considered). In this case, the characteristic equation of the unity feedback system is

$$\delta(s) = 1 + K_c e^{-j\phi} G(s, \mathbf{q} \in Q) = 0 = 1 + K_c e^{-j\phi} \frac{K}{s^n + q_{n-1}s^{n-1} + \ldots\ldots + q_0} \tag{4.15}$$

Setting $K_c = 1$, one gets

$$\delta(s) = s^n + q_{n-1}s^{n-1} + q_{n-2}s^{n-2} + \ldots\ldots\ldots + q_0 + K(cos(\phi) - jsin(\phi)) \tag{4.16}$$

where $q_i \in [\underline{q_i}, \overline{q_i}], i = 0, 1, 2, \ldots\ldots, n-1$. Substituting $s = j\omega$,

$$\delta(j\omega) = U(\omega) + jV(\omega) = q_0 + Kcos(\phi) - q_2\omega^2 + q_4\omega^4 - \ldots\ldots + j(-Ksin(\phi) + q_1\omega - q_3\omega^3 + \ldots\ldots) \tag{4.17}$$

Thus, the four extreme polynomials for $\omega \geq 0$ are

$$\begin{aligned}
maxU^{+}(\omega) &= \overline{q_0} + Kcos(\phi) - \underline{q_2}\omega^2 + \overline{q_4}\omega^4 - \underline{q_6}{}^6 + ... \\
minU^{+}(\omega) &= \underline{q_0} + Kcos(\phi) - \overline{q_2}\omega^2 + \underline{q_4}\omega^4 - \overline{q_6}\omega^6 + ... \\
maxV^{+}(\omega) &= -Ksin(\phi) + \overline{q_1}\omega - \underline{q_3}\omega^3 + \overline{q_5}\omega^5 - \underline{q_7}\omega^7 + ... \\
minV^{+}(\omega) &= -Ksin(\phi) + \underline{q_1}\omega - \overline{q_3}\omega^3 + \underline{q_5}\omega^5 - \overline{q_7}\omega^7 + ...
\end{aligned} \tag{4.18}$$

and for the negative range of ω, the four extreme polynomials are

$$\begin{aligned}
maxU^{-}(\omega) &= \overline{q_0} + Kcos(\phi) - \underline{q_2}\omega^2 + \overline{q_4}\omega^4 - \underline{q_6}{}^6 + ... \\
minU^{-}(\omega) &= \underline{q_0} + Kcos(\phi) - \overline{q_2}\omega^2 + \underline{q_4}\omega^4 - \overline{q_6}\omega^6 + ... \\
maxV^{-}(\omega) &= -Ksin(\phi) + \underline{q_1}\omega - \overline{q_3}\omega^3 + \underline{q_5}\omega^5 - \overline{q_7}\omega^7 + ... \\
minV^{-}(\omega) &= -Ksin(\phi) + \overline{q_1}\omega - \underline{q_3}\omega^3 + \overline{q_5}\omega^5 - \underline{q_7}\omega^7 + ...
\end{aligned} \tag{4.19}$$

From the Eqs.(4.18-4.19), it can be seen that $maxU^{+}(\omega) = maxU^{-}(\omega)$, $minU^{+}(\omega) = minU^{-}(\omega)$, $maxV^{+}(\omega) = minV^{-}(\omega)$ and $minV^{+}(\omega) = maxV^{-}(\omega)$. Therefore, one needs to consider only four equations, namely those for $\omega \geq 0$ or $\omega < 0$. Incrementing ϕ and computing the roots of these equations, there will be four possibilities to get the robust phase margin. These four possibilities are:

1. From the $maxU^{+}(\omega)$ and the $maxV^{+}(\omega)$. The related parameter set is

$$S_1 := \{\overline{q_0}, \overline{q_1}, \underline{q_2}, \underline{q_3}, \overline{q_4}, \overline{q_5}, \underline{q_6}, ...\}$$

2. From the $maxU^{+}(\omega)$ and the $minV^{+}(\omega)$. The related parameter set is

$$S_2 := \{\overline{q_0}, \underline{q_1}, \underline{q_2}, \overline{q_3}, \overline{q_4}, \underline{q_5}, \underline{q_6}, ...\}$$

3. From the $minU^{+}(\omega)$ and the $maxV^{+}(\omega)$. The related parameter set is

$$S_3 := \{\underline{q_0}, \overline{q_1}, \overline{q_2}, \underline{q_3}, \underline{q_4}, \overline{q_5}, \overline{q_6}, ...\}$$

4. From the $minU^{+}(\omega)$ and the $minV^{+}(\omega)$. The related parameter set is

$$S_4 := \{\underline{q_0}, \underline{q_1}, \overline{q_2}, \overline{q_3}, \underline{q_4}, \underline{q_5}, \overline{q_6}, ...\}$$

The four Kharitonov plants are

$$\begin{aligned}
G_1(s) &= \frac{K}{s^n + ... + \underline{q_4}s^4 + \overline{q_3}s^3 + \overline{q_2}s^2 + \underline{q_1}s + \underline{q_0}} \\
G_2(s) &= \frac{K}{s^n + ... + \underline{q_4}s^4 + \underline{q_3}s^3 + \overline{q_2}s^2 + \overline{q_1}s + \underline{q_0}} \\
G_3(s) &= \frac{K}{s^n + ... + \overline{q_4}s^4 + \overline{q_3}s^3 + \underline{q_2}s^2 + \underline{q_1}s + \overline{q_0}} \\
G_4(s) &= \frac{K}{s^n + ... + \overline{q_4}s^4 + \underline{q_3}s^3 + \underline{q_2}s^2 + \overline{q_1}s + \overline{q_0}}
\end{aligned} \tag{4.20}$$

It is clear that the parameters in the sets (S_1,S_2,S_3 and S_4) belong to the Kharitonov plants. Thus, one can conclude that the robust phase margin of a stable *nth* order all pole interval system is achieved at one of the Kharitonov plants. The calculation of the minimum gain margin is similar to the calculation of the minimum phase margin with ϕ set equal to zero in Eq.(4.14).

By making some modification in Figure 4.2, it can be shown that the outer boundary of the Nyquist envelope of a stable *nth* order all pole interval system comes from the Nyquist plots of the Kharitonov plants of this system. If one multiplies the given interval plant with a complex gain and then apply the procedure which is used for computing the gain and phase margins, it can be proved that a point on the outer portion of the Nyquist envelope belongs to a Kharitonov plant as follows:

Consider a point on the outer portion of the Nyquist envelope of a stable *nth* order all pole interval system as

$$z = x + jy \ \ and \ \ arg[z] = tan^{-1}(\frac{y}{x}) \tag{4.21}$$

this point can be written as

$$x^2 + y^2 = r^2 \tag{4.22}$$

which represents a circle with radius r and centred at the origin. Now, replace the frequency-independent gain-phase compensator ($G_c = K_c e^{-j\phi}$) with $G_c = \frac{1}{r}e^{-j\phi}$. Then, the characteristic equation of the unity feedback system which is shown in Figure 4.2 becomes

$$\delta(s) = 1 + \frac{1}{r}e^{-j\phi}G(s, \mathbf{q}) = 1 + \frac{1}{r}e^{-j\phi}\frac{K}{s^n + q_{n-1}s^{n-1} + ... + q_0} = 0 \tag{4.23}$$

or

$$\delta(s) = rs^n + rq_{n-1}s^{n-1} + rq_{n-2}s^{n-2} + ... + rq_0 + Kcos(\phi) - jKsin(\phi) \tag{4.24}$$

Substituting $s = j\omega$,

$$\begin{aligned} &\delta(j\omega) = U(\omega) + jV(\omega) = \\ &\quad rq_0 + Kcos(\phi) - rq_2\omega^2 + rq_4\omega^4 - ...... + j(-Ksin(\phi) + rq_1\omega - rq_3\omega^3 + ...) \end{aligned} \tag{4.25}$$

Thus, the four extreme polynomials for $\omega \geq 0$ are

$$\begin{aligned} maxU^+(\omega) &= r\overline{q_0} + Kcos(\phi) - r\underline{q_2}\omega^2 + r\overline{q_4}\omega^4 - r\underline{q_6}{}^6 + ... \\ minU^+(\omega) &= r\underline{q_0} + Kcos(\phi) - r\overline{q_2}\omega^2 + r\underline{q_4}\omega^4 - r\overline{q_6}\omega^6 + ... \\ maxV^+(\omega) &= -Ksin(\phi) + r\overline{q_1}\omega - r\underline{q_3}\omega^3 + r\overline{q_5}\omega^5 - r\underline{q_7}\omega^7 + ... \\ minV^+(\omega) &= -Ksin(\phi) + r\underline{q_1}\omega - r\overline{q_3}\omega^3 + r\underline{q_5}\omega^5 - r\overline{q_7}\omega^7 + ... \end{aligned} \tag{4.26}$$

If one increases ϕ and calculates the roots of these equations, from the generalized Hermite-Biehler theorem for real and complex interval polynomials it can be observed that the strict robust stability conditions for interval polynomials will be violated at the point $z = x + jy$ which belongs to a Kharitonov plant. Therefore, one can say that the outer Nyquist envelope of a stable *nth* order all pole interval system is covered by the Nyquist plots of the Kharitonov plants.

Example 4.2

Consider an interval system as

$$G(s, \mathbf{q}, \mathbf{r}) = \frac{1.5}{s^4 + [1.8, 2.2]s^3 + [3.6, 4.4]s^2 + [3.6, 4.4]s + [0.9, 1.1]} \tag{4.27}$$

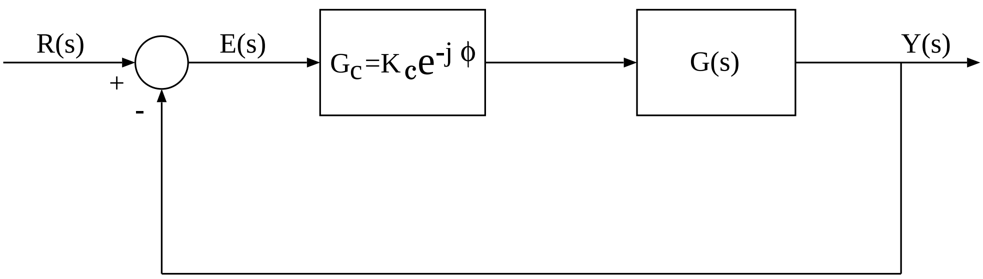

Figure 4.2: A unity feedback system

which has the following Kharitonov plants

$$\begin{aligned}
G_1(s) &= \frac{1.5}{s^4 + 2.2s^3 + 4.4s^2 + 3.6s + 0.9} \\
G_2(s) &= \frac{1.5}{s^4 + 1.8s^3 + 4.4s^2 + 4.4s + 0.9} \\
G_3(s) &= \frac{1.5}{s^4 + 2.2s^3 + 3.6s^2 + 3.6s + 1.1} \\
G_4(s) &= \frac{1.5}{s^4 + 1.8s^3 + 3.6s^2 + 4.4s + 1.1}
\end{aligned} \tag{4.28}$$

The minimum gain margin is 1.15 and is achieved at $G_4(s)$. The minimum phase margin is 86.77 and is achieved at $G_1(s)$. The Nyquist plots of the Kharitonov plants and the outer boundary of the Nyquist envelope are shown in Figures 4.3 and 4.4.

4.3.2 Bode envelope

The magnitude and phase extremums of the interval plant of Eq.(2.27) can be found as

a) For $s = j\omega^*$, the maximum and the minimum magnitudes of $G(j\omega^*, \mathbf{q}, \mathbf{r})$ occur on one of the Kharitonov or on an edge plant (by edge plant we mean a plant which belongs to the thirty-two systems of Eq.(2.34)).

b) The maximum and the minimum phases of $G(s, \mathbf{q}, \mathbf{r})$ at $s = j\omega^*$ are always generated by Kharitonov plants.

The maximum and minimum magnitudes of Eq.(2.27) at $s = j\omega^*$ can be written as

$$max|G(j\omega^*, \mathbf{q}, \mathbf{r})| = \frac{max|N(j\omega^*, \mathbf{r})|}{min|D(j\omega^*, \mathbf{q})|} \tag{4.29}$$

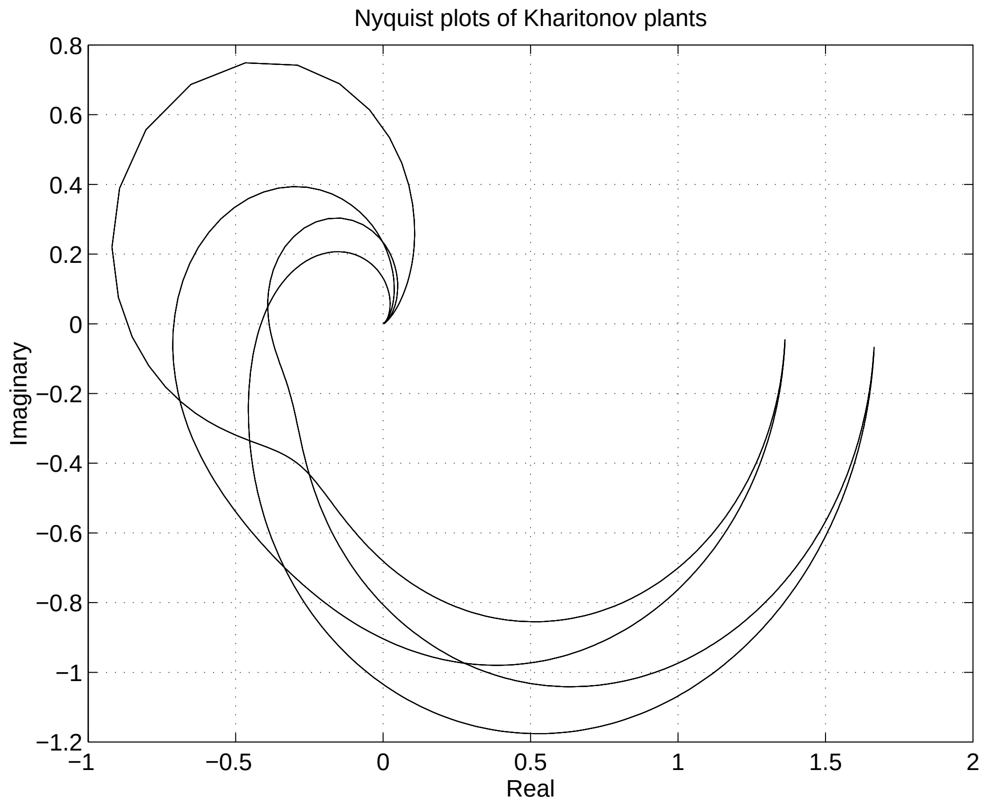

Figure 4.3: Nyquist plots of the four Kharitonov plants

and

$$min|G(j\omega^*, \mathbf{q}, \mathbf{r})| = \frac{min|N(j\omega^*, \mathbf{r})|}{max|D(j\omega^*, \mathbf{q})|} \tag{4.30}$$

Similarly, the maximum and minimum phases of $G(j\omega^*, \mathbf{q}, \mathbf{r})$ are

$$maxarg[G(j\omega^*, \mathbf{q}, \mathbf{r})] = maxarg[N(j\omega^*, \mathbf{r})] - minarg[D(j\omega^*, \mathbf{q})] \tag{4.31}$$

and

$$minarg[G(j\omega^*, \mathbf{q}, \mathbf{r})] = minarg[N(j\omega^*, \mathbf{r})] - maxarg[D(j\omega^*, \mathbf{q})] \tag{4.32}$$

The value sets of the numerator, $N(s, \mathbf{r})$, and the denominator, $D(s, \mathbf{q})$, for $s = j\omega^*$ are shown in Figure 4.5 where N_1, N_2, N_3, N_4, D_1, D_2, D_3 and D_4 represent the Kharitonov polynomials of the numerator and the denominator of $G(s, \mathbf{q}, \mathbf{r})$. Since the value sets are rectangular, the maximum magnitude of $N(j\omega^*, \mathbf{r})$ and $D(j\omega^*, \mathbf{q})$ always occur at one of the Kharitonov polynomials and the minimum magnitude of $N(j\omega^*, \mathbf{r})$ and $D(j\omega^*, \mathbf{q})$ occur on a Kharitonov segment or on a Kharitonov polynomial. For the phase of $G(s, \mathbf{q}, \mathbf{r})$, it is

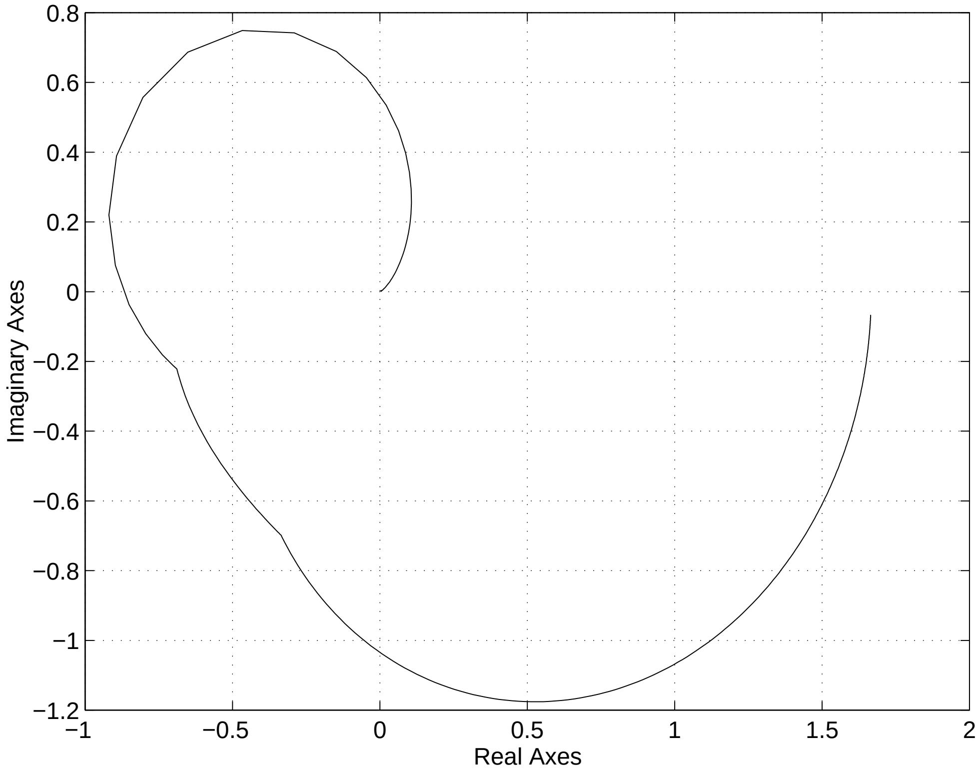

Figure 4.4: Outer boundary of the Nyquist envelope

clear that the maximum and minimum arguments of $N(j\omega^*, \mathbf{r})$ and $D(j\omega^*, \mathbf{q})$ are achieved at the corners of the value sets which correspond to the Kharitonov polynomials of the numerator and the denominator.

Thus, as a result, one can say that the boundary of the Bode envelope can be calculated from the Kharitonov or edge plants and the boundary of the phase envelope can be found from the phases of the Kharitonov plants.

4.3.3 Gain Crossover, Phase Crossover and Bandwidth Frequencies of Interval Systems

Several frequencies such as gain crossover, phase crossover and bandwidth frequencies are used in control systems in order to calculate the gain and phase margins and to characterize the speed of response of the system. The gain and phase crossover frequencies (ω_{cg} and ω_{cp}) are defined as the frequencies at which the magnitude of the system is equal to unity ($0db$) and the phase angle is equal to -180^o, respectively. Two important frequency-domain measures, gain and phase margins which are used as design criteria, are calculated at these

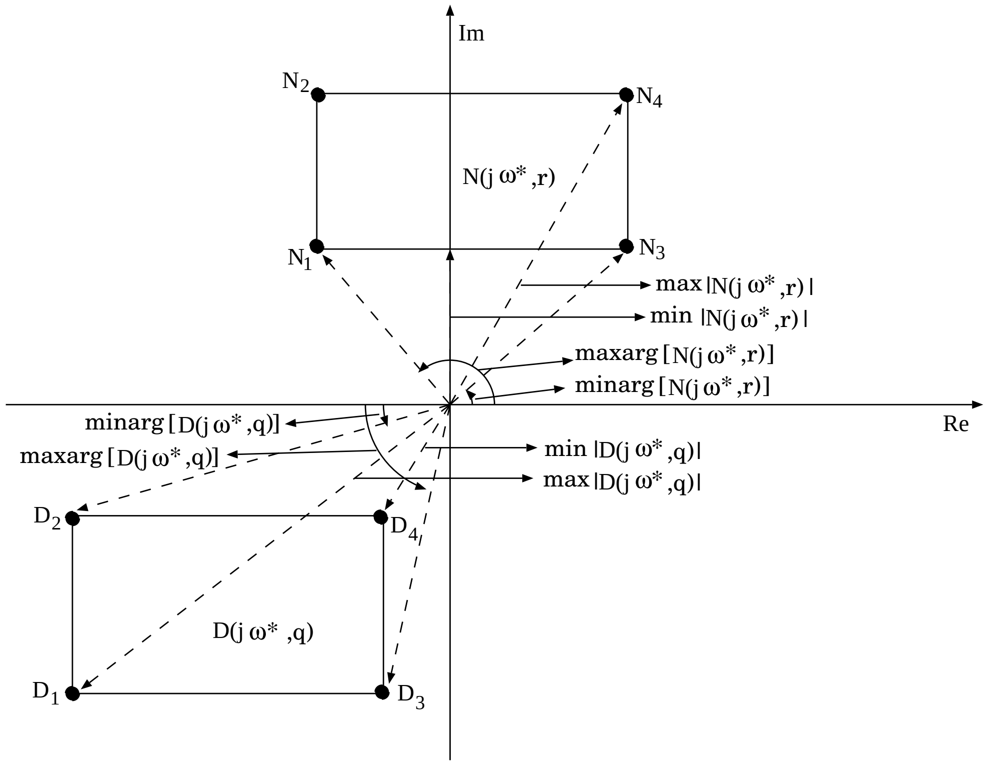

Figure 4.5: Value sets of $N(s, \mathbf{r})$ and $D(s, \mathbf{q})$ at $s = j\omega^*$

frequencies. Also, the bandwidth frequency, ω_b, is the frequency at which the magnitude of the complementary sensitivity function of the system is equal to 0.707 ($-3db$). The bandwidth frequency of the system indicates how fast or how well the system will track an input signal.

In general, fixed systems except conditionally stable systems and some higher-order systems with complicated numerator have one gain crossover and one phase crossover frequency. Therefore, the calculation of these frequencies for a fixed system is straightforward. However, for interval systems, there are many gain crossover, phase crossover and bandwidth frequencies due to the uncertain parameters. So, it is of value to find the bounds of these frequencies for uncertain systems. These bounds may offer a convenient means for designing interval control systems. With this motivation, the gain and the phase crossover and the bandwidth frequencies of the interval plant of Eq.(2.27) are formulated as follows:

1) The relationship of the gain crossover frequencies of $G(s, \mathbf{q}, \mathbf{r})$ can be written as

$$min\omega_{cg} \leq \omega_{cg1} \leq \omega_{cg2} \leq .... \leq max\omega_{cg} \tag{4.33}$$

where $min\omega_{cg}$ and $max\omega_{cg}$ are achieved at the Kharitonov or edge plants.

From Figure 4.6, the intersection points of the magnitude envelope of $G(s, \mathbf{q}, \mathbf{r})$ with the $0db$ line give the gain crossover frequencies. Since both sides of the magnitude envelope of $G(s, \mathbf{q}, \mathbf{r})$ comes from Kharitonov and edge plants, one can say that the $min\omega_{cg}$ and the $max\omega_{cg}$ belong to one of the Kharitonov or edge plants.

Remark 4.1: If the portion of the phase envelope between $min\omega_{cg}$ and the $max\omega_{cg}$ is approximately linear and decreasing, the $max\omega_{cg}$ occurs on the Kharitonov plant which gives the robust phase margin (pm_{min}).

2) The range of phase crossover frequencies of $G(s, \mathbf{q}, \mathbf{r})$ is

$$min\omega_{cp} \leq \omega_{cp1} \leq \omega_{cp2} \leq .... \leq max\omega_{cp} \tag{4.34}$$

where $min\omega_{cp}$ and $max\omega_{cp}$ are achieved at the Kharitonov plants.

From Figure 4.6, since both sides of the phase envelope of $G(s, \mathbf{q}, \mathbf{r})$ come from Kharitonov plants, the $min\omega_{cp}$ and the $max\omega_{cp}$ belong to the Kharitonov plants and the other phase crossover frequencies must lie between $min\omega_{cp}$ and $max\omega_{cp}$.

Remark 4.2: If the portion of the magnitude envelope of $G(s, \mathbf{q}, \mathbf{r})$ between $minw_{cp}$ and $maxw_{cp}$ is approximately linear and decreasing then the Kharitonov plant which gives the robust gain margin (gm_{min}) has $min\omega_{cp}$.

3) The relationship of the bandwidth frequencies of $G(s, \mathbf{q}, \mathbf{r})$ can be written as

$$min\omega_{b} \leq \omega_{b1} \leq \omega_{b2} \leq .... \leq max\omega_{b} \tag{4.35}$$

where $min\omega_{b}$ and $max\omega_{b}$ are achieved at the Kharitonov or edge plants.

In order to prove this result, it is necessary to consider the complementary sensitivity function of the system. The complementary sensitivity function of $G(s, \mathbf{q}, \mathbf{r})$ can be written as

$$T(s,\mathbf{q},\mathbf{r}) = \frac{G(s,\mathbf{q},\mathbf{r})}{1+G(s,\mathbf{q},\mathbf{r})} \tag{4.36}$$

It is known that the magnitude envelope of $G(s,\mathbf{q},\mathbf{r})$ is bounded by Kharitonov and edge plants. Now, the question is "can one say that the magnitude envelope of $T(s,\mathbf{q},\mathbf{r})$ is covered by Kharitonov and edge plants of $G(s,\mathbf{q},\mathbf{r})$?". For $s = j\omega^*$, the value set of $G(s,\mathbf{q},\mathbf{r})$ is covered by Kharitonov and edge plants. If one shifts the value set of $G(s,\mathbf{q},\mathbf{r})$ along the horizontal(real) axis by 1, the value set of $1+G(j\omega^*,\mathbf{q},\mathbf{r})$ is obtained. Therefore,

$$min|T(j\omega^*,\mathbf{q},\mathbf{r})| = \frac{min|G(j\omega^*,\mathbf{q},\mathbf{r})|}{1+max|G(j\omega^*,\mathbf{q},\mathbf{r})|} \tag{4.37}$$

and

$$max|T(j\omega^*,\mathbf{q},\mathbf{r})| = \frac{max|G(j\omega^*,\mathbf{q},\mathbf{r})|}{1+min|G(j\omega^*,\mathbf{q},\mathbf{r})|} \tag{4.38}$$

Thus, one can say that the magnitude envelope of $T(s,\mathbf{q},\mathbf{r})$ is bounded by the magnitude envelope of the complementary sensitivity functions of the Kharitonov and edge plants of $G(s,\mathbf{q},\mathbf{r})$.

Now, from the magnitude envelope of $T(s,\mathbf{q},\mathbf{r})$, if one draws a line which is parallel to the frequency axis at $-3db$, the line will intersect the magnitude envelope of the complementary sensitivity functions. From the intersection points, one can calculate the bandwidth frequencies. From Figure 4.7, since the magnitude envelope of $T(s,\mathbf{q},\mathbf{r})$ is bounded by Kharitonov and edge plants of the system, then the minimum and the maximum bandwidth frequencies ($min\omega_b$ and $max\omega_b$) of the system occur on the Kharitonov and the edge plants.

4.3.4 Nichols Envelope

The boundary of a Nyquist template of an interval transfer function (by a Nyquist template we mean the value set of $G(s,\mathbf{q},\mathbf{r})$ at $s = j\omega^*$) is contained in the boundary of Nyquist template of its thirty-two systems. Thus, the Nichols envelope of an interval plant can be constructed by using the thirty-two systems. The Nichols envelope can also be generated approximately from the magnitude and phase envelopes of the family.

As a concluding remark, the Nyquist, Nichols and Bode envelopes of interval systems can be computed using the thirty-two systems of the interval plant family.

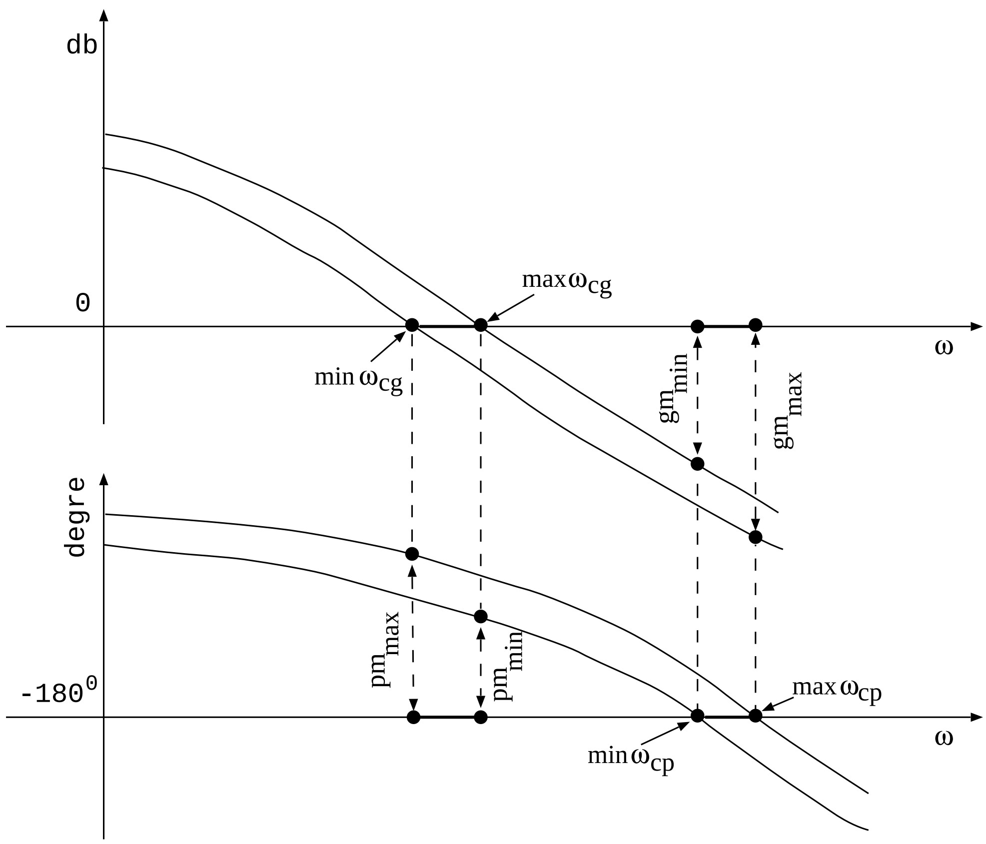

Figure 4.6: Magnitude and phase envelopes of an interval plant

4.4 Maximum Allowable Perturbation Bounds of Parameters of a Linear System

One of the main problems in robustness of linear systems is to find the maximum allowable perturbation bounds of parameters of a linear system while preserving stability. The interest in this area has greatly increased since the publication of the Kharitonov theorem. Although the stability of an interval system can be checked by Kharitonov's test, there is no direct indication as to what extent the bounds of parameters can be increased before the system becomes unstable. Following the Kharitonov theorem, this problem has been treated in [14, 136, 120, 40]. In this section, the method of [14] is used in order to prepare an algorithm for computing the maximum allowable perturbation.

Consider a linear unity feedback system with the nominal transfer function as

$$G(s) = \frac{N(s)}{D(s)} = \frac{b_m s^m + b_{m-1}s^{m-1} + ... + b_0}{a_n s^n + a_{n-1}s^{n-1} + ... + a_0}, \quad n \geq m \tag{4.39}$$

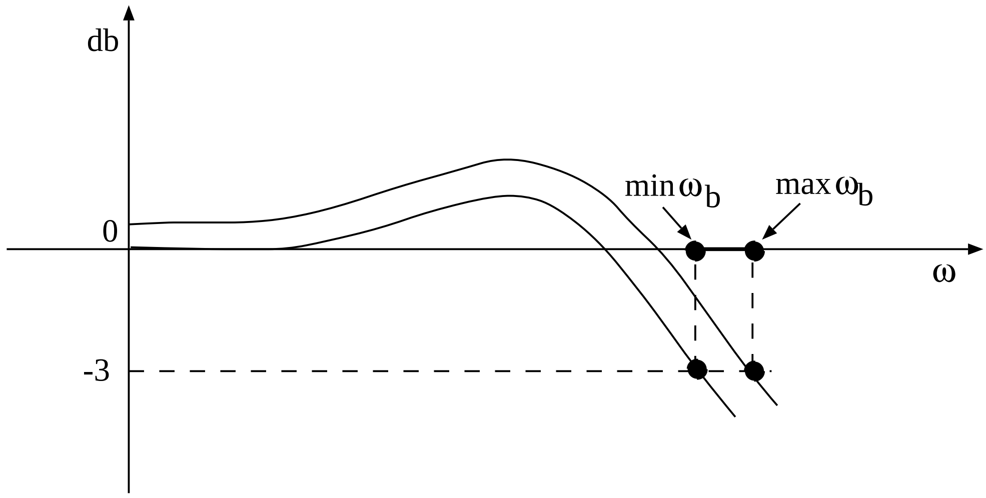

Figure 4.7: Magnitude envelope of the complementary sensitivity function of an interval plant

The closed loop characteristic equation of this nominal system can be written as

$$\delta(s) = \sum_{i=m+1}^{n} a_i s^i + \sum_{i=0}^{m} (a_i + b_i) s^i \tag{4.40}$$

Assume that the nominal unity feedback system is Hurwitz stable. Given any allowable variations in the coefficients $\epsilon > 0$, Eq.(4.39) can be written with an interval plant structure as

$$G(s, \mathbf{q}, \mathbf{r}) = \frac{N(s, \mathbf{r})}{D(s, \mathbf{q})} = \frac{r_m s^m + r_{m-1} s^{m-1} + ... + r_0}{q_n s^n + q_{n-1} s^{n-1} + ... + q_0} \tag{4.41}$$

where

$$\begin{aligned} r_i &\in [\underline{r}_i, \overline{r}_i],\ i = 0, 1, 2, ..., m,\ \underline{r}_i = b_i - \epsilon,\ \overline{r}_i = b_i + \epsilon \\ q_i &\in [\underline{q}_i, \overline{q}_i],\ i = 0, 1, 2, ..., n,\ \underline{q}_i = a_i - \epsilon,\ \overline{q}_i = a_i + \epsilon \end{aligned} \tag{4.42}$$

and the closed loop characteristic equation of the system of Eq.(4.41) is

$$\delta(s, \mathbf{q}, \mathbf{r}) = \sum_{i=m+1}^{n} q_i s^i + \sum_{i=0}^{m} (q_i + r_i) s^i \tag{4.43}$$

Now, we seek the largest value of ϵ, say ϵ_{max}, such that the interval system is Hurwitz stable. If one writes the Kharitonov polynomials of the characteristic equation, Eq.(4.43),(assuming $n = m + 1$), one gets

$$\begin{aligned}
\delta_1(s) &= \underline{q_n}s^n + (\overline{q_{n-1}} + \overline{r_{n-1}})s^{n-1} + (\overline{q_{n-2}} + \overline{r_{n-2}})s^{n-2} + (\underline{q_{n-3}} + \underline{r_{n-3}})s^{n-3} + ...\\
\delta_2(s) &= \underline{q_n}s^n + (\underline{q_{n-1}} + \underline{r_{n-1}})s^{n-1} + (\overline{q_{n-2}} + \overline{r_{n-2}})s^{n-2} + (\overline{q_{n-3}} + \overline{r_{n-3}})s^{n-3} + ...\\
\delta_3(s) &= \overline{q_n}s^n + (\underline{q_{n-1}} + \underline{r_{n-1}})s^{n-1} + (\underline{q_{n-2}} + \underline{r_{n-2}})s^{n-2} + (\overline{q_{n-3}} + \overline{r_{n-3}})s^{n-3} + ...\\
\delta_4(s) &= \overline{q_n}s^n + (\overline{q_{n-1}} + \overline{r_{n-1}})s^{n-1} + (\underline{q_{n-2}} + \underline{r_{n-2}})s^{n-2} + (\underline{q_{n-3}} + \underline{r_{n-3}})s^{n-3} + ...
\end{aligned} \tag{4.44}$$

Thus, for any $\epsilon > 0$, if all these four Kharitonov polynomials of the perturbed system are Hurwitz stable then stability of the perturbed system is guaranteed. If the maximum perturbations of $\delta_1(s)$, $\delta_2(s)$, $\delta_3(s)$ and $\delta_4(s)$ are respectively ϵ_1, ϵ_2, ϵ_3 and ϵ_4, then from

$$\epsilon_{max} = min\{\epsilon_1, \epsilon_2, \epsilon_3, \epsilon_4\} \tag{4.45}$$

the maximum allowable perturbation can be determined.

Example 4.3

Let the feedforward transfer function of a unity feedback system be

$$G(s) = \frac{b_2s^2 + b_1s + b_0}{s^3 + a_2s^2 + a_1s + a_0} = \frac{4s^2 + 6s + 2}{s^3 + 5s^2 + 2s + 6} \tag{4.46}$$

This nominal system is Hurwitz stable. Now, the question is "how much can one perturb the parameters $(b_0, b_1, b_2, a_0, a_1, a_2)$ while preserving stability?". The output of the algorithm for maximum perturbation is

$$\epsilon_{max} = 2.438$$

Thus, for this perturbation value, the following interval system

$$G(s, \mathbf{q}, \mathbf{r}) = \frac{[1.562, 6.438]s^2 + [3.562, 8.438]s + [-0.4384, 4.438]}{s^3 + [2.562, 7.438]s^2 + [-0.4384, 4.438]s + [3.562, 8.438]} \tag{4.47}$$

is Hurwitz stable.

4.5 AISTK-A Software Package for the Analysis of Interval Systems

MATLAB with its large collection of fast and efficient functions and various toolboxes, such as the control systems toolbox, provides an ideal interactive environment for linear control system analysis and design. Its graphical user interface (GUI) allows a user to build up user friendly toolboxes. A graphical user interface is a user interface made up of graphical objects such as buttons, menus, figures and so on. A GUI provides an interface between an application and a user. When the user chooses an object from the GUI, it is expected that a certain kind of action will take place. In addition a great majority of the control community are familiar with MATLAB and its toolboxes. These reasons have been chosen for the development of the Analysis of Interval Systems ToolKit (AISTK) in MATLAB.

AISTK is a user friendly MATLAB based software package. It deals with analysis of uncertain systems defined by an interval plant structure. Various functions (M-files) have been developed in the MATLAB environment using the theory given in Chapter 2 and in this chapter. The objective in developing AISTK was to gather these functions under a toolkit and make them easily usable by students and other users.

When AISTK is run the window of Figure 4.8 appears on the screen where $G(s, \mathbf{q}, \mathbf{r})$ is an interval plant and $C(s)$ and $H(s)$ are fixed controllers. Double clicking on $G(s, \mathbf{q}, \mathbf{r})$, $C(s)$ or $H(s)$ opens up a window in which the user can enter the parameters of an interval plant and controllers in MATLAB form. There are four pull down menus namely *File, Model, Analysis* and *Plot.* The *File* menu allows for clearing the workspace and quitting from the program. The controller type and model to be analysed can be selected from the menu *Model.* The *Analysis* menu has many submenus which are shown in Figure 4.9. Briefly, the features provided in the program enable the user to

— enter data through a very friendly graphical user interface (GUI);

— find the Kharitonov plants of $G(s, \mathbf{q}, \mathbf{r})$. From the *Analysis* menu, clicking on the "Kharitonov Plant" button opens up the window of Figure 4.10 in which the user can see the number of Kharitonov plants and the parameters of any selected Kharitonov plant can be displayed by using "Show Parameters" button;

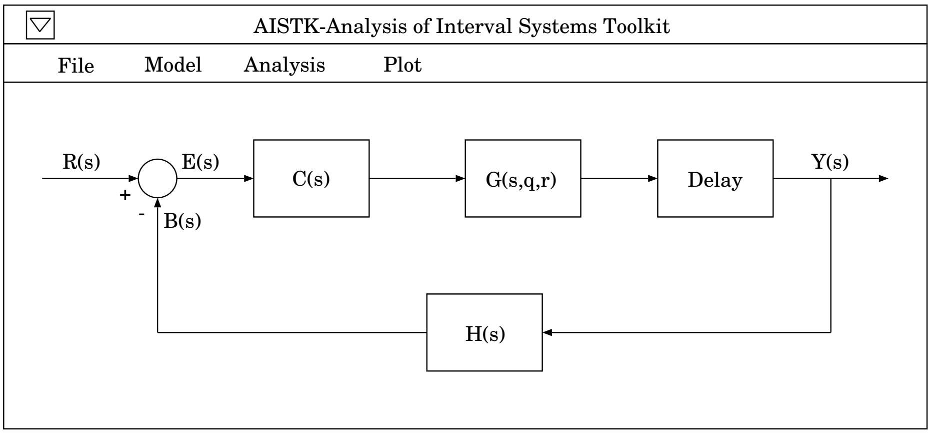

Figure 4.8: The block diagram of AISTK

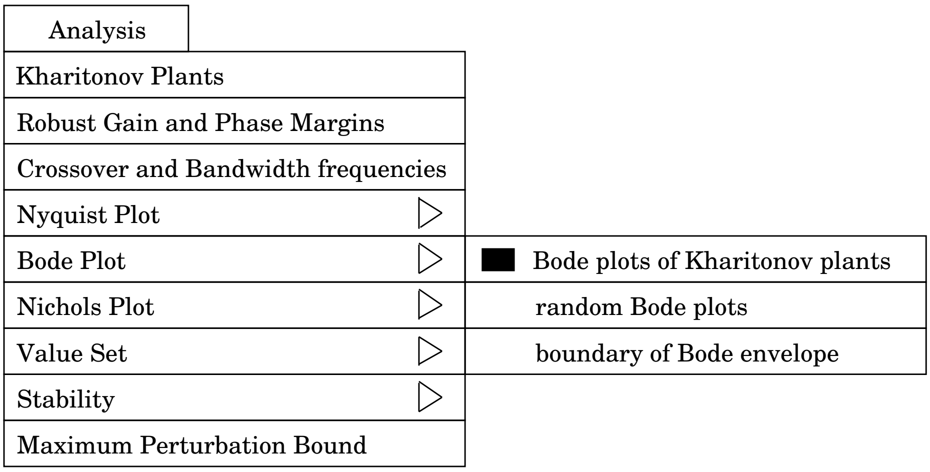

Figure 4.9: Analysis menu

— find the minimum gain and phase margins and the plants which yield each. When the user clicks on the submenu "Robust Gain and Phase Margins" of Figure 4.9, the window of Figure 4.11 is displayed where the robust gain and phase margins can be read;

— plot the robust versions of the Nyquist, Bode and Nichols diagrams;

— obtain the plots of the value set of the characteristic equation, numerator or denominator of the system;

— compute the bounds of the gain crossover, phase crossover and bandwidth frequencies;

— compute the maximum allowable perturbation bounds of parameters of a fixed system;

— check the stability of the system and see if the interlacing property is satisfied.

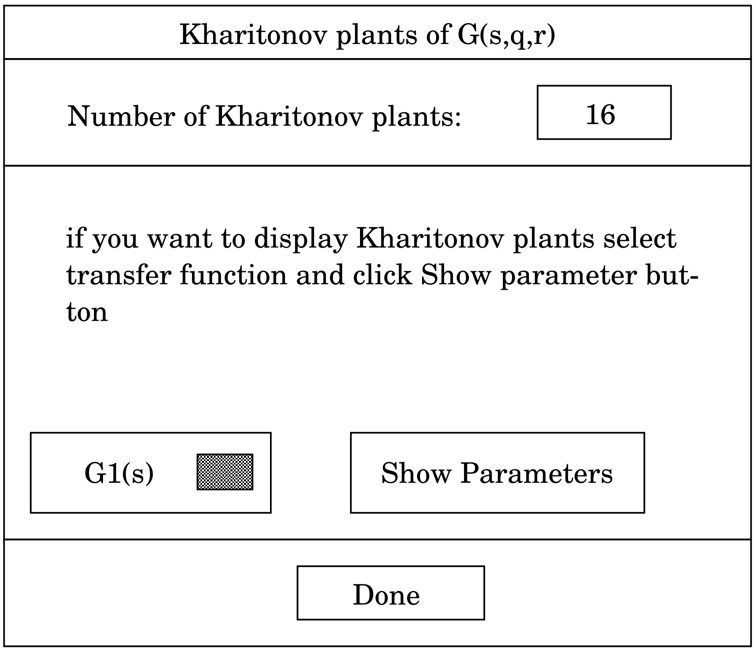

Figure 4.10: The Kharitonov plants window

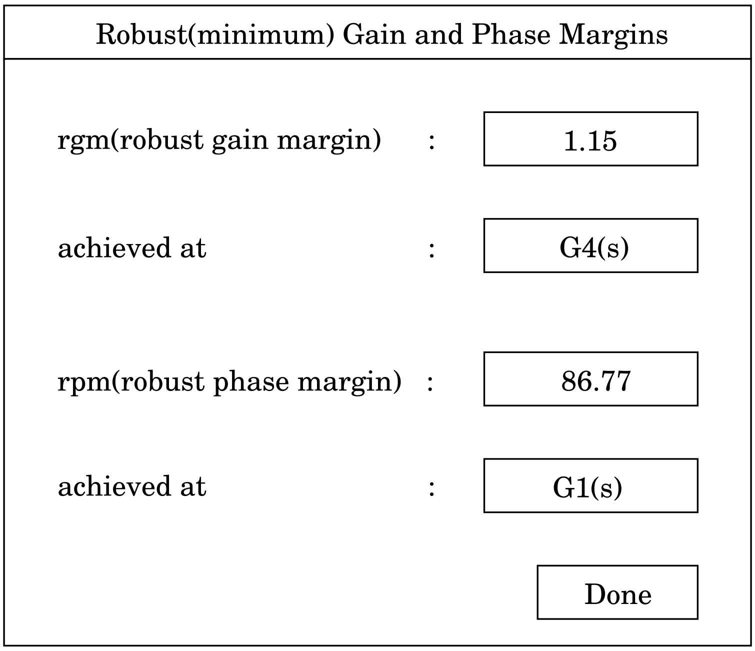

Figure 4.11: Gain and phase margins window

Example 4.4

Consider an interval plant as

$$G(s, \mathbf{q}, \mathbf{r}) = \frac{[2,3]s + [1,2]}{s^3 + [3,6]s^2 + [2,3]s + [1,2]} \tag{4.48}$$

and the controller as

$$C(s) = \frac{s+3}{4s+7} \tag{4.49}$$

The robust gain margin is infinity and the phase margin is equal to 85.39° which is achieved at $C(s)G(s) \in C(s)G(s, \mathbf{q}, \mathbf{r}) = (2s^2+8s+6)/(4s^4+31s^3+50s^2+18s+7)$. Figures 4.12 and 4.13 show the Nyquist and Nichols templates. The value set of the characteristic equation at $\omega = 1rad/sec$ is shown in Figures 4.14. Figures 4.15 and 4.16 show random Bode plots and the boundary of the Bode envelopes.

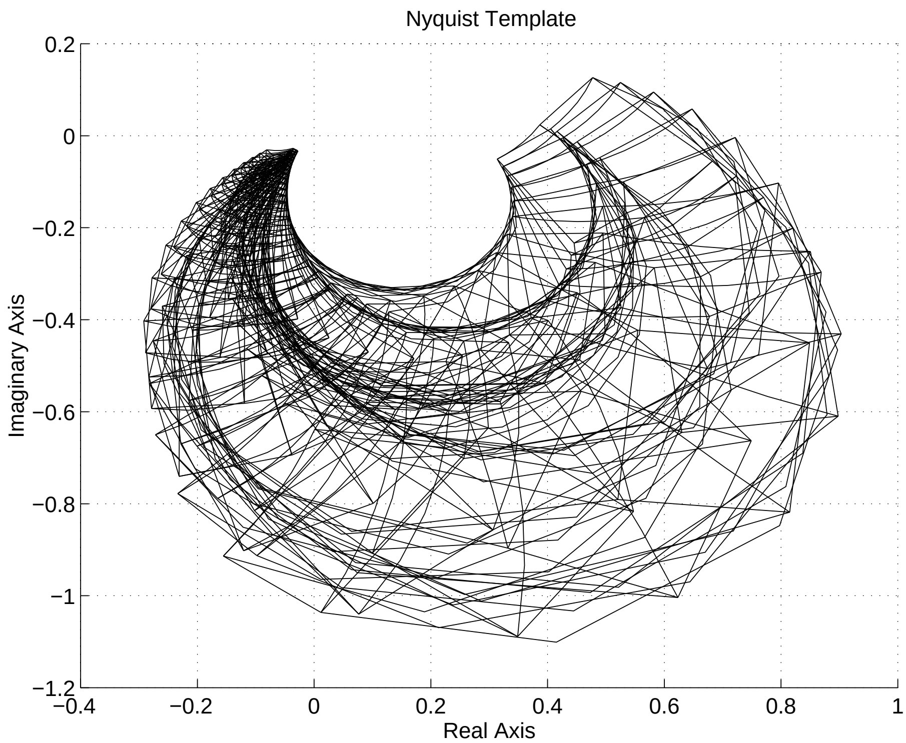

Figure 4.12: Nyquist envelope

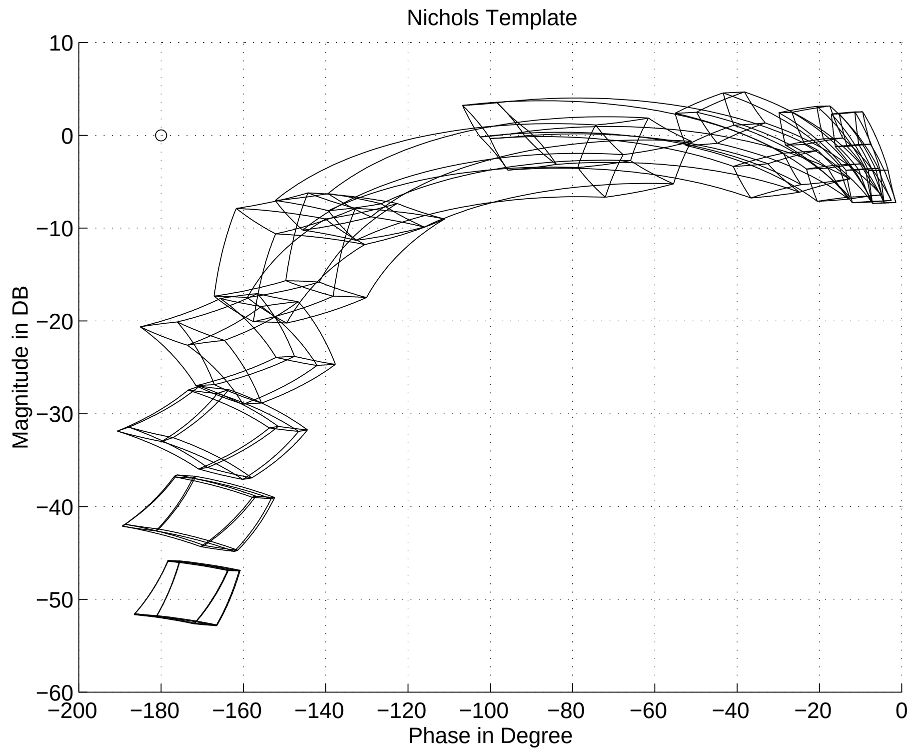

Figure 4.13: Nichols envelope

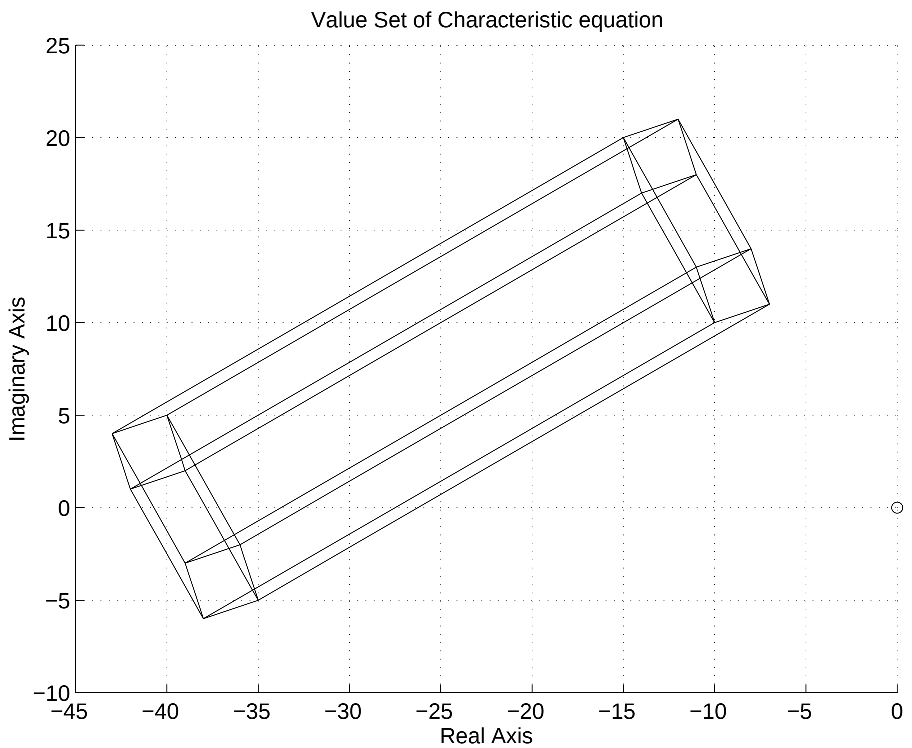

Figure 4.14: Value set of the characteristic equation at $\omega = 1 rad/sec$

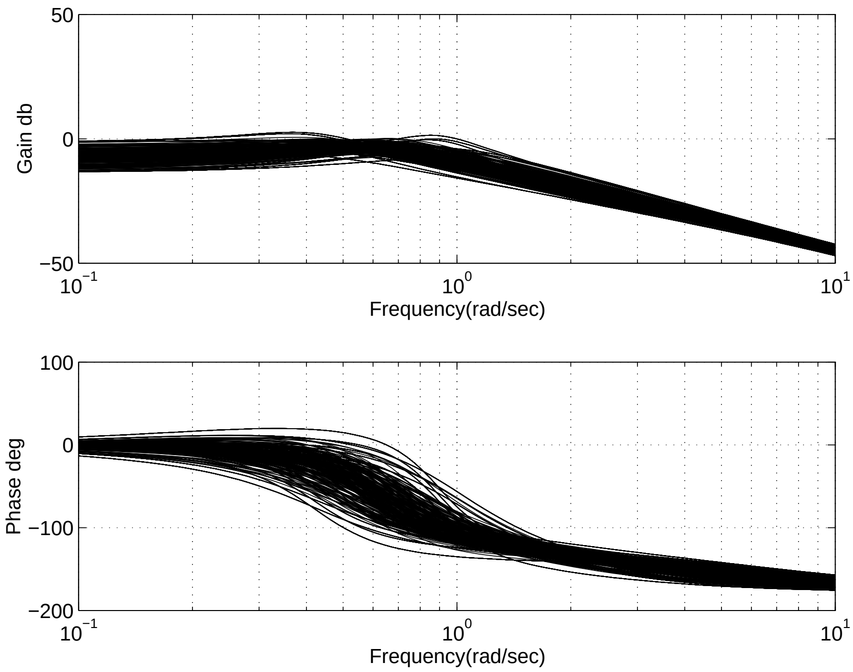

Figure 4.15: Random Bode plots

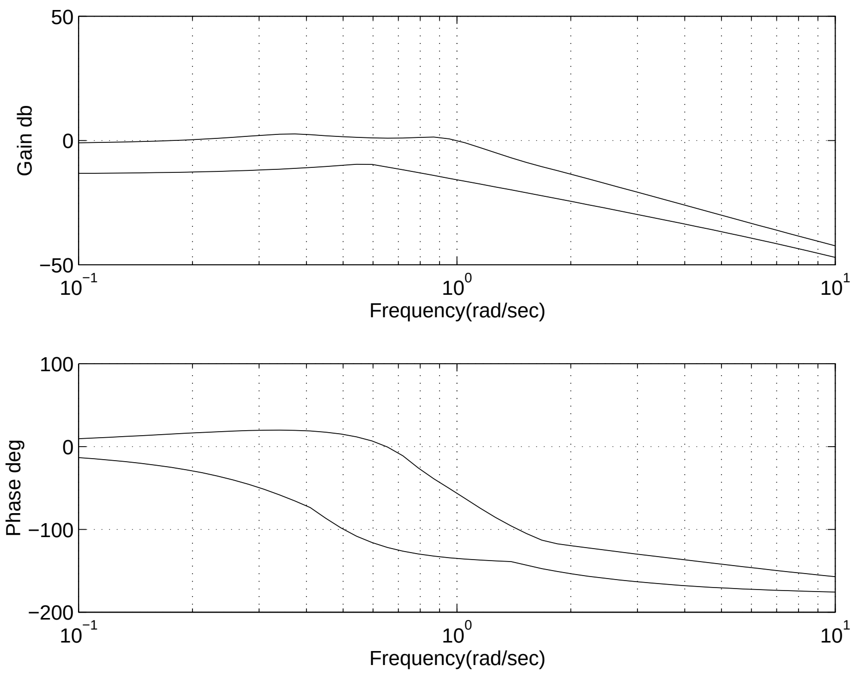

Figure 4.16: Boundary of the Bode envelope

Example 4.5

In this example, the Astrom-Hagglund controller tuning method [7] is used in order to find the parameters of a PID controller which gives a desired minimum phase margin for an interval plant family. The Astrom-Hagglund controller tuning method is based on the idea that a point on the Nyquist plot of a given transfer function can be moved to an arbitrary point in the complex plane by choosing suitable controller parameters. Such an appropriate point for tuning is the intersection of the Nyquist curve with the negative real axis which is traditionally described as the *critical point.* However, for an interval plant there are many Nyquist curves which cross the negative real axis or for a fixed frequency there are many points in the Nyquist plane. Therefore, it is necessary to find the worst case transfer function.

Consider an interval transfer function as

$$G(s, \mathbf{q}, \mathbf{r}) = \frac{1}{[0.002, 0.072]s^4 + [0.335, 0.405]s^3 + [1.295, 1.365]s^2 + [1.965, 2.035]s + [0.965, 1.035]} \tag{4.50}$$

The aim is to find the parameters of the PID controller of the form of

$$C(s) = K_p(1 + sT_d + \frac{1}{sT_i}) \tag{4.51}$$

for which the phase margin of the system is at least $\varphi_m = 45°$.

From the toolbox, it was computed that the bound of phase crossover frequencies of $G(s, \mathbf{q}, \mathbf{r})$ is

$$\omega_{cp} = [2.20, 2.46] \tag{4.52}$$

The minimum gain margin of the system is equal to 3.55 at the frequency $\omega = 2.20 = min\omega_{cp}$. Using this frequency and the gain at this frequency, the following PID controller was designed using the Astrom-Hagglund method

$$C(s) = \frac{3.012s^2 + 5.5s + 2.51}{2.193s} \tag{4.53}$$

The minimum phase margin of the overall system is 45.22°. Figure 4.17 shows the closed loop step responses of $G_K(s)$ (Kharitonov plant family) and Figure 4.18 shows the closed

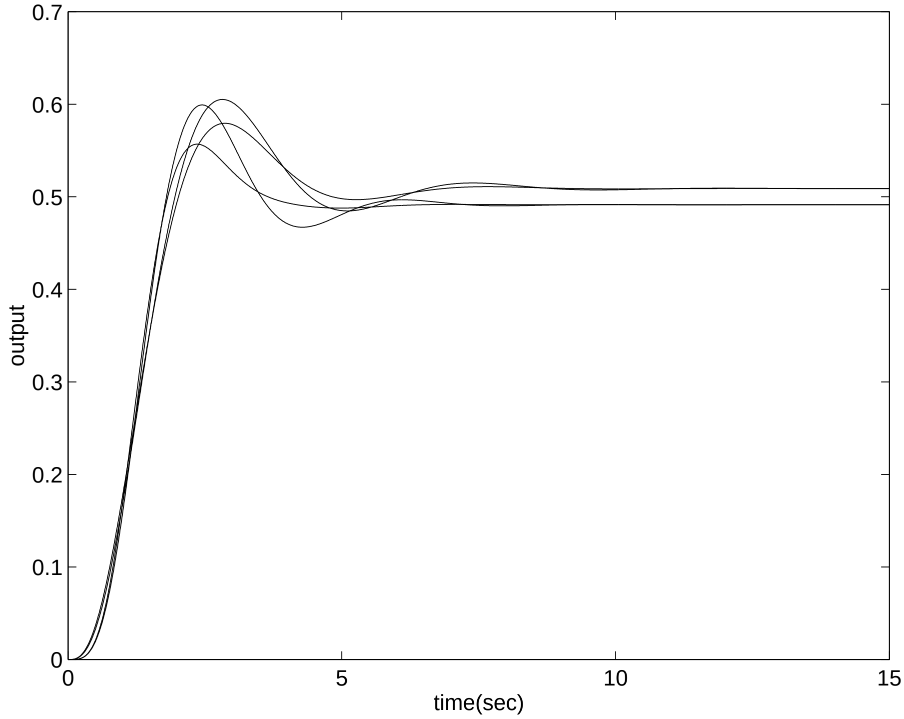

Figure 4.17: Step responses of $G_K(s)$

loop step responses of $C(s)G_K(s)$. The Nyquist envelopes of $G(s,\mathbf{q},\mathbf{r})$ and $C(s)G(s,\mathbf{q},\mathbf{r})$ are shown in Figure 4.19.

4.6 Conclusion

This chapter has described an easy to use software program developed for the analysis of interval systems. The program allows the user to compute the frequency responses, check the stability, construct the value sets, find the Kharitonov plants and determine the minimum gain and phase margins of control systems with an interval plant. The program is a collection of algorithms developed in the MATLAB environment. The logic behind the algorithms is based on the the results summarized in Chapter 2 and this chapter. Although the package is developed to deal with interval systems, it can be successfully used for the analysis of control systems with more complex uncertainty structure using the so-called overbounding technique.

Some theoretical results have been also developed in this chapter. An alternative proof of why the outer boundary of the Nyquist envelope of a stable interval plant is covered by

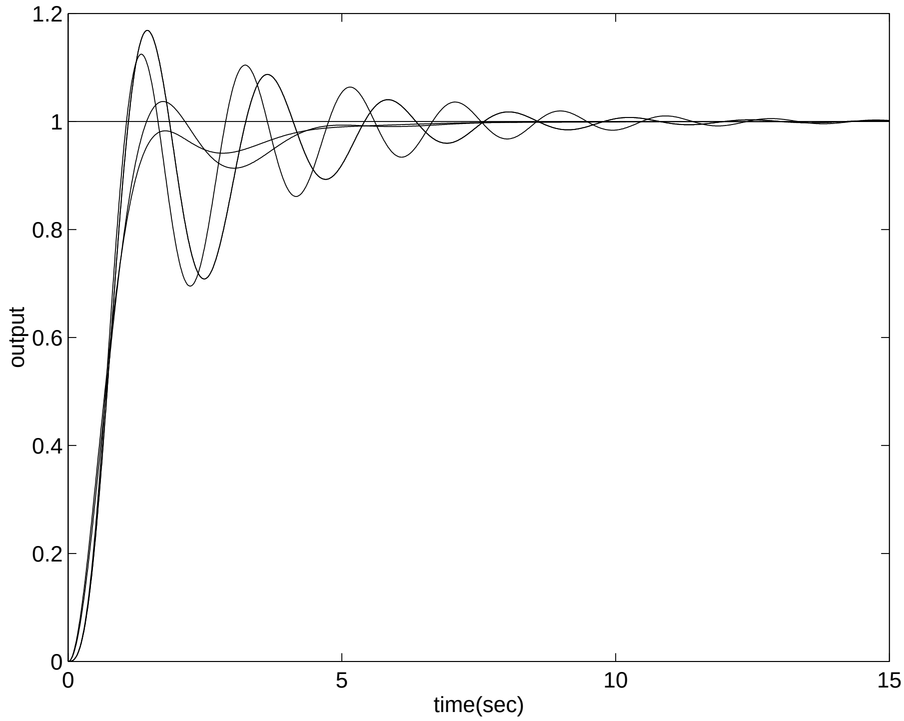

Figure 4.18: Step responses of $C(s)G_K(s)$

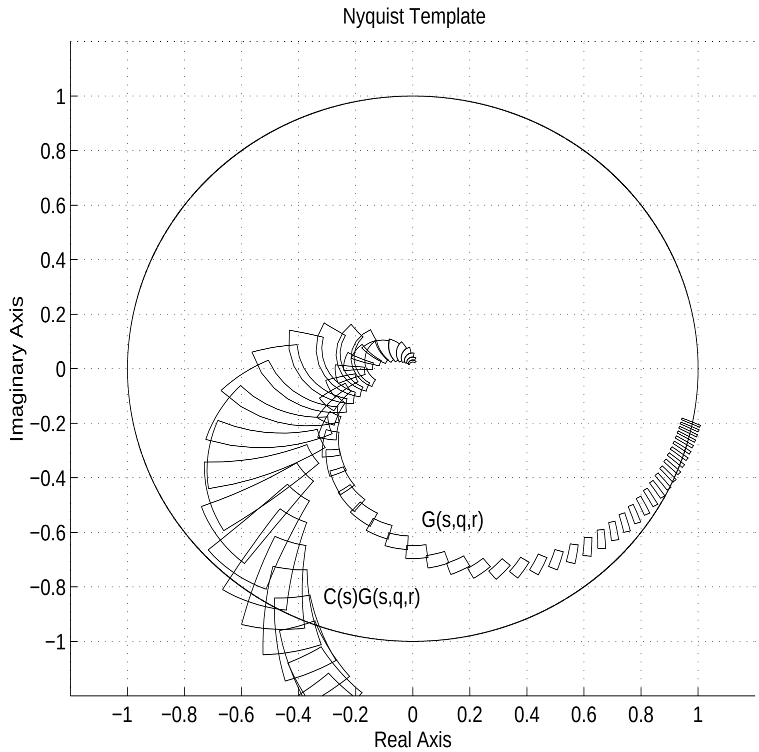

Figure 4.19: Nyquist envelopes of $G(s, \mathbf{q}, \mathbf{r})$ and $C(s)G(s, \mathbf{q}, \mathbf{r})$

the Nyquist plots of the Kharitonov plants has been given. The bounds of phase crossover, gain crossover and bandwidth frequencies of an interval plant has been formulated. An application of the Astrom-Hagglund controller design method to an interval plant has been given via an example.

Chapter 5

FREQUENCY RESPONSE OF SYSTEMS WITH AFFINE LINEAR UNCERTAINTY

5.1 Introduction

As mentioned in Chapter 4, several papers, motivated by the results obtained in the parametric area, have studied the computation of the frequency response of control systems under parametric uncertainty. It is also necessary to mention that a large part of the literature in the field of robust parametric control has been devoted to the robust stability analysis paradigm, rather than the robust performance paradigm. This is not because the robust performance problems of systems with parametric uncertainty have been solved, but simply because the research has had little success in this field so far. The paper by Keel and Bhattacharyya [87] addresses robust versions of the powerful graphical tools such as the Nyquist plot, Bode plot, and the Nichols chart for uncertain systems defined by an interval plant structure, where the numerator and denominator polynomial coefficients change independently, and then the problem of controller design using extensions of a classical approach. However, in practical feedback system analysis and design problems the coefficients of the plant transfer function do not necessarily vary independently.

In this chapter, the numerator and the denominator polynomials of the transfer function of a given system are assumed to be a polynomial family of the form

$$P(s,\mathbf{q}) = a_0(\mathbf{q}) + a_1(\mathbf{q})s + ... + a_n(\mathbf{q})s^n \tag{5.1}$$

whose coefficients $a_i(\mathbf{q})$ depend linearly on $\mathbf{q} = [q_1, q_2, ..., q_q]^T$ and the uncertainty box is

$$Q = \{\mathbf{q} : q_i \in [\underline{q_i}, \overline{q_i}], i = 1, 2, ..., q\} \tag{5.2}$$

where $\underline{q_i}$ and $\overline{q_i}$ are specified lower and upper bounds of the ith perturbation q_i, respectively. In other words, the system's transfer function is assumed to be

$$G(s,\mathbf{q},\mathbf{r}) = \frac{N(s,\mathbf{r})}{D(s,\mathbf{q})} = \frac{b_0(\mathbf{r}) + b_1(\mathbf{r})s + ... + b_m(\mathbf{r})s^m}{a_0(\mathbf{q}) + a_1(\mathbf{q})s + ... + a_n(\mathbf{q})s^n} \tag{5.3}$$

where $\mathbf{q} = [q_1, q_2, ..., q_q]^T \in Q$ and $\mathbf{r} = [r_1, r_2, ..., r_r]^T \in R$.

Using the method given in [116], where a simplification algorithm was given for testing the stability of a polytopic polynomial family of the form of Eq.(5.1) by constructing its $2q$-convex parpolygons (for each $s = j\omega$, the $2q$-convex parpolygon is defined as the outer edges of the image of the exposed edges ($(2^{q-1})q$ edges) of the Q-box), the amplitude and phase extremums of Eq.(5.1) at $s = j\omega^*$ ($\omega^* \in [0, \infty)$) are obtained. The amplitude and phase extremums of $P(s,\mathbf{q})$ multiplied with a fixed polynomial, $\delta(s)$, are also discussed. Once the edges of a $2q$-convex parpolygon are identified then the maximum magnitude and phase extremums of $P(s,\mathbf{q})$ at $s = j\omega^*$ can be calculated from the vertices of the $2q$-convex parpolygon. For the minimum magnitude, instead of sweeping over the edges of the $2q$-convex parpolygon, an exact equation is derived. Then, the procedures for constructing the Bode, Nyquist and Nichols envelopes of a control system defined by Eq.(5.3) are presented. Finally, using these envelopes, a controller design strategy is given. The distinguishing feature of the results given in this chapter is the efficient procedure introduced for constructing the $2q$-convex parpolygon of $P(s, \mathbf{q})$. Thus, the approach presented in this chapter allows one to eliminate some exposed edges of $N(s, \mathbf{r})$ and $D(s, \mathbf{q})$ which are not useful for constructing the Bode, Nyquist and Nichols envelopes.

The most closely related work to that of this chapter is that given in [25] and also [10, 62, 22, 23]. The boundary results for Eq.(5.3) given in [25] are based on using all the exposed edges of $N(s, \mathbf{r})$ and $D(s, \mathbf{q})$. In [10], the transfer function of the system was assumed similar to Eq.(5.3) and an angle sweeping technique was proposed in order to compute the Nichols template boundary. In [62, 22], it was assumed that the coefficients of the numerator and the denominator polynomials of Eq.(5.3) were correlated with each other and it was shown that the Nyquist envelope was contained in the set obtained by mapping the exposed edges of the uncertainty box in the complex plane. Some improvements of the results of [62] and [22] were given in [23] for computing the Bode and Nyquist envelopes of uncertain systems. Since a more general uncertainty structure has been considered in [62, 22, 23], the results of [62, 22, 23] are to date the best known results. However, the exponential growth of the edges with respect to the number of uncertain parameters can lead to serious computational difficulties. On the other hand, as is stated above, a novel feature of the approach given in this chapter is the use of the $2q$-convex parpolygonal value set. Therefore, if the given plant has the structure of Eq.(5.3) then the results of this chapter can be more helpful than existing results for computing the Bode, Nyquist and Nichols envelopes.

The outline of the chapter is as follows: In Section 5.2 the construction of the $2q$-convex parpolygon is given. The magnitude and phase extremums of Eq.(5.1) are obtained in Section 5.3 and the construction of the Bode, Nyquist and Nichols envelopes of a control system with an uncertain transfer function of the form of Eq.(5.3) are discussed in Section 5.4. Section 5.5 deals with the computation of the robust gain and phase margins of $G(s, \mathbf{q}, \mathbf{r})$. In Section 5.6, examples are given to illustrate the benefits of the method presented. Section 5.7 gives concluding remarks.

5.2 Construction of 2q-Convex Parpolygon

In Chapter 2, it was stated that the corresponding polytope of a family of polynomials of Eq.(5.1) in the coefficient space has 2^q vertices and $(2^{q-1})q$ exposed edges [13] and it can be rewritten as

$$P(s,\mathbf{q}) = f_0(s) + f_1(s)q_1 + f_2(s)q_2 + f_3(s)q_3 + ... + f_q(s)q_q, \quad \mathbf{q}{\in}Q \tag{5.4}$$

The 2^q vertex polynomials of the polytope of $P(s,\mathbf{q})$ can be written in the following pattern

$$\begin{aligned}
c_1(s,\mathbf{q}) &= f_0(s) + f_1(s)\underline{q_1} + f_2(s)\underline{q_2} + f_3(s)\underline{q_3} + ... + f_q(s)\underline{q_q} \\
c_2(s,\mathbf{q}) &= f_0(s) + f_1(s)\overline{q_1} + f_2(s)\underline{q_2} + f_3(s)\underline{q_3} + ... + f_q(s)\underline{q_q} \\
c_3(s,\mathbf{q}) &= f_0(s) + f_1(s)\underline{q_1} + f_2(s)\overline{q_2} + f_3(s)\underline{q_3} + ... + f_q(s)\underline{q_q} \\
&\cdots \\
&\cdots \\
c_{2^q}(s,\mathbf{q}) &= f_0(s) + f_1(s)\overline{q_1} + f_2(s)\overline{q_2} + f_3(s)\overline{q_3} + ... + f_q(s)\overline{q_q}
\end{aligned} \tag{5.5}$$

The value set of Eq.(5.1) can be obtained by mapping the $(2^{q-1})q$ exposed edges in the complex plane for each $s = j\omega$ and the outer edges of the value set define a $2q$-convex parpolygon. The $(2^{q-1})q$ edges in the complex plane can be divided into q groups where each group has the same number of edges (2^{q-1} edges) [116]. All edges in group i ($i = 1, 2, ..., q$) are parallel to each other with the same slope. Thus, knowing one edge from each group is sufficient to construct the $2q$-convex parpolygon. For example, let $e(c_i, c_j)$ denote the edge with end points c_i and c_j and for clarity of presentation consider Figure 5.1a which is the image of the exposed edges of a polytope with $q = 3$ parameters. It can be easily shown that the edges $e(c_1, c_2)$, $e(c_3, c_4)$, $e(c_5, c_6)$ and $e(c_7, c_8)$ are parallel to each other as shown in Figure 5.1a. Two of them which have the maximum and minimum intersections with the imaginary axis identify two edges of a $2q$-convex parpolygon as shown in Figure 5.1. Similarly, the other edges needed for construction of the $2q$-convex parpolygon can be identified. If there are vertical edges which have no intersection with the imaginary axis, in this case from the maximum and the minimum intersections with the

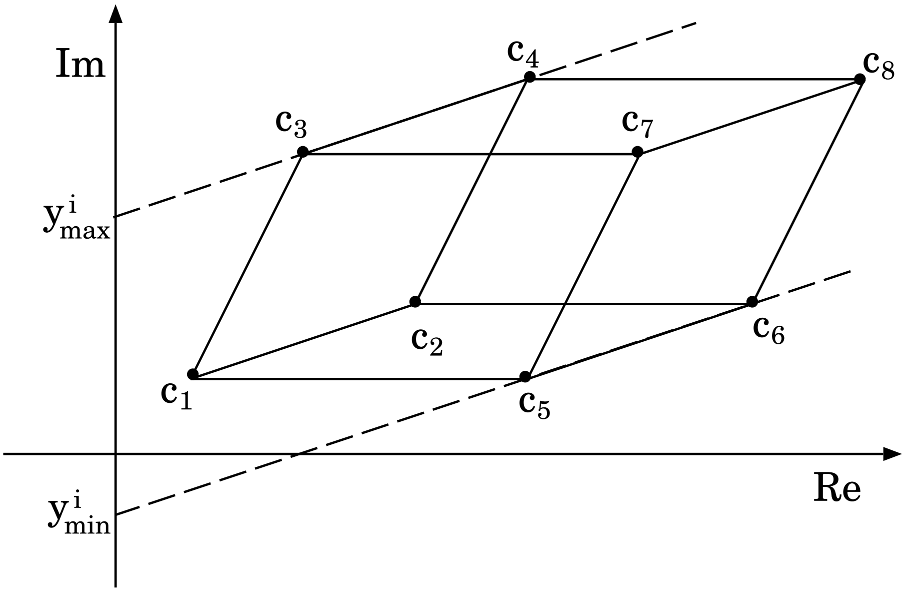

(a)

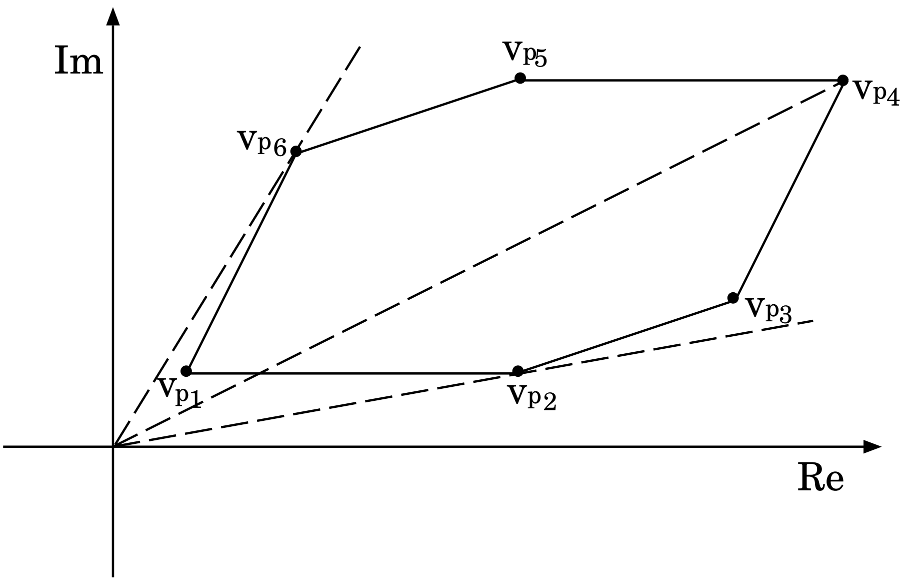

(b)

Figure 5.1: a) Image of exposed edges b) $2q$-convex parpolygon

real axis, the two required edges can be found. A general formula [116] for the intersection point of the edge line with the imaginary axis is

$$y^i = \frac{\omega}{E_i} \sum_{k=1}^{q} (O_k E_i - O_i E_k)(q_k - \underline{q_k}),\ k \neq i \tag{5.6}$$

and with the real axis is

$$x^i = \frac{1}{O_i} \sum_{k=1}^{q} (O_i E_k - O_k E_i)(q_k - \underline{q_k}),\ k \neq i \tag{5.7}$$

where $i = 1, 2, ..., q$, q_k takes either $\underline{q_k}$ or $\overline{q_k}$ depending on which edge it is associated with and E_i and O_i are the even and odd parts of $f_i(s)$. Further information about the value set of the uncertain polynomials and the construction of the $2q$-convex parpolygon can be found in [13] and [116].

For different values of frequency, the edges of a $2q$-convex parpolygon may be different. The following theorem is given in order to divide the frequency axis, $\omega \in [0, \infty)$, into a finite number of intervals where in each interval the edges of the $2q$-convex parpolygon remain the same.

Theorem 5.1: The positive real roots of

$$Re[f_i]Im[f_j] - Re[f_j]Im[f_i] = 0,\ i, j = 1, 2, ..., q, i \neq j \tag{5.8}$$

divide the frequency axis into finite intervals where in each interval the $2q$ edges of the $(2^{q-1})q$ exposed edges which constitute the outer boundary of the convex parpolygon remain unchanged. The frequencies where the outer edges of the convex parpolygon may change will be referred to as *transition frequencies.*

Proof: It is clear that when the frequency changes, the value of $f_i(j\omega)$, $i = 0, 1, 2, ..., q$ changes and this may lead to a change of the specific subset of $(2^{q-1})q$ edges which constitute the $2q$-convex parpolygon. The *transition frequency*, where the image of an edge of a Q-box changes from the boundary into the interior and vice versa, occurs when the phases of two of $f_i(j\omega)$, $i = 1, 2, ..., q$ are equal to each other [1]. Thus, at a *transition frequency*

$$arg[f_i(j\omega)] = arg[f_j(j\omega)],\ i, j = 1, 2, ..., q \ and\ i \neq j \tag{5.9}$$

or

$$tan^{-1}(\frac{Im[f_i]}{Re[f_i]}) = tan^{-1}(\frac{Im[f_j]}{Re[f_j]}), \quad i,j = 1,2,...,q \ \ and \ \ i{\neq}j \tag{5.10}$$

From Eq.(5.10), the following equation

$$Re[f_i]Im[f_j] - Re[f_j]Im[f_i] = 0 \tag{5.11}$$

is obtained. □

Remark 5.1: This theorem is not new. Indeed, a similar result is given in [116]. However, the proof given here is based on the condition which may lead to the change of the edges of the $2q$-convex parpolygon explained in the book by Ackermann [1, pp. 137]. Therefore, it may be considered as an alternative proof.

Example 5.1

Consider

$$P(s,\mathbf{q}) = q_5 s^4 + q_4 s^3 + (q_2 + q_3)s^2 + (q_1 + 0.5q_2 + q_3)s + q_1 \tag{5.12}$$

$$Q = \{\mathbf{q} : q_1{\in}[0.965, 1.035], q_2{\in}[0.59, 0.73], q_3{\in}[0.5, 0.65], q_4{\in}[0.33, 0.41], q_5{\in}[0.02, 0.072]\} \tag{5.13}$$

From theorem 5.1 it was computed that there was no *transition frequency* for $P(s,\mathbf{q})$ of Eq.(5.12). Thus, one single value of frequency within $\omega{\in}(0,\infty)$ is sufficient to identify the edges of the $2q$-convex parpolygons of $P(s,\mathbf{q})$. For example, writing Eq.(5.6) for $i = 1$

$$y^1 = \omega[(0.5 + \omega^2)(q_2 - \underline{q_2}) + (1 + \omega^2)(q_3 - \underline{q_3}) - \omega^4(q_4 - \underline{q_4}) - \omega^4(q_5 - \underline{q_5})] \tag{5.14}$$

and from this equation the maximum value of y^1 occurs for any value of $\omega{\in}(0,\infty)$ when $q_2 = \overline{q_2}$, $q_3 = \overline{q_3}$, $q_4 = \underline{q_4}$, $q_5 = \underline{q_5}$ and the minimum occurs for $q_2 = \underline{q_2}$, $q_3 = \underline{q_3}$, $q_4 = \overline{q_4}$, $q_5 = \overline{q_5}$. So, the edges $e(c_7, c_8)$ and $e(c_{25}, c_{26})$, (here, c_7, c_8, c_{25}, ... are the vertex polynomials of the polytope of $P(s,\mathbf{q})$ which constitute the edges of a $2q$-convex parpolygon and they can be obtained by using Eq.(5.5)), are the two outer edges of the convex parpolygon. Similarly, the other edges, $e(c_{22}, c_{24})$, $e(c_9, c_{11})$, $e(c_{18}, c_{22})$, $e(c_{11}, c_{15})$, $e(c_{18}, c_{26})$, $e(c_7, c_{15})$, $e(c_8, c_{24})$ and $e(c_9, c_{25})$, are found to constitute the boundary of the $2q$-convex parpolygons of $P(s,\mathbf{q})$. Thus for all $\omega{\in}(0,\infty)$, the set of the vertex polynomials is

$$
\begin{aligned}
S_{P_V} \; = \; & \{0.02s^4+0.33s^3+1.38s^2+1.98s+0.965, 0.02s^4+0.33s^3+1.38s^2+2.05s+1.035, \\
& 0.072s^4+0.33s^3+1.38s^2+2.05s+1.035, 0.072s^4+0.33s^3+1.24s^2+1.98s+1.035, \\
& 0.072s^4+0.33s^3+1.09s^2+1.83s+1.035, 0.072s^4+0.41s^3+1.09s^2+1.83s+1.035, \\
& 0.072s^4+0.41s^3+1.09s^2+1.76s+0.965, 0.02s^4+0.41s^3+1.09s^2+1.76s+0.965, \\
& 0.02s^4+0.41s^3+1.23s^2+1.83s+0.965, 0.02s^4+0.41s^3+1.38s^2+1.98s+0.965\} \quad (5.15)
\end{aligned}
$$

and the set of edge polynomials is

$$
\begin{aligned}
S_{P_E} = & \{0.02s^4+0.33s^3+1.38s^2+(1.98+0.07\lambda)s+(0.965+0.07\lambda), \\
& (0.02+0.052\lambda)s^4+0.33s^3+1.38s^2+2.05s+1.035, \\
& 0.072s^4+0.33s^3+(1.24+0.14\lambda)s^2+(1.98+0.07\lambda)s+1.035, \\
& 0.072s^4+0.33s^3+(1.09+0.15\lambda)s^2+(1.83+0.15\lambda)s+1.035, \\
& 0.072s^4+(0.33+0.08\lambda)s^3+1.09s^2+1.83s+1.035, \\
& 0.072s^4+0.41s^3+1.09s^2+(1.76+0.07\lambda)s+(0.965+0.07\lambda), \\
& (0.02+0.052\lambda)s^4+0.41s^3+1.09s^2+1.76s+0.965, \\
& 0.02s^4+0.41s^3+(1.09+0.14\lambda)s^2+(1.76+0.07\lambda)s+0.965, \\
& 0.02s^4+0.41s^3+(1.23+0.15\lambda)s^2+(1.83+0.15\lambda)s+0.965, \\
& 0.02s^4+(0.33+0.08\lambda)s^3+1.38s^2+1.98s+0.965\} \qquad (5.16)
\end{aligned}
$$

Since the polynomial of Eq.(5.12) has $q = 5$ uncertain parameters, the value set at each frequency is contained in the image of $2q = 10$ edges, which are given by Eq.(5.16). Using these edge polynomials, the value set of $P(s, \mathbf{q})$ can be constructed. The $2q$-convex parpolygons of $P(s, \mathbf{q})$ for $\omega \in [0, 3]$ are shown in Figure 5.2

5.3 Magnitude and Phase Extremums of $P(s, \mathbf{q})$ and $\delta(s)P(s, \mathbf{q})$

In this section, the magnitude and phase extremums of an uncertain polynomial family, $P(s, \mathbf{q})$ of Eq.(5.1), at $s = j\omega^*$ are first investigated. Then, the magnitude and phase extremums of $P(s, \mathbf{q})$ multiplied by a fixed polynomial, $\delta(s)$, are obtained. These results

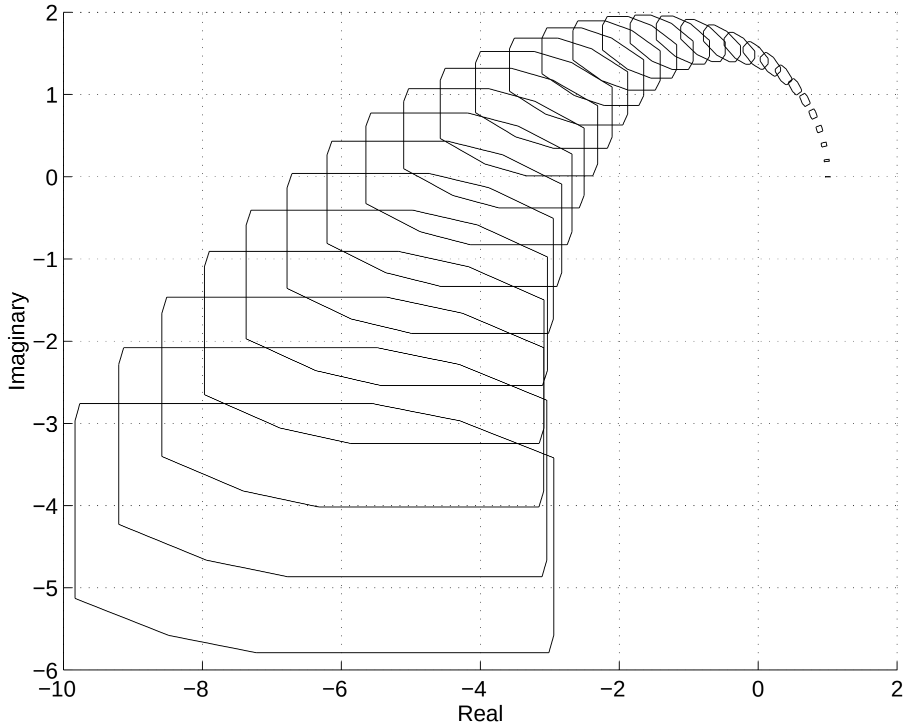

Figure 5.2: $2q$-convex parpolygons for the polynomial of Eq.(5.12)

will be used in the next section in order to develop the robust versions of the frequency-domain analysis and design tools such as the Nyquist, Bode and Nichols envelopes for the transfer function of Eq.(5.3).

5.3.1 Magnitude and Phase Extremums of $P(s, \mathbf{q})$

Let the $2q$ vertices of the $2q$-convex parpolygon of $P(s, \mathbf{q})$ at $s = j\omega^*$ be v_{p1}, v_{p2}, v_{p3}, ..., v_{p2q} (see Figure 5.1b). Then,

Theorem 5.2: The maximum magnitude of $P(s, \mathbf{q})$ at $s = j\omega^*$ is

$$max|P(j\omega^*, \mathbf{q})| = max(|v_{p1}|, |v_{p2}|, |v_{p3}|, ..., |v_{p2q}|) \tag{5.17}$$

and the phase extremums of $P(j\omega^*, \mathbf{q})$ are

$$\begin{aligned} minarg[P(j\omega^*, \mathbf{q})] &= min(arg[v_{p1}], arg[v_{p2}], arg[v_{p3}], ..., arg[v_{p2q}]) \\ maxarg[P(j\omega^*, \mathbf{q})] &= max(arg[v_{p1}], arg[v_{p2}], arg[v_{p3}], ..., arg[v_{p2q}]) \end{aligned} \tag{5.18}$$

Proof: The proof of this theorem follows in a straightforward manner from the geometric structure of the value set of $P(s, \mathbf{q})$ at $s = j\omega^*$. Since the value set of $P(j\omega^*, \mathbf{q})$ is contained in a $2q$-convex parpolygon, the maximum distance from the origin to the point which belongs to the parpolygon edges is achieved at a corner of the $2q$-convex parpolygon and the phase extremums will be on the vertices of the $2q$-convex parpolygon (see Figure 5.1b). $\square$

To find the minimum magnitude, the following theorem is given,

Theorem 5.3: Define

$$|v_{pi}| = min(|v_{p1}|, |v_{p2}|, |v_{p3}|, ..., |v_{p2q}|) \tag{5.19}$$

where $i = 1, 2, 3, ..., 2q$. Considering Figure 5.3a let $e(v_{pi}, v_{px})$ and $e(v_{pi}, v_{py})$ be two edges of the $2q$-convex parpolygon which have the common vertex v_{pi}. Let ϕ_{pi}, ϕ_{px} and ϕ_{py} be the angles of v_{pi}, v_{px} and v_{py} respectively. Draw the lines l_1 and l_2 which pass through the points (v_{px}, v_{pi}) and (v_{py}, v_{pi}). Let ϕ_{h_1} and ϕ_{h_2} be the angles of the lines h_1 and h_2 which are drawn from the origin and are perpendicular to the lines l_1 and l_2, respectively. Assume also that the $2q$-convex parpolygon does not include the origin (if the value set includes the origin for $s = j\omega^*$ then the minimum magnitude is equal to zero). Then,

$$min|P(j\omega^*, \mathbf{q})| = \begin{cases} |v_{pi}| & \text{if } \phi_{h_1} \notin (\phi_{pi}, \phi_{px}) \& \phi_{h_2} \notin (\phi_{py}, \phi_{pi}) \\ \frac{\sigma_1}{2\rho_1} & \text{if } \phi_{h_1} \in (\phi_{pi}, \phi_{px}) \\ \frac{\sigma_2}{2\rho_2} & \text{if } \phi_{h_2} \in (\phi_{py}, \phi_{pi}) \end{cases} \tag{5.20}$$

where

$$\begin{aligned} \sigma_1 &= [(2|v_{pi}|\rho_1)^2 - (|v_{pi}|^2 - |v_{px}|^2 + \rho_1^2)^2]^{1/2} \\ \sigma_2 &= [(2|v_{pi}|\rho_2)^2 - (|v_{pi}|^2 - |v_{py}|^2 + \rho_2^2)^2]^{1/2} \\ \rho_1 &= [(Re[v_{px}] - Re[v_{pi}])^2 + (Im[v_{px}] - Im[v_{pi}])^2]^{1/2} \\ \rho_2 &= [(Re[v_{py}] - Re[v_{pi}])^2 + (Im[v_{py}] - Im[v_{pi}])^2]^{1/2} \end{aligned} \tag{5.21}$$

Proof: First of all, the minimum magnitude of $P(s, \mathbf{q})$ at $s = j\omega^*$ should be achieved at the edges of a $2q$-convex parpolygon. If $|v_{pi}| = min(|v_{p1}|, |v_{p2}|, ..., |v_{p2q}|)$ at $s = j\omega^*$, geometrically the $min|P(j\omega^*, \mathbf{q})|$ must be on the edge $e(v_{pi}, v_{py})$ or $e(v_{pi}, v_{px})$. From the figure, it is seen that $\phi_{h_2} \notin (\phi_{py}, \phi_{pi})$ so it is not possible that the edge, $e(v_{pi}, v_{py})$, has a point whose magnitude is smaller than $|v_{pi}|$. However, since $\phi_{h_1} \in (\phi_i, \phi_x)$, it is possible that the edge, $e(v_{pi}, v_{px})$, has a point whose magnitude is less than $|v_{pi}|$ and it can be calculated as

$$\rho_1 = [(Re[v_{px}] - Re[v_{pi}])^2 + (Im[v_{px}] - Im[v_{pi}])^2]^{1/2} \tag{5.22}$$

$$|v_{px}|^2 - (\rho_1 - \tau)^2 = |v_{pi}|^2 - \tau^2 \tag{5.23}$$

From Eqs.(5.22-5.23)

$$\begin{gathered} min|P(j\omega^*, \mathbf{q})| = h_1 = [|v_{pi}|^2 - \tau^2]^{1/2} = \frac{\sigma_1}{2\rho_1} = \\ \frac{[(2|v_{pi}|\rho_1)^2 - (|v_{pi}|^2 - |v_{px}|^2 + \rho_1^2)^2]^{1/2}}{2[(Re[v_{px}] - Re[v_{pi}])^2 + (Im[v_{px}] - Im[v_{pi}])^2]^{1/2}} \quad \square \end{gathered} \tag{5.24}$$

The application of this theorem, however, may give some difficulties, since for each frequency, one needs to find the lines l_1, l_2, h_1 and h_2 and the phases ϕ_{pi}, ϕ_{px}, ϕ_{py}, ϕ_{h1} and ϕ_{h2}. Therefore, an equivalent result which is easily applied is given by the following lemma.

Lemma 5.1: Define the segments

$$s_1 = (1 - \lambda)v_{pi} + \lambda v_{px}, \quad s_2 = (1 - \lambda)v_{pi} + \lambda v_{py} \tag{5.25}$$

where $\lambda \in [0, 1]$. Take a value for λ, say λ^*, which is very close to zero such as $0 < \lambda^* \leq 10^{-6}$ and write

$$k_1 = (1 - \lambda^*)v_{pi} + \lambda^* v_{px}, \quad k_2 = (1 - \lambda^*)v_{pi} + \lambda^* v_{py} \tag{5.26}$$

Then, the minimum magnitude of $P(s, \mathbf{q})$ at $s = j\omega^*$ is

$$min|P(j\omega^*, \mathbf{q})| = \begin{cases} |v_{pi}| & \text{if } |v_{pi}| < |k_1| \& |v_{pi}| < |k_2| \\ \frac{\sigma_1}{2\rho_1} & \text{if } |k_1| < |v_{pi}| \\ \frac{\sigma_2}{2\rho_2} & \text{if } |k_2| < |v_{pi}| \end{cases} \tag{5.27}$$

where σ_1, σ_2, ρ_1 and ρ_2 are given in Eq.(5.21) and $|v_{pi}|$ is defined by Eq.(5.19).

Proof: The proof of this lemma is similar to the proof of theorem 5.3. Here, instead of using the lines l_1 and l_2 and corresponding perpendicular lines h_1 and h_2, we can calculate the minimum magnitude of $P(j\omega^*, \mathbf{q})$ by choosing the points k_1 and k_2 on the edges $e(v_{pi}, v_{px})$ and $e(v_{pi}, v_{py})$ and checking the magnitude of these points. Of course, the points k_1 and k_2 must be very close to the point v_{pi}. In other words, we have to assume that , it is not possible to draw a perpendicular line to the edge $e(v_{pi}, k_1)$ or $e(v_{pi}, k_2)$ which passes through the origin. Therefore, by taking the value of λ^* very close to zero, this assumption can be fulfilled. From Figure 5.3b, since $|k_1| < |v_{pi}|$, the minimum magnitude is

$$min|P(j\omega^*, \mathbf{q})| = h = [|v_{pi}|^2 - \tau^2]^{1/2} = \frac{\sigma_1}{2\rho_1}$$

Likewise, when $|k_2| < |v_{pi}|$, the related equation for the minimum magnitude can be derived. $\square$

Remark 5.2: For $s = j\omega^*$, if $|v_{px}| = |v_{pi}| = min(|v_{p1}|, |v_{p2}|, ..., |v_{p2q}|)$ where $i, x = 1, 2, ..., 2q$ and $i \neq x$, in this case, the minimum magnitude of $P(j\omega^*, \mathbf{q})$ will be on the edge $e(v_{px}, v_{pi})$ and its value is

$$min|P(j\omega^*, \mathbf{q})| = \frac{\sigma_1}{2\rho_1} = \frac{[(2|v_{pi}|)^2 - \rho_1^2]^{1/2}}{2} \tag{5.28}$$

5.3.2 Magnitude and Phase Extremums of $\delta(s)P(s, \mathbf{q})$

The magnitude and phase extremums of an uncertain polynomial $P(s, \mathbf{q})$ multiplied with a fixed polynomial $\delta(s) = \delta_0 + \delta_1 s + ... + \delta_n s^n$ at $s = j\omega^*$ are given by the following theorem:

Theorem 5.4: The magnitude and phase extremums of $\delta(s)P(s, \mathbf{q})$ at $s = j\omega^*$ are

$$\begin{aligned} min|\delta(j\omega^*)P(j\omega^*, \mathbf{q})| &= |\delta(j\omega^*)|min|P(j\omega^*, \mathbf{q})| \\ max|\delta(j\omega^*)P(j\omega^*, \mathbf{q})| &= |\delta(j\omega^*)|max|P(j\omega^*, \mathbf{q})| \end{aligned} \tag{5.29}$$

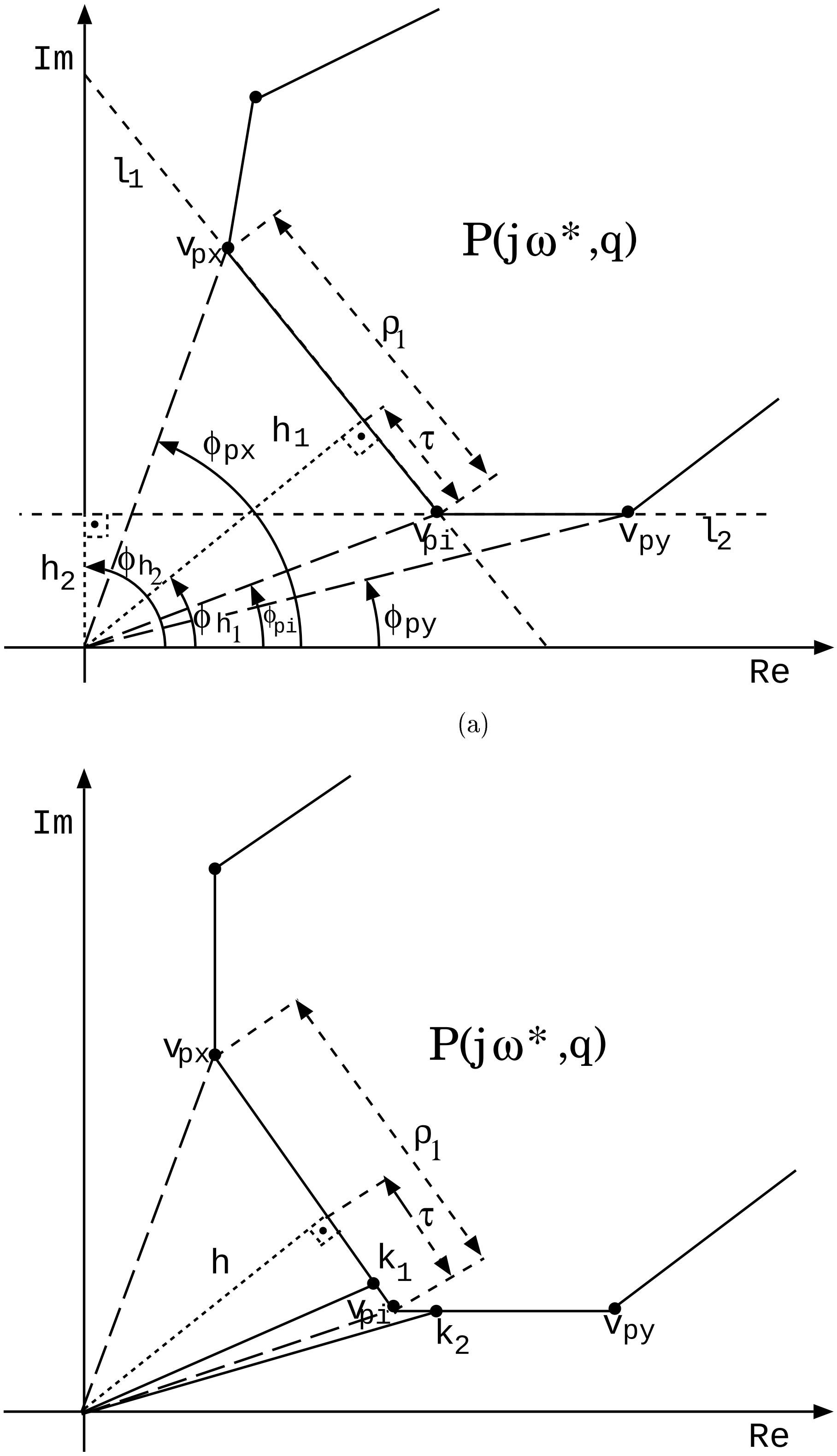

(a)

(b)

Figure 5.3: $2q$-convex parpolygon of $P(s, \mathbf{q})$ at $s = j\omega^*$

$$minarg[\delta(j\omega^*)P(j\omega^*,\mathbf{q})] = arg[\delta(j\omega^*)] + minarg[P(j\omega^*,\mathbf{q})]$$
$$maxarg[\delta(j\omega^*)P(j\omega^*,\mathbf{q})] = arg[\delta(j\omega^*)] + maxarg[P(j\omega^*,\mathbf{q})] \qquad (5.30)$$

Proof: For $s = j\omega^*$, $\delta(s)$ can be written as

$$\delta(j\omega^*) = M(\omega^*)e^{j\theta(\omega^*)} \qquad (5.31)$$

where $M(\omega^*) = (Re[\delta(j\omega^*)]^2 + Im[\delta(j\omega^*)]^2)^{1/2}$ and $\theta(\omega^*) = tan^{-1}[Im(\delta(j\omega^*))/Re(\delta(j\omega^*))]$. Thus, geometrically, the effect of multiplying $P(j\omega^*,\mathbf{q})$ by $\delta(j\omega^*) = M(\omega^*)e^{j\theta(\omega^*)}$ is to rotate and scale the value set of $P(s,\mathbf{q})$ at $s = j\omega^*$, but not to distort its shape. Therefore, the value set of $\delta(j\omega^*)P(j\omega^*,\mathbf{q})$ is still a $2q$-convex parpolygon. So, from the results obtained in Section 5.3.1, the magnitude and phase extremums of $\delta(s)P(s,\mathbf{q})$ can be computed using Eqs.(5.29-5.30). $\square$

5.4 Bode, Nyquist and Nichols Envelopes

In this section, the construction of the Bode, Nyquist and Nichols envelopes of a given uncertain transfer function of the form of Eq.(5.3) is discussed. Throughout this section, it is assumed that $0 \notin D(s,\mathbf{q})$. If this assumption fails to hold one can exclude the values of the frequencies which violate the assumption. Now, consider the transfer function given in Eq.(5.3) and let v_{n1}, v_{n2}, v_{n3}, ..., v_{n2r} and v_{d1}, v_{d2}, v_{d3}, ..., v_{d2q} be the vertices of the $2r$ and $2q$-convex parpolygons of $N(s,\mathbf{r})$ and $D(s,\mathbf{q})$ at $s = j\omega^*$. Then define the sets S_{N_V} and S_{N_E} which contain the vertices and the edges of the $2r$-convex parpolygon of $N(s,\mathbf{r})$ at $s = j\omega^*$ as

$$S_{N_V} = \{v_{n1}, v_{n2}, ..., v_{n2r}\} \qquad (5.32)$$

$$S_{N_E} = \{e_{n1}, e_{n2}, ..., e_{n2r}\} = \{(1-\lambda)v_{n1} + \lambda v_{n2}, (1-\lambda)v_{n2} + \lambda v_{n3}, ..., (1-\lambda)v_{n2r} + \lambda v_{n1}\}, \lambda \in [0,1] \qquad (5.33)$$

similarly define S_{D_V} and S_{D_E} for the denominator as

$$S_{D_V} = \{v_{d1}, v_{d2}, ..., v_{d2q}\} \qquad (5.34)$$

$$S_{D_E} = \{e_{d1}, e_{d2}, ..., e_{d2q}\} = \{(1-\lambda)v_{d1}+\lambda v_{d2}, (1-\lambda)v_{d2}+\lambda v_{d3}, ..., (1-\lambda)v_{d2q}+\lambda v_{d1}\}, \lambda\in[0,1] \tag{5.35}$$

Then, the magnitude and phase extremums of $G(s, \mathbf{q}, \mathbf{r})$ at $s = j\omega^*$ can be found by the following theorem

Theorem 5.5: The magnitude extremums of $G(s, \mathbf{q}, \mathbf{r})$ at $s = j\omega^*$ are

$$max|G(j\omega^*, \mathbf{q}, \mathbf{r})| = \frac{max|N(j\omega^*, \mathbf{r})|}{min|D(j\omega^*, \mathbf{q})|} = \frac{max_{v_{ni}\in S_{N_V}}|v_{ni}|}{min_{e_{dj}\in S_{D_E}}|e_{dj}|} \tag{5.36}$$

$$min|G(j\omega^*, \mathbf{q}, \mathbf{r})| = \frac{min|N(j\omega^*, \mathbf{r})|}{max|D(j\omega^*, \mathbf{q})|} = \frac{min_{e_{ni}\in S_{N_E}}|e_{ni}|}{max_{v_{dj}\in S_{D_V}}|v_{dj}|} \tag{5.37}$$

and the phase extremums are

$$\begin{aligned} maxarg[G(j\omega^*, \mathbf{q}, \mathbf{r})] &= maxarg[N(j\omega^*, \mathbf{r})] - minarg[D(j\omega^*, \mathbf{q})] \\ &= maxarg_{v_{ni}\in S_{N_V}}[v_{ni}] - minarg_{v_{dj}\in S_{D_V}}[v_{dj}] \end{aligned} \tag{5.38}$$

$$\begin{aligned} minarg[G(j\omega^*, \mathbf{q}, \mathbf{r})] &= minarg[N(j\omega^*, \mathbf{r})] - maxarg[D(j\omega^*, \mathbf{q})] \\ &= minarg_{v_{ni}\in S_{N_V}}[v_{ni}] - maxarg_{v_{dj}\in S_{D_V}}[v_{dj}] \end{aligned} \tag{5.39}$$

where $i = 1, 2, ..., 2r$ and $j = 1, 2, ..., 2q$.

Proof: The proof of this theorem follows immediately from the results of the previous section. Since at each frequency, the value sets of $N(s, \mathbf{r})$ and $D(s, \mathbf{q})$ are contained in $2r$ and $2q$-convex parpolygons, the magnitude and phase extremums of $G(s, \mathbf{q}, \mathbf{r})$ can be found from the magnitude and phase extremums of the $2r$ and $2q$-convex parpolygons. □

For the computation of the Nyquist and Nichols envelopes of the transfer function of Eq.(5.3), it has been shown in [25, pp. 362-363] that $\partial G(s, \mathbf{q}, \mathbf{r})\subset G_E(s)$ where ∂ denotes the boundary and

$$G_E(s) = \{G(s, \alpha) : \alpha\in\Omega_E\} \tag{5.40}$$

where $\alpha = [q_1, q_2, ..., q_q, r_1, r_2, ..., r_r]^T$ denotes the parameter vector and Ω_E denotes the exposed edges of the uncertainty polytope $\Omega = \{\alpha : q_i\in[\underline{q_i}, \overline{q_i}], r_j\in[\underline{r_j}, \overline{r_j}], i = 1, 2, ..., q, j =$

$1, 2, ..., r\}$. However, it is clear that the uncertainty polytope, Ω, has $(2^{(q+r)-1})(q+r)$ exposed edges. By using the $2q$-convex parpolygonal value set of a polynomial family of Eq.(5.1), the following theorem, which is not computationally expensive, is given

Theorem 5.6: At $s = j\omega^*$,

$$\partial G(j\omega^*, \mathbf{q}, \mathbf{r}) \subset G_E(j\omega^*) = \frac{S_{N_V}}{S_{D_E}} \cup \frac{S_{N_E}}{S_{D_V}} \tag{5.41}$$

where ∂ denotes the boundary and S_{N_V}, S_{N_E}, S_{D_V} and S_{D_E} are defined in Eqs.(5.32-5.35).

Proof: Let A and B be the two complex plane polygons with vertex sets S_{A_V} and S_{B_V}, and edge sets S_{A_E} and S_{B_V}, respectively. Then, from the complex plane geometry, the following is known [25, pp. 335]:

$$\partial(\frac{A}{B}) \subset (\frac{S_{A_V}}{S_{B_E}} \cup \frac{S_{A_E}}{S_{B_V}}) \tag{5.42}$$

Since the value set of the numerator $N(s, \mathbf{r})$ and the denominator $D(s, \mathbf{q})$ of Eq.(5.3) at $s = j\omega^*$ are independent $2r$ and $2q$-convex parpolygons, we can write

$$S_{A_V} = S_{N_V},\ S_{B_V} = S_{D_V},\ S_{A_E} = S_{N_E},\ S_{B_E} = S_{D_E}$$

Thus,

$$\partial G(j\omega^*, \mathbf{q}, \mathbf{r}) \subset \frac{S_{N_V}}{S_{D_E}} \cup \frac{S_{N_E}}{S_{D_V}} = G_E(j\omega^*) \quad \square \tag{5.43}$$

A more generalized version of theorem 5.6 which will be essential for the computation of the robust gain and phase margins can be given under the assumption of no *transition frequency* (a discussion on this assumption can be found in Chapter 6). Assume that neither $N(s, \mathbf{r})$ nor $D(s, \mathbf{q})$ has any *transition frequency.* This assumption guarantees that the identified edges for a single frequency which constitute the $2r$ and $2q$-convex parpolygons remain unchanged for all $\omega \in (0, \infty)$. Thus an extremal subset which characterizes the boundary of the Nyquist envelope for all frequencies can be obtained. This is given as follows:

Theorem 5.7: Assume that neither $N(s, \mathbf{r})$ nor $D(s, \mathbf{q})$ has any *transition frequency.* Then,

$$\partial G(j\omega, \mathbf{q}, \mathbf{r}) \subset G_E(j\omega) = \frac{S_{N_V}}{S_{D_E}} \cup \frac{S_{N_E}}{S_{D_V}} \tag{5.44}$$

where ∂ denotes the boundary and S_{N_V}, S_{N_E}, S_{D_V} and S_{D_E} are defined in Eqs.(5.32-5.35).

The results of Section 5.2 enable one to identify the edges which constitute a $2q$-convex parpolygon of a polynomial family of Eq.(5.1). Therefore, the advantage of the results presented is that it is not necessary to consider all the exposed edges and vertices of the corresponding polytopes of the numerator and denominator polynomials. For example, in order to find a Nyquist template of a transfer function of Eq.(5.3) with $r = 4$ and $q = 5$ uncertain parameters then using known results one needs to find the image of $9(2^8) = 2304$ edges, however, from theorem 5.6, one needs to find the image of only 160 edges.

The following procedure is given to compute the Bode, Nyquist and Nichols envelopes of $G(s, \mathbf{q}, \mathbf{r})$

1. Rewrite $N(s, \mathbf{r})$ and $D(s, \mathbf{q})$ in the form of Eq.(5.4).

2. Solve Eq.(5.8) both for $N(s, \mathbf{r})$ and $D(s, \mathbf{q})$ and find the *transition frequencies* of $N(s, \mathbf{r})$ and $D(s, \mathbf{q})$.

3. Obtain the frequency intervals, within these intervals the edges of the $2r$ and $2q$-convex parpolygons of $N(s, \mathbf{r})$ and $D(s, \mathbf{q})$ remain unchanged, as

$$(0, \omega_{n1}), (\omega_{n1}, \omega_{n2}), ..., (\omega_{n\epsilon 1}, \infty) \ for \ N(s, \mathbf{r})$$

$$(0, \omega_{d1}), (\omega_{d1}, \omega_{d2}), ..., (\omega_{d\epsilon 2}, \infty) \ for \ D(s, \mathbf{q})$$

where $\omega_{n1} < \omega_{n2} < ... < \omega_{n\epsilon 1}$ and $\omega_{d1} < \omega_{d2} < ... < \omega_{d\epsilon 2}$ are the *transition frequencies* of $N(s, \mathbf{r})$ and $D(s, \mathbf{q})$, respectively.

4. Choose an arbitrary value of frequency within each interval found in **3** and by using Eqs.(5.6-5.7), identify the $2r$ and $2q$-convex parpolygons edges and obtain the vertex and edge sets (S_{N_V}, S_{N_E}, S_{D_V} and S_{D_E}) of the numerator and the denominator polynomials for each interval.

5. For each $s = j\omega$, using the sets (S_{N_V}, S_{N_E}, S_{D_V} and S_{D_E}) found in **4** and the results given in Section 5.3 and in this section, obtain the Bode, Nyquist and Nichols envelopes.

Remark 5.3: The results of this section can be extended to a system with a fixed controller and a transfer function given by Eq.(5.3). From Section 5.3.2 it has been seen that the value set of an uncertain polynomial of the form of Eq.(5.1) multiplied with a fixed polynomial at $s = j\omega^*$ is still a $2q$-convex parpolygon. Also, the procedures given above can be used for computing the frequency response of the more general uncertainty structure such as $G(s, \mathbf{q}{\in}Q) = N(s, \mathbf{q})/D(s, \mathbf{q})$ (the numerator and the denominator coefficients are correlated with each other) by defining new uncertainty boxes for the numerator and the denominator polynomials. However, the result will be conservative.

5.5 Robust Gain and Phase Margins

As stated in Chapter 4, the gain and phase margins are two important frequency domain specifications. This section deals with the calculation of the robust gain and phase margins for systems with an uncertain transfer function of the form of Eq.(5.3) using the theory presented in the previous sections.

Suppose that a closed loop system with an uncertain plant of the form of Eq.(5.3) is stable then the robust gain margin is the largest value of the gain K greater than 1 for which the stability of $KG(s, \mathbf{q}, \mathbf{r})$ is preserved and the robust phase margin is the largest value of phase θ for which the uncertain system with $e^{-j\theta}G(s, \mathbf{q}, \mathbf{r})$ is robustly stable. Thus, the worst case gain margin K^* and phase margin θ^* can be stated as

$$K^* = inf_{G(s)\in G(s,\mathbf{q},\mathbf{r})} K_G, \quad \theta^* = inf_{G(s)\in G(s,\mathbf{q},\mathbf{r})} \theta_G \tag{5.45}$$

where K_G stands for gain margin of $G(s)$ and θ_G stands for phase margin of $G(s)$.

Using the following theorem, the values of K^* and θ^* can be computed from the extremal system, $G_E(s)$ of Eq.(5.44).

Theorem 5.8: Suppose a unity feedback system with $G(s, \mathbf{q}, \mathbf{r})$ is stable and assume that neither $N(s, \mathbf{r})$ nor $D(s, \mathbf{q})$ has any *transition frequency* (if there is transition frequency, see Remark 5.4). Then, the robust gain and phase margins are

$$K^* = inf_{G(s)\in G_E(s)} K_G, \quad \theta^* = inf_{G(s)\in G_E(s)} \theta_G \tag{5.46}$$

where $G_E(s) = (S_{N_V}/S_{D_E}) \cup (S_{N_E}/S_{D_V})$ and S_{N_V}, S_{N_E}, S_{D_V} and S_{D_E} are defined in Eqs.(5.32-5.35).

Proof: Let A and B be the two complex plane polygons with vertex sets S_{A_V} and S_{B_V}, and edge sets S_{A_E} and S_{B_E}, respectively. Then, from the complex plane geometry, the following is known

$$\partial(A+B)\subset(S_{A_E}+S_{B_V})\cup(S_{A_V}+S_{B_E}) \tag{5.47}$$

Now, for the calculation of the gain margin, one needs to find the maximum value of K greater than 1 for which

$$\Lambda(s) = KN(s,\mathbf{r}) + D(s,\mathbf{q}) \tag{5.48}$$

is Hurwitz stable. From theorem 5.1, it is clear that if there is no *transition frequency* then the identified edges which constitute the $2r$ and $2q$-convex parpolygons for a single frequency remain unchanged for all $\omega\in(0,\infty)$. The multiplication of a $2r$-convex parpolygon with a fixed K is still a $2r$-convex parpolygon. Thus, for a fixed value of K, one can write

$$S_{A_V} = KS_{N_V},\ S_{B_V} = S_{D_V},\ S_{A_E} = KS_{N_E},\ S_{B_E} = S_{D_E}$$

and from Eq.(5.48), the following equation can be written

$$\Lambda(j\omega)\subset\Lambda_E(j\omega) = (KS_{N_E}+S_{D_V})\cup(KS_{N_V}+S_{D_E}) \tag{5.49}$$

Therefore, the stability of $\Lambda_E(s)$ implies the stability of $\Lambda(s)$. For the phase margin calculation, the gain K of Eq.(5.48) will be a complex gain such as $K = e^{-j\theta} = cos(\theta) - jsin(\theta)$ and the same proof will be valid. $\Box$

Remark 5.4: For clarity of presentation, theorem 5.8 is given for the no *transition frequency* case. If there is a *transition frequency* then the Nyquist envelope can be obtained by using theorem 5.6. Thus, the result of theorem 5.8 can be reformulated for this case. However, the $G_E(s)$ of Eq.(5.44) may be different for different frequency intervals.

5.6 Controller Synthesis Technique

In this section, using the tools (Bode, Nyquist and Nichols envelopes) developed in the previous section, classical controller design methods are used to design robust controllers for systems with affine linear uncertainty. Classical controller design techniques are basically based on two approaches. One is the Root-locus approach and the other is the frequency-response approach. Here, the frequency-response approach is used in order to design a controller which compensates a system of the form of Eq.(5.3). The design procedure is given by the following two examples. The first example deals with a *Lead* controller design. The objective of the second example is to design a robust *PI* controller for a given uncertain system.

Example 5.2

Consider a feedback system with an uncertain transfer function

$$G(s,\mathbf{q},\mathbf{r}) = \frac{N(s,\mathbf{r})}{D(s,\mathbf{q})} = \frac{r_1}{q_4 s^3 + (q_2+q_3)s^2 + (q_1+0.5q_2+q_3)s + q_1} \tag{5.50}$$

where

$$R = \{\mathbf{r} = [r_1] : r_1 \in [5,7]\} \tag{5.51}$$

$$Q = \{\mathbf{q} = [q_1\ q_2\ q_3\ q_4]^T : q_1 \in [0.05, 0.25], q_2 \in [0.4, 0.5], q_3 \in [0.5, 0.7], q_4 \in [0.09, 0.11]\} \tag{5.52}$$

The objective is to design a *Lead* controller of the form

$$C(s) = K_c \frac{Ts+1}{\alpha Ts+1},\ 0 < \alpha < 1 \tag{5.53}$$

which guarantees that the system has a phase margin of at least $\varphi = 45^\circ$ and a gain margin of not less than $\kappa = 12db$. It is desired that the bandwidth of the closed loop system be equal to or greater than $0.5rad/sec$.

Since $N(s,\mathbf{r}) = r_1$, the sets S_{N_V} and S_{N_E} are

$$S_{N_V} = \{5,7\}\ and\ S_{N_E} = \{5+2\lambda\}\ \ \forall\omega\in(0,\infty),\ \lambda\in[0,1] \tag{5.54}$$

Using theorem 1 it was computed that there is no *transition frequency* for $D(s,\mathbf{q})$. Thus, one single value of frequency within $\omega\in(0,\infty)$ is sufficient to identify the edges of the $2q$-convex parpolygons of $D(s,\mathbf{q})$. The edges, $e(c_7,c_8)$, $e(c_9,c_{10})$, $e(c_6,c_8)$, $e(c_9,c_{11})$, $e(c_2,c_6)$, $e(c_{11},c_{15})$, $e(c_2,c_{15})$ and $e(c_7,c_{15})$, were found to constitute the boundary of the $2q$-convex parpolygons of $D(s,\mathbf{q})$. Thus for all $\omega\in(0,\infty)$, the vertex and edge sets of $D(s,\mathbf{q})$ are

$$S_{D_V} = \{0.09s^3 + 0.9s^2 + 0.95s + 0.25,$$

$$
\begin{aligned}
&0.09s^3 + 1.1s^2 + 1.15s + 0.25, \\
&0.09s^3 + 1.2s^2 + 1.2s + 0.25, \\
&0.09s^3 + 1.2s^2 + s + 0.05, \\
&0.11s^3 + 1.2s^2 + s + 0.05, \\
&0.11s^3 + s^2 + 0.8s + 0.05, \\
&0.11s^3 + 0.9s^2 + 0.75s + 0.05, \\
&0.11s^3 + 0.9s^2 + 0.95s + 0.25\}
\end{aligned} \tag{5.55}
$$

and

$$
\begin{aligned}
S_{D_E} = \{&0.09s^3 + (0.9 + 0.2\lambda)s^2 + (0.95 + 0.2\lambda)s + 0.25, \\
&0.09s^3 + (1.1 + 0.1\lambda)s^2 + (1.15 + 0.05\lambda)s + 0.25, \\
&0.09s^3 + 1.2s^2 + (1.2 - 0.2\lambda)s + 0.25 - 0.2\lambda, \\
&(0.09 + 0.02\lambda)s^3 + 1.2s^2 + s + 0.05, \\
&0.11s^3 + (1.2 - 0.2\lambda)s^2 + (1 - 0.2\lambda)s + 0.05, \\
&0.11s^3 + (1 - 0.1\lambda)s^2 + (0.8 - 0.05\lambda)s + 0.05, \\
&0.11s^3 + 0.9s^2 + (0.75 + 0.2\lambda)s + 0.05 + 0.2\lambda, \\
&(0.11 - 0.02\lambda)s^3 + 0.9s^2 + 0.95s + 0.25\}
\end{aligned} \tag{5.56}
$$

Using the result given in [25], it can be seen that the extremal system, $G_E(s)$, has 80 systems with one unknown parameter $\lambda \in [0, 1]$. On the other hand, from theorem 5.6, it is clear that there are 24 systems each of which has one unknown parameter namely $\lambda \in [0, 1]$. So, the computational gain for this example is about 70%. Figure 5.4 shows the Nyquist template of $G(s, \mathbf{q}, \mathbf{r})$ at $\omega = 2rad/sec$ by using the results of [25] and a Nyquist template of $G(s, \mathbf{q}, \mathbf{r})$ at $\omega = 2rad/sec$ obtained by using the results developed in this paper is shown in Figure 5.5.

From the magnitude and phase envelopes of $G(s, \mathbf{q}, \mathbf{r})$, which are shown in Figure 5.6, the gain margin of the uncompensated system is $-1.21db$ and the phase margin is $-2.5°$.

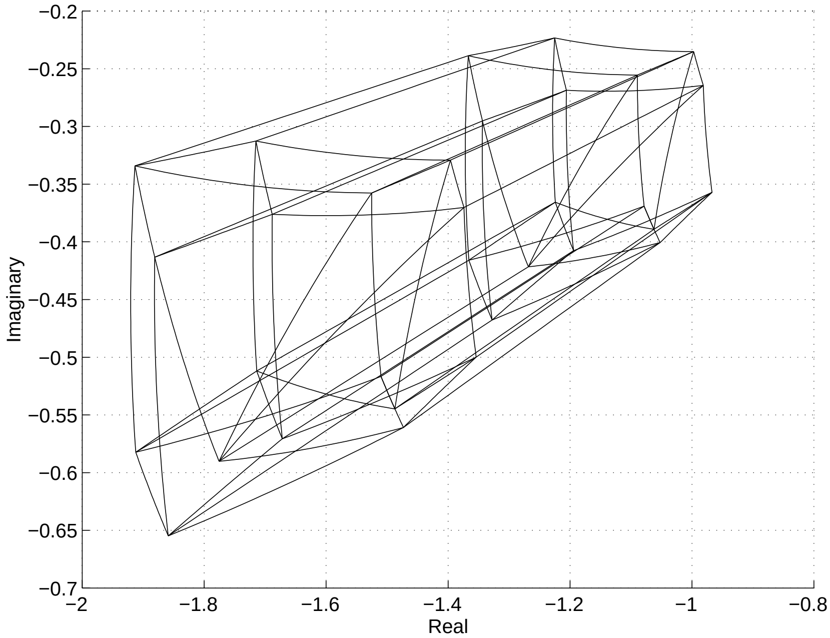

Figure 5.4: A Nyquist template at $\omega = 2rad/sec$

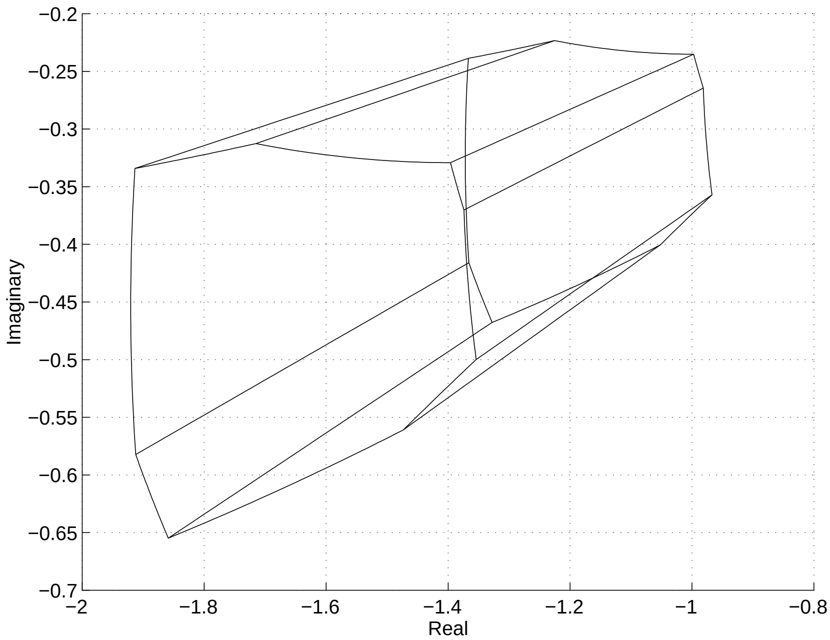

Figure 5.5: A Nyquist template at $\omega = 2rad/sec$

Thus, it is necessary to adjust the phase of the open loop transfer function by an amount

$$\phi_m = 45° - (-2.5°) = 47.5° \tag{5.57}$$

At $\omega = 2.64 rad/sec.$, the minimum phase of $G(s, \mathbf{q}, \mathbf{r})$ is about $-180°$. Therefore, we need a phase lead controller with a maximum phase value $\phi_m = 47.5°$ at $\omega_m = 2.64 rad/sec.$ So, from

$$\alpha = \frac{1 - sin\phi_m}{1 + sin\phi_m} \ \ and \ \ \omega_m = \frac{1}{T\sqrt{\alpha}} \tag{5.58}$$

one obtains $\alpha = 0.15$ and $T = 0.97$. However, a phase lead compensator will shift the gain crossover frequency to a higher frequency where the phase is less than at the original gain crossover frequency. Therefore, in order to bring the Bode envelope of $(0.97s+1)/(0.146s+1)G(s, \mathbf{q}, \mathbf{r})$ to $0db$, at this frequency requires

$$20log_{10}K_c = -9.5db \tag{5.59}$$

giving $K_c = 0.34$. Thus, the *Lead* controller

$$C(s) = 0.34\frac{0.97s + 1}{0.146s + 1} \tag{5.60}$$

is obtained.

The phase and gain margins of the compensated system were computed to be 47.7° and $13.5db$, respectively. From the magnitude envelope of the closed loop transfer function of the compensated system, it was found that the bandwidth of every system in the family lies between $0.68 rad/sec$ and $1.28 rad/sec.$. Therefore, the designed *Lead* controller satisfies the design specification robustly. The Bode, Nyquist and Nichols envelopes of the uncompensated and compensated systems are shown in Figures 5.6, 5.7 and 5.8, respectively.

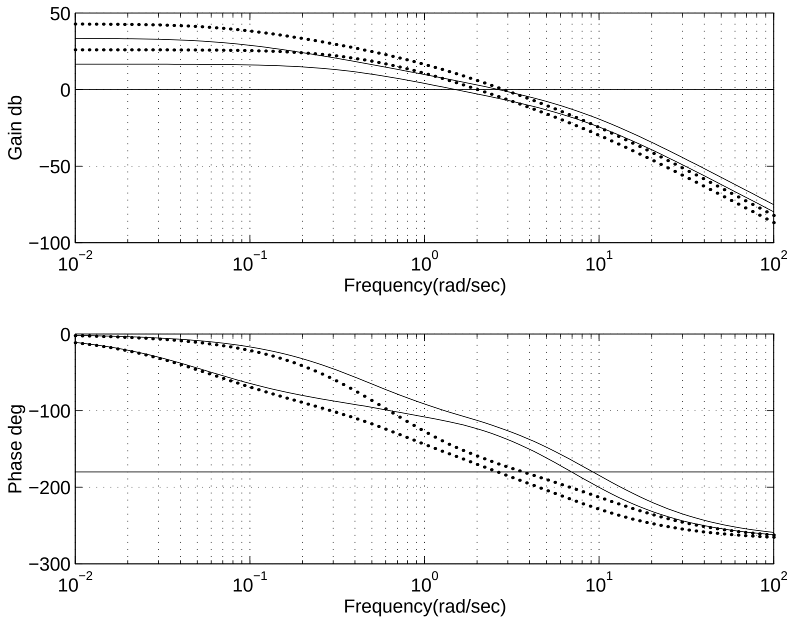

Figure 5.6: Bode envelopes(...uncomp., -comp.)

Example 5.3

Consider

$$G(s,\mathbf{q},\mathbf{r}) = \frac{N(s,\mathbf{r})}{D(s,\mathbf{q})} = \frac{(0.5r_1 + r_2 + 0.2r_3)s + (r_1 + r_3)}{(q_4 + q_1)s^4 + (q_4 + q_3 + q_2)s^3 + (q_2 + q_1)s^2 + q_3 s} \tag{5.61}$$

where

$$R = \{\mathbf{r} = [r_1\ r_2\ r_3]^T : r_1 \in [0.4, 0.8], r_2 \in [0.01, 0.08], r_3 \in [0.2, 0.6]\} \tag{5.62}$$

$$Q = \{\mathbf{q} = [q_1\ q_2\ q_3\ q_4]^T : q_1 \in [0.4, 0.8], q_2 \in [0.2, 0.6], q_3 \in [0.02, 0.08], q_4 \in [0.001, 0.005]\} \tag{5.63}$$

The aim is to design a PI controller of the form

$$C(s) = \frac{K_p s + K_i}{s} \tag{5.64}$$

which guarantees that the entire family has a phase margin of at least $\varphi = 45°$.

From theorem 5.1 it was computed that there was no *transition frequency* for $N(s,\mathbf{r})$. Thus, one single value of frequency within $\omega \in (0, \infty)$ is sufficient to identify the edges of the $2r$-convex parpolygons of $N(s,\mathbf{r})$. However, for $D(s,\mathbf{q})$, it was found that there is one *transition frequency* at $1 rad/sec$. The edges of the $2r$-convex parpolygons of $N(s,\mathbf{r})$

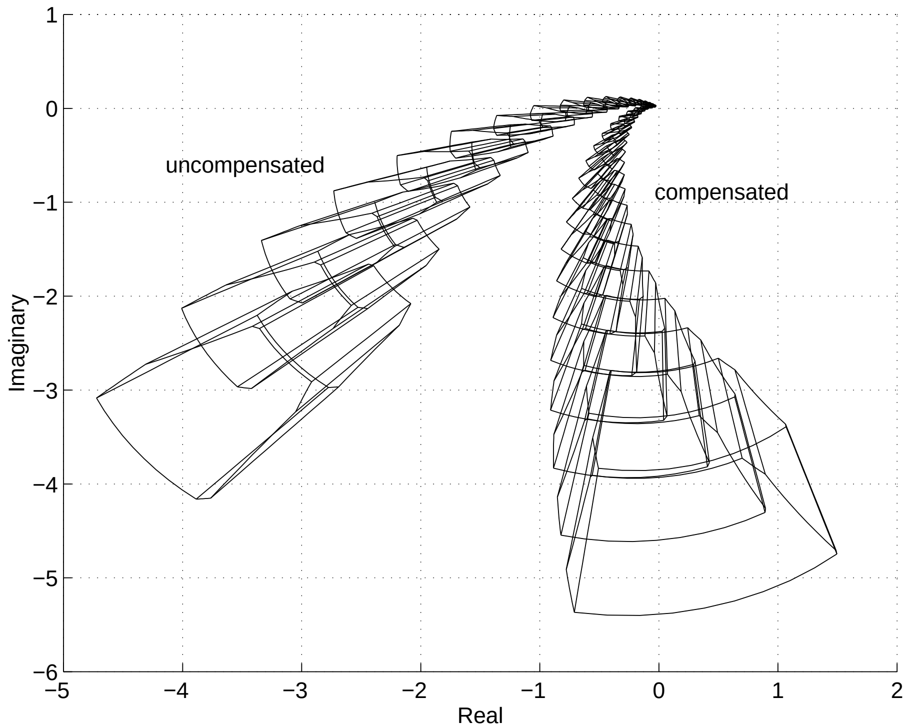

Figure 5.7: Nyquist envelopes

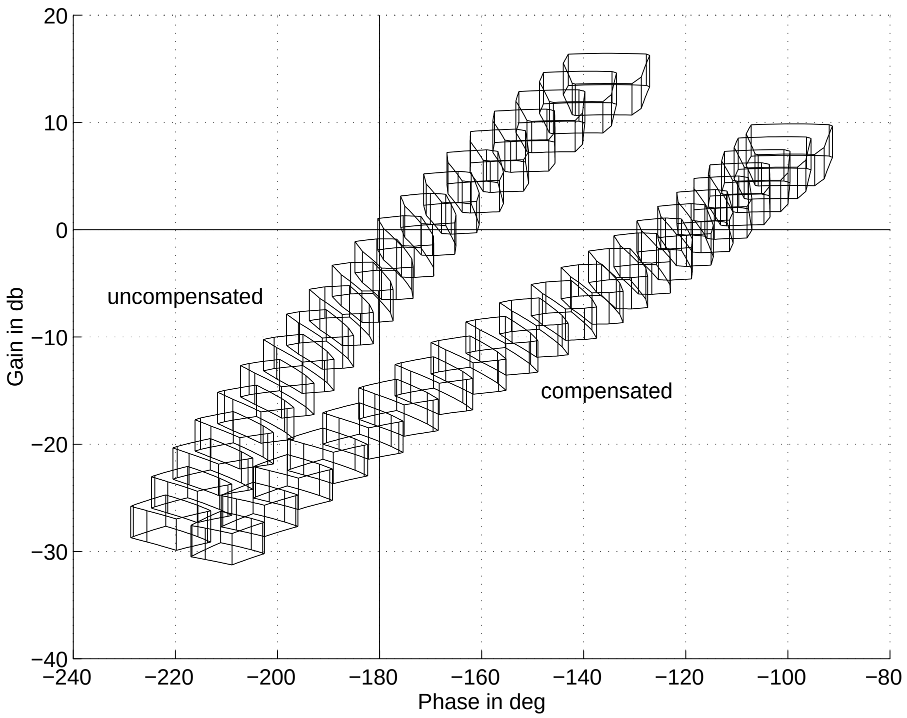

Figure 5.8: Nichols envelopes

for $\omega\in(0,\infty)$ and the edges of the $2q$-convex parpolygons of $D(s,\mathbf{q})$ within $\omega\in(0,1)$ and $\omega\in(1,\infty)$ are shown in Table 5.1.

Edges of $2r$-convex parpolygon for $\omega\in(0,\infty)$	Edges of $2q$-convex parpolygon for $\omega\in(0,1)$	Edges of $2q$-convex parpolygon for $\omega\in(1,\infty)$
$e(c_4,c_3)$	$e(c_5,c_6)$	$e(c_1,c_2)$
$e(c_5,c_6)$	$e(c_{11},c_{12})$	$e(c_{15},c_{16})$
$e(c_6,c_8)$	$e(c_6,c_8)$	$e(c_1,c_3)$
$e(c_1,c_3)$	$e(c_9,c_{11})$	$e(c_{14},c_{16})$
$e(c_4,c_8)$	$e(c_9,c_{13})$	$e(c_{10},c_{14})$
$e(c_1,c_5)$	$e(c_4,c_8)$	$e(c_3,c_7)$
	$e(c_5,c_{13})$	$e(c_2,c_{10})$
	$e(c_4,c_{12})$	$e(c_7,c_{15})$

Table 5.1: Identified edges which constitute the boundary of the $2r$ and $2q$-convex parpolygons

Now

$$\phi_m = 45^\circ + 5^\circ(additional\ phase) = 50^\circ \tag{5.65}$$

and from

$$\phi_m = 50^\circ = 180^\circ + minarg[G(j\omega_1,\mathbf{q},\mathbf{r})] \tag{5.66}$$

the value of ω_1 is $0.01203 rad/sec.$ and the maximum magnitude of $G(s,\mathbf{q},\mathbf{r})$ at $s = j\omega_1$ is $77.8db$. From

$$-20log_{10}K_p = max|G(j\omega_1,\mathbf{q},\mathbf{r})|db = 77.8db \tag{5.67}$$

$K_p = 1.29\times10^{-4}$. If one chooses the corner frequency K_i/K_p to be one decade below ω_1 then $K_i = (\omega_1/10)K_p = 1.55\times10^{-7}$. Thus, the designed PI controller is

$$C(s) = \frac{1.29\times10^{-4}s + 1.55\times10^{-7}}{s} \tag{5.68}$$

It was computed that the phase margin of the compensated system is greater than 56.7°. Figures 5.9, 5.10 and 5.11 show the Bode, Nyquist and Nichols envelopes of the uncompensated and compensated systems.

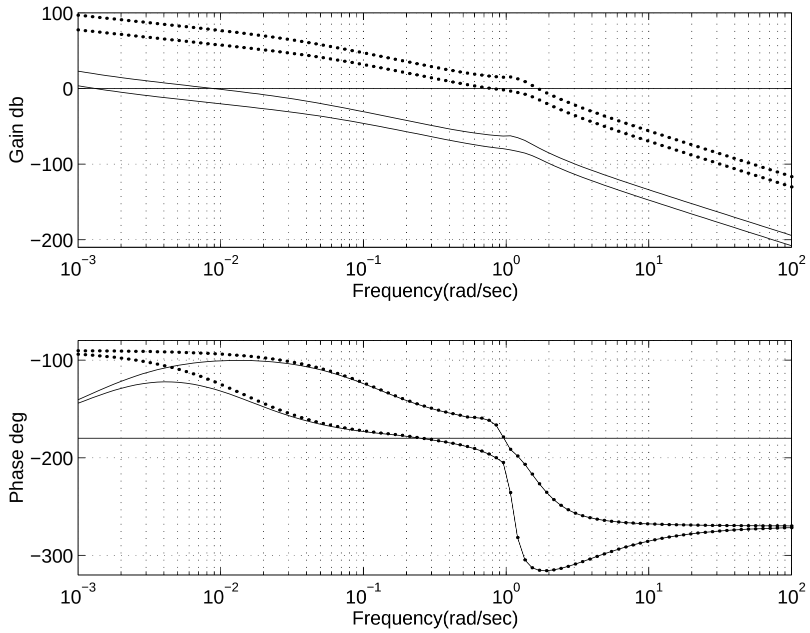

Figure 5.9: Bode envelopes(...uncomp., -comp.)

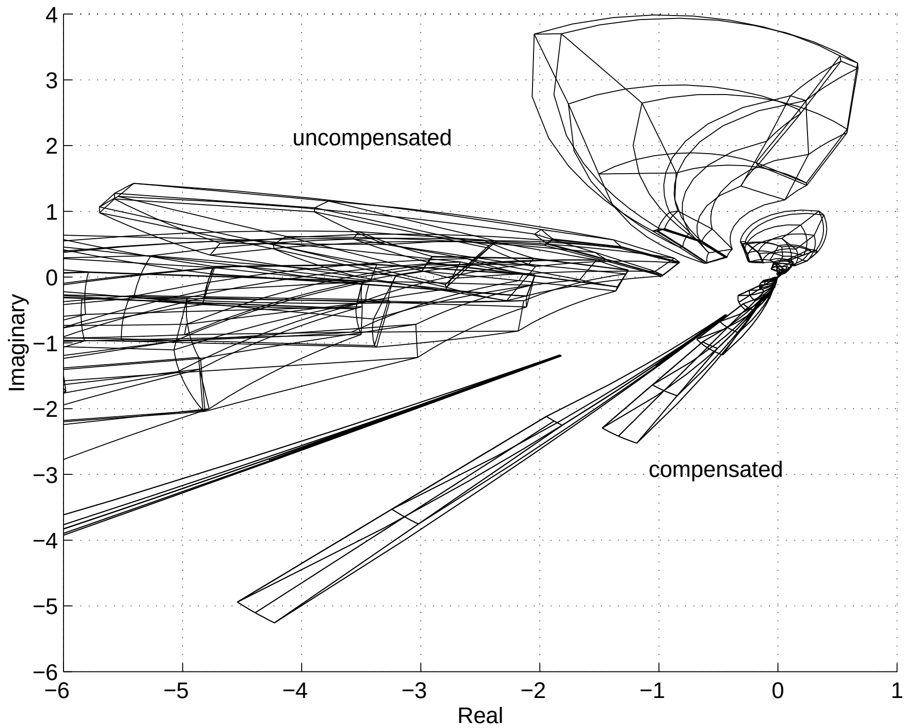

Figure 5.10: Nyquist envelopes

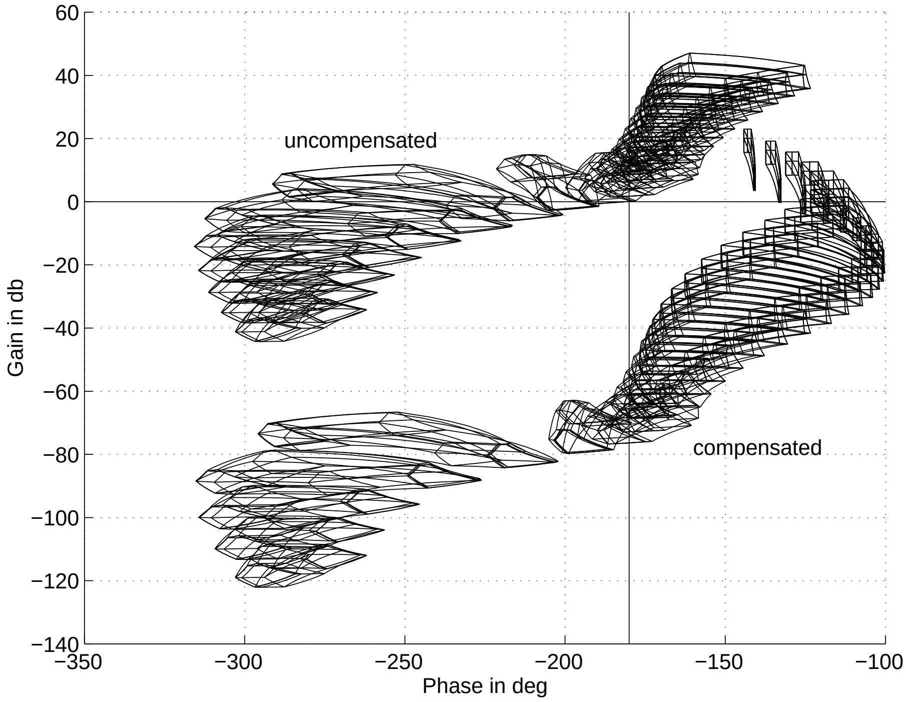

Figure 5.11: Nichols envelopes

5.7 Conclusion

A technique has been presented for plotting the frequency response of a transfer function with affine linear uncertainty structure. The technique is based on a $2q$-convex parpolygonal value set. Several new results have been derived for construction of the Bode, Nyquist, and Nichols envelopes of control systems with uncertain parameters. These results have been used to design compensators that provide a guaranteed level of performance, in the sense of gain and phase margins, for systems with affine linear uncertainty.

Chapter 6

ANALYSIS OF CONTROL SYSTEMS WITH MIXED PERTURBATIONS

6.1 Introduction

This chapter is an extension of the results contained in the previous chapter. It considers control systems with parametric as well as unstructured uncertainty. It is known that in most practical systems at least two types of uncertainties are present, namely unstructured (or nonparametric) uncertainty which represents unmodeled dynamics, nonlinearities etc., and structured (or parametric) uncertainty, representing a lack of precise knowledge of the actual parameters. The robust stability analysis of a control system in the presence of unstructured uncertainty is an important and well-developed subject in control theory. The well-known absolute stability problem [134] which was formulated in the 1950s is an important robustness problem regarding unstructured uncertainty. In this problem, a fixed linear system is subjected to perturbations consisting of all possible nonlinear feedback gains lying in a sector. A similar problem was studied in the 1980's by modelling the perturbations as H_∞ norm bounded perturbations of a fixed linear system. And in recent years, as mentioned before, a substantial amount of research [13] concerning robustness analysis of control systems affected by real parametric uncertainty has been done.

The aim of this chapter is to study the determination of the robust small gain theorem, robust performance, strict positive realness and absolute stability problem of control systems with parametric as well as unstructured uncertainty. Thus, the system under investigation contains a mixed type uncertainty structure. Parametric uncertainty is modelled by a transfer function whose numerator and denominator polynomials are of the form of Eq.(5.1). The unstructured uncertainty is modelled as H_∞ norm bounded perturbations and perturbations consisting of a family of nonlinear sector bounded feedback gains. These problems for systems with parametric uncertainty are studied in [37, 48, 38, 67, 129, 39, 46, 59, 107]. The main ideas of the approaches presented in these references regarding these problems are based on the boundary results developed for uncertain transfer functions by using the Kharitonov theorem [88], the generalized Kharitonov theorem [34] and the edge theorem [21]. The majority of these results dealt with uncertain systems defined by an interval plant structure. On the other hand, in this chapter, it is assumed that the uncertain transfer function of the system is in the form of Eq.(5.3). Under the assumption of no *transition frequency* and using the boundary results developed in Chapter 5, which are based on the $2q$-convex parpolygonal value set of the polynomial of the form of Eq.(5.1), the classical small gain theorem, robust performance, strict positive realness and the absolute stability problem of a control system with an uncertain transfer function of the form of Eq.(5.3) are formulated.

The chapter is organized as follows: In Section 6.2 a discussion on the assumption of no *transition frequency* is given. In Section 6.3, the robust version of the small gain theorem is derived. The robust performance of a feedback system with parametric uncertainty is discussed in Section 6.4. In Section 6.5, the strict positive realness conditions of the transfer function of Eq.(5.3) are investigated. The problem of robust absolute stability of systems with parametric uncertainty is discussed in Section 6.6. Section 6.7 gives concluding remarks.

6.2 Assumption of No Transition Frequency

In this chapter, the results are presented under the assumption of no *transition frequency*. Therefore, theorem 5.7 is mainly used in order to prove the results. A polynomial of the form of Eq.(5.1) has no *transition frequency*, if Eq.(5.8) does not have any positive real root. The assumption of no *transition frequency* does not mean that the results are not helpful in the case of a *transition frequency*. The reason for making such an assumption is to allow results to be presented in a clear and closed form. Therefore, the results given in the next sections can be reformulated for the case of a *transition frequency*. The following example is given to clarify the situation (assumption of no *transition frequency*).

Example 6.1

Consider

$$G(s,\mathbf{q},\mathbf{r}) = \frac{N(s,\mathbf{r})}{D(s,\mathbf{q})} = \frac{r_3 s^2 + (r_1 + r_2 + r_3)s + 2r_1 + r_2}{q_4 s^3 + q_2 s^2 + (q_1 + q_2 + q_4)s + q_1 + q_3} \tag{6.1}$$

where

$$R = \{\mathbf{r} = [r_1\ r_2\ r_3]^T : r_1 \in [1,3], r_2 \in [4,6], r_3 \in [0.2, 2.8]\} \tag{6.2}$$

$$Q = \{\mathbf{q} = [q_1\ q_2\ q_3\ q_4]^T : q_1 \in [1,2], q_2 \in [3,5], q_3 \in [0.25, 1.5], q_4 \in [0.4, 1.4]\} \tag{6.3}$$

From theorem 5.1 it was computed that there was no *transition frequency* for $N(s,\mathbf{r})$. Thus, one single value of frequency within $\omega \in (0,\infty)$ is sufficient to identify the edges of the $2r$-convex parpolygons of $N(s,\mathbf{r})$. However, for $D(s,\mathbf{q})$, it was found that there is one *transition frequency* at $1 rad/sec$. The edges of the $2r$-convex parpolygons of $N(s,\mathbf{r})$ for $\omega \in (0,\infty)$ and the edges of the $2q$-convex parpolygons of $D(s,\mathbf{q})$ within $\omega \in (0,1)$ and $\omega \in (1,\infty)$ are shown in Table 6.1. For frequency response computation, the result given in theorem 5.6 is always superior to the boundary results of [25, pp.362-363]. For this example, using the boundary result given in [25] it can be seen that the extremal system, $G_E(s)$, has 448 systems. On the other hand, the extremal system obtained by theorem

Edges of $2r$-convex parpolygon for $\omega\in(0,\infty)$	Edges of $2q$-convex parpolygon for $\omega\in(0,1)$	Edges of $2q$-convex parpolygon for $\omega\in(1,\infty)$
$e(c_1, c_2)$	$e(c_{11}, c_{12})$	$e(c_3, c_4)$
$e(c_2, c_4)$	$e(c_5, c_6)$	$e(c_{13}, c_{14})$
$e(c_1, c_5)$	$e(c_{14}, c_{16})$	$e(c_6, c_8)$
$e(c_5, c_7)$	$e(c_1, c_3)$	$e(c_9, c_{11})$
$e(c_4, c_8)$	$e(c_{12}, c_{16})$	$e(c_4, c_8)$
$e(c_7, c_8)$	$e(c_1, c_5)$	$e(c_9, c_{13})$
	$e(c_6, c_{14})$	$e(c_6, c_{14})$
	$e(c_3, c_{11})$	$e(c_3, c_{11})$

Table 6.1: Identified edges which constitute the boundary of the $2r$ and $2q$-convex parpolygons

5.6 contains 96 systems for each frequency. Therefore, the computational gain at each frequency is about 78.5%. However, for other control problems such as the computation of the maximum H_∞ norm of the family or calculation of robust gain and phase margins, the scenario is a little different. For example, in order to compute the maximum H_∞ norm of the system given in Eq.(6.1), one needs to consider two extremal systems namely $G_{E1}(s)$ and $G_{E2}(s)$ for $\omega\in(0,1)$ and $\omega\in(1,\infty)$, respectively. Since there is no *transition frequency* for $N(s,\mathbf{r})$, six exposed edges of $N(s,\mathbf{r})$ are eliminated. For $D(s,\mathbf{q})$, from Table 6.1, it can be seen that the edges $e(c_6, c_{14})$ and $e(c_3, c_{11})$ remain unchanged for all frequencies. Thus, 36 systems of $G_{E2}(s)$ are similar to the 36 systems of $G_{E1}(s)$. So, it is necessary to consider a total of $96 + 60 = 156$ systems for calculating the maximum H_∞ norm of the family and the computational gain reduces to 65%.

From this example, it is clear that extensions of the results of the present chapter to the transfer function with *transition frequency* is obvious. There will always be a considerable computational reduction as long as the number of the total extremal systems is not equal to the extremal system given in [25].

6.3 Small Gain Theorem

This is a very useful theorem in robust stability studies. The small gain theorem can be posed in any normed algebra, and it gives conditions under which a system of interconnected components is stable. Generally, the classical small gain theorem studies the

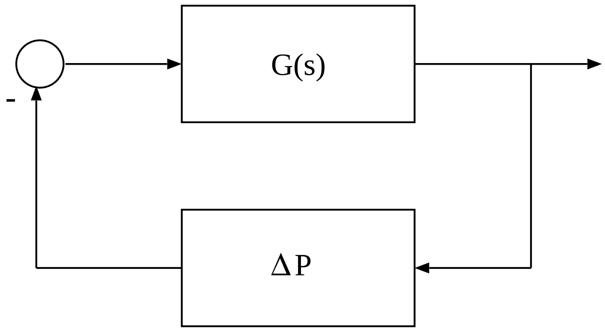

Figure 6.1: Closed loop system with H_∞ norm bounded perturbation

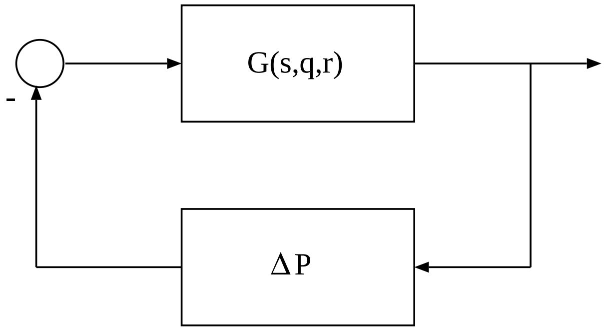

Figure 6.2: Closed loop system with mixed perturbations

robust stability of the closed-loop system of Figure 6.1 where $G(s)$ is a stable linear time-invariant system which is perturbed via feedback by a stable transfer function ΔP with bounded H_∞ norm. It states that the configuration of Figure 6.1 remains stable for all feedback perturbations ΔP satisfying $\|\Delta P\|_\infty < \alpha$ if and only if

$$\|G\|_\infty \leq \frac{1}{\alpha} \tag{6.4}$$

In the following theorem this result is extended to the case where in addition to unstructured feedback perturbations, the $G(s)$ of Figure 6.1 is subject to parameter perturbations defined by Eq.(5.3).

Theorem 6.1 (small gain theorem for configuration of Figure 6.2): Given an uncertain family $G(s, \mathbf{q}, \mathbf{r})$ of stable proper plants with no *transition frequency*, the closed loop system of Figure 6.2 remains stable for all stable perturbations ΔP such that $\|\Delta P\|_\infty < \alpha$ if and only if

$$\alpha \leq \frac{1}{max_{G \in G_E(s)} \|G\|_\infty} \tag{6.5}$$

where $G_E(s)$ is given by Eq.(5.44).

Proof: The proof of this theorem comes from theorem 5.7. From theorem 5.7, for all frequencies, since $\partial G(j\omega, \mathbf{q}, \mathbf{r}) \subset G_E(j\omega)$, the maximum H_∞ norm over the parameter set occurs over the subset $G_E(s)$ of Eq.(5.44). □

Now, consider the control system block diagrams given in Figures 6.3 and 6.4 where $C(s)$ is a stabilizing controller for the entire family. In order to determine the amount of

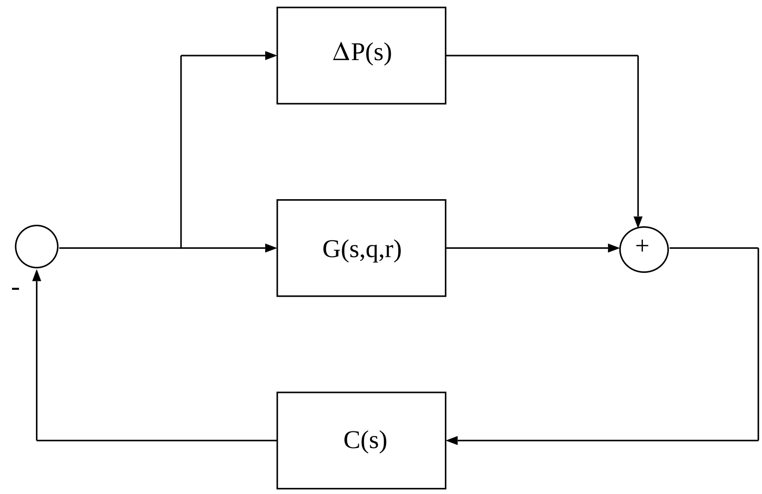

Figure 6.3: Closed loop system with additive perturbations

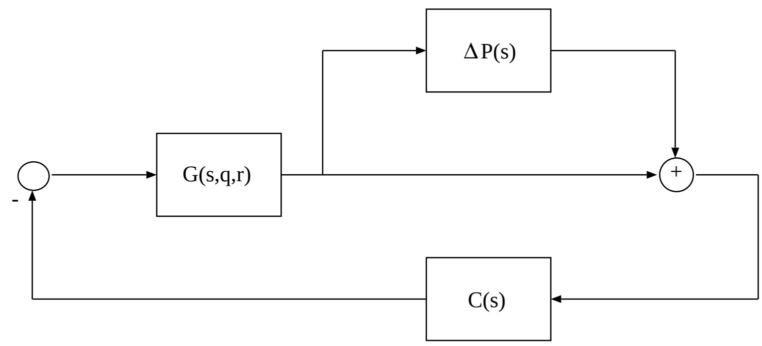

Figure 6.4: Closed loop system with multiplicative perturbations

unstructured perturbations that can be tolerated by the additively perturbed uncertain system shown in Figure 6.3, one needs to find the maximum of the H_∞ norm of the closed loop transfer function

$$C(s)(1 + C(s)G(s))^{-1} \tag{6.6}$$

over all elements $G(s) \in G(s, \mathbf{q}, \mathbf{r})$. In the case of the multiplicative perturbations shown in

Figure 6.4, it is necessary to find the maximum of the H_∞ norm of the closed loop transfer function

$$C(s)G(s)(1+C(s)G(s))^{-1} \tag{6.7}$$

for all elements $G(s) \in G(s,\mathbf{q},\mathbf{r})$.

The following theorem is given for computing the level of unstructured perturbations that can be tolerated in both the additive and multiplicative cases shown in Figures 6.3 and 6.4, respectively.

Theorem 6.2 (small gain theorem for Figures 6.3 and 6.4): Let $G(s,\mathbf{q},\mathbf{r})$ of Figures 6.3 and 6.4 be a proper family of plants with no *transition frequency* and $C(s)$ be a stabilizing controller then the closed loop sytem in Figures 6.3 and 6.4 remains stable for all stable perturbations ΔP satisfying $\|\Delta P\|_\infty < \alpha$ if and only if,

$$\alpha \leq \frac{1}{sup_{G(s)\in G_E(s)}\|C(s)(1+C(s)G(s))^{-1}\|_\infty} \quad for \;\; figure\; 6.3 \tag{6.8}$$

and

$$\alpha \leq \frac{1}{sup_{G(s)\in G_E(s)}\|C(s)G(s)(1+C(s)G(s))^{-1}\|_\infty} \quad for \;\; figure\; 6.4 \tag{6.9}$$

where $G_E(s)$ is defined by Eq.(5.44).

Proof: Let the polynomial $P(s,\mathbf{q})$ of Eq.(5.1) be multiplied with a fixed polynomial $\delta(s) = \delta_0 + \delta_1 s + ... + \delta_n s^n$. At $s = j\omega^*$, the value set of $P(j\omega^*,\mathbf{q})$ is contained in a $2q$-convex parpolygon. For $s = j\omega^*$, geometrically, the affect of multiplying $P(j\omega^*,\mathbf{q})$ by $\delta(j\omega^*)$ is to rotate and scale the value set of $P(s,\mathbf{q})$ at $s = j\omega^*$, but not to distort its shape. Therefore, the value set of $\delta(j\omega^*)P(j\omega^*,\mathbf{q})$ is still a $2q$-convex parpolygon (see section 5.3.2). Thus,

$$\partial(C(j\omega)(1+C(j\omega)G(j\omega,\mathbf{q},\mathbf{r}))^{-1}) \subset C(j\omega)(1+G_E(j\omega)C(j\omega))^{-1} \tag{6.10}$$

From this equation

$$sup_{G(s)\in G(s,\mathbf{q},\mathbf{r})}|C(j\omega)(1+C(j\omega)G(j\omega))^{-1}| = sup_{G(s)\in G_E(s)}|C(j\omega)(1+G_E(j\omega)C(j\omega))^{-1}| \tag{6.11}$$

Hence,

$$sup_{G(s)\in G(s,\mathbf{q},\mathbf{r})}\|C(j\omega)(1{+}C(j\omega)G(j\omega))^{-1}\|_\infty{=}sup_{G(s)\in G_E(s)}\|C(j\omega)(1{+}G_E(j\omega)C(j\omega))^{-1}\|_\infty \tag{6.12}$$

Similarly, it can be shown that $sup_{G(s)\in G(s,\mathbf{q},\mathbf{r})}\|C(j\omega)G(j\omega)(1+C(j\omega)G(j\omega))^{-1}\|_\infty =$ $sup_{G(s)\in G_E(s)}\|C(j\omega)G_E(j\omega)(1+G_E(j\omega)C(j\omega))^{-1}\|_\infty$ for Eq.(6.9). $\square$

Example 6.2

Consider

$$G(s,\mathbf{q},\mathbf{r}) = \frac{N(s,\mathbf{r})}{D(s,\mathbf{q})} = \frac{r_2 s + r_1}{(q_2+q_3)s^3 + (q_1+q_2+q_3)s^2 + (q_1+q_2)s + q_1+q_2+q_3} \tag{6.13}$$

where

$$R = \{\mathbf{r} = [r_1\ r_2]^T : r_1\in[1,2], r_2\in[0.2, 0.8]\} \tag{6.14}$$

$$Q = \{\mathbf{q} = [q_1\ q_2\ q_3]^T : q_1\in[4,5], q_2\in[0.5, 1.2], q_3\in[0.5, 0.8]\} \tag{6.15}$$

Since $N(s,\mathbf{r})$ is an interval polynomial, from the Kharitonov theorem the sets S_{N_V} and S_{N_E} $\forall\omega\in(0,\infty)$ are

$$S_{N_V} = \{0.2s+1,\ 0.2s+2,\ 0.8s+2,\ 0.8s+1\} \tag{6.16}$$

and

$$S_{N_E} = \{0.2s+1+\lambda,\ (0.2+0.6\lambda)s+2,\ 0.8s+2-\lambda,\ (0.8-0.6\lambda)s+1\} \tag{6.17}$$

where $\lambda\in[0,1]$. Using theorem 5.1 it is easily shown that there is no *transition frequency* for $D(s,\mathbf{q})$. Thus, one single value of frequency within $\omega\in(0,\infty)$ is sufficient to identify the edges of the $2q$-convex parpolygons of $D(s,\mathbf{q})$. The edges, $e(c_1,c_2)$, $e(c_2,c_4)$, $e(c_5,c_7)$, $e(c_4,c_8)$, $e(c_1,c_5)$ and $e(c_7,c_8)$, are found to constitute the boundary of the $2q$-convex parpolygons of $D(s,\mathbf{q})$. Thus for all $\omega\in(0,\infty)$, from Eqs.(5.32-5.35) the vertex, S_{D_V}, and the edge, S_{D_E}, sets of $D(s,\mathbf{q})$ can be written as

$$S_{D_V} \;=\; \{s^3+5s^2+4.5s+5,$$

$$
\begin{aligned}
& s^3 + 6s^2 + 5.5s + 6, \\
& 1.7s^3 + 6.7s^2 + 6.2s + 6.7, \\
& 2s^3 + 7s^2 + 6.2s + 7, \\
& 2s^3 + 6s^2 + 5.2s + 6, \\
& 1.3s^3 + 5.3s^2 + 4.5s + 5.3\}
\end{aligned}
\tag{6.18}
$$

and

$$
\begin{aligned}
S_{D_E} = \{ & s^3 + (5+\lambda)s^2 + (4.5+\lambda)s + 6 + \lambda, \\
& (1+0.7\lambda)s^3 + (6+0.7\lambda)s^2 + (5.5+0.7\lambda)s + 6 + 0.7\lambda, \\
& (1.7+0.3\lambda)s^3 + (6.7+0.3\lambda)s^2 + 6.2s + 6.7 + 0.3\lambda, \\
& 2s^3 + (6+\lambda)s^2 + (5.2+\lambda)s + 6 + \lambda, \\
& (1.3+0.7\lambda)s^3 + (5.3+0.7\lambda)s^2 + (4.5+0.7\lambda)s + 5.3 + 0.7\lambda, \\
& (1+0.3\lambda)s^3 + (5+0.3\lambda)s^2 + 4.5s + 5 + 0.3\lambda\}
\end{aligned}
\tag{6.19}
$$

Using these vertex and edge sets the maximum H_∞ norm of the family can be computed as 0.6782. Thus, from theorem 6.1, the entire family of systems remains stable under any unstructured feedback perturbations of H_∞ norm less than

$$\alpha = \frac{1}{0.6782} = 1.47$$

The Nyquist envelope of the extremal system, $G_E(s)$, of $G(s, \mathbf{q}, \mathbf{r})$ is shown in Figure 6.5.

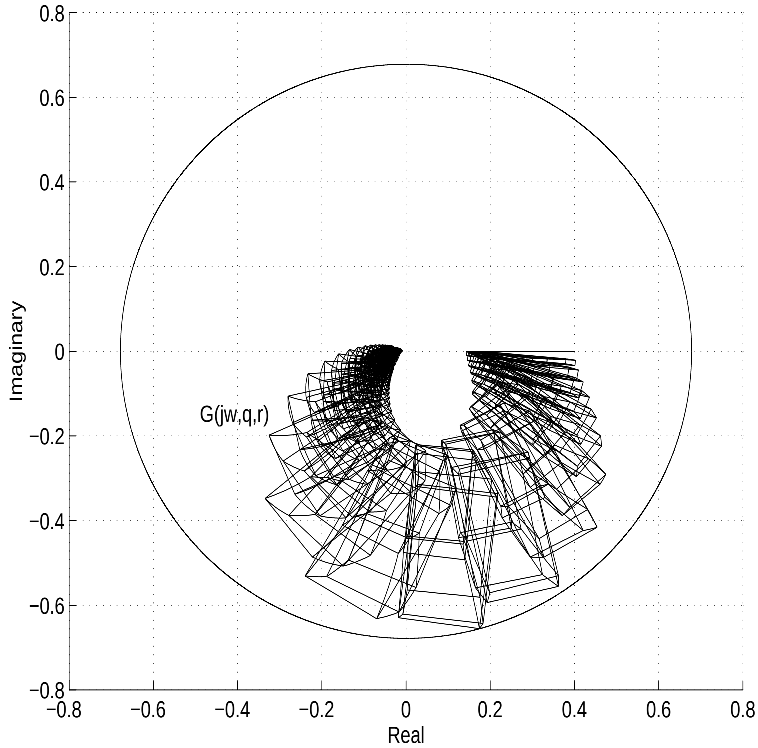

Figure 6.5: Nyquist envelope of $G(s, \mathbf{q}, \mathbf{r})$ and H_∞ stability margin

6.4 Robust Performance

The error, output and control signal transfer functions from the input for the control system block diagram shown in Figure 6.6 can be written as

$$\begin{aligned} T^e(s) &= (1 + C(s)G(s, \mathbf{q}, \mathbf{r}))^{-1} \\ T^y(s) &= C(s)G(s, \mathbf{q}, \mathbf{r})(1 + C(s)G(s, \mathbf{q}, \mathbf{r}))^{-1} \\ T^u(s) &= C(s)(1 + C(s)G(s, \mathbf{q}, \mathbf{r}))^{-1} \end{aligned} \tag{6.20}$$

In the H_∞ approach to robust control problems, system performance is measured by the size of the H_∞ norm of error, output and other transfer functions. The worst case performance of the transfer functions given in Eq.(6.20) can be determined by the following theorem

Theorem 6.3 (robust performance): The maximum value of the H_∞ norms of $T^e(s)$,

$T^y(s)$ and $T^u(s)$ are:

$$\begin{aligned} sup_{G(s)\in G(s,\mathbf{q},\mathbf{r})}\|(1+C(s)G(s))^{-1}\|_\infty &= sup_{G(s)\in G_E(s)}\|(1+G(s)C(s))^{-1}\|_\infty \\ sup_{G(s)\in G(s,\mathbf{q},\mathbf{r})}\|C(s)G(s)(1+C(s)G(s))^{-1}\|_\infty &= sup_{G(s)\in G_E(s)}\|C(s)G(s)(1+G(s)C(s))^{-1}\|_\infty \\ sup_{G(s)\in G(s,\mathbf{q},\mathbf{r})}\|C(s)(1+C(s)G(s))^{-1}\|_\infty &= sup_{G(s)\in G_E(s)}\|C(s)(1+G(s)C(s))^{-1}\|_\infty \end{aligned} \tag{6.21}$$

Proof: The proof of this theorem is similar to the proof of theorem 6.1. Therefore, it is omitted.

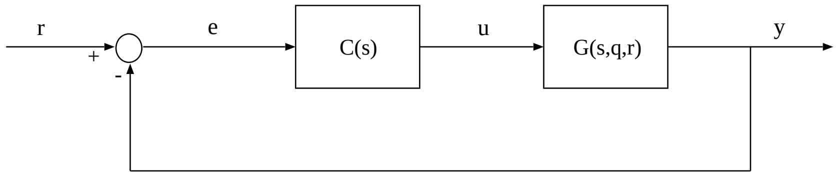

Figure 6.6: A unity feedback system with parametric uncertainty

6.5 SPR (Strict Positive Realness) Conditions

Strictly positive real transfer functions are of importance in control theory. Such transfer functions are stable and their Nyquist diagrams are in the first and fourth quadrants of the complex plane. A definition of a strictly positive real transfer function is given as

Definition 6.1 [1, pp. 211]: A proper transfer function, $G(s) = N(s)/D(s)$, is called strictly positive real if

i) $D(s)$ is Hurwitz and

ii) $Re[G(j\omega)] > 0, \ \forall\omega\geq 0$

In other words, a transfer function is strictly positive real if it is stable and its Nyquist plot is completely contained in the right half complex plane. With this definition, one can proceed to investigate the SPR property of the transfer function of the form of Eq.(5.3) which is given by the following theorem

Theorem 6.4: Assume that neither $N(s,\mathbf{r})$ nor $D(s,\mathbf{q})$ has any transition frequency. Let the vertex and edge sets of $N(s,\mathbf{r})$ and $D(s,\mathbf{q})$ be given by Eqs.(5.32-5.35). Then, $G(s,\mathbf{q},\mathbf{r})$ is a strictly positive real transfer function family if

a) S_{D_E} has at least one stable member and the $2q$-convex parpolygons of $D(s,\mathbf{q})$ do not include the origin for all frequencies.

b) For all frequencies

$$|arg_{v_{ni}\in S_{N_V}}[v_{ni}] - arg_{v_{dj}\in S_{D_V}}[v_{dj}]| < \frac{\pi}{2} \tag{6.22}$$

where $i = 1, 2, ..., 2r$ and $j = 1, 2, ..., 2q$.

Proof:

a) From definition 6.1, $D(s,\mathbf{q})$ must be stable. The stability of $D(s,\mathbf{q})$ can be checked by using the *zero exclusion principle* and *value set concept*. The value set of $D(s,\mathbf{q})$ at $s = j\omega^*$ is contained in a $2q$-convex parpolygon. The assumption of no *transition frequency* guarantees that the identified edges for a single frequency which constitute the edges of a $2q$-convex parpolygon remain unchanged. Thus, from the *zero exclusion principle*, for stability of $D(s,\mathbf{q})$, the edge set, S_{D_E}, of $D(s,\mathbf{q})$ must be stable. This implies that there must be at least one stable member of S_{D_E} and the $2q$-convex parpolygonal value set of $D(s,\mathbf{q})$ will not include the origin.

b) The value set of the numerator $N(s,\mathbf{r})$ and the denominator $D(s,\mathbf{q})$ for a fixed $s = j\omega^*$ are $2r$ and $2q$-convex parpolygons. The phase condition of $G(s,\mathbf{q},\mathbf{r})$ to be strictly positive real is

$$|arg[G(j\omega,\mathbf{q},\mathbf{r})]| = |arg[N(j\omega,\mathbf{r})] - arg[D(j\omega,\mathbf{q})]| < \frac{\pi}{2} \tag{6.23}$$

This means that for each frequency both the $2r$ and $2q$-convex parpolygonal value sets must be included in a $\pi/2$-sector, see Figure 6.7. This is guaranteed if the transfer functions obtained by the vertex sets (S_{N_V} and S_{D_V}) achieve this phase condition. Therefore, for SPR of $G(s,\mathbf{q},\mathbf{r})$, Eq.(6.23) can be written as

$$|arg_{v_{ni}\in S_{N_V}}[v_{ni}] - arg_{v_{dj}\in S_{D_V}}[v_{dj}]| < \frac{\pi}{2} \quad \square \tag{6.24}$$

Example 6.3

Consider the uncertain transfer function given in Example 6.1. The edges which constitute the boundary of the $2r$ and $2q$-convex parpolygons were given in Table 6.1. Here, the

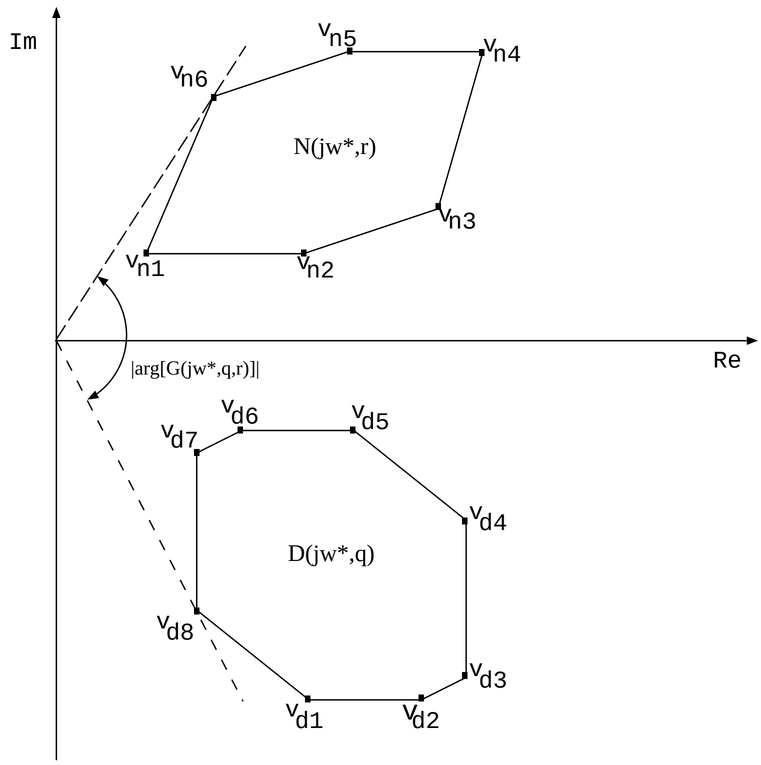

Figure 6.7: Convex parpolygons for $r = 3$ and $q = 4$ uncertain parameters

objective is to check whether the transfer function of Eq.(6.1) is a strictly positive real transfer function or not. Using Eqs.(5.32-5.35) and the identified edges given in Table 6.1, the vertex and edge sets S_{N_V} and S_{N_E} for $N(s,\mathbf{r})$ and S_{D_V} and S_{D_E} for $D(s,\mathbf{q})$ can be obtained. Since one member of S_{D_E}, for example $p(s) \in S_{D_E} = s^3 + 3s^2 + 4.4s + 1.25$, is stable and the $2q$-convex parpolygons which are shown in Figure 6.8 exclude the origin, one can conclude that S_{D_E} and subsequently $D(s,\mathbf{q})$ is stable. However, it was found that there are transfer functions obtained from vertex sets of the numerator and denominator polynomials that violate the condition given in Eq.(6.22). For example, the absolute value of the phase of $G(s) \in S_{N_V}/S_{D_V} = (0.2s^2 + 5.2s + 6)/(0.4s^3 + 3s^2 + 4.4s + 3.4)$ at $\omega = 10 rad/sec$ is equal to $125.13°$ which is greater than $\pi/2$. Therefore, one can say that the uncertain family of Eq.(6.1) is not a strictly positive real family. The Nyquist envelope of the family is shown in Figure 6.9.

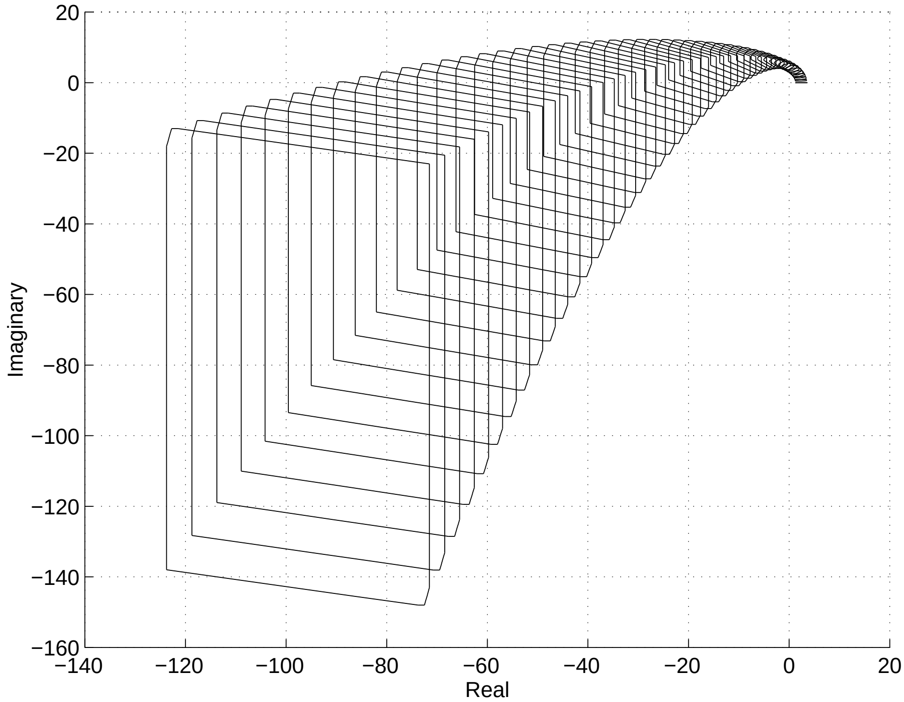

Figure 6.8: $2q$-convex parpolygon of $D(s, \mathbf{q})$

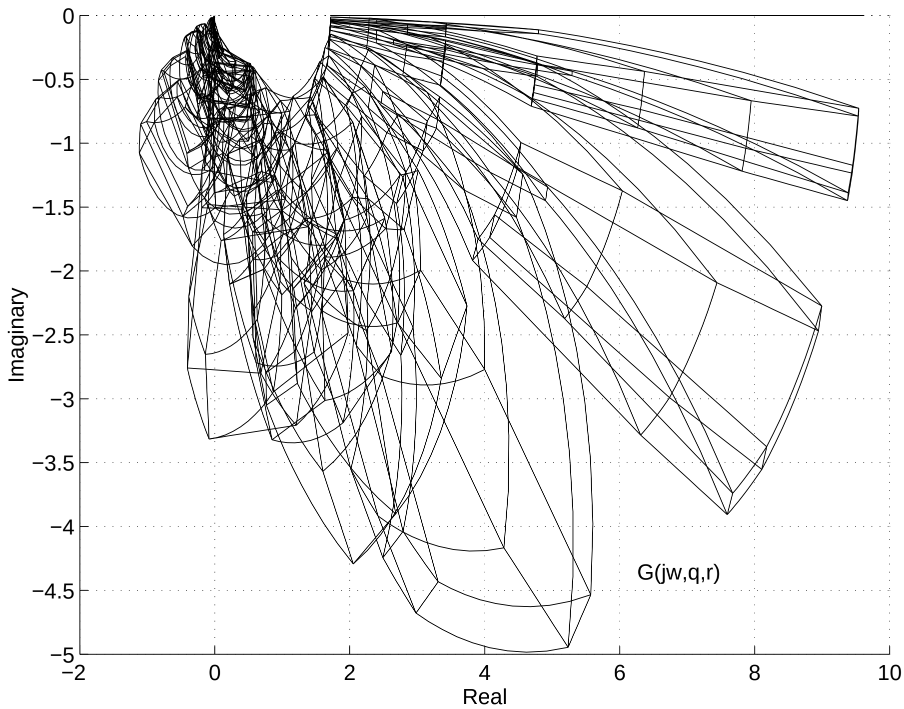

Figure 6.9: Nyquist envelope

6.6 Absolute Stability Problems

Here, the robust versions of the classical absolute stability criteria for systems with parametric uncertainty defined by Eq.(5.3) are derived. The proofs of the theorems given below can be done by using theorem 5.7 and the proofs given in previous sections. Therefore, the proofs are omitted.

Theorem 6.5: (*Lur'e Criterion*) if $G(s, \mathbf{q}, \mathbf{r})$ of Figure 6.10 is a stable transfer function with no *transition frequency* and the nonlinearity ϕ belongs to the sector $[0, k_l]$ then the condition for absolute stability is

$$\frac{1}{k_l} + Re[G_E(j\omega)] > 0, \quad \forall\omega\geq 0 \tag{6.25}$$

where $G_E(s)$ is given by Eq.(5.44).

Theorem 6.6: (*Popov Criterion*) If $G(s, \mathbf{q}, \mathbf{r})$ of Figure 6.10 is a stable transfer function with no *transition frequency* and ϕ is a time-invariant nonlinearity which belongs to the sector $[0, k_p]$ then the condition for absolute stability is that there exists a real number θ such that

$$\frac{1}{k_p} + Re[(1 + \theta j\omega)G_E(j\omega)] > 0, \quad \forall\omega\geq 0 \tag{6.26}$$

where $G_E(s)$ is defined by Eq.(5.44).

For the circle criterion define a circle C which is centered on the negative real axis at the point $(-(k_1 + k_2)/2k_1k_2, 0)$ and cutting the negative real axis at $-1/k_1$ and $-1/k_2$ where $k_1 > 0$, $k_2 > 0$ and $k_1 < k_2$. Then,

Theorem 6.7: (*Circle Criterion*) If $G(s, \mathbf{q}, \mathbf{r})$ of Figure 6.10 is a stable transfer function with no *transition frequency* and ϕ is a time-invariant nonlinearity which belongs to the sector $[k_1, k_2]$ then the condition for absolute stability is that the Nyquist plots of $G_E(s)$ which are given by Eq.(5.44) stay outside of the circle C.

Remark 6.1: The results given above, can be extended to the systems of Figures 6.11 and 6.12. It can be easily shown that

$$\partial C(j\omega)G(j\omega, \mathbf{q}, \mathbf{r})\subset C(j\omega)G_E(j\omega) \tag{6.27}$$

for the system of Figure 6.11 and

$$\partial C(j\omega)G(j\omega,\mathbf{q},\mathbf{r})(1+C(j\omega)G(j\omega,\mathbf{q},\mathbf{r}))^{-1} \subset C(j\omega)G_E(j\omega)(1+C(j\omega)G_E(j\omega))^{-1} \quad (6.28)$$

for the system of Figure 6.12.

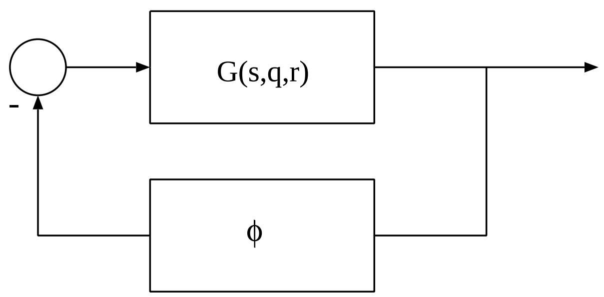

Figure 6.10: A plant with nonlinear feedback perturbations

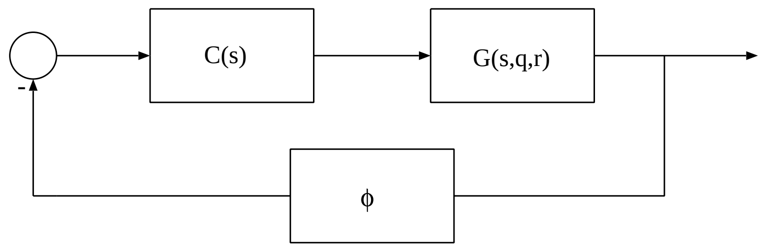

Figure 6.11: A control system with nonlinear feedback perturbations

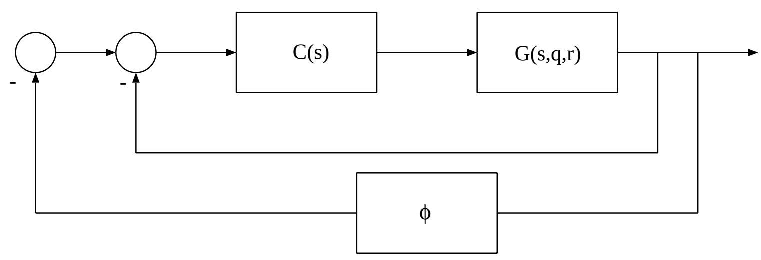

Figure 6.12: A closed loop system with nonlinear feedback perturbations

Example 6.4

Let the controller of Figure 6.11 be

$$C(s) = 0.3\frac{1.2s+1}{0.12s+1} \tag{6.29}$$

and the plant be $G(s,\mathbf{q},\mathbf{r})$ of Eq.(5.50). In example 5.2, the vertex and edge sets of the numerator and denominator of $G(s,\mathbf{q},\mathbf{r})$ were found and given by Eq.(5.54) and Eqs.(5.55-5.56), respectively. Thus, using these vertex and edge sets the Nyquist envelope and Popov plots of $C(s)G(s,\mathbf{q},\mathbf{r})$ can be obtained.

Using theorem 6.5 and Figure 6.13, the robust Lur'e gain was computed as $k_l = 1.5361$. From Figure 6.14, it was found that the robust Popov gain was $k_p = 5.026$, and from Figure 6.15 that the radii of the smallest circles C_1, C_2 and C_3 centered at $(-0.5, 0)$, $(-1, 0)$ and $(-1.25, 0)$ and touching the envelope are equal to 0.196, 0.622 and 0.835, respectively. Thus, the robust absolute stability sector for C_1 is $[k_1, k_2] = [1.436, 3.289]$, for C_2 is $[k_1, k_2] = [0.617, 2.645]$ and for C_3 is $[k_1, k_2] = [0.479, 2.409]$.

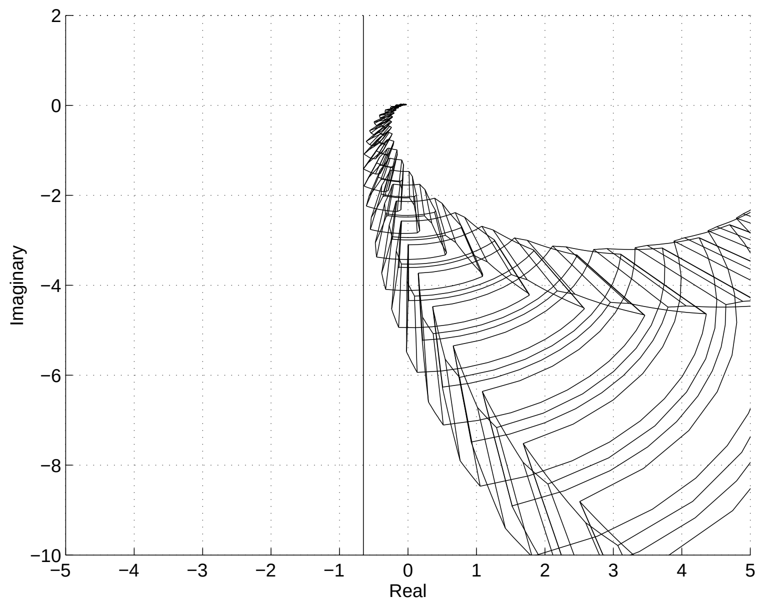

Figure 6.13: Lur'e criterion

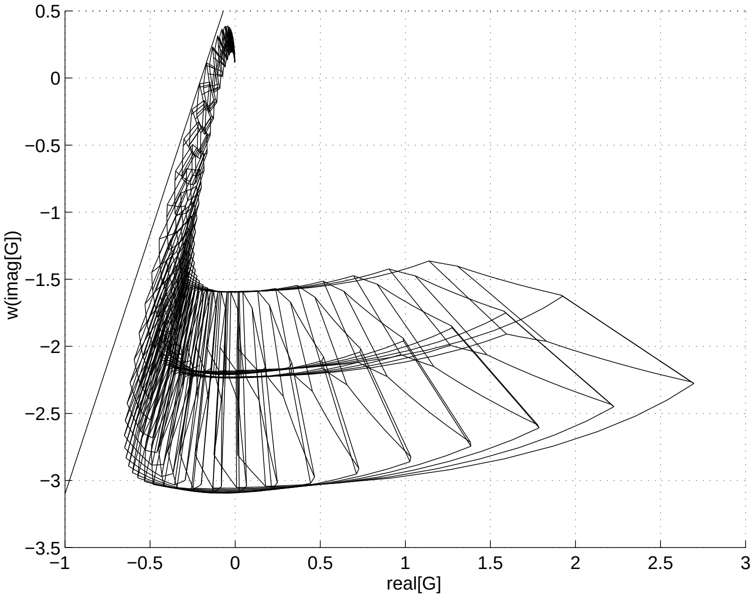

Figure 6.14: Popov criterion

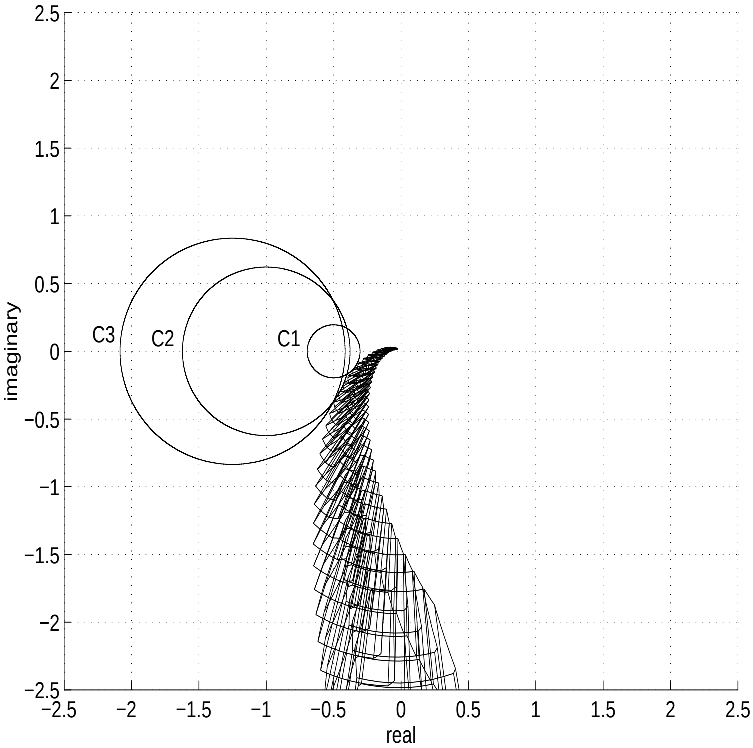

Figure 6.15: Circle criterion

6.7 Conclusion

The robust stability of a control system subject to both unstructured uncertainty, modelled as norm bounded H_∞ perturbations and sector bounded nonlinear feedback gains, and parametric uncertainty, modelled as parameter variations in the coefficients of the plant has been studied. A novel feature of the results given in this chapter is the use of the $2q$-convex parpolygonal value set of a polynomial with affine linear uncertainty. The examples given clearly show the benefit of the method presented for determination of the robust small gain theorem, robust performance, SPR conditions and absolute stability problem of control systems with mixed perturbations.

Chapter 7

THE DESCRIBING FUNCTION ANALYSIS OF NONLINEAR DISCRETE INTERVAL SYSTEMS

7.1 Introduction

It is well-known that many physical systems are not linear, although they are often represented approximately by linear equations. The principle of superposition does not hold for nonlinear systems with the result that the system response depends on the magnitude and type of the input. For example, the response of a nonlinear system to step inputs of different magnitudes may be completely different. Therefore, procedures for finding the solutions of problems involving nonlinear systems, in general, are extremely complicated.

Because of this mathematical difficulty attached to nonlinear systems, one often finds it necessary to use equivalent linearization techniques and to solve the resulting linearized problem. Linearization is the procedure in which a set of nonlinear differential equations is approximated by a linear set. The Describing Function method is one of the popular equivalent linearization methods for dealing with nonlinear control problems [8, 64, 91].

Describing Function (DF) based methods play a major part in the analysis of nonlinear discrete and continuous systems. In particular, these methods are used for assessing the system stability where instability is envisaged in the form of limit cycles. However, the classical DF method was developed for fixed nominal systems and in general is inapplicable when several uncertain parameters are present. In these situations, it is necessary to develop DF based methods for nonlinear uncertain systems in order to carry out analysis. The DF analysis of nonlinear continuous systems with parametric uncertainty was studied in [58, 57, 81] by using the μ-synthesis framework, the Kharitonov theorem and the mapping theorem [139]. However, for nonlinear discrete systems with parametric uncertainty, there are not any results to date.

In this chapter, the extension of the results given in [57, 81] to nonlinear discrete systems is given. Some of the now well developed results from the area of parametric robust control are combined with the describing function method to analyze the stability problem of uncertain discrete time systems with separable nonlinearities. The system under investigation is shown in Figure 7.1a where both the linear and nonlinear elements contain parametric uncertainties. The characteristic equation of such systems turns out to be a discrete uncertain polynomial. Using the so-called overbounding method and results given in the literature about the Schur stability of interval polynomials [30, 77, 44, 92, 93, 85, 111, 89], a method is proposed for the prediction of limit cycles.

The chapter is organized as follows: A review of the classical DF method is given in Section 7.2. Section 7.3 investigates the robust Schur stability of interval polynomials. A stability result for discrete interval plants with separable nonlinearity is derived in section 7.4. Section 7.5 gives some concluding remarks.

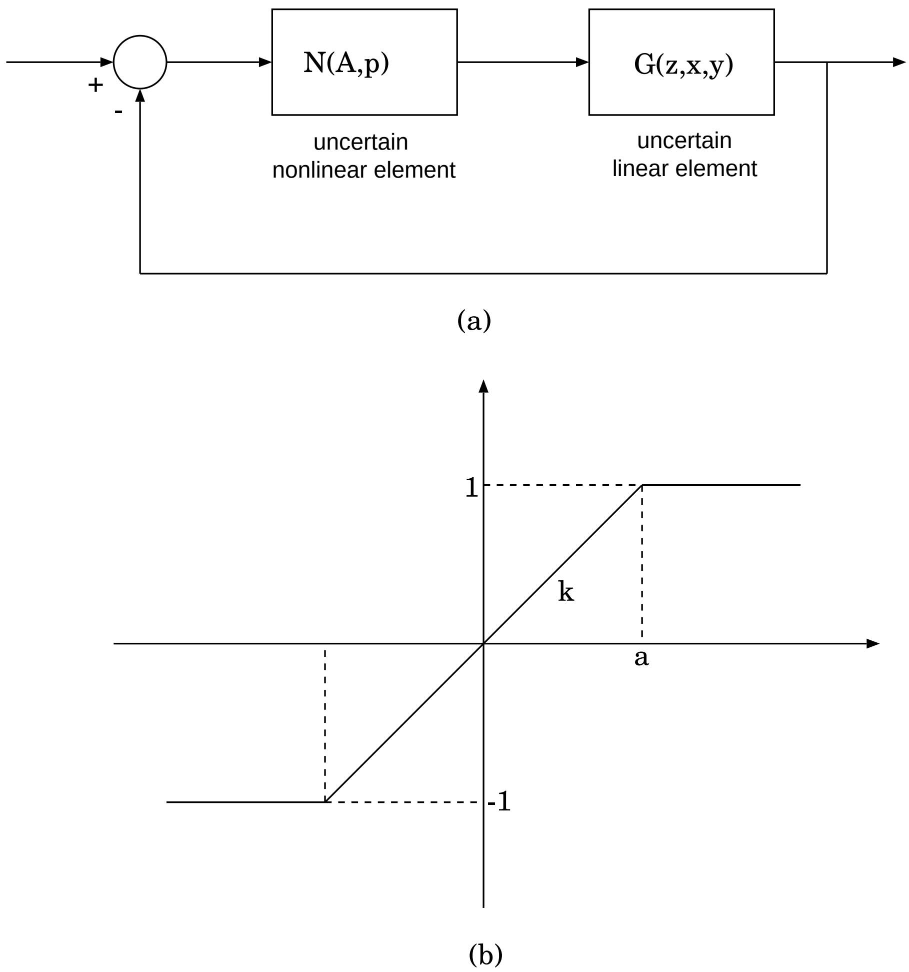

Figure 7.1: a) Uncertain nonlinear discrete system b) Saturation nonlinearity

7.2 Describing Function Analysis

The DF method is an approximate procedure for investigating the existence of limit cycles in control systems with separable nonlinearities. The details of this method can be found in the books by Atherton [8, 9]. The basic idea is that a steady-state sinusoidal input into a nonlinear element will produce an output that has components of the same frequency as the input as well as the harmonics. Describing function analysis assumes that only the fundamental component of the output is important. Thus, the DF of a nonlinear element can be defined as the complex ratio of the fundamental component of the output to the sinusoidal input.

Consider an input $x(t) = Asin(\omega t)$ to the nonlinear element, the output can be expressed in a Fourier series as follows:

$$y(t) = \frac{a_0}{2} + \sum_{n=1}^{\infty}[a_n cos(n\omega t) + b_n sin(n\omega t)] \tag{7.1}$$

where

$$a_n = \frac{1}{\pi}\int_0^{2\pi} y(t)cos(n\omega t)d(\omega t) \tag{7.2}$$

and

$$b_n = \frac{1}{\pi}\int_0^{2\pi} y(t)sin(n\omega t)d(\omega t) \tag{7.3}$$

For an odd nonlinearity a_0 is zero. Using the fundamental component of $y(t)$, the nonlinearity is represented with the describing function as

$$N(A) = \frac{b_1 + ja_1}{A} \tag{7.4}$$

Since Eq.(7.4) is a scalar quantity, any parametric uncertainty in the nonlinearity can be easily represented by varying the describing function in an interval. Therefore, the uncertain describing function can be denoted with $N(A, \mathbf{p})$ where $\mathbf{p}$ is a vector of uncertain parameters. Now, the characteristic equation of the uncertain system shown in Figure 7.1a can be written as

$$1 + N(A, \mathbf{p})G(z, \mathbf{x}, \mathbf{y}) = 0 \tag{7.5}$$

where $G(z, \mathbf{x}, \mathbf{y})$ is an interval discrete plant. From Eq.(7.5), the following equation can be obtained

$$G(z, \mathbf{x}, \mathbf{y}) = -\frac{1}{N(A, \mathbf{p})} \tag{7.6}$$

Thus, the possible range of (A, ω) values can be investigated by plotting $G(e^{j\omega T}, \mathbf{x}, \mathbf{y})$ and $-1/N(A, \mathbf{p})$ together. If an intersection exists, the system may have limit cycles in those ranges of (A, ω) determined by the intersection points. The stability of the system can be assessed by applying the Nyquist criterion. In this case, the single $(-1, 0)$ critical point is replaced by a locus of critical points, which are given by $-1/N(A, \mathbf{p})$.

The advantage of the DF method is its simplicity and its easy usability with classical control methods. However, its down side is that, since it is an approximate procedure, it may give incorrect results. The accuracy of the DF method depends on two factors which are the distortion produced by the nonlinearity assuming a sinusoidal input and the frequency characteristic of the linear element. In the presence of uncertainty, the results of the DF method may deteriorate further. Thus, using the results developed in the field of parametric robust control some reliable results can be obtained.

7.3 Schur Stability of Interval Polynomials

The problem of the stability of interval polynomials was solved in continuous time systems by the Kharitonov theorem. To date, such a solution does not exist for discrete time polynomials of the form

$$P(z, \mathbf{a}) = \sum_{i=0}^{n} a_i z^{n-i} \tag{7.7}$$

where $a_i \in [\underline{a_i}, \overline{a_i}], i = 0, 1, ..., n$ and as usual $\underline{a_i}$ and $\overline{a_i}$ are specified lower and upper bounds of the ith perturbation a_i, respectively. For example, consider the following interval polynomials

$$P(z, \mathbf{a}) = z^4 + [-1.3, -1]z^3 + [0.42, 0.5]z^2 + [-0.16, -0.1]z + 0.0096 \tag{7.8}$$

The four Kharitonov polynomials

$$\begin{aligned} p_1(z) &= z^4 - z^3 + 0.5z^2 - 0.16z + 0.0096 \\ p_2(z) &= z^4 - 1.3z^3 + 0.5z^2 - 0.1z + 0.0096 \\ p_3(z) &= z^4 - z^3 + 0.42z^2 - 0.16z + 0.0096 \\ p_4(z) &= z^4 - 1.3z^3 + 0.42z^2 - 0.1z + 0.0096 \end{aligned} \tag{7.9}$$

are all Schur stable. However, the polynomial

$$p(z) \in P(z, \mathbf{a}) = z^4 - 1.28z^3 + 0.42z^2 - 0.155z + 0.0096 \tag{7.10}$$

is not Schur Stable. This shows that the stability of the Kharitonov polynomials does not guarantee the Schur stability of the entire family. Furthermore, it is known that [25] even the Schur stability of all the vertex polynomials of interval discrete polynomials does not guarantee the stability of the entire family.

One method for tackling the robust discrete-stability of the polynomials is based on the bilinear transformation. If $P(z, \mathbf{a})$ has all zeros $|z| < 1$, then

$$Q(s, \mathbf{a}) = (s-1)^n P(\frac{s+1}{s-1}, \mathbf{a}) \tag{7.11}$$

has all zeros in $Re(s) < 0$. However, the problem is that if the coefficients of $P(z, \mathbf{a})$ lie in rectangular boxes with sides parallel to the axes, this is not the case for the coefficients of $Q(s, \mathbf{a})$, nor conversely. So, the bilinear transformation distorts regions in the coefficient space which makes the problem difficult. Another method is the edge theorem. As stated in Chapter 2, the edge theorem is a very useful tool for robust $\mathcal{D}$ stability of uncertain polynomials. In the case of discrete polynomials the region $\mathcal{D}$ is a unit circle in the complex plane. Therefore, from the edge theorem, one can say that a discrete interval polynomial is Schur stable if all the exposed edges of the family are Schur stable. However, since the number of exposed edges is dependent exponentially on the number of the uncertain parameters, this procedure is computationally expensive.

Kharitonov like results for monic low order (first, second and third order) discrete interval polynomials were developed in [77, 44]. For higher orders and when all the coefficients of a given polynomial are subject to perturbation, the problem of robust Schur stability was solved in [85] using a Kharitonov parameter box. The results given in [77] are reviewed as follows:

Theorem 7.1 (Hollot and Bartlett [77]): Assume that all the a_i's of $P(z, \mathbf{a})$ are constant for $i = 0, 1, 2, ..., n/2\perp$ (by $n/2\perp$ we mean next lower integer with respect to $n/2$). Then the interval polynomial family $P(z, \mathbf{a})$ is Schur stable if and only if all the corner polynomials are Schur stable. These corner polynomials can be represented as

$$C^k(z) = \sum_{i=0}^{n/2\perp} a_i z^{n-i} + \sum_{j=n/2\perp+1}^{n} a_j z^{n-j} \tag{7.12}$$

where $\underline{a_i} = \overline{a_i}$ and $a_j \in \{\underline{a_j}, \overline{a_j}\}$.

With this theorem, one can consider the special case of interval polynomials whose order $n \leq 3$. For monic interval polynomials of order $n = 1$ and $n = 2$, the robust Schur stability is equivalent to the robust Schur stability of Kharitonov polynomials. A monic third order discrete interval polynomial is robust Schur stable if all $2^3 = 8$ extreme polynomials are stable (instead of only four polynomials in Kharitonov's test). However, when all the $(n+1)$ coefficients of $P(z, \mathbf{a})$ are subject to change, the robust Schur stability of corner polynomials or Kharitonov polynomials are not sufficient for stability of all the family. In this case Katbab and Jury [85] have used a Kharitonov parameter box in order to determine robust Schur stability. This method is actually a simplification of the edge theorem for discrete interval polynomials. The method is summarized as follows:

Consider two different boxes corresponding to the lower, $P_l(z)$, and upper, $P_u(z)$, parts of a polynomial $P(z, \mathbf{a})$ which is represented in Eq.(7.7) form as

$$P(z, \mathbf{a}) = P_l(z) + P_u(z) = \sum_{i=0}^{n/2\perp} a_i z^{n-i} + \sum_{j=n/2\perp+1}^{n} a_j z^{n-j} \tag{7.13}$$

The upper box, $P_u(z)$, has $K = 2^{n-n/2\perp}$ corners. The upper part of the kth such corner can be written as

$$C_u^k(z) = \sum_{j=n/2\perp+1}^{n} a_j z^{n-j} \tag{7.14}$$

where $a_j \in \{\underline{a_j}, \overline{a_j}\}$ and $k = 1, 2, ..., K$. Also, the total number of all a_i-edges of the lower box, $P_l(z)$, is $h = n'2^{n'-1}$ for monic and $h = (n'+1)2^{n'}$ for non-monic polynomials, where $n' = n/2\perp$. The lower part of the eth such a_i-edge, $e = 1, 2, ..., h$, has the general form

$$E_l^e(z) = \sum_{i=0}^{n/2\perp} [(1-\lambda_i)\underline{a_i} + \lambda_i \overline{a_i}] z^{n-i} \tag{7.15}$$

where only one of the λ_is, $i = 0, 1, ..., n/2\perp$ belongs to the interval $[0, 1]$ and the others are either 0 or 1. Thus, in order to check the stability of $P(z, \mathbf{a})$, one needs to check $H = K \times h$ edge polynomials. The hth one is shown below:

$$E^h(z) = E_l^e + C_u^k = \sum_{i=0}^{n/2\perp} [(1-\lambda_i)\underline{a_i} + \lambda_i \overline{a_i}] z^{n-i} + \sum_{j=n/2\perp+1}^{n} a_j z^{n-j} \tag{7.16}$$

where $h = 1, 2, ..., H$, $k = 1, 2, ..., K$, $e = 1, 2, ..., h$, and as mentioned before only one of the λ_i's, $i = 1, 2, ..., n/2\perp$ belongs to the interval $[0, 1]$ and the others are either 0 or 1.

Example 7.1

Consider

$$P(z,\mathbf{a}) = a_0 z^3 + a_1 z^2 + a_2 z + a_3 \tag{7.17}$$

where $a_0 \in [0.9, 1.1]$, $a_1 \in [-0.35, -0.15]$, $a_2 \in [-0.85, -0.65]$ and $a_3 \in [0.08, 0.28]$. Since there are four unknown parameters, from the edge theorem the corresponding polytope of the family has 32 exposed edges. However, using the method of Katbab and Jury, it is possible to reduce the number of edges which are necessary for the stability of the family by 50% as follows:

The lower polynomial

$$P_l(z) = a_0 z^3 + a_1 z^2 \tag{7.18}$$

has $h = 4$ edges as follows

$$\begin{aligned}
E_l^1 &= [(1-\lambda)\underline{a_0} + \lambda\overline{a_0}]z^3 + \underline{a_1}z^2 = [(1-\lambda)0.9 + \lambda 1.1]z^3 - 0.35z^2 \\
E_l^2 &= [(1-\lambda)\underline{a_0} + \lambda\overline{a_0}]z^3 + \overline{a_1}z^2 = [(1-\lambda)0.9 + \lambda 1.1]z^3 - 0.15z^2 \\
E_l^3 &= \underline{a_0}z^3 + [(1-\lambda)\underline{a_1} + \lambda\overline{a_1}]z^2 = 0.9z^3 + [-(1-\lambda)0.35 - \lambda 0.15]z^2 \\
E_l^4 &= \overline{a_0}z^3 + [(1-\lambda)\underline{a_1} + \lambda\overline{a_1}]z^2 = 1.1z^3 + [-(1-\lambda)0.35 - \lambda 0.15]z^2
\end{aligned} \tag{7.19}$$

and the upper polynomial

$$P_u(z) = a_2 z + a_3 \tag{7.20}$$

has $K = 4$ corners as follows:

$$\begin{aligned}
C_u^1 &= \underline{a_2}z + \underline{a_3} = -0.85z + 0.08 \\
C_u^2 &= \underline{a_2}z + \overline{a_3} = -0.85z + 0.28 \\
C_u^3 &= \overline{a_2}z + \underline{a_3} = -0.65z + 0.08 \\
C_u^4 &= \overline{a_2}z + \overline{a_3} = -0.65z + 0.28
\end{aligned} \tag{7.21}$$

Thus, for the stability of $P(z,\mathbf{a})$, it is necessary to check the stability of $H = K \times h = 16$ edge polynomials. These edge polynomials can be obtained from Eq.(7.16). For example, one of these edge polynomials is

$$E^1 = E_l^1 + C_u^1 = [(1-\lambda)\underline{a_0} + \lambda\overline{a_0}]z^3 + \underline{a_1}z^2 + \underline{a_2}z + \underline{a_3} \tag{7.22}$$

Similarly, the other edges can be obtained. The value sets of these 16 edges are shown in Figure 7.2. It can be tested that the four Kharitonov polynomials of the family are Schur stable. However, since the value sets include the origin from the zero exclusion principle, one can conclude that the discrete interval polynomial of Eq.(7.17) is not Schur stable.

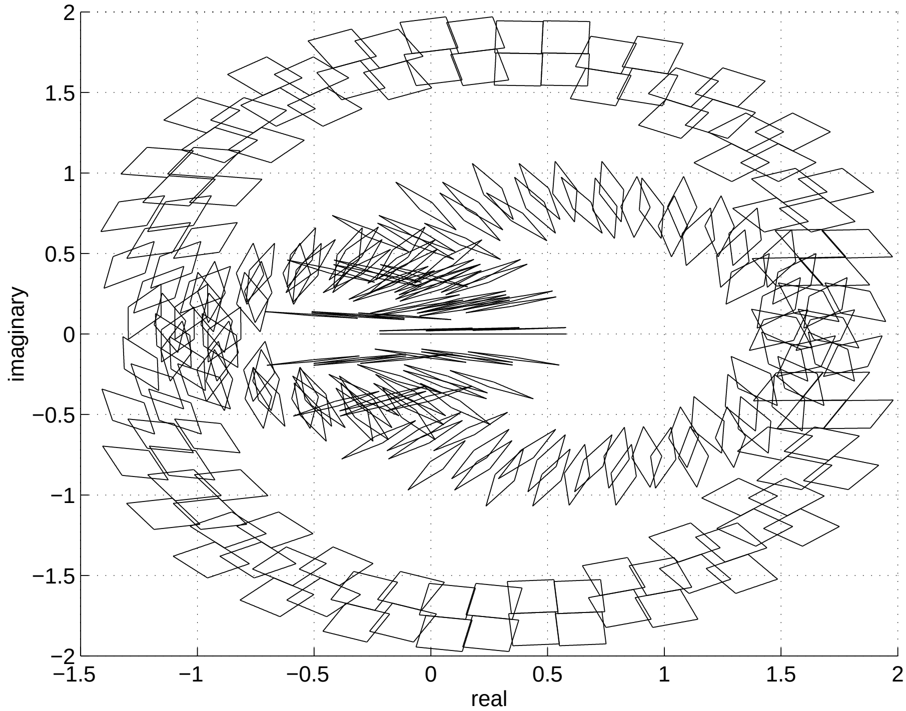

Figure 7.2: Value sets of 16 edges

7.4 Nonlinear Discrete Systems with Uncertain Parameters

The describing function analysis of continuous systems with parametric uncertainty has been studied in [57] and [81]. In [57], it was assumed that the linear part was an interval plant of the form of Eq.(2.27) and the nonlinear element was represented by an uncertain gain with lower and upper values. Then, it is easy to show that the characteristic equation of such a system is a polynomial with multilinear uncertainty structure unless the numerator of the linear part is constant. By overbounding the coefficients of the characteristic equation and using the Kharitonov theorem, a stability result has been given in [57]. However, since the overbounding technique has been used in [57], the given results are conservative. On the other hand, by using the mapping theorem and also assuming that the linear part may have an affine linear uncertainty structure, some improved results in this direction have been given by Impram and Munro [81]. The extension of these results to the discrete nonlinear system is considered in this section. In particular, the aim of this section is to study the stability of systems of Figure 7.1a.

Let the describing function of the nonlinear element which contains uncertain parameters be

$$N(A,\mathbf{p}) = [\underline{p_r}, \overline{p_r}] + j[\underline{p_i}, \overline{p_i}] \tag{7.23}$$

For a memoryless nonlinearity, the interval describing function is

$$N(A,\mathbf{p}) = [\underline{p_r}, \overline{p_r}] \tag{7.24}$$

and let the discrete interval plant, G(z,**x**,**y**), of Figure 7.1a be given as

$$G(z,\mathbf{x},\mathbf{y}) = \frac{N(z,\mathbf{x})}{D(z,\mathbf{y})} = \frac{\sum_{i=0}^{m} x_i z^{m-i}}{\sum_{i=0}^{n} y_i z^{n-i}}, \quad m \le n \tag{7.25}$$

where $x_i \in [\underline{x_i}, \overline{x_i}]$ and $y_i \in [\underline{y_i}, \overline{y_i}]$. Then the characteristic equation of the system can be written as

$$1 + N(A,\mathbf{p})G(z,\mathbf{x},\mathbf{y}) = 1 + [\underline{p_r}, \overline{p_r}] \frac{\sum_{i=0}^{m} x_i z^{m-i}}{\sum_{i=0}^{n} y_i z^{n-i}} =$$
$$\sum_{i=0}^{n} [\underline{y_i}, \overline{y_i}] z^{n-i} + [\underline{p_r}, \overline{p_r}] \sum_{i=0}^{m} [\underline{x_i}, \overline{x_i}] z^{m-i} = 0 \tag{7.26}$$

It can be seen that the characteristic equation of the system has a multilinear uncertainty structure. In order to apply the results summarized in the previous section, one needs to obtain an independent uncertainty structure. To do this, the so-called overbounding method which enables one to convert a dependent uncertainty structure to an independent one is used. Thus, by overbounding the parameters, Eq.(7.26) can be written as

$$\sum_{i=0}^{n-(m+1)} [\underline{y_i}, \overline{y_i}] z^{n-i} + \sum_{i=n-m}^{n} [\underline{p_r x_{i-(n-m)}} + \underline{y_i}, \overline{p_r x_{i-(n-m)}} + \overline{y_i}] z^{n-i} = 0 \tag{7.27}$$

or writing Eq.(7.27) in the form of Eq.(7.7)

$$\delta(z) = \sum_{i=0}^{n-(m+1)} [\underline{y_i}, \overline{y_i}] z^{n-i} + \sum_{i=n-m}^{n} [\underline{p_r x_{i-(n-m)}} + \underline{y_i}, \overline{p_r x_{i-(n-m)}} + \overline{y_i}] z^{n-i} = \sum_{i=0}^{n} a_i z^{n-i} \tag{7.28}$$

where

$$a_i \in [\underline{a_i}, \overline{a_i}] = [\underline{y_i}, \overline{y_i}] \;\; for \;\; 0 \leq i \leq n-(m+1)$$

and

$$a_i \in [\underline{a_i}, \overline{a_i}] = [\underline{p_r}\, \underline{x_{i-(n-m)}} + \underline{y_i}, \overline{p_r}\, \overline{x_{i-(n-m)}} + \overline{y_i}] \;\; for \;\; n-m \leq i \leq n$$

Then, in the light of the results given in the previous section, the robust stability of the nonlinear discrete interval systems of Figure 7.1a can be stated as follows:

i) If the closed loop characteristic equation of the system, $\delta(z)$ of Eq.(7.28), is a monic first or second order interval polynomial then the given system is robustly Schur stable if and only if the following Kharitonov polynomials are robustly stable.
monic first order:

$$\begin{aligned} \delta_1(z) &= z + \underline{a_1} \\ \delta_2(z) &= z + \overline{a_1} \end{aligned} \tag{7.29}$$

monic second order:

$$\begin{aligned} \delta_1(z) &= z^2 + \underline{a_1} z + \underline{a_2} \\ \delta_2(z) &= z^2 + \overline{a_1} z + \underline{a_2} \\ \delta_3(z) &= z^2 + \underline{a_1} z + \overline{a_2} \\ \delta_4(z) &= z^2 + \overline{a_1} z + \overline{a_2} \end{aligned} \tag{7.30}$$

ii) If the characteristic equation is a monic third order one, the following 8 extreme polynomials will be enough for robust stability of the system:

$$\begin{aligned} \delta_1(z) &= z^3 + \underline{a_1} z^2 + \underline{a_2} z + \underline{a_3} \\ \delta_2(z) &= z^3 + \underline{a_1} z^2 + \underline{a_2} z + \overline{a_3} \end{aligned}$$

$$\begin{aligned}
\delta_3(z) &= z^3 + \underline{a_1} z^2 + \overline{a_2} z + \overline{a_3} \\
\delta_4(z) &= z^3 + \underline{a_1} z^2 + \overline{a_2} z + \underline{a_3} \\
\delta_5(z) &= z^3 + \overline{a_1} z^2 + \underline{a_2} z + \underline{a_3} \\
\delta_6(z) &= z^3 + \overline{a_1} z^2 + \underline{a_2} z + \overline{a_3} \\
\delta_7(z) &= z^3 + \overline{a_1} z^2 + \overline{a_2} z + \underline{a_3} \\
\delta_8(z) &= z^3 + \overline{a_1} z^2 + \overline{a_2} z + \overline{a_3}
\end{aligned} \tag{7.31}$$

iii) When all coefficients of $\delta(z)$ of Eq.(7.28) are subject to perturbation then the robust Schur stability of H ($H = K \times h$ where $K = 2^{n-n/2\perp}$, $h = n'2^{n'-1}$ for monic and $h = (n'+1)2^{n'}$ for non-monic polynomials and $n' = n/2\perp$) edges guarantees the robust stability of the system. The general form of such an edge is shown in Eq.(7.16).

Example 7.2

Consider the nonlinear system of Figure 7.1a with

$$G(z, \mathbf{x}, \mathbf{y}) = \frac{0.1746z + 0.1529}{z^2 + y_1 z + y_2} \tag{7.32}$$

where $y_1 \in [-1.5746, -1.3746]$ and $y_2 \in [0.7, 0.8]$ and let the nonlinear element have the saturation characteristic, with a and k as shown in Figure 7.1b. If $A < a$ the describing function is a constant k. For $A > a$, the describing function is

$$N(A, k) = \frac{2k}{\pi}[arcsin(\frac{a}{A}) + (\frac{a}{A})\sqrt{1 - \frac{a^2}{A^2}}\,] \tag{7.33}$$

For $k \in [1, 4]$, the describing function becomes $N(A, k) \in [0, 4]$. Then, the characteristic equation of the system can be written as

$$1 + N(A, k)G(z, \mathbf{x}, \mathbf{y}) = 0 = 1 + [0, 4]\frac{0.1746z + 0.1529}{z^2 + [-1.5746, -1.3741]z + [0.7, 0.8]} \tag{7.34}$$

and from Eq.(7.34), the characteristic equation reduces to

$$\delta(z) = z^2 + [-1.5746, -0.6757]z + [0.7, 1.4116] = 0 \tag{7.35}$$

and the four Kharitonov polynomials are

$$\begin{aligned}
\delta_1(z) &= z^2 - 1.5746z + 0.7 \\
\delta_2(z) &= z^2 - 0.6757z + 0.7 \\
\delta_3(z) &= z^2 - 1.5746z + 1.4116 \\
\delta_4(z) &= z^2 - 0.6757z + 1.4116 \qquad (7.36)
\end{aligned}$$

The roots of $\delta_3(z)$ and $\delta_4(z)$ are $0.7873 \pm j0.8898$ and $0.3378 \pm j1.1391$ respectively, which are not inside the unit circle. This shows that the nonlinear system is not robust Schur stable. The frequency response of $G(e^{j\omega T}, \mathbf{x}, \mathbf{y})$ and describing function $-1/N(A,k)$ are shown in Figure 7.3. It can be seen that the describing function plot intersects with the Nyquist envelope of $G(e^{j\omega T}, \mathbf{x}, \mathbf{y})$. Therefore, one can say that a limit cycle is likely to occur.

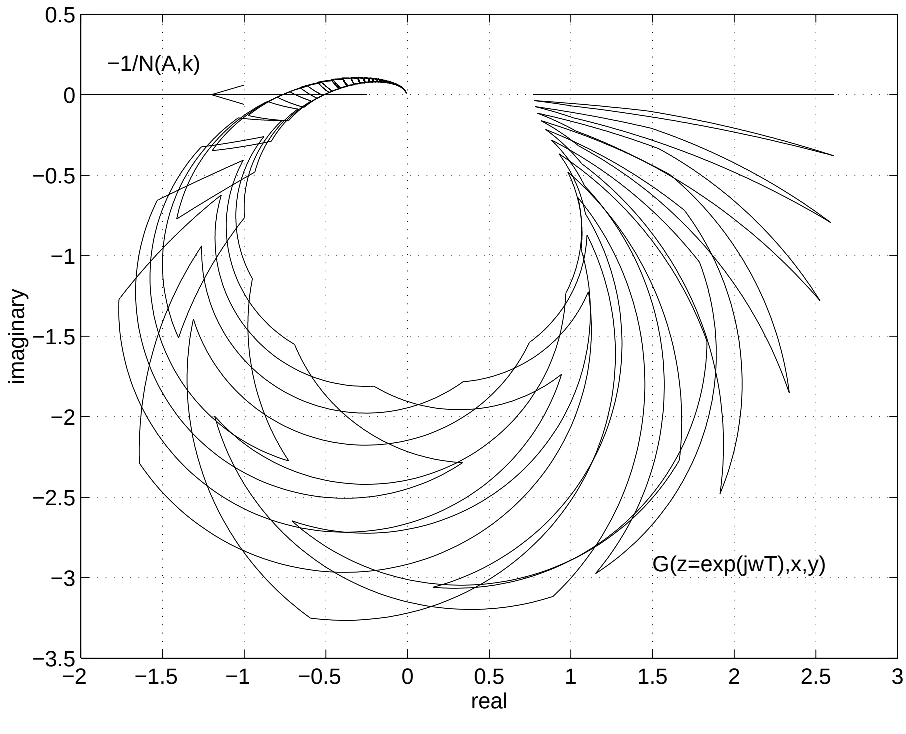

Figure 7.3: Graphical prediction of limit cycle

Example 7.3

Here, we consider the system of Figure 7.1a to have

$$G(z,\mathbf{x},\mathbf{y}) = \frac{0.1}{y_0 z^2 + y_1 z + y_2} \tag{7.37}$$

where $y_0 \in [2.5, 4]$, $y_1 \in [-0.1, 0.25]$ and $y_2 \in [0.1, 0.7]$ and again consider the saturation non-linearity as in Example 7.2. The closed loop characteristic equation of the system is

$$1 + N(A,k)G(z,\mathbf{x},\mathbf{y}) = 0 = 1 + [0,4]\frac{0.1}{[2.5,4]z^2 + [-0.1,0.25]z + [0.1,0.7]} \tag{7.38}$$

and it can be written as

$$\delta(z) = [2.5,4]z^2 + [-0.1,0.25]z + [0.1,1.1] \tag{7.39}$$

which is a non-monic second order polynomial. Therefore, the robust Schur stability of the Kharitonov polynomials alone will not be sufficient. From the results of Section 7.3,

$$\delta_l(z) = [2.5,4]z^2 \tag{7.40}$$

which has the $h = 1$ edge as follows

$$E_l^1 = [(1-\lambda)2.5 + 4\lambda],\ \lambda \in [0,1] \tag{7.41}$$

The upper box

$$\delta_u(z) = [-0.1,0.25]z + [0.1,1.1] \tag{7.42}$$

has $K = 4$ corners as follows:

$$\begin{aligned} C_u^1 &= -0.1z + 0.1 \\ C_u^2 &= -0.1z + 1.1 \\ C_u^3 &= 0.25z + 0.1 \\ C_u^4 &= 0.25z + 1.1 \end{aligned} \tag{7.43}$$

Thus, there are $H = K \times h = 4$ edge polynomials to check the stability of $\delta(z)$, which are

$$\begin{aligned} E^1(\lambda, z) &= E_l^1 + C_u^1 = (2.5 + 1.5\lambda)z^2 - 0.1z + 0.1 \\ E^2(\lambda, z) &= E_l^1 + C_u^2 = (2.5 + 1.5\lambda)z^2 - 0.1z + 1.1 \\ E^3(\lambda, z) &= E_l^1 + C_u^3 = (2.5 + 1.5\lambda)z^2 + 0.25z + 0.1 \\ E^4(\lambda, z) &= E_l^1 + C_u^4 = (2.5 + 1.5\lambda)z^2 + 0.25z + 1.1 \end{aligned} \tag{7.44}$$

The stability of these four edge polynomials can be checked by using the zero exclusion principle. The image set (value set) of $E^h(\lambda, e^{j\omega T})$, $h = 1, 2, 3, 4$ is shown in Figure 7.4. It can be seen that the image set excludes the origin $(0 \notin E^h(\lambda, e^{j\omega T}))$, which shows that the entire family is asymptotically stable. The Nyquist envelope of $G(z, \mathbf{x}, \mathbf{y})$ of Eq.(7.37) and the describing function $-1/N(A, k)$ are shown in Figure 7.5.

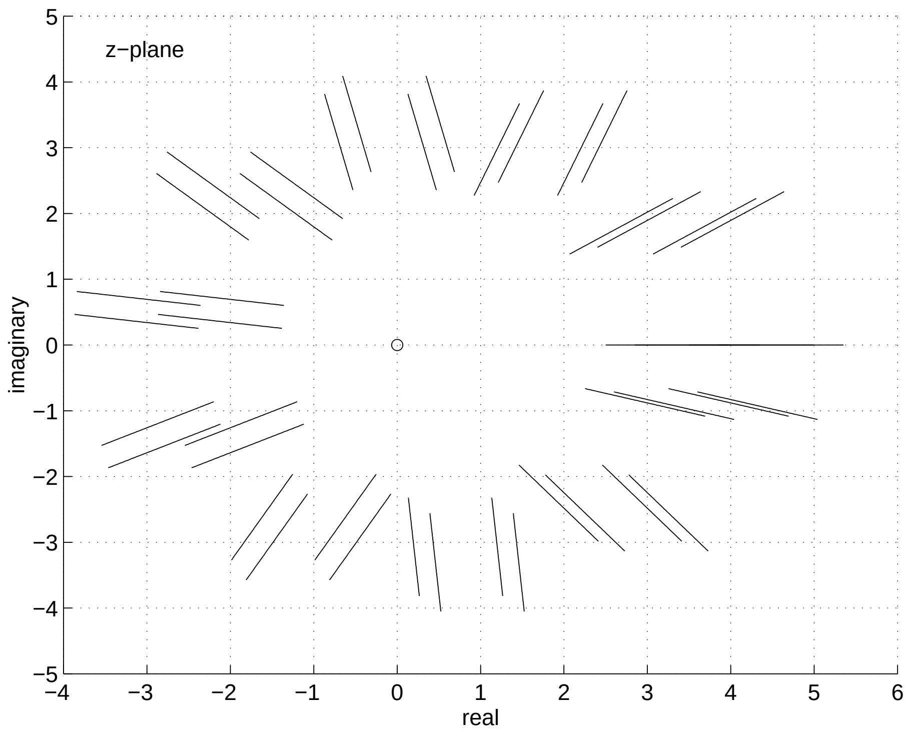

Figure 7.4: Image set(value set) of $E^h(\lambda, e^{j\omega T})$, $h = 1, 2, 3, 4$.

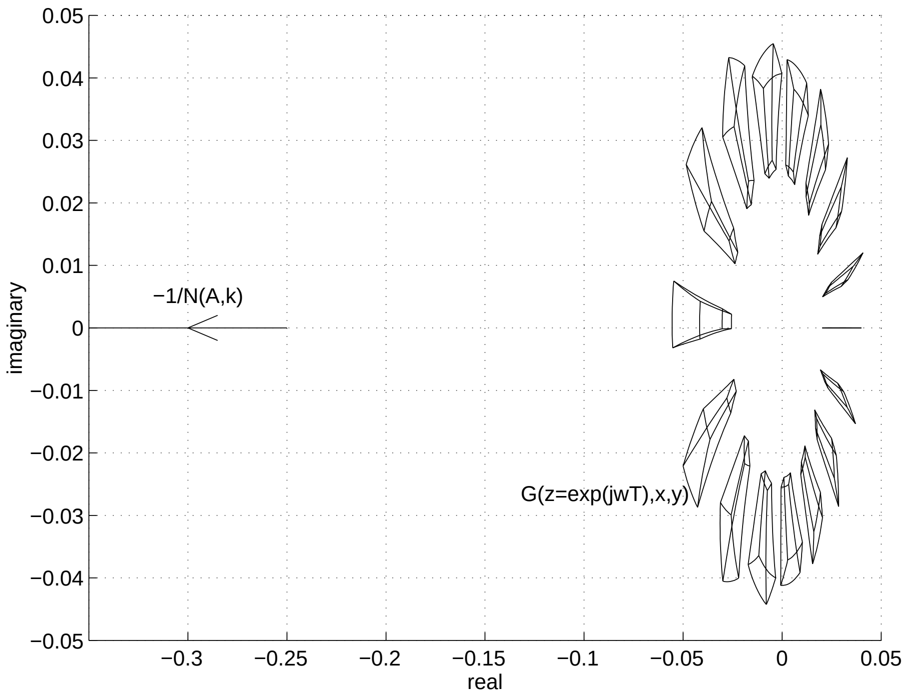

Figure 7.5: Nyquist envelope and Describing function

7.5 Conclusion

In this chapter, the describing function analysis of nonlinear discrete systems with parametric uncertainty has been studied. It has been shown that the characteristic equation of such systems with an interval plant and an uncertain describing function turns out to be a polynomial with multilinear uncertainty structure. Using the so-called overbounding procedure and combining the describing function method with some well established results from the area of robust control under parametric uncertainty, a method has been proposed for the prediction of limit cycles in uncertain discrete systems with separable nonlinearities. Since the DF technique is an approximate procedure, it may give inaccurate results. However, the results which are produced by the DF method can be relied upon if the linear subsystem is sufficiently low pass and the DF approximation is valid.

Chapter 8

CONCLUSIONS

8.1 New Contributions

Several important control problems have been addressed in this thesis. The new contributions of the thesis are summarized below:

1. Extension of the Ho *et al.* method [72] to a *Lag/Lead* controller structure for stabilizing a given fixed plant;

2. Extension of the Ho *et al.* method to PI, $Lag/Lead$ and PID controllers for relative stabilization of a fixed plant;

3. Extension of the Ho *et al.* method to interval plant stabilization;

4. Development of an alternative approach, which is based on the generalized Hermite-Biehler theorem, for computing the robust gain and phase margins and outer boundary of the Nyquist envelope of an interval plant family;

5. Formulation of the gain crossover, phase crossover and bandwidth frequencies of an interval plant;

6. Development of a user friendly software program to analyse interval systems;

7. Application of a simple autotuning method to an interval plant via an example;

8. An alternative proof of the idea that the edges of the $2q$-convex parpolygon of $P(s, \mathbf{q})$ of Eq.(5.1) remain unchanged within some frequency intervals (Theorem 5.1);

9. It was shown that the maximum magnitude and the phase extremums of $P(s, \mathbf{q})$ of Eq.(5.1) and $\delta(s)P(s, \mathbf{q})$, where $\delta(s)$ is a fixed polynomial, at $s = j\omega^*$ can be found from vertices of the $2q$-convex parpolygon. For computing the minimum magnitude, an exact equation was derived (Theorem 5.1, Theorem 5.3, Lemma 5.1 and Theorem 5.4);

10. It has been shown that the magnitude extremums, the phase extremums and the boundary of a Nyquist template of $G(s, \mathbf{q}, \mathbf{r})$ of Eq.(5.3) at $s = j\omega^*$ can be computed from the vertex and edge sets of $2r$ and $2q$-convex parpolygons of the numerator and denominator polynomials of $G(s, \mathbf{q}, \mathbf{r})$ (Theorem 5.5, Theorem 5.6 and Theorem 5.7);

11. A procedure has been given for computing the Bode, Nyquist and Nichols envelopes of a transfer function with affine linear uncertainty;

12. It was shown that the robust gain and phase margins of $G(s, \mathbf{q}, \mathbf{r})$ of Eq.(5.3) can be found from the vertex and edge sets of $2r$ and $2q$-convex parpolygons of the numerator and denominator polynomials of $G(s, \mathbf{q}, \mathbf{r})$ (Theorem 5.8);

13. Extension of classical control design methods to systems with affine linear uncertainty;

14. A robust version of the small gain theorem for a control system with $G(s, \mathbf{q}, \mathbf{r})$ of Eq.(5.3) was derived (Theorem 6.1 and Theorem 6.2);

15. Robust performance of control systems with affine linear uncertainty was formulated (Theorem6.3);

16. Strict positive realness conditions of a transfer function of the form of Eq.(5.3) have been investigated (Theorem 6.4);

17. Robust versions of absolute stability criteria were derived (Theorem 6.6, Theorem 6.7 and Theorem 6.8);

18. A method has been given to investigate the stability of nonlinear discrete interval systems.

8.2 Future Work

There are several possibilities for future work which include:

1. Development of analogous results to those obtained in Chapter 3 for cone stabilization and stabilization of uncertain systems with an affine linear uncertainty structure;

2. Extension of the program described in Chapter 4 to systems with affine linear uncertainty and the addition of some algorithms to design robust controllers for uncertain systems;

3. In Chapter 5, it was shown that the magnitude and phase extremums of $P(s, \mathbf{q})$ of Eq.(5.1) at $s = j\omega^*$ can be computed from the boundary of the $2q$-convex parpolygon. It would be beneficial to obtain frequency intervals within which the polynomials that give the magnitude and phase extremums remain unchanged. Thus, a further reduction for computing the Bode envelope of $G(s, \mathbf{q}, \mathbf{r})$ of Eq.(5.3) will be possible;

4. Using the boundary results developed in Chapter 5 to find the maximum time-delay, τ_{max}, such that the stability of a feedback system with $C(s)G(s, \mathbf{q}, \mathbf{r})e^{-\tau s}$, where $C(s)$ is a fixed controller and $G(s, \mathbf{q}, \mathbf{r})$ is a transfer function of the form of Eq.(5.3), is preserved for all $0 \leq \tau < \tau_{max}$;

5. The critical direction theory proposed in [98] can be extended to a control system with a transfer function of the form of Eq.(5.3). The critical direction method states that, at any given frequency, there is only one direction of perturbations which is important for stability analysis. The critical direction is defined by a vector with origin at the nominal transfer function and pointing towards the point $-1 + j0$. Thus, at each frequency, the points on the Nyquist template which do not lie on the critical vector can be ignored. This would be a helpful method for checking the robust stability of control systems with affine linear uncertainty by combining this theory with the boundary results developed in Chapter 5;

6. The results given in Chapter 5 can be further developed to compute frequency responses of multilinear affine systems whose numerator and denominator polynomials are multilinear affine polynomials such as

$$P(s, \mathbf{q}_1, \mathbf{q}_2, ..., \mathbf{q}_3) = P_1(s, \mathbf{q}_1)P_2(s, \mathbf{q}_2) \cdots P_m(s, \mathbf{q}_m) \tag{8.1}$$

where each $P_i(s, \mathbf{q}_i), i = 1, 2, ..., m$ is a polynomial of the form of Eq.(5.1).

7. Development of similar results to those presented in Chapter 6 for multilinear affine systems.

8. Extensions of the results given in Chapter 7 to nonlinear discrete systems with more complex uncertainty structures.

Appendix A

Using The Root Locus for Narrowing the Sweeping Range

In Chapter 3, the generalized Hermite-Biehler theorem was used to find the controller parameters which stabilize a given plant. It was seen that in order to apply the Hermite-Biehler theorem successfully, it is necessary to find the positive real roots of the real or imaginary part of the closed loop characteristic equation. However, the real and the imaginary parts of the closed loop characteristic equation are dependent on the controller parameters. Therefore, the following root locus idea which is given in [74] can be used for narrowing the sweeping range.

"Consider the problem of determining the root locus of $U(x)+kV(x)=0$, where $U(x)$ and $V(x)$ are real and coprime polynomials and k varies from $-\infty$ to ∞. Then, one can make the following observations:

1) The real breakaway points on the root locus of $U(x)+kV(x)=0$ correspond to a real multiple root and must, therefore, satisfy

$$\frac{d(\frac{V(x)}{U(x)})}{dx}=0$$

Then one obtains

$$\frac{U(x)\frac{dV(x)}{dx}-V(x)\frac{dU(x)}{dx}}{U^2(x)}=0$$

The real breakaway points are the real zeros of the above equation.

2) Let $k_1 < k_2 < ... < k_z$ be the distinct, finite, values of k corresponding to the real breakaway points $x_i, i = 1, 2, ..., z$ on the root locus of $U(x) + kV(x) = 0$. Also define $k_0 = -\infty$ and $k_{z+1} = \infty$. Then $x_i, i = 1, 2, ..., z$ are the multiple real roots of $U(x) + kV(x) = 0$ and the corresponding k's are the k_i's. Note that for $k \in (k_i, k_{i+1})$, the real roots of $U(x) + kV(x) = 0$ are simple and the number of real roots of $U(x) + kV(x) = 0$ is invariant.

3) if $U(0) + kV(0) \neq 0$ for all $k \in (k_i, k_{i+1})$, then the distribution of the real roots of $U(x) + kV(x) = 0$ with respect to the origin is invariant over this range of k values.

Example A.1

Let

$$U(x) = (x+1)^3(x-1)(x^2-x+1)^2$$

and

$$V(x) = (x-2)^2(x+3)(x^2+2x+2)$$

Then,

$$\frac{U(x)\frac{dV(x)}{dx} - V(x)\frac{dU(x)}{dx}}{U^2(x)} =$$
$$[-3x^{12} - 4x^{11} + 41x^{10} + 38x^9 - 82x^8 - 188x^7 + 77x^6 + 82x^5 - 265x^4$$
$$+28x^3 + 160x^2 - 36x - 8]/(x+1)^6(x-1)^2(x^2-x+1)^4$$

The breakaway points x_i which are the real zeros of the above equation are: $x_1 = 2.96872$, $x_2 = -1$, $x_3 = 0.42142$, $x_4 = 0.66720$, $x_5 = -0.14008$ and $x_6 = -1$ and the corresponding finite k_i's (arranged in ascending order of magnitude) are: $k_1 = -61.44924$, $k_2 = 0$, $k_3 = 0.03689$, $k_4 = 0.03791$, $k_5 = 0.04279$ and $k_6 = 163.73847$. Also, $U(x) + kV(x) = 0$ has a root at the origin when $k = k^* = 0.04167$.

Now, for $k \in (k_i, k_{i+1})$ and $k^* \notin (k_i, k_{i+1})$, the distribution of the real roots of $U(x) + kV(x) = 0$ with respect to the origin is invariant. Thus, one can simply check an arbitrary $k \in (k_i, k_{i+1})$ and determine the real root distribution of $U(x) + kV(x) = 0$ with respect to the origin, and this distribution is valid for all k in that interval. In this example, $k^* \in (k_4, k_5)$, and so the the real root distribution of $U(x) + kV(x) = 0$ with respect to the origin may not be invariant over the entire interval (k_4, k_5). Therefore, one needs to split the interval (k_4, k_5) into two subintervals (k_4, k^*), (k^*, k_5), and then check the real root distribution for each of these subintervals.

The real root distribution, with respect to the origin, of $U(x) + kV(x) = 0$ for k belonging to the different intervals, is given below:

$$k \in (-\infty, -61.44924) : \ 3 \, positive \ and \ 1 \ negative \ real \ roots$$

$$k \in (-61.44924, 0) : \ 1 \, positive \ and \ 1 \ negative \ real \ roots$$

$$K \in (0, 0.03689) : \ 1 \, positive \ and \ 1 \ negative \ real \ roots$$

$$k \in (0.03689, 0.03791) : \ 3 \, positive \ and \ 1 \ negative \ real \ roots$$

$$k \in (0.03791, 0.04167) : \ 1 \, positive \ and \ 1 \ negative \ real \ roots$$

$$k \in (0.04167, 0.04279) : \ 2 \ negative \ real \ roots$$

$$k \in (0.04279, 163.73847) : \ no \ real \ roots$$

$$k \in (163.73847, \infty) : \ 2 \ negative \ real \ roots$$

This example shows how the root locus ideas can be used to determine the distribution of the real zeros of $U(x) + kV(x) = 0$, with respect to the origin, as k varies from $-\infty$ to ∞."

References

[1] Ackermann, J. *Robust Control: Systems with Uncertain Physical Parameters*, Springer-Verlag, 1993.

[2] Anderson, B. D. O., Jury, E. I. and Mansour, M., "On robust Hurwitz polynomials," *IEEE Trans. on Automat. Contr.*, Vol. 32, pp. 909-913, 1987.

[3] Argoun, M. B., "Allowable coefficeent perturbations with preserved stability of a Hurwitz polynomial," *Int. J. of Contr.*, Vol.44, pp. 927-934, 1986.

[4] Argoun, M. B., "Frequency domain conditions for stability of perturbed polynomials," *IEEE Trans. on Automat. Contr.*, Vol. 32, pp. 913-916, 1987.

[5] Argoun, M. B. and Bayoumi, M. M., "Robust gain and phase margins for interval uncertain systems," *1993 Canadian Conf. on Electrical and computers Engineering*, Vol. 1, pp. 349-352, 1993.

[6] Arhipov, V. V., Kharitonov, V. L. and Zhapko, A. P., "Robust stability of polynomials and quasipolynomials under polynomial perturbations," *IFAC Robust Control Design*, Budapest, Hungary, pp. 73-78, 1997.

[7] Astrom, K. J. and Hagglund, T., "Automatic tuning of simple regulators with specification on phase and gain margins," *Automatica*, Vol. 20, pp. 645-651, 1984.

[8] Atherton, D. P., *Stability of Nonlinear Systems*, Research Studies Press, 1981.

[9] Atherton, D. P., *Nonlinear Control Engineering*, Van Nostrand Reinhold, London, 1982.

[10] Bailey, F. N. and Panzer D., "A fast algorithm for computing interval rational functions," *Proc. of Amer. Contr. Conf.*, pp. 22-23, 1988.

[11] Bailey, F. N., Panzer, D., and Gu, G., "Two algorithms for frequency domain design of robust control systems," *Int. J. of Contr.*, Vol. 48, pp. 1787-1806, 1988.

[12] Bailey, F. N. and Hui, C. H., "A fast algorithm for computing parametric rational functions," *IEEE Trans. on Automat. Contr.*, Vol. 34, pp. 1209-1212, 1989.

[13] Barmish, B. R. *New Tools for Robustness of Linear Systems*, MacMillan, NY, 1994.

[14] Barmish, B. R., "Invariance of the strict Hurwitz property for polynomials with perturbed coefficients," *IEEE Trans. on Automat. Contr.*, Vol. 29, pp. 935-936, 1984.

[15] Barmish, B. R., "A generalization of Kharitonov's four-polynomial concept for robust stability problems with linearly dependent coefficient perturbations," *IEEE Trans. on Automat. Contr.*, Vol. 34, pp. 157-165, 1989.

[16] Barmish, B. R., Hollot, C. V., Kraus, F. J. and Tempo, R., "Extreme point results for robust stabilization of interval plants with first order compensators," *IEEE Trans. on Automat. Contr.*, Vol. 37, pp. 707-714, 1992.

[17] Barmish, B. R. and Tempo, R., "The robust root locus," *Automatica*, Vol. 26, pp. 283-292, 1990.

[18] Barmish, B. R. and Shi, Z., "Robust stability of perturbed systems with time delay," *Automatica*, Vol. 25, pp. 371-381, 1989.

[19] Barmish, B. R., Lagoa, C. M. and Tempo, R., "Radially truncated uniform distributions for probabilistic robustness of control systems," *Proc. of Amer. Ctrl. Conf.*, 1997.

[20] Barmish, B. R. and Kang, H. I., "A survey of extreme point results for robustness of control systems," *Automatica*, Vol. 29, pp. 13-35, 1993.

[21] Bartlett, A. C., Hollot, C. V., and Lin H., "Root location of an entire polytope of polynomials: it suffices to check the edges," *Mathematics of Controls, Signals and Systems*, Vol. 1, pp. 61-71, 1988.

[22] Bartlett, A. C., "Nyquist, Bode and Nichols plots of uncertain systems," *Proc. of Amer. Contr. Conf.*, pp. 2033-2036, 1990.

[23] Bartlett, A. C., "Computation of frequency response of systems with uncertain parameters: a simplification," *Int. J. of Contr.*, Vol. 57, pp. 1293-1309, 1993.

[24] Bartlett, A. C., Tesi, A., and Vicino, A., "Frequency response of uncertain systems with interval plants," *IEEE Trans. on Automat. Contr.*, Vol. 38, pp. 929-933, 1993.

[25] Bhattacharyya, S. P., Chapellat, H., and Keel, L. H., *Robust Control: The Parametric Approach.* Prentice Hall, 1995.

[26] Bhattacharyya, S. P. and Keel, L. H., "Comments on "extreme point results for robust stabilization of interval plants with first order compensators"," *IEEE Trans. on Automat. Contr.,* Vol. 38, pp.1734-1735, 1993.

[27] Blanchini, F., Tempo, R. and Dabbene, F., "Computation of the minimum destabilizing valume for interval and affine families of polynomials", *Proc. of Amer. Contr. Conf.*, 1997.

[28] Bode, H. W., *Network Analysis and Feedback Design,* Van Nostrand Reinhold, New York, 1945.

[29] Bose, N.K. and Shi, Y. Q., "A simple general proof of Kharitonov's generalized stability criterion," *IEEE Trans. on Circuit and Systems*, Vol. 34, pp. 1233-1237, 1987.

[30] Bose, N. K., Jury, E. I and Zehep, E., "On robust Hurwitz and Schur polynomials," *Proc. of the 25th CDC*, pp. 739-744, 1986.

[31] Cailler, F. M. and Desoer, C. A., *Multivariable Feedback Systems*, Springer-Verlag, New York, 1982.

[32] Chandrasekharan, P. C., *Robust Control of Linear Dynamical Systems*, Kluwer Academic Press, 1996.

[33] Chang, B. C. and Pearson, J. B, "Optimal disturbance reduction in linear multivariable systems," *IEEE Trans. on Automat. Contr.*, Vol. 29, pp. 880-887, 1984.

[34] Chapellat, H. and Bhattacharyya, S. P., "A generalization of Kharitonov's theorem: robust stability of interval plants," *IEEE Trans. on Automat. Contr.*, Vol. 34, pp. 306-311, 1989.

[35] Chapellat, H. and Bhattacharyya, S. P., "An alternative proof of Kharitonov's theorem," *IEEE Trans. on Automat. Contr.*, Vol. 34, pp. 448-450, 1989.

[36] Chapellat, H., Mansour, M. and Bhattacharyya, S. P., "Elementary proofs of some classical stability criteria," *IEEE Trans. on Automat. Contr.*, Vol. 33, pp.232-239, 1990.

[37] Chapellat, H., Dahleh, M. and Bhattacharyya, S. P., "Robust stability under structured and unstrucured perturbations," *IEEE Trans. on Automat. Contr.*, Vol. 35, pp. 1100-1108, 1990.

[38] Chapellat, H., Dahleh, M. and Bhattacharyya, S. P., "On robust nonlinear stability of interval control systems," *IEEE Trans. on Automat. Contr.*, Vol. 36, pp. 59-67, 1991.

[39] Chapellat, H., *Robust stability and Control under Structured and Unstructured Perturbations*, PhD thesis, Department of Electrical Engineering Texas AM University, Collage Station, Texas, U.S.A, 1990.

[40] Chapellat, H., Bhattacharyya, S. P. and Keel, L. H., "Stability margins for Hurwitz polynomials," *Proc. of the 27th CDC*, pp. 1392-1398, 1988.

[41] Chen, C. L., Yang, S. K. and Chen, C. K., "On determining the root locations of an interval system," *Control-Theory and Advanced Technology*, Vol. 8, pp. 789-802, 1992.

[42] Chen, X. and Zhou, K., "On the probabilistic characterization of model uncertainty and robustness," *Proc. of the 36th CDC*, pp. 3616-3621, 1997.

[43] Chen, X. and Zhou, K., "A probabilistic approach to robust control," *Proc. of the 36th CDC*, pp. 4894-3895, 1997.

[44] Cieslek, J., "On possibilities of extension of Kharitonov's stability test for interval polynomials to discrete-time case," *IEEE Trans. on Automat. Contr.*, Vol. 32, pp. 237-238, 1987.

[45] Dahleh, M., Tesi, A. and Vicino, A., "An overview of extremal properties for robust control of interval plants," *Automatica*, Vol. 29, pp. 707-721, 1993.

[46] Dahleh, M., Tesi, A. and Vicino, A., "On the robust Popov criterion for interval Lur'e system," *IEEE Trans. on Automat. Contr.*, Vol. 38, pp. 1400-1405, 1993.

[47] Dasgupta, S., "Kharitonov's theorem revisited," *Syst. Contr. Lett.*, Vol. 11, pp. 381-384, 1988.

[48] Dasgupta, S., "Kharitonov like theorem for systems under nonlinear passive feedback," *Proc. of the 26th CDC*, pp. 2062-2063, 1987.

[49] Datta, A. D. and Bhattacharyya, S. P., "On determining δ and θ Hurwitz stability of interval polynomials," *Proc. of Amer. Contr. Conf.*, pp. 2396-2398, 1995.

[50] Delsarte, P. H., Genin, Y. and Kamp, Y., "The Nevanlinna-Pick problem in circuit and system theory," *Int. J. Circuit Theory and Applications*, Vol. 9, pp. 177-187, 1981.

[51] Desoer, C. A., Liu, R. W., Murray, J. and Saeks, R., "Feedback system design: The fractional representation approach to analysis and synthesis," *IEEE Trans. on Automat. Contr.*, Vol. 25, pp. 339-412, 1980.

[52] Djaferis, T. E., *Robust Control Design: A Polynomial Approach*, Kluwer Academic Publishers, Boston, 1995.

[53] Djaferis, T. E. and Hollot, C. V., "Parameter partitioning via shaping conditions for the stability of families of polynomials," *IEEE Trans. on Automat. Contr.*, Vol. 34, pp. 1205-1209, 1989.

[54] Djaferis, T. E., "To stabilize an interval plant family it sufficies to simultaneously stabilize sixty-four polynomials," *IEEE Trans. on Automat. Contr.*, Vol. 38, pp. 760-764, 1993.

[55] Doyle, J. C. and Stein, G., "Multivariable feedback design: concepts for a classical modern synthesis," *IEEE Trans. on Automat. Contr.*, Vol. 26, pp. 4-16, 1981.

[56] Evans, W. R., "Graphical analysis of control systems," *AIEE Trans. Part II*, Vol. 67, pp. 547-551, 1948.

[57] Fadali, M. S. and Chachavalvoong, N., "Describing function analysis of nonlinear systems using the Kharitonov approach," *Proc. of Amer. Contr. Conf.*, pp. 2906-2912, 1995.

[58] Ferreres, G. and Fromion, V., "Nonlinear analysis in the presence of parametric uncertainty," *Int. J. of Contr.*, Vol. 69, pp. 695-716, 1998.

[59] Foo, Y. K. and Soh, Y. C., "Closed-loop hyperstability of inerval plants," *IEEE Trans. on Automat. Contr.*, Vol. 39, pp. 151-154, 1994.

[60] Francis, B. A. and Zames, G., "On H_∞ optimal sensitivity theory for SISO systems," *IEEE Trans. on Automat. Contr.*, Vol. 29, pp. 9-16, 1984.

[61] Francis, B. A., Helton, J. W. and Zames, G., "H_∞ optimal controller for linear multivariable systems," *IEEE Trans. on Automat. Contr.*, Vol. 29, pp. 888-990, 1984.

[62] Fu, M., "Computing the frequency response of linear systems with parametric perturbations," *Syst. Contr. Lett.*, Vol. 15, pp. 45-52, 1990.

[63] Fu, M., Olbrot, A. W. and Polis, M. P., "Robust stability for time-delay systems: the edge theorem and graphical tests," *IEEE Trans. on Automat. Contr.*, Vol. 34, pp. 813-819, 1989.

[64] Franklin, F., Powell, J. D. and Workman, K. L., *Digital Control of Dynamic Systems*, Addison-Wesley, 1990.

[65] Ghosh, B. K., "Some new results on the simultaneous stabilization of a family of single input, single output systems," *Syst. Contr. Lett.,* Vol. 6, pp. 39-45, 1985.

[66] Glover, K., "Optimal Hankel norm approximation of linear multivariable systems and their L_∞ error bounds" *Int. J. of Contr.,* Vol. 39, pp. 1115-1193, 1984.

[67] Grujic, L. T. and Petkovski, D., "On robustness of Lurie systems with multiple nonlinearities," *Automatica*, Vol.23, pp. 327-334, 1987.

[68] Helton, J. W., "Worst case analysis in the frequency domain: The H_∞ approach to control," *IEEE Trans. on Automat. Contr.*, Vol. 30, pp. 1154-1170, 1985.

[69] Hernandez, R., Dormido, S. and Dormido, R., "On the thirty-two virtual polynomials to stabilize an interval plant," *IEEE Trans. on Automat. Contr.*, Vol. 43, pp. 1460-1465, 1998.

[70] Ho, M. T., Datta, A. and Bhattacharyya, S. P., "Design of P, PI and PID controllers for interval plants," *Proc. of Amer. Ctrl. Conf.*, 1998.

[71] Ho, M. T., Datta, A. and Bhattacharyya, S. P., "A generalization of the Hermite-Biehler theorem," *Proc. of the 34th CDC*, pp.130-131, 1995.

[72] Ho, M. T., Datta, A. and Bhattacharyya, S. P., "A new approach to feedback stabilization," *Proc. of the 35th CDC*, pp. 4643-4648, 1996.

[73] Ho, M. T., Datta, A. and Bhattacharyya, S. P., "A linear programming characterization of all stabilizing PID controllers," *Proc. of Amer. Contr. Conf.,* 1997.

[74] Ho, M. T., Datta, A. and Bhattacharyya, S. P., "A new approach to feedback design part I: generalized interlacing and proportional control and part II: PI and PID controllers," *Department of Electrical Engg., Texas AM Univ., College Station, TX, Tech. Report TAMU-ECE97-001-A and 001-B.*, 1997.

[75] Hollot, C. V. and Tempo, R.,"On the Nyquist envelope of an interval plant family," *Proc. of Amer. Contr. Conf.*, pp. 861-864, 1991. Also in, *IEEE Trans. on Automat. Contr.*, Vol. 39, pp. 391-396, 1994.

[76] Hollot, C. V. and Yang F., "Robust stabilization of interval plants using lead or lag compensators," *Syst. Contr. Lett.*, Vol. 14, pp. 9-12, 1990.

[77] Hollot, C. V. and Bartlett, A. C., "Some discrete time counterparts of Kharitonov's stability criterion for uncertain systems," *IEEE Trans. on Automat. Contr.*, Vol. 31, pp. 355-356, 1986.

[78] Horowitz, I. M., *Synthesis of Feedback Systems*, Academic Press, New York, 1963.

[79] Hwang, C., Chen, J. J. and Chen, U. Y., "An improved technique for plotting robust root locus", *J. of Chineese Inst. of Eng.*, Vol. 19, pp. 551-559, 1996.

[80] Hwang, C. and Chen, J. J., "Plotting robust root loci for linear systems with multilinearly parametric uncertainties," *Proc. of Amer. Ctrl. Conf.*, pp. 1958-1962, 1998.

[81] Impram, S. T. and Munro, N., "Describing function analysis of nonlinear systems with parametric uncertainties," *Inter. Conf. on Contr.'98, UKACC*, Swansea, UK, 1998.

[82] Kalman, R. E., "A new approach to linear filtering and prediction problems," *J. of Basic Eng.*, Vol. 82, pp. 35-45, 1960.

[83] Karamancioglu, A., Dzhafarov, V. and Ozdemir, C., "Frequency response of PID-controlled linear interval systems," *Circuits, Systems and Signal Processing*, Vol. 15, pp. 735-748, 1996.

[84] Katbab, A. and Jury, E. I., "Robust Schur-stability of control systems with interval plants," *Int. J. of Contr.*, Vol. 51, pp. 1343-1352, 1990.

[85] Katbab, A. and Jury, E. I., "Generalization and comparsion of two recent frequency-domain stability robustness results," *Int. J. of Contr.*, Vol. 53, pp. 463-475, 1991.

[86] Ke, N. P., "An algorithm for symbolic computation of stability margin", *Proc. of Amer. Contr. Conf.*, 1998.

[87] Keel, L. H. and Bhattacharyya, S. P., "Control system design for parametric uncertainty," *Int. J. of Contr.*, Vol. 4, pp. 87-100, 1994.

[88] Kharitonov, V. L., "Asymptotic stability of an equilibrium position of a family of systems of linear differential equations," *Differential Equations*, Vol. 14, pp.1483-1485, 1979.

[89] Kharitonov, V. L., "Robust stability of continuous-time difference systems," *Int. J. of Contr.*, Vol. 64, pp. 985-990, 1996.

[90] Kimura, H., "Robust stabilization of a class of transfer functions," *IEEE Trans. on Automat. Contr.*, Vol. 29, pp. 778-793, 1984.

[91] Kuo, B. C., *Analysis and Synthesis of Sampled-Data Control Systems*, Prentice-Hall, 1963.

[92] Kraus, F., Anderson, B. D. O., Jury, E. I. and Mansour, M., "Robust Schur polynomial stability and Kharitonov's theorem," *Int. J. of Contr.*, Vol. 47, pp. 1213-1225, 1988.

[93] Kraus, F., Anderson, B. D. O. and Mansour, M., "On robustness of low order Schur polynomials," *IEEE Trans. on Automat. Contr.*, Vol. 35, pp. 570-577, 1988.

[94] Kogan, J. and Leizarowitz, A., "Frequency domain criterion for robust stability of interval time-delay systems," *Automatica*, Vol. 31, pp. 463-469, 1995.

[95] Kontogiannis, E. and Munro, N., "The fundamental dominance condition for MIMO systems with parametric uncertainty," *Proc. of IEE/IFAC Control'96*, Exeter, U.K., pp. 1202-1207, 1996.

[96] Kontogiannis, E. and Munro, N., "Extreme point solutions to the diagonal dominance problem and stability analysis of uncertain systems," *Proc. of Amer. Contr. Conf.*, pp. 3936-3940, 1997.

[97] Lagoa, C. M., Shcherbakov, P. S. and Barmish, B. R., "Probabilistic enhancement of classical robustness margins: the unirectangularity concept," *Proc. of the 36th CDC*, pp. 4874-4879, 1997.

[98] Latchman, H. A., Crisalle, O. D. and Basker, V. R., "The Nyquist robust stability margin-a new metric for the stability of uncertain systems," *Int. J. of Robust and Nonlinear Control*, Vol. 7, pp. 211-226, 1997.

[99] Latchman, H. A., Crisalle, O. D. and Basker, V. R., "Robustness of uncertain MIMO systems- an overview and a new perspective," *Proc. of the 35th CDC*, pp. 2929-2935, 1996.

[100] Latchman, H. A., Crisalle, O. D. and Yen, K. H., "A design metric for systems with parametric uncertainties," *Proc. of IASTED Int. Conf. on Applied Modelling and Simulation*, pp. 588-590, 1995.

[101] Levkovich, A., Cohen, N. and Zehep, E., "A root-distribution criterion for an interval polynomial in a sector," *Journal of Mat. Contr. and Inform.*, Vol. 13, pp. 321-333, 1996.

[102] Levkovich, A. and Zehep, E., "Frequency response envelopes of a family of uncertain continuous-time systems," *IEEE Trans. Circuits and Sys.,* Vol. 42, pp. 156-165, 1995.

[103] MacFarlane, A. G. J., "Linear multivariable feedback theory: a survey," *IFAC Symp. on Multivariable Contr. Sys.*, Dusseldorf, Germany, 1971.

[104] Mahon, H. M., Crisalle, O. D., Lantchmen, H. and Yen, K. H., "A new method for computing robustness margins for real parametric uncertainties", *Proc. of Amer. Contr. Conf.*, 1998.

[105] Mayne, D. Q., "The design of linear multivariable systems," *Automatica*, Vol. 9, pp. 201-207, 1973.

[106] Minninchalli, R. J., Anagnost, J. J., and Desoer, C. A., "An elementary proof of Kharitonov's stability theorem with extensions," *IEEE Trans. on Automat. Contr.*, Vol. 34, pp. 995-998, 1989.

[107] Mori, T., Nishimura, T. and Kokame, H., "Comments on "on the robust Popov criterion for interval Lur'e systems"," *IEEE Trans. on Automat. Contr.*, Vol.40, pp.136-137, 1995.

[108] Naimark, L. and Zehep, E., "All constant gain stabilizing controllers for an interval delay system with uncertain parameters," *Automatica*, Vol. 33, pp. 1669-1675, 1997.

[109] Nichols, N. B., "Backlash in a velocity lag servomechanism," *AIEE Trans. Part II.*

[110] Nyquist, H., "Regeneration theory," *Bell System Tech. J.*, Vol.11, pp. 126-147, 1932.

[111] Omorov, R. O., "Robustness of interval dynamical systems. II. Robustness of discrete linear interval dynamical systems," *Int. J. of Sys. Sciences*, Vol. 34, pp. 1-5, 1996.

[112] Polis, M. P., Olbrot, A. W. and Fu, M., "An overview of recent results on the parametric approach to robust stability," *Proc. of the 28th CDC*, pp. 23-29, 1989.

[113] Rantzer, A.,"Stability conditions for polytopes of polynomials," *IEEE Trans. on Automat. Contr.*, Vol. 37, pp. 79-89, 1992.

[114] Rosenbrock, H. H., *Computer Aided Control Systems Design*, Academic Press, London, 1974.

[115] Santis, E. D. and Vicino, A., "Diagonal dominance for robust stability of MIMO interval systems," *IEEE Trans. on Automat. Contr.*, Vol. 41, 1996.

[116] Shaw, J. and Jayasuriya, S., "A new algorithm for testing the stability of a polytope: a geometric approach for simplification," *Journal of Dynamic Sys., Meas., and Contr.*, Vol. 118, pp. 611-614, 1996.

[117] Siljak, D. D., *Nonlinear Systems*, Wiley, New York, 1969.

[118] Siljak, D. D.,"Parameter space methods for robust control design: a guided tour," *IEEE Trans. on Automat. Contr.*, Vol. 34, pp. 674-688, 1989.

[119] Soh, C. B.,"On damping ratio of polynomials with perturbed coefficients," *IEEE Trans. on Automat. Contr.*, Vol. 37, pp. 277-279, 1992.

[120] Soh, Y. C., Xie, L. and Foo, Y. K., "Maximal perturbations bound for perturbed polynomials with roots in the left-sector," *IEEE Trans. on Circuits and Systems-I: Fundamental Theory and Applications,* Vol. 41, pp. 281-285, 1994.

[121] Tan, N. and Atherton, D. P., "AISTK-A software package for the analysis of interval systems," *IEE Colloquium: Robust Control-Theory, Software and Applications*, London, UK, Digest No. 97/380, pp. 4/1-4/7, 1997.

[122] Tan, N. and Atherton, D. P., "Magnitude and phase envelopes of systems with affine linear uncertainty," *International Conf. on Control'98, UKAC*, Swansea UK, pp. 1039-1044, 1-4 Sept. 1998.

[123] Tan, N. and Atherton, D. P., "Frequency response of uncertain systems: A 2q-convex parpolygonal approach," submitted to *IEE Proc., Control Theory and Applications.*

[124] Tan, N. and Atherton, D. P., "Controller synthesis technique for systems with affine linear uncertainty," *14th World Congress of IFAC*, Vol. G, pp. 133-138, July 5-9, 1999.

[125] Tan, N. and Atherton, D. P., "Feedback stabilization using the Hermite Biehler theorem ," *2nd International Conf. on the Control of the Industrial Processes*, March 30-31, 1999.

[126] Tan, N. and Atherton, D. P., "Describing function analysis of nonlinear discrete interval systems," *European Control Conference*, Karlsruhe, Germany, 31. August-3. September, 1999.

[127] Tan, N. and Atherton, D. P., "Absolute stability problem of systems with parametric uncertainties," *European Control Conference*, Karlsruhe, Germany, 31. August-3. September, 1999.

[128] Tan, N. and Atherton, D. P., "Analysis of control systems with mixed perturbations," submitted to *European Journal of Control(EJC)*.

[129] Tesi, A. and Vicino, A., "Robust absolute stabilty of Lur'e control system in parameter space," *Automatica*, Vol. 27, No.1, pp. 147-151, 1991.

[130] Truol, W. and Kraus, F. J., "Computation of value sets of uncertain transfer functions," in *Robustness of Dynamical Systems with Parameter Uncertainty*, M. Mansour, S. Balemi and W. Truol, eds., Birkhauser, Basel, Switzerland, 1992.

[131] Tsypkin, Y. Z. and Fu, M., "Robust stability of time-delay systems with an uncertain time-delay constant," *Int. J. of Contr.*, Vol. 57, pp. 865-879, 1993.

[132] Vidyasagar, M., *Control Systems Synthesis-A Factorization Approach*, Cambridge MA: MIT Press, 1985.

[133] Vidyasagar, M. and Kimura, H., "Robust controller for uncertain linear multivariable systems," *Automatica*, Vol. 28, pp. 85-94, 1986.

[134] Vidyasagar, M., *Nonlinear Systems Analysis*, Englewood Cliffs, Prentice-Hall, 1978.

[135] Yeung, L. F. and Winnie, H. Y. N., "Dominance measures for uncertain multivariable systems," *Proc. of the 35th CDC*, pp. 2892-2893, 1996.

[136] Yeung, K. S., "Linear system stability under parameter uncertainties," *Int. J. of Control*, Vol. 38, pp. 459-464, 1983.

[137] Youla, D. C., Bongiorno, J. J. and Lu, C. N., "Modern Wiener-Hopf design of optimal controllers, Part I: The single input case," *IEEE Trans. on Automat. Contr.*, Vol. 21, pp. 3-14, 1976.

[138] Youla, D. C., Jabar, H. A. and Bongiorno, J. J., "Modern Wiener-Hopf design of optimal controllers, Part II: The multivariable case," *IEEE Trans. on Automat. Contr.*, Vol. 21, pp. 319-338, 1976.

[139] Zadeh, L. A. and Desoer, C. A., *Linear System Theory-A State Space Approach*, McGraw Hill, New York, 1963.

[140] Zames, G., "Feedback and optimal sensitivity: Model reference transformations, multiplicative semi-norms and approximate inverses," *IEEE Trans. on Automat. Contr.*, Vol. 26, pp. 301-320, 1981.

[141] Zames, G. and Francis, B. A., "Feedback, minimax sensitivity and optimal robustness," *IEEE Trans. on Automat. Contr.*, Vol. 28, pp. 585-601, 1983.

List of Publications

1. Tan, N. and Atherton, D. P., "AISTK-A software package for the analysis of interval systems," *IEE Colloquium: Robust Control-Theory, Software and Applications*, London UK, Digest No. 97/380, pp. 4/1-4/7, 1997.

2. Tan, N. and Atherton, D. P., "Magnitude and phase envelopes of systems with affine linear uncertainty," *International Conf. on Control'98, UKAC*, Swansea UK, pp.1039-1044, 1-4 September, 1998.

3. Tan, N. and Atherton, D. P., "Feedback stabilization using the Hermite Biehler theorem," *2nd International Conf. on the Control of the Industrial Processes*, March 30-31, 1999.

4. Tan, N. and Atherton, D. P., "Controller synthesis technique for systems with affine linear uncertainty," *14th World Congress of IFAC*, Vol. G, pp. 133-138, July 5-9, 1999.

5. Tan, N. and Atherton, D. P., "Absolute stability problem of systems with parametric uncertainties," *European Control Conference*, Karlsruhe, Germany, 31. August - 3. September, 1999.

6. Tan, N. and Atherton, D. P., "Describing function analysis of nonlinear discrete interval systems," *European Control Conference*, Karlsruhe, Germany, 31. August - 3. September, 1999.

7. Tan, N. and Atherton, D. P., "A user friendly toolbox for the analysis of interval systems," submitted to *ROCOND2000.*

8. Tan, N. and Atherton, D. P., "Frequency response of uncertain systems: A 2q-convex parpolygonal approach," submitted to *IEE Proc., Control Theory and Applications.*

9. Tan, N. and Atherton, D. P., "Analysis of control systems with mixed perturbations," submitted to *European Journal of Control.*

10. Tan, N. and Atherton, D. P., "Stability and Performance analysis in an uncertain world," submitted to *Computing and Control Engineering Journal.*